



LEVEL *14*

P

Research and Development Technical Report

ECOM - 75-1344-F SUPPLEMENT

ADA064375

DDC FILE COPY

**A TWO-DIMENSIONAL COMPUTER MODEL
FOR THE STEADY-STATE OPERATION
OF MOSFETs**

prepared by

Alan D. Sutherland
University of Florida
Electron Device Research Center
College of Engineering
Gainesville, Florida 32611

September 1977

Supplemental Final Report for Period 1 March 1977-30 June 1977

Distribution Statement
Approved for Public Release, Distribution Unlimited

Prepared for

Advanced Research Agency
1400 Wilson Boulevard
Arlington, Va. 22209



79 02 07 018

The findings in this report are not to be construed as an official Department of the Army position unless so designated by other authorized documents.

Citation of manufacturers' or trade names does not constitute an official endorsement or approval of the use thereof.

Destroy this report when it is no longer needed.
Do not return it to the originator.

ACCESSION for	
NTIS	White Section <input checked="" type="checkbox"/>
DDC	Buff Section <input type="checkbox"/>
UNCLASSIFIED	<input type="checkbox"/>
DISPATCH SYMBOL AVAILABILITY CODES	
SPECIAL	
A	

79 02 07 018

19 REPORT DOCUMENTATION PAGE		READ INSTRUCTIONS BEFORE COMPLETING FORM
1. REPORT NUMBER 18 ECOM-75-1344-F-Supplement	2. GOVT ACCESSION NO.	3. RECIPIENT'S CATALOG NUMBER
4. TITLE (and Subtitle) A Two-Dimensional Computer Model for the Steady-State Operation of MOSFET's Supplement.	5. TYPE OF REPORT & PERIOD COVERED Supplemental Final Report 1 March 1977 - June 30 1977	
7. AUTHOR(s) 10 Alan D. Sutherland	6. CONTRACT OR GRANT NUMBER(s) 15 DAAB07-75-C-1344 V ARPA Order - 2985	
9. PERFORMING ORGANIZATION NAME AND ADDRESS University of Florida Department of Electrical Engineering Gainesville, FL 32611	10. PROGRAM ELEMENT, PROJECT, TASK AREA & WORK UNIT NUMBERS 61101E6010	
11. CONTROLLING OFFICE NAME AND ADDRESS Advanced Research Projects Agency (ARPA) 1400 Wilson Blvd. Arlington, VA 22209	12. REPORT DATE 11 Sep 1977	
14. MONITORING AGENCY NAME & ADDRESS (if different from Controlling Office) U.S. Army Electronics Command ATTN: DRSEL-TL-IG Ft. Monmouth, NJ 07703	13. NUMBER OF PAGES 200	
	15. SECURITY CLASS. (of this report) UNCLASSIFIED	
15a. DECLASSIFICATION/DOWNGRADING SCHEDULE		
16. DISTRIBUTION STATEMENT (of this Report) Approved for public release; distribution unlimited.		
17. DISTRIBUTION STATEMENT (of the abstract entered in Block 20, if different from Report)		
18. SUPPLEMENTARY NOTES This research was sponsored by the Defense Advanced Research Project Agency (DARPA) pursuant to ARPA Order No. 2985 dated 18 February 1975, Program Code W15P8W.		
19. KEY WORDS (Continue on reverse side if necessary and identify by block number) MOSFET model IGFET model TWO-DIMENSIONAL model		
20. ABSTRACT (Continue on reverse side if necessary and identify by block number) This report describes in detail a two-dimensional computer model for the steady-state operation of an MOSFET, and is intended to serve as a USER'S MANUAL for that model. Detailed flow charts are included. The model is shown to produce results in good agreement with those produced by a prototype model which is the proprietary property of IBM. It is also shown to agree well with experimental data obtained from a p-channel device whose para- meters have been well characterized by means of test sites.		

DD FORM 1473
1 JAN 73EDITION OF 1 NOV 68 IS OBSOLETE
S/N 0102-014-6601

SECURITY CLASSIFICATION OF THIS PAGE (When Data Entered)

404 825

Gm

FOREWORD

Custom integrated semiconductor circuits are often needed for military applications that involve a vast number of different, highly specialized, electronic systems, although seldom are these systems called for in large quantity. This combination produces an economically prohibitive situation. The large initial cost for designing integrated circuits, in conjunction with a small production requirement, creates an unreasonably large cost per IC chip. The source of this difficulty lies in empirical, and costly, engineering techniques used during both IC design, and production start-up. Empirical techniques are used during IC design to solve problems for which there is inadequate basic understanding. Similar empirical techniques are also used during production start-up to overcome problems that presently cannot be solved by design engineers.

An important source of this problem lies in the lack of adequate models for the design and development of IC structures. This effort is part of the DARPA funded research, pursued to ARPA Order No. 2985, and is intended to replace the empirical and costly conventional engineering approach to IC development for military systems with a computed aided cost effective method. In particular, this report describes, in detail, a two-dimensional computer model for the steady-state operation of an MOSFET and is intended to serve as a USER's MANUAL for that model.

CONTENTS

	<u>Page</u>
CHAPTER I A Two-Dimensional Model for MOSFET Operation	7
1.0 Introduction	7
2.0 Description of the Model	8
2.01 Basic Geometry	8
2.02 Dimensionless Variables	10
2.03 Basic Equations	10
2.04 Boundary Conditions	14
2.04.1 Boundary Conditions on ψ and n	15
2.04.2 Boundary Conditions on θ	18
2.05 Determination of the Drain Current Factor J_0	19
3.0 Finite-Difference Algorithm	20
3.01 Finite-Difference Algorithms for ψ	22
3.01.1 Implementation of the Boundary Conditions on ψ	24
3.01.2 Numerical Algorithm for the Charge Term Q_p	29
3.02 Finite-Difference Algorithm for the Stream Function θ	30
3.02.1 Implementation of the Boundary Conditions on θ	34
3.03 Finite-Difference Algorithm for the Drain Current Factor J_0	5
3.04 Finite-Difference Algorithm for the Electron Number Density n	36
4.0 The Iterative Procedure	39
4.01 Picard Iteration	39
4.02 Gummel's Algorithm	42
4.03 A Modification of Mock's Iterative Procedure	43
4.04 Initial Estimates for $\psi(x,y)$, $\theta(x,y)$, $n(x,y)$ and $p(x,y)$	47
4.04.1 Initial Estimate for $\psi(x,y)$	47
4.04.2 Initial Estimate for $\theta(x,y)$	51
4.04.3 Initial Estimates for $n(x,y)$ and $p(x,y)$	51
CHAPTER II Evaluation of The Computer Model's Performance	52
1.0 Comparison with Mock's Program	52
2.0 Comparison with Experiment	77

	<u>Page</u>
CHAPTER III Instructions for Using the Computer Program	81
1.0 Input Data	81
1.01 NAMELIST/PRMTRS/	81
1.02 NAMELIST/VOLTGE/	83
1.03 NAMELIST/CONTRL/	84
2.0 Output Data	86
3.0 Glossary of the Variables Appearing in COMMON Statements	88
3.01 COMMON/ARRAYS/	88
3.02 COMMON/COEFF/	106
3.03 COMMON/REAL/	107
3.04 COMMON/INTGR/	108
3.05 COMMON/NRMLZE/	109
3.06 COMMON/CNTRL/	109
CHAPTER IV Program Listing, with Flowcharts	110
1.0 MAIN	112
2.0 GRID	117
3.0 BORDER	123
4.0 INITAL	127
5.0 VZERO & DERIV	138
6.0 ONEDIM	142
7.0 RELAX & GRELAX	146
8.0 STREAM	152
9.0 BLOCK	161
10.0 DNSITY	165
11.0 CURDNS	169
12.0 EIGEN	172
13.0 POISSN	175
14.0 STONE & STONE1	179
15.0 CHARGE	189
16.0 OUTPUT	192
CHAPTER V Conclusions	197
DISTRIBUTION LIST	198

FIGURES

<u>Figure</u>	<u>Title</u>	<u>Page</u>
1	(a) Cross-section of an n-channel MOSFET (b) Rectangular region modeled.	9
2	Graded lattice of points used in the finite-difference equations dealt with in the computer model.	11
3	Boundary conditions for (a) $\psi(x,y)$, (b) $\theta(x,y)$, and (c) $n(x,y)$.	16
4	Layout of the interlaced ψ and θ lattices used in the finite-difference equations.	21
5	Five-point "star" of ψ -lattice points used in the finite-difference equation for ψ .	23
6	Boundary conditions on ψ at the oxide-silicon interface are enforced through an appropriate choice for the location of the interface, leading to special finite-difference equations applicable for the two ψ -lattice rows bracketing the interface.	26
7	Five-point "star" of θ -lattice points used in the finite-difference equation for θ .	31
8	Number of iterations required for convergence of ψ to within .02 kT/q versus the gate voltage V_G , comparing Mock's iterative procedure with the overrelaxed Gummel procedure.	44
9	Number of iterations required for convergence of ψ to within .02 kT/q versus the overrelaxation parameter Ω used with Gummel's algorithm. The numerical values show CPU time, in seconds, required with an Amdahl 470 V/6-II computer.	46
10	(a) Sketch of the equipotential contours in an MOSFET operating in saturation, providing insight into how to supply an initial estimate for $\psi(x,y)$. (b) Sketch of the potential $\psi(x)$ along the oxide-silicon interface, and $\psi_B^s(x)$ deep within the bulk material.	48
11	Comparison of the potential $\psi(x)$ along the oxide-silicon interface, generated by this model and by Mock's model.	53
14		56
17		59
20		62
23		65
26		68
29		71
32		74

<u>Figure</u>	<u>Title</u>	<u>Page</u>
12	Comparison of the potential $\psi(y)$ along the plane midway between source and drain, generated by this model and by Mock's model	54
15		57
18		60
21		63
24		66
27		69
30		72
33		75
13	Comparison of the electron number density $n(y)$ along the plane midway between source and drain, generated by this model and by Mock's model	55
16		58
19		61
22		64
25		67
28		70
31		73
34		76
35	Comparison of the theory with experimental data obtained from a p-channel MOSFET device whose parameters were characterized by means of test sites on its chip. The curve shows I_D versus V_{DS} , with $V_{GS} = 10$ volts	79
36	Comparison of the theory with experimental data obtained from a p-channel MOSFET device whose parameters were characterized by means of test sites on its chip. The curve shows I_D versus V_{GS} , with $V_{DS} = V_{GS}$.	80

TABLES

	<u>Page</u>
I Definition of Dimensionless Variables	12
II Comparison of Drain Current Calculations	77
III Sample Input Data Set	81
IV Recommended Control Parameters	85
V Sample Listing of Output Data	89
VI Symbols Appearing in the Flowcharts	111

CHAPTER I

A Two-Dimensional Model for MOSFET Operation

1.0 Introduction

This report is an addendum to the Final Research and Development Technical Report under this contract on Computer Aided Engineering of Semiconductor Integrated Circuits, dated August 31, 1977. The present report presents further details concerning a two-dimensional mathematical model for an MOSFET, and is intended to serve as a USER's MANUAL for the computer program which has been developed to implement that model.

The model described herein is patterned from the earlier work of M.S. Mock who developed a two-dimensional MOSFET model for IBM [1-3]. This useful analytic tool, which has produced results in good agreement with experiment [4], was provided to us by IBM with the understanding that it would be regarded as their proprietary property. That computer program was utilized extensively in the development of a one-dimensional MOSFET model described in detail in Chapter I of the Final Report named above.

In order to make such a two-dimensional analytic tool available to government laboratories, and to the semiconductor industry, the development of the model reported herein was undertaken with the intention of disseminating the resultant computer program to those desiring it, accompanied by this USER's MANUAL.

-
- [1] M.S. Mock, Solid State Electronics, 16, 601 (1973).
 - [2] D.P. Kennedy, Mathematical Simulation of the Effects of Ionizing Radiation on Semiconductors, Scientific Report No. 1, AFCRL-71-0272 (1971).
 - [3] D.P. Kennedy, Mathematical Simulation of the Effects of Ionizing Radiation on Semiconductors, Final Report, AFCRL-72-0257 (1972).
 - [4] D.P. Kennedy, Private Communication.

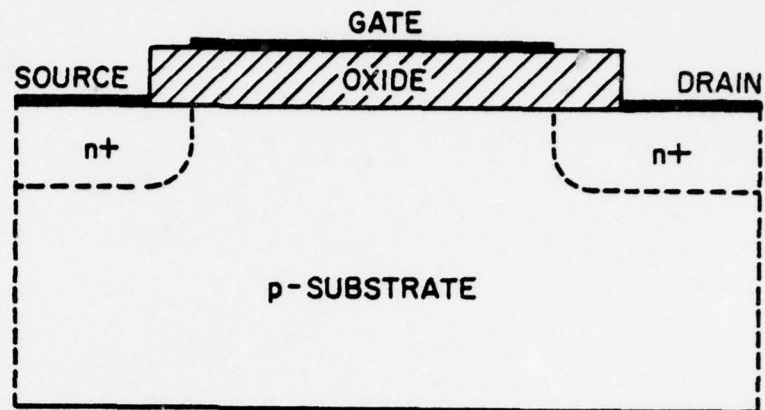
It should be emphasized that the proprietary nature of the IBM program has been scrupulously observed during this development. Some of the algorithms implemented in our model are due to Mock, but only those which he has described in the literature [1-3]. No attempt has been made to copy the IBM program. We have, of course, made liberal use of that program as a means of providing numerical checks of the performance of our model. The availability of that program for this purpose is gratefully acknowledged.

2.0 Description of the Model

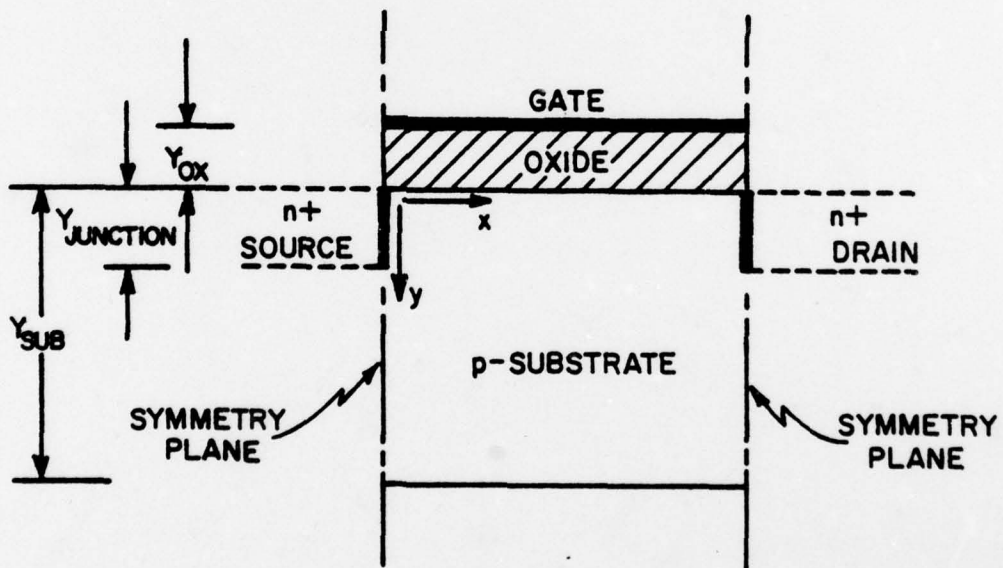
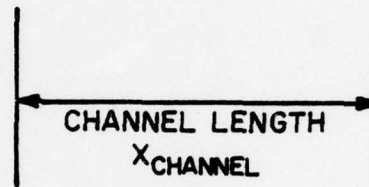
The computer model treats an n-channel enhancement mode MOSFET in which the conducting channel is formed by a gate-induced inversion layer just below the interface between a uniformly doped p-type substrate and the SiO_2 layer (hereinafter named the oxide) upon which the gate metallization is deposited. The inherent thinness of the inversion layer justifies the assumptions made that the net electron-hole recombination rate and the hole current are negligible in the steady state operation of this device. Details are given in the following subsections.

2.01 Basic Geometry

Figure 1(a) depicts such an n-channel device in which the source and drain consist of n^+ islands diffused into the p-substrate. The thinness of the gate-induced inversion layer of mobile electrons formed just below the oxide-silicon interface makes possible the adoption of the simplified rectangular geometry of Figure 1(b), wherein the vertical metallurgical p-n junctions (assumed to be abrupt transitions between p and n^+ regions) are located at the left and right borders of the rectangular region treated. Large gradients in electric potential and, consequently, in the electron and hole densities are expected in the immediate vicinity of those junctions, requiring a rather dense array of the geometric points at which those variables are calculated with the finite-difference equa-



(a)



(b)

Figure 1

(a) Cross-section of an n-channel MOSFET.

(b) Rectangular region modeled. The abrupt metallurgical junctions between source-substrate and drain-substrate are regarded as planar and at the left and right borders of the region modeled.

tions employed. The same is true in the region just below the oxide-silicon interface where the inversion layer forms. On the other hand, the density of such points in regions remote from those surfaces can be relatively sparse. By placing the source and drain junctions at the borders of the rectangular region treated, such a graded lattice of points is readily defined. Figure 2 illustrates the graded lattice employed by the model with a 41 (horizontal) by 25 (vertical) array overlayed on the rectangle. The prescription adopted for generating this graded lattice is precisely that suggested by Mock [1].

2.02 Dimensionless Variables

For computational purposes, the adoption of dimensionless (normalized) variables at the outset results in two benefits: (1) unnecessary multiplications by redundant constants such as ϵ_0 , q , kT/q , n_i , etc. can be precluded, and (2) numerical scaling causing most variables to lie within reasonable numerical ranges can be achieved.

Understanding that such dimensionless variables will be utilized in all of which follows (with few exceptions which will be clearly flagged), we shall designate physical variables (i.e., those which possess dimensions) in this subsection by means of primed symbols, using corresponding unprimed symbols for their dimensionless counterparts. This convention provides the advantage of utilizing conventional symbols such as \bar{J} for current density, n and p for electron and hole densities, ψ for electric potential, etc., even though those variables are normalized. In this vein, the dimensionless variables employed in our model are defined in Table I.

2.03 Basic Equations

Having adopted the assumptions of negligible hole current and electron-hole recombination, the dimensionless equations describing the physical mechanisms within this semiconductor device are:

GRADED LATTICE

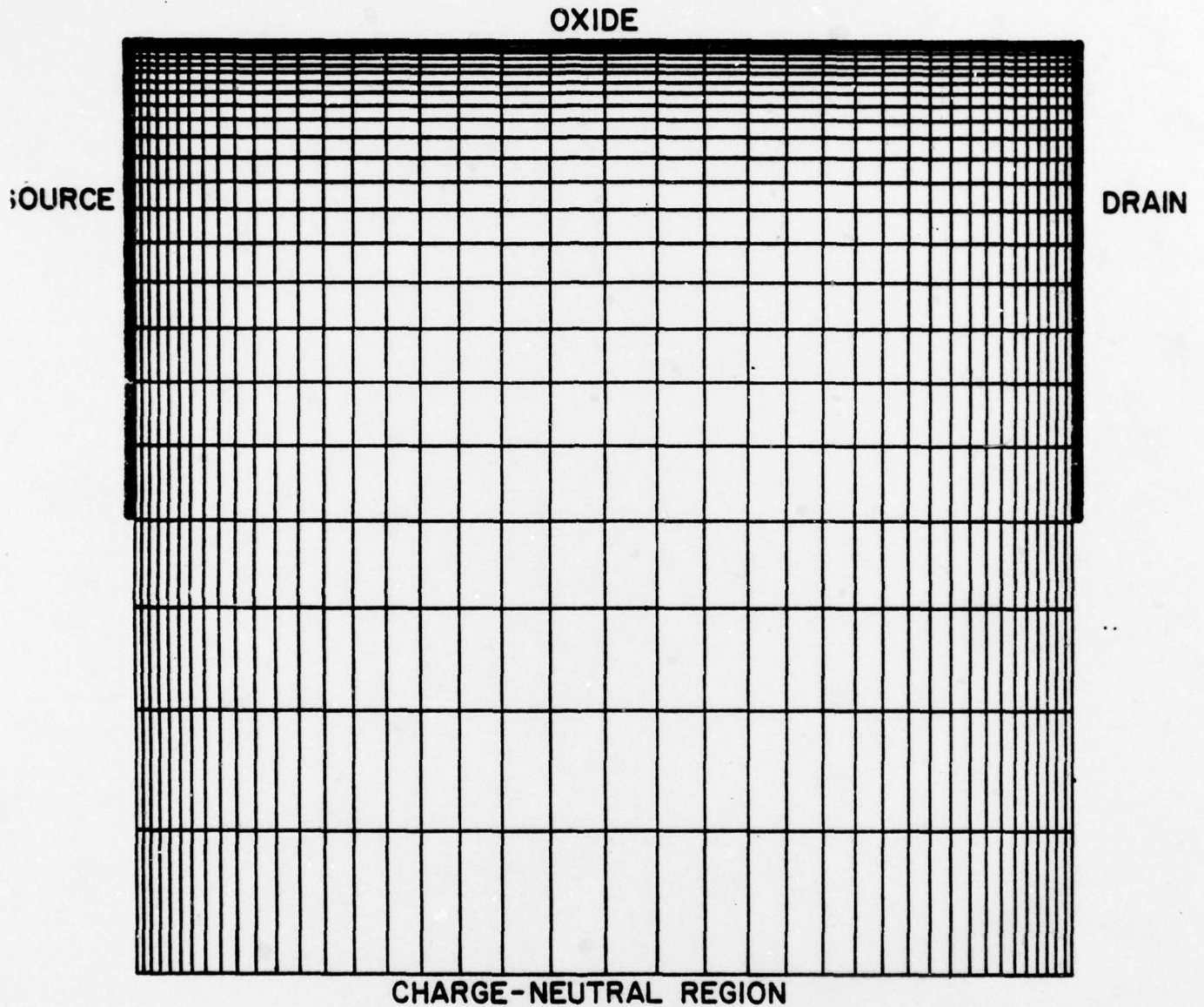


Figure 2 Graded lattice of points used in the finite-difference equations dealt with in the computer model.

TABLE I--DEFINITION OF DIMENSIONLESS VARIABLES
(κ_s is the relative permittivity of silicon)

Define:

$$L_D' = \sqrt{\frac{\kappa_s \epsilon_0' (k'T'/q')}{q' n_i'}} , \quad \text{Intrinsic Debye length of silicon}$$

$$\mu_n' , \quad \text{Low field electron mobility}$$

Then Let:

$$\left. \begin{aligned} \psi' &= (k'T'/q') \psi \\ \phi_n' &= (k'T'/q') \phi_n \\ \phi_p' &= (k'T'/q') \phi_p \end{aligned} \right\} , \quad \text{Electric potential, and electron and hole quasi-Fermi potentials}$$

$$\left. \begin{aligned} N_D' &= n_i' N_D \\ N_A' &= n_i' N_A \\ n' &= n_i' n \\ p' &= n_i' p \end{aligned} \right\} , \quad \text{Donor, acceptor, electron, and hole number densities}$$

$$\left. \begin{aligned} x' &= L_D' x \\ y' &= L_D' y \end{aligned} \right\} , \quad \text{Cartesian coordinates}$$

$$\bar{J}' = \left[\frac{(k'T'/q') \mu_n' n_i' q'}{L_D'} \right] \bar{J} , \quad \text{Electron current density}$$

$$Q_{ss}' = \left[\frac{(k'T'/q') \kappa_s \epsilon_0'}{L_D'} \right] Q_{ss} , \quad \text{Surface charge density}$$

$$\mu' = \mu_n' \mu , \quad \text{Electron mobility}$$

$$\nabla^2 \psi = N_A + n - p , \quad (1)$$

$$n = \exp(\psi - \phi_n) , \quad (2)$$

$$p = \exp(\phi_p - \psi) , \quad (3)$$

$$\bar{J} = -\mu n \nabla \phi_n , \quad (4)$$

$$0 = \nabla \phi_p , \quad (5)$$

$$\nabla \cdot \bar{J} = 0 . \quad (6)$$

Equation (1) is Poisson's equation for the electric potential ψ , eqs. (2) and (3) express the use of Boltzmann statistics for the electron and hole number densities n and p (i.e., nondegenerate doping of the p-substrate is implied), eq. (4) relates the electron current density vector \bar{J} to the electron quasi-Fermi potential ϕ_n and number density n in the usual manner [5], eq. (5) enforces zero hole current density, while eq. (6) assures conservation of charge under the assumed condition of zero net recombination of electron-hole pairs.

The above equations apply only in the rectangular p-substrate region. The conditions in the oxide are described by:

$$\nabla^2 \psi = 0 , \quad (7)$$

and $n = p = \bar{J} \equiv 0$, with appropriate boundary conditions to match the tangential and normal electric field at the oxide-silicon interface.

The divergence-free flow of electron current expressed by (6) can be enforced by introducing a stream function $\theta(x,y)$, as did Mock, such that the x and y components of \bar{J} are given by:

$$J_x = J_0 \frac{\partial \theta}{\partial y} , \quad (8)$$

$$J_y = -J_0 \frac{\partial \theta}{\partial x} , \quad (9)$$

[5] S.M. Sze, *Physics of Semiconductor Devices*, p. 96, Wiley, N.Y. (1969).

thereby assuring that $\nabla \cdot \bar{J} = 0$. Here, J_0 is a scalar constant whose determination will be discussed later. We next seek the differential equation which must be satisfied by this stream function.

Solving (2) for the electron quasi-Fermi potential ϕ_n , and substituting the result into (4), we obtain:

$$\bar{J} = \mu e^\psi \nabla (n e^{-\psi}) . \quad (10)$$

Identifying the x and y components of (10) with the corresponding expressions of (8) and (9), we have:

$$J_0 \frac{\partial \theta}{\partial y} = \mu e^\psi \frac{\partial}{\partial x} (n e^{-\psi}) , \quad (11)$$

$$J_0 \frac{\partial \theta}{\partial x} = -\mu e^\psi \frac{\partial}{\partial y} (n e^{-\psi}) . \quad (12)$$

Divide both sides of these intermediate equations by μe^ψ , then differentiate the first partially with respect to y, the second partially with respect to x, and add the two, obtaining:

$$\frac{\partial}{\partial x} \left[\mu^{-1} e^{-\psi} \frac{\partial \theta}{\partial x} \right] + \frac{\partial}{\partial y} \left[\mu^{-1} e^{-\psi} \frac{\partial \theta}{\partial y} \right] = 0 . \quad (13)$$

Eq. (13) is a second order differential equation in θ , given $\mu(x,y)$ and $\psi(x,y)$. Given its solution, the electron current density vector \bar{J} is then known, from (8) and (9).

The manner in which the current density scale factor J_0 is determined is best deferred until after a discussion of the boundary conditions which must be satisfied by the solutions of these basic equations.

2.04 Boundary Conditions

We regard the left and right borders of the rectangular region dealt with by the model as symmetry planes such that ψ , θ , n , p , and J_y are even functions of x , while J_x is an odd function. Image theory then requires that these functions all be periodic in x , the periodicity being twice the channel

length X_{channel} of Figure 1(b). A consequence of this implied periodicity is that the source and drain islands shown dotted in Figure 1(a) are "squeezed out of the picture," being replaced by infinitesimally thin source and drain "contacts" which serve as sources or sinks for current and electric flux lines. The assignment of boundary conditions on ψ and n to these "contacts" bears careful scrutiny.

2.04.1 Boundary Conditions on ψ and n --We select the charge-neutral source island as the zero reference for electric potential, $\psi = 0$ (even though that region has been "squeezed out of the picture" in the model), and assume that the contact potentials of all metal-semiconductor and metal-oxide contacts are identical and, therefore, can be ignored.* The p-substrate, in the absence of any external bias voltages, assumes the normalized "built-in" potential:

$$\psi_{EQ} = -\ln(N_D N_A) , \quad (14)$$

which is also assumed by the gate. If the substrate and gate are then biased positively** with respect to the source at potentials V_{SUB} and V_G , respectively, the boundary conditions stipulated along the two horizontal borders in Figure 3(a) are obtained.

Consider next the source and drain "contacts" which, as stated above, are assumed to coincide with the metallurgical junction planes. Letting U be the normalized potential with zero reference redefined (for the present discussion) to be that of the charge-neutral p-region, Kennedy [6] shows rigorously that the potential U_j resulting in the plane of the metallurgical junction defining an abrupt p-n junction is:

*Differences in contact potential of the gate and substrate contacts and of the oxide-silicon interface can be modeled by assigning appropriate numerical values to the surface charge term Q_{SS} , for which our model does account.

**Later in this development, we tacitly assume that V_{SUB} will always be a negative numeric.

[6] D.P. Kennedy, IEEE Trans. Electron Devices, ED-22, 988 (1975).

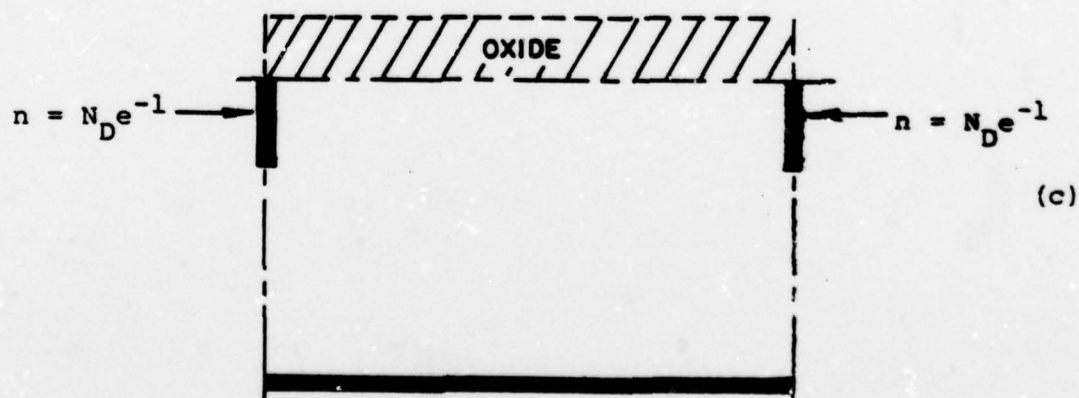
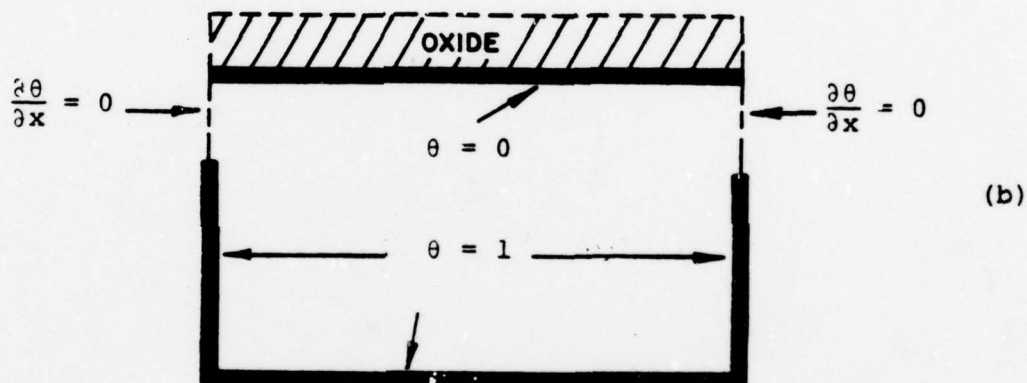
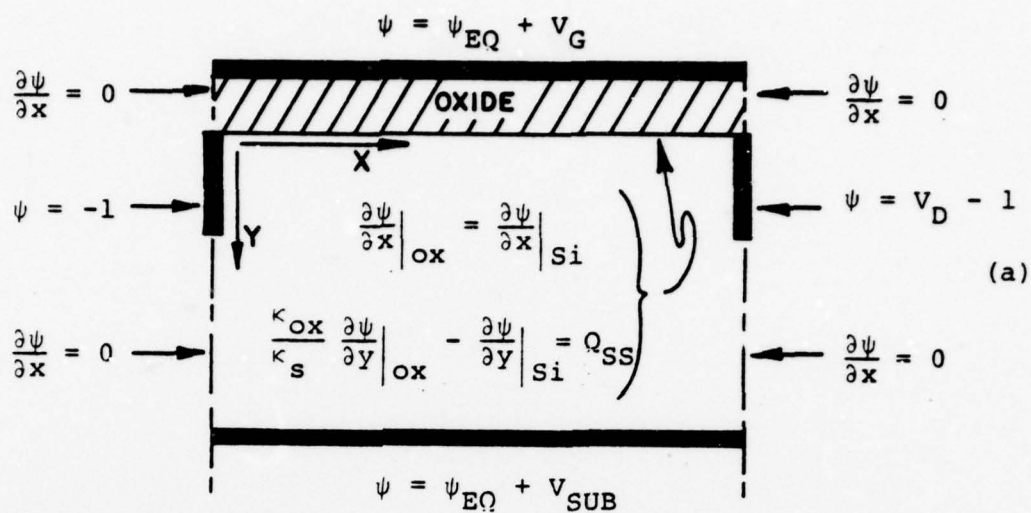


Figure 3 Boundary conditions for: (a) $\psi(x, y)$, (b) $\theta(x, y)$, and (c) $n(x, y)$.

$$U_J = U_T \left[\frac{N_D}{N_A + N_D} \right] + \left[\frac{N_A - N_D}{N_A + N_D} \right] \left[1 - \exp(-U_T) \right], \quad (15)$$

where U_T is the total potential appearing across the p-n junction:

$$U_T = \ln(N_D N_A) + U_{\text{applied}}. \quad (16)$$

(Note that positive U_{applied} in (16) results in a reverse-biased junction, consistent with Kennedy's convention.)

Consider some typical numerical values in (15) and (16). With $n'_i = 1.5 \times 10^{10} \text{ cm}^{-3}$, $N'_D = 10^{19} \text{ cm}^{-3}$, $N'_A = 10^{16} \text{ cm}^{-3}$ (the primes flag unnormalized constants), $\ln(N_D N_A)$ assumes the numerical value 33.7, and the exponential term in (15) is entirely negligible except for negative values of U_{applied} (i.e., forward bias) approaching that numerical magnitude. Furthermore, since $N_D \gg N_A$, (15) simplifies tremendously, becoming:

$$U_J \approx U_T - 1. \quad (17)$$

Since the drain junction is always operated reverse-biased, with $V_D > 0$, (17) is valid at the drain "contact."

Consider the source "contact," which does become forward-biased due to band bending near the oxide-silicon interface as the applied gate potential V_G is made positive with respect to the source. At the onset of strong inversion, the total normalized potential drop across the n^+p source junction right at the oxide-silicon interface will be reduced to $U_T = \ln(N_D/N_A)$, which assumes the value $U_T = 6.9$, using the same numerical values for N'_D and N'_A assumed above. Again, the exponential term in (15) is negligible. We conclude that (17) is still a valid approximation for the source contact, at least for N_D/N_A ratios of 10^3 or higher. The approximation begins to become questionable only when $N_D/N_A < 10^2$, but at the source "contact" only.

Reverting to our convention of selecting the charge-neutral source island for zero reference potential, we conclude from (17) that the appropriate boundary conditions on ψ at the source and drain "contacts" are $\psi = -1$, and $\psi = V_D - 1$, respectively, as shown in Figure 3(a).

The remaining boundary conditions on ψ shown in that figure assure the symmetry assumed at the left and right borders of the region, and assure proper matching of the solutions of (1) and (7) at the oxide-silicon interface. Note that the condition imposed upon the normal derivatives of ψ at that interface allows for the inclusion of surface charge Q_{ss} , a feature not included by Mock. (The condition stated in the figure for the normal derivatives assumes an unfamiliar form because of the normalized variables employed.)

The numerical method later to be described for determining the electron number density $n(x,y)$ requires that n be specified along the borders of the rectangular region only at the source and drain "contacts." The fact that those "contacts" have potentials one normalized unit lower than those of the corresponding charge-neutral source and drain islands (where $n = N_D$) leads to the boundary conditions on n depicted in Figure 3(c).

2.04.2 Boundary Conditions on θ --Referring to (8) and (9), we note that θ is defined only in terms of its spatial derivatives. This means that its magnitude can be arbitrarily bounded. A convenient choice for those bounds is $0 \leq \theta \leq 1$, with θ specified to be zero along the oxide-silicon interface as in Figure 3(b). Tacitly assuming that the substrate (back-gate) will always be biased negatively with respect to the source ($V_{SUB} \leq 0$), so that no back-gate current flows, the appropriate boundary conditions on θ along the remaining borders in the figure are those shown. The stipulation $\frac{\partial \theta}{\partial x} = 0$ along the source and drain "contacts" assures zero tangential current at those "contacts," and is consistent with the implied symmetry conditions discussed earlier.

Bounding θ between zero and unity has two useful consequences, both stemming from eq. (8): 1) the numerical value of θ at any point (x,y) is the decimal fraction of the total drain current which crosses the plane x through the layer bounded by the oxide-silicon interface and the plane y and, 2) the constant J_0 appearing in (8) and (9) represents, physically, the total drain current per unit width of the inversion channel.

2.05 Determination of the Drain Current Factor J_0 :

The drain current per unit width of channel, J_0 , is obtained as follows. Eq. (11) gives:

$$\frac{\partial}{\partial x} (ne^{-\psi}) = \mu^{-1} e^{-\psi} J_0 \frac{\partial \theta}{\partial y} . \quad (18)$$

Integrating with respect to x along a horizontal line ($y = \text{constant}$) which intersects the source and drain "contacts," one obtains:

$$N_D [e^{-V_D} - 1] = J_0 \int_0^{x_{\text{channel}}} \mu^{-1} e^{-\psi} \frac{\partial \theta}{\partial y} dx . \quad (19)$$

Solving for J_0 :

$$J_0 = \frac{-N_D [1 - e^{-V_D}]}{\int_0^{x_{\text{channel}}} \mu^{-1} e^{-\psi} \frac{\partial \theta}{\partial y} dx} . \quad (20)$$

This is the same result used by Mock for calculating J_0 , except for the factor N_D appearing in (20), which is absent in Mock's result ([1], eq. (10)). The reason for this difference is seated in the fact that Mock chose to set the electron quasi-Fermi Potential ϕ_n equal to zero in the charge-neutral source region, which makes $\psi = \ln(N_D)$ in that region, whereas we have chosen to set $\psi = 0$ there. Note that the sign

of J_0 changes if one were to perform the integration from $x = 0$ to the "image" drain contact at $x = -x_{\text{channel}}$. Thus, J_0 is an odd function of x , as it must be in order to satisfy the symmetry conditions on J_x and J_y described in Section 2.04.

3.0 Finite-Difference Algorithms

Figure 4 defines the indices (I,J) , and their bounds, used to identify each lattice point involved in implementing finite-difference algorithms for determining ψ , θ , and n . (The figure does not attempt to convey the graded nature of the lattice actually used.) As shown, two "interlaced" lattices are employed. The first, depicted by circles, represents the set of points at which the electrostatic potential ψ and the corresponding electron and hole densities n and p are numerically determined while the second, depicted by squares, represents the set of points at which the stream function θ is evaluated. This choice, although complicating the satisfaction of the boundary conditions on θ , allows the use of simple differencing between adjacent lattice points in evaluating $\partial\theta/\partial x$ and $\partial\theta/\partial y$.^{*} Mock also employed such an interlaced pair of lattices.

Note that the oxide-silicon interface coincides with the upper border, $J = J_{\text{MAX}}$, of the θ lattice. Although not shown in Figure 4, the ψ lattice extends vertically an additional four rows (uniformly spaced) beyond the row $J = J_{\text{MAX}} + 1$ shown, to model the electrostatic potential

^{*}In an earlier version of the model, the author chose to deal with a single lattice of points, rather than the interlaced lattices presently employed. In the development of the computer code for that choice, it was soon discovered that the nonuniform point spacings of the lattice precluded the use of simple differencing for evaluating derivatives. It was found necessary to fit parabolas through sets of three adjacent points in a row or column in order to evaluate the partial derivatives needed. While this was easily accomplished with a single subroutine for that purpose, nonetheless each such operation required 7 multiplications and 7 additions each time the subroutine was called. This imposed an unacceptable cost in computation time, and the approach was abandoned.

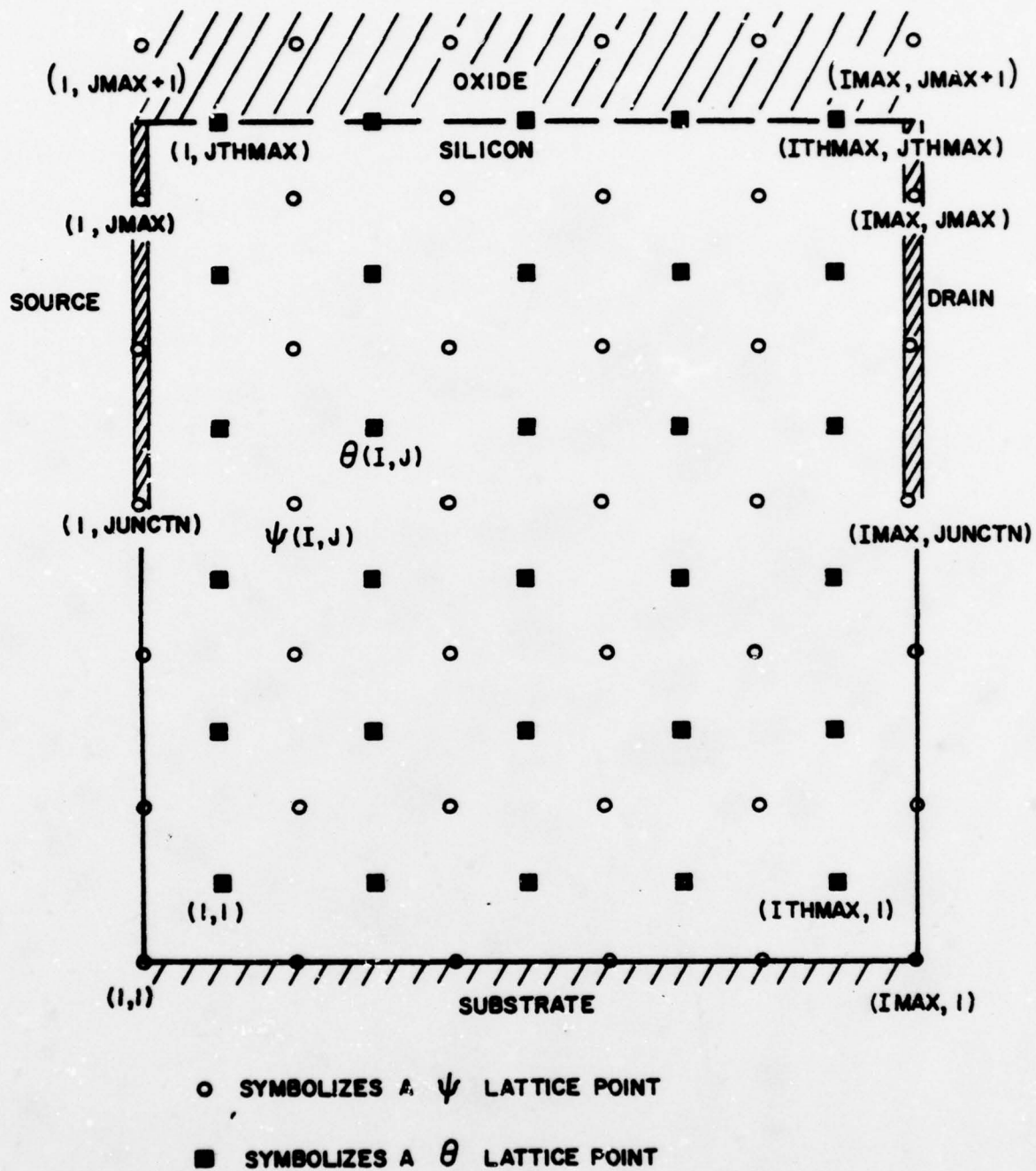


Figure 4 Layout of the interlaced ψ and θ lattices used in the finite-difference equations.

within the oxide region. Note, also, the convention adopted for the indices of the ψ lattice with respect to those of the θ lattice. (Given the ordered pair (I,J) , the point of the θ lattice so identified is "northeast" of the corresponding point of the ψ lattice.)

3.01 Finite-Difference Algorithms for ψ

Consider the five point "star" of points in the ψ lattice shown in Figure 5. The dotted rectangle shown in that figure, having dimensions $\tilde{\Delta}x(I)$ by $\tilde{\Delta}y(J)$, is bounded at its four corners by the corresponding θ lattice points "NE, NW, SE and SW" of the central point P. (We shall adopt "points of the compass" notation, using subscripts in the difference equations to follow, to avoid repeated use of the index pairs (I,J) , $(I+1,J)$, etc., which are used in their FORTRAN counterparts in the computer program.) The lengths $\tilde{\Delta}x(I)$, $\tilde{\Delta}y(J)$, abbreviated $\tilde{\Delta}x_P$ and $\tilde{\Delta}y_P$ in the difference equations, are defined to be:

$$\left. \begin{aligned} \tilde{\Delta}x_P &= (\tilde{\Delta}x_E + \Delta x_W)/2 , \\ \tilde{\Delta}y_P &= (\Delta y_N + \Delta y_S)/2 . \end{aligned} \right\} \quad (21)$$

This locates the θ lattice points always midway between their neighboring ψ lattice points.

Applying Gauss's law to the rectangular region surrounding the point (I,J) in Figure 5, one obtains:

$$B_P \psi_S + D_P \psi_W + E_P \psi_P + F_P \psi_E + H_P \psi_N = Q_P , \quad (22)$$

where:

$$\left. \begin{aligned} B_P &= \tilde{\Delta}x_P / \Delta y_S , \\ D_P &= \tilde{\Delta}y_P / \Delta x_W , \\ E_P &= -(B_P + D_P + F_P + H_P) , \\ F_P &= \tilde{\Delta}y_P / \Delta x_E , \\ H_P &= \tilde{\Delta}x_P / \Delta y_N , \\ Q_P &= \iint_{\text{BOX}} (N_A + n - p) dx dy . \end{aligned} \right\} \quad (23)$$

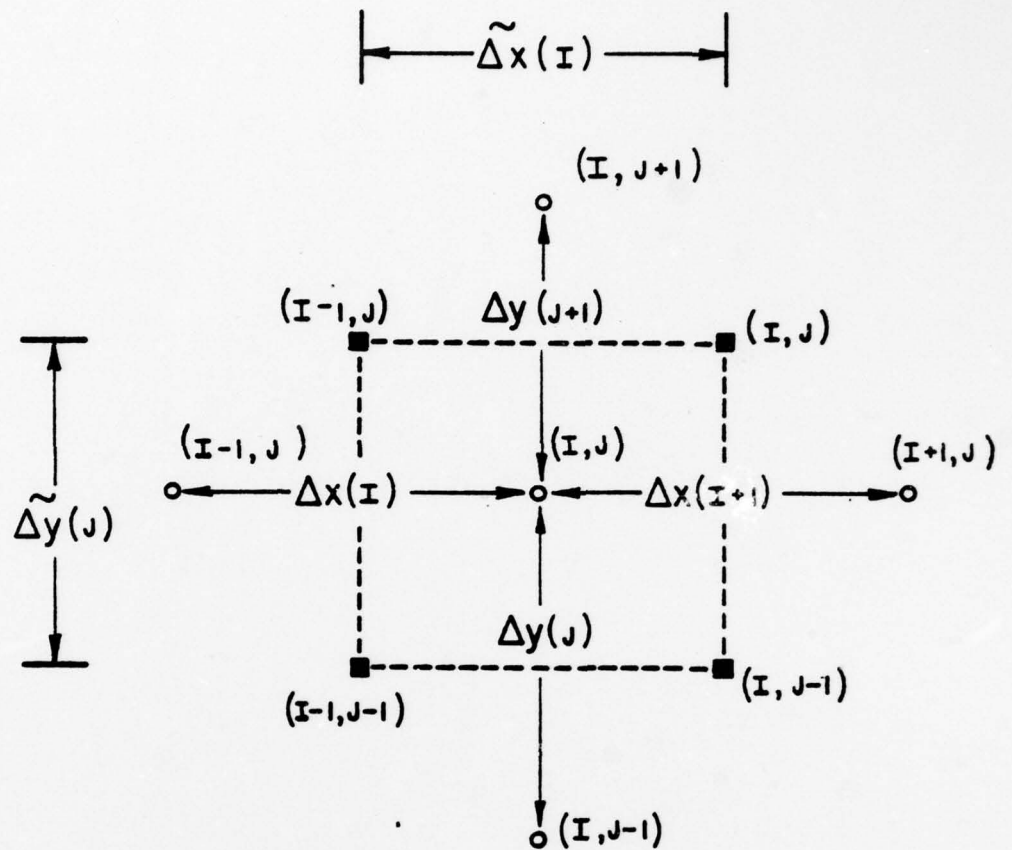


Figure 5 Five-point "star" of ψ -lattice points used in the finite-difference equation for ψ .

With a ψ lattice whose dimensions are I_{MAX} by $(JMAX+5)$, the set of equations represented by (22) can be expressed in the matrix form:

$$[L] \cdot [\psi] = [Q] , \quad (24)$$

where $[\psi]$ and $[Q]$ are rectangular matrices having the same dimensions as those of the ψ lattice, while $[L]$ is a square matrix of dimensions $(IMAX) \cdot (JMAX+5)$ by $(IMAX) \cdot (JMAX+5)$. This matrix is sparse, having only five nonzero symmetrically positioned diagonal elements. Stone's iterative matrix factorization method [7] is employed in our model to solve (24) for the array ψ , given the array Q .

3.01.1 Implementation of the Boundary Conditions on ψ

The boundary conditions on ψ depicted in Figure 3(a) are enforced by appropriate modifications of the factors B_p , D_p , E_p , F_p , H_p , and Q_p in (22) at those ψ lattice points coinciding with the borders of the rectangular region modeled. These are next discussed.

3.01.1(a) Border Segments where ψ Is Specified--For ψ lattice points at which ψ is fixed, the coefficients B_p , D_p , F_p , and H_p are set to zero, while E_p is set to unity. Then the term Q_p in (22) is set equal to the known value of ψ at the point in question. In accordance with (22), this forces ψ_p to assume that known value at such border points.

3.01.1(b) Border Segments along Symmetry Planes--The boundary condition $\partial\psi/\partial x = 0$ is enforced at the symmetry planes in the following manner. At the left border, the coefficient D_p in (22) is set to zero, while F_p is doubled. The converse is applied at the right border. This assures the required symmetry of ψ at those border segments.

3.01.1(c) The Oxide-Silicon Interface--Since the ψ lattice has no points coinciding with the interface, the enforcement

[7] H.L. Stone, SIAM Jour. Numer. Anal., 5, 530 (1968).

of the proper boundary conditions on ψ there is somewhat more involved. We develop special forms of the finite-difference equation for ψ , which apply for the two rows of the ψ lattice, viz. $J = J_{\text{MAX}}$ and $J = (J_{\text{MAX}}+1)$, which bracket that interface. Figure 6 shows one set of points in those rows of the ψ lattice, and defines spacings $\Delta\eta_{\text{ox}}$ and $\Delta\eta_{\text{si}}$ which locate the interface. Through an appropriate choice of the ratio $(\Delta\eta_{\text{ox}}/\Delta\eta_{\text{si}})$, we develop an expression for the potential ψ_{surf} at the interface, in terms of the known potentials ψ_{ox} and ψ_{si} of the ψ lattice points north and south of it, such that the required discontinuity in $\partial\psi/\partial y$ is automatically satisfied. Then, an application of Gauss's law to the two rectangular regions shown crosshatched in the figure leads to the required special forms of the finite-difference equation in ψ for the two rows in question.

The boundary condition on $\partial\psi/\partial y$ at the interface is:

$$\left(\frac{\partial\psi}{\partial y}\right)_{\text{si}} = \left(\frac{\kappa_{\text{ox}}}{\kappa_{\text{si}}}\right) \left(\frac{\partial\psi}{\partial y}\right)_{\text{ox}} - Q_{\text{ss}} , \quad (25)$$

which comes from applying Gauss's law to an infinitesimally thin gaussian "pillbox" bracketing the interface, with the result expressed in terms of the normalized variables employed in our model. Here, κ_{ox} and κ_{si} are the relative permittivity of the oxide and silicon regions, respectively, while Q_{ss} is the surface charge density (if any) residing at the interface. In addition to this condition, we have:

$$\psi_{\text{si}} = \psi_{\text{ox}} + \left(\frac{\partial\psi}{\partial y}\right)_{\text{ox}} \Delta\eta_{\text{ox}} + \left(\frac{\partial\psi}{\partial y}\right)_{\text{si}} \Delta\eta_{\text{si}} , \quad (26)$$

$$\left(\frac{\partial\psi}{\partial y}\right)_{\text{ox}} = \left[\frac{\psi_{\text{surf}} - \psi_{\text{ox}}}{\Delta\eta_{\text{ox}}} \right] , \quad (27)$$

$$\left(\frac{\partial\psi}{\partial y}\right)_{\text{si}} = \left[\frac{\psi_{\text{si}} - \psi_{\text{surf}}}{\Delta\eta_{\text{si}}} \right] , \quad (28)$$

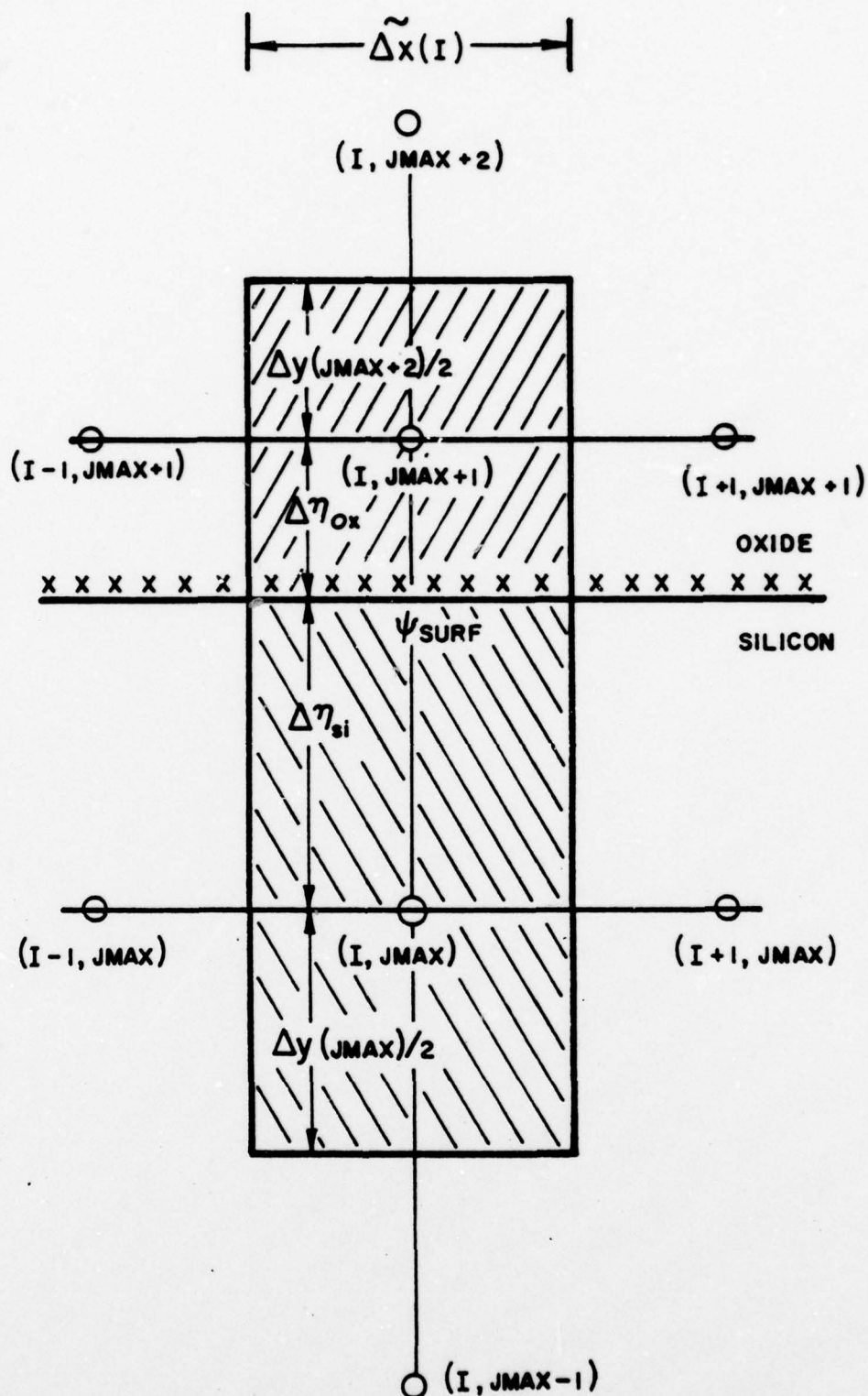


Figure 6 Boundary conditions on ψ at the oxide-silicon interface are enforced through an appropriate choice for the location of the interface, leading to special finite-difference equations applicable for the two ψ -lattice rows bracketing the interface.

with positive y defined to be vertically downward from the interface. These four equations relate five unknowns-- $\Delta\eta_{ox}$, $\Delta\eta_{si}$, ψ_{surf} , $(\partial\psi/\partial y)_{ox}$, $(\partial\psi/\partial y)_{si}$ --which means that the ratio $(\Delta\eta_{ox}/\Delta\eta_{si})$ can be specified at our convenience.

To find ψ_{surf} (and discover a convenient choice for $\Delta\eta_{ox}/\Delta\eta_{si}$), substitute (25) for $(\partial\psi/\partial y)_{si}$ and (27) for $(\partial\psi/\partial y)_{ox}$ into (26), obtaining:

$$\psi_{surf} = \left\{ \frac{\psi_{si} + \left(\frac{\kappa_{ox}}{\kappa_{si}} \right) \left(\frac{\Delta\eta_{si}}{\Delta\eta_{ox}} \right) \psi_{ox} + Q_{SS} \Delta\eta_{si}}{1 + \left(\frac{\kappa_{ox}}{\kappa_{si}} \right) \left(\frac{\Delta\eta_{si}}{\Delta\eta_{ox}} \right)} \right\}. \quad (29)$$

Choosing:

$$\Delta\eta_{ox} = \left(\frac{\kappa_{ox}}{\kappa_{si}} \right) \Delta\eta_{si}, \quad (30)$$

we obtain the simple relationship:

$$\psi_{surf} = \left[\frac{\psi_{ox} + \psi_{si}}{2} \right] + Q_{SS} \frac{\Delta\eta_{si}}{2}. \quad (31)$$

Furthermore, since $(\Delta\eta_{ox} + \Delta\eta_{si}) = \Delta y(JMAX+1)$, we find:

$$\Delta\eta_{si} = \Delta y(JMAX+1) / [1 + (\kappa_{ox}/\kappa_{si})], \quad (32)$$

$$\Delta\eta_{ox} = \Delta y(JMAX+1) \left[\frac{(\kappa_{ox}/\kappa_{si})}{1 + (\kappa_{ox}/\kappa_{si})} \right]. \quad (33)$$

The result of the above procedure is that the potential at the interface, ψ_{surf} , is now known in terms of the potential at its north and south ψ lattice neighbors, with the simple relationship expressed by (31) resulting from locating the interface as prescribed by (32) and (33). These three equations assure that the boundary condition on $(\partial\psi/\partial y)$ at the interface is automatically satisfied, as is the boundary condition on $(\frac{\partial\psi}{\partial x})$.

Now apply Gauss's law to the rectangular region shown in Figure 6 which encompasses the ψ lattice point (I,JMAX) just below the interface. Again, adopting "points of the compass" notation, the electrostatic flux entering the upper surface of that rectangle is $-\tilde{\Delta}x_p(\psi_p - \psi_{\text{surf}})/\Delta\eta_{\text{si}}$. Using (31) to relate ψ_{surf} to ψ_N and ψ_p , the resulting finite-difference equation still assumes the form given by (22). However, the terms H_p and Q_p appearing in (23) (and only those) are now modified becoming:

$$\left. \begin{aligned} H_p &= \tilde{\Delta}x_p/2\Delta\eta_{\text{si}} , \\ Q_p &= \iint_{\text{BOX}} (N_A + n - p) dx dy - Q_{\text{SS}} \tilde{\Delta}x_p/2 , \end{aligned} \right\} \quad (34)$$

which apply for any ψ lattice point in the row $J = \text{JMAX}$.

An identical procedure, applied to the rectangular region encompassing the point (I,JMAX+1) in Figure 6 shows the terms B_p and Q_p to be:

$$\left. \begin{aligned} B_p &= \tilde{\Delta}x_p/2\Delta\eta_{\text{ox}} , \\ Q_p &= -\left(\frac{\kappa_{\text{si}}}{\kappa_{\text{ox}}}\right) Q_{\text{SS}} \tilde{\Delta}x_p/2 , \end{aligned} \right\} \quad (35)$$

which apply for any ψ lattice point in the row $J = \text{JMAX}+1$.

As a check of these results, it is satisfying to find that if there were no interface (i.e., if $\kappa_{\text{ox}} \equiv \kappa_{\text{si}}$, and $Q_{\text{SS}} \equiv 0$), then (32) and (33) result in $\Delta\eta_{\text{si}} = \Delta\eta_{\text{ox}} = \Delta y(\text{JMAX}+1)/2$, so that both (34) and (35) reduce to the corresponding expressions for B_p , H_p , and Q_p given in (23), which apply for all rows of the ψ lattice except the two which bracket the oxide-silicon interface.

Mock did not use the above procedure for dealing with the interface. Instead, he defined a transformation of coordinate variable $y \rightarrow z$ in the oxide region, chosen so that $(\partial\psi/\partial z)_{\text{ox}} = (\partial\psi/\partial y)_{\text{si}}$ at the interface, even though

$(\partial\psi/\partial y)$ is discontinuous there. (This is equivalent to defining a modified oxide thickness.) While this approach possesses the advantage of requiring no special forms of the finite-difference equations at the interface, it precludes the inclusion of surface charge Q_{ss} in the model. Since we wish to include such, we choose not to follow Mock's approach, and implement the above described procedure instead.

3.01.2 Numerical Algorithm for the Charge Term Q_p

The charge term Q_p in (23) represents the net bulk charge enclosed by the rectangular region surrounding each ψ -lattice point, the corners of that region coinciding with the points of the θ -lattice NE, NW, SE, and SW of the point P. A simple approximation for Q_p is obtained from (23) to be:

$$Q_p \approx (N_A + n - p) \tilde{\Delta}x_p \tilde{\Delta}y_p , \quad (36)$$

which assumes that n and p can be regarded as constant throughout the rectangular region.

While more elaborate approximations for Q_p are possible (e.g., a two-dimensional implementation of Simpson's rule) they involve more complex programming logic to handle lattice points adjacent to the four borders of the lattice, and are more costly in terms of computation time. Such more sophisticated procedures were tried by the author, but were found to be unnecessary, and were subsequently abandoned.

3.02 Finite-Difference Algorithm for the Stream Function θ

The partial differential equation in θ , eq. (13), is repeated here for convenience of reference:

$$\frac{\partial}{\partial x} \left(\mu^{-1} e^{-\psi} \frac{\partial \theta}{\partial x} \right) + \frac{\partial}{\partial y} \left(\mu^{-1} e^{-\psi} \frac{\partial \theta}{\partial y} \right) = 0 . \quad (13)$$

Our present version of the computer model does not incorporate provisions for field-dependent electron mobility. Therefore, μ^{-1} can be factored from (13), and ignored. If the field dependence of μ is to be retained, as a refinement to be later incorporated, several subroutines in the computer program will require revision.

Figure 7 focuses upon a point (I,J) of the θ lattice, and its nearest neighbors. Simple differencing gives the partial derivatives of θ at the four points shown as crosses in the figure:

$$\left. \begin{aligned} \left(\frac{\partial \theta}{\partial x} \right)_E &= \left[\frac{\theta_E - \theta_P}{\Delta x_E} \right] , \\ \left(\frac{\partial \theta}{\partial x} \right)_W &= \left[\frac{\theta_P - \theta_W}{\Delta x_W} \right] , \\ \left(\frac{\partial \theta}{\partial y} \right)_N &= \left[\frac{\theta_P - \theta_N}{\Delta y_N} \right] , \\ \left(\frac{\partial \theta}{\partial y} \right)_S &= \left[\frac{\theta_S - \theta_P}{\Delta y_S} \right] . \end{aligned} \right\} \quad (37)$$

The numerical value of $e^{-\psi}$ at each of those four points is determined in the manner next to be described.

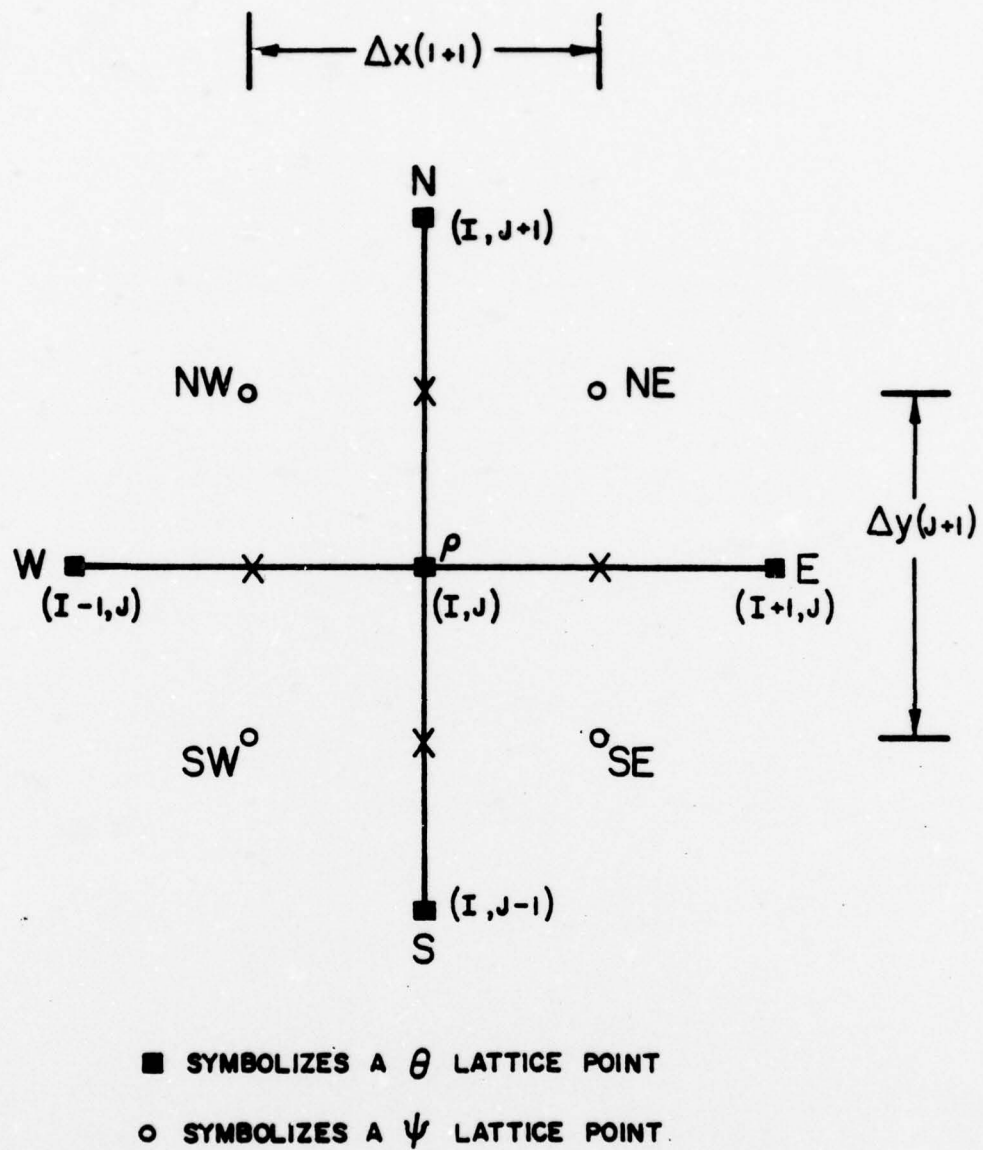


Figure 7

Five point "star" of θ -lattice points used in the finite-difference equation for θ .

Consider the four ψ lattice points located NE, SE, SW, and NW of the θ lattice point P. Assume a linear dependence of ψ along the borders of the rectangle defined by those four points, then evaluate an average value of $e^{-\psi}$ along each of those four borders, as did Mock [1], assigning the four averaged values to the respective points indicated by the crosses in the figure. (Mock describes this approach as a critical factor in achieving accuracy.) The result is:

$$\left. \begin{aligned} \langle e^{-\psi} \rangle_E &= \left[\frac{e^{-\psi_{NE}} - e^{-\psi_{SE}}}{\psi_{SE} - \psi_{NE}} \right] , \\ \langle e^{-\psi} \rangle_W &= \left[\frac{e^{-\psi_{NW}} - e^{-\psi_{SW}}}{\psi_{SW} - \psi_{NW}} \right] , \\ \langle e^{-\psi} \rangle_N &= \left[\frac{e^{-\psi_{NE}} - e^{-\psi_{NW}}}{\psi_{NW} - \psi_{NE}} \right] , \\ \langle e^{-\psi} \rangle_S &= \left[\frac{e^{-\psi_{SE}} - e^{-\psi_{SW}}}{\psi_{SW} - \psi_{SE}} \right] . \end{aligned} \right\} \quad (38)$$

With the $e^{-\psi}$ values thus determined at the four points midway between the N, E, S, and W points of the θ lattice, the finite-difference form of (13) becomes (assuming constant mobility μ):

$$\begin{aligned} &\Delta y_P \left[\langle e^{-\psi} \rangle_E \left(\frac{\theta_E - \theta_P}{\tilde{\Delta} x_E} \right) - \langle e^{-\psi} \rangle_W \left(\frac{\theta_P - \theta_W}{\tilde{\Delta} x_W} \right) \right] \\ &+ \Delta x_P \left[\langle e^{-\psi} \rangle_S \left(\frac{\theta_S - \theta_P}{\tilde{\Delta} y_S} \right) - \langle e^{-\psi} \rangle_N \left(\frac{\theta_P - \theta_N}{\tilde{\Delta} y_N} \right) \right] = 0 , \end{aligned} \quad (39)$$

where Δx_P and Δy_P have been introduced as shorthand notation for $\Delta x(I+1)$, $\Delta y(J+1)$ in Figure 7. (See Figure 5 for the geometric definitions of the $\tilde{\Delta} x$ and $\tilde{\Delta} y$ factors in the above equation.)

As was the case with the finite-difference equation for ψ discussed earlier, the set of equations (39) can be represented in matrix form. The resulting sparse matrix contains only five nonzero symmetrically positioned diagonal elements. The matrix equation is solved for θ , given ψ , using the block-line iterative procedure described by Varga [8].

The finite-difference equation for θ expressed by (39) is deceptively simple. Its implementation produces nontrivial challenges because of the exponential dependence upon ψ evident in (38). To illustrate, consider a modest drain voltage of 10 volts. In our normalized variables, this translates to a numerical value on the order of 400. But the IBM 370/165 used in this development produces overflow and underflow with the operation $e^{\pm|x|}$ when $|x|$ exceeds approximately 175. Not only is this limit obviously violated in regions near the drain, in the example cited, but along the entire channel as well when the gate voltage exceeds about 4.5 volts.

The modus operandi developed for dealing with this problem is the following. One never deals with positive x values in the operation e^x . One always alters the equation being treated so that only negative exponents are encountered. Furthermore, one endeavors always to reformulate that equation so that x represents differences in the potential between adjacent ψ lattice points, rather than the magnitude of ψ itself. Finally, one always tests the magnitude of the negative exponent before attempting the operation of exponentiation, avoiding "underflow" messages by use of the approximation $e^{-x} \approx 0$ when x is found sufficiently large.

[8] R.S. Varga, Matrix Iterative Analysis, p. 194, Prentice-Hall, New York (1962).

To implement these restrictions, the average $e^{-\psi}$ functions in (38) are first reexpressed by factoring the exponential term whose exponent is least negative. This leaves within the brackets an exponential term whose negative exponent represents differences in ψ between adjacent lattice points. Following this, the four terms in (38) are again factored by the exponential term outside of the brackets whose exponent is least negative. Since the right hand side of (39) is zero, the latter factor can be cancelled from the equation. Again, this results in exponential terms whose negative exponents represent differences in ψ between adjacent lattice points. The subprogram which implements this procedure selects one of 16 possible cases in the process of determining which exponents are least negative.

3.02.1 Implementation of the Boundary Conditions on θ

The finite-difference equation in θ , equation (39), can be reexpressed to read:

$$B_P^{\theta} S + D_P^{\theta} W + E_P^{\theta} P + F_P^{\theta} E + H_P^{\theta} N = 0, \quad (40)$$

which then takes on the same form as the finite-difference equation in ψ , equation (22). As was the case with ψ , the boundary conditions on θ shown in Figure 3(b) are established by means of appropriate modifications in the coefficients B_P , D_P , E_P , F_P , and H_P in (40).

3.02.1(a) Border Segments where $\theta=1$ --The fact that the θ lattice interlaces the ψ lattice (Figure 4) means that the boundary condition $\theta=1$ cannot strictly be enforced at the borders where that condition applies (Figure 3). However, those borders are remote from the region under the oxide-silicon interface where "the action" occurs, so this is not considered to be a serious drawback. What is done is to enforce $\theta=1$ along the column (or row) of θ lattice points

imagined to be present just outside of the rectangular region modeled. Thus, for example, at the left border in Figure 4 the coefficient D_p is calculated in the usual manner. Then the right hand side of (40) is set equal to the negative of D_p and the term involving θ_W in (40) is omitted, which is equivalent to enforcing θ_W to be unity. Similar procedures are applied at the right border and along the lower border of the substrate.

3.02.1(b) Border Segments where $\partial\theta/\partial x = 0$ --Again, we imagine two columns of the θ lattice just outside of the rectangular region modeled in Figure 4. At the left border, therefore, we wish to enforce $\theta_W = \theta_p$. This is achieved by calculating D_p and E_p in the usual manner, then summing them to obtain a revised value for E_p . The coefficient D_p in (40) is then set to zero. A similar procedure is applied at the right border.

3.02.1(c) The Oxide-Silicon Interface where $\theta=0$ --Here, the row $J = JTHMAX$ of the θ lattice coincides with the interface. The condition $\theta=0$ is enforced along that row by setting B_p , D_p , F_p , and H_p to zero, while setting E_p to unity in (40).

3.03 Finite-Difference Algorithm for the Drain Current Factor J_0

The row of the ψ lattice just below the oxide-silicon interface is selected for the line integral contained in (20), to evaluate the drain current factor J_0 . The trapezoidal rule is applied to evaluate the integral. Simple differencing of θ on the interlaced θ lattice provides $\partial\theta/\partial y$ at the centroid of each interval Δx . The value of $e^{-\psi}$ at that centroid is again specified to be an average obtained by assuming a linear variation of ψ between adjacent ψ lattice points along the row:

$$\langle e^{-\psi} \rangle = \left[\frac{e^{-\psi_E} - e^{-\psi_W}}{\psi_W - \psi_E} \right] . \quad (41)$$

As in the case of evaluating θ discussed earlier, special procedures are employed to avoid overflow and underflow due to machine limitations.

3.04 Finite-Difference Algorithm for the Electron Number Density n

Equation (10) when separated into its x and y components, gives:

$$\frac{\partial}{\partial x} (n e^{-\psi}) = \frac{J_x}{\mu} e^{-\psi}, \quad (42)$$

$$\frac{\partial}{\partial y} (n e^{-\psi}) = \frac{J_y}{\mu} e^{-\psi}. \quad (43)$$

Expressing (42) in finite-difference form:

$$\left[\frac{n(I+1, J) e^{-\psi(I+1, J)} - n(I, J) e^{-\psi(I, J)}}{\Delta x(I+1)} \right] = \frac{J_x}{\mu} \langle e^{-\psi(I, J)} \rangle. \quad (44)$$

(Here we resort to the use of the indices (I, J) identifying ψ lattice points because the "points of the compass" notation employed earlier becomes awkward.) Note that an average value for $e^{-\psi}$ is assigned to the point midway between the points $I+1$ and I of the row J . That is:

$$\langle e^{-\psi(I, J)} \rangle = \left[\frac{e^{-\psi(I+1, J)} - e^{-\psi(I, J)}}{\psi(I, J) - \psi(I+1, J)} \right]. \quad (45)$$

Equations (44) and (45), when combined, can be reexpressed so as to involve only differences in ψ :

$$n(I+1, J) = n(I, J) e^{-[\psi(I, J) - \psi(I+1, J)]} + \frac{J_x}{\mu} \left[\frac{1 - e^{-[\psi(I, J) - \psi(I+1, J)]}}{\psi(I, J) - \psi(I+1, J)} \right] \Delta x(I+1). \quad (46)$$

Alternatively:

$$n(I,J) = n(I+1,J)e^{-[\psi(I+1,J)-\psi(I,J)]} - \frac{J_x}{\mu} \left[\frac{1 - e^{-[\psi(I+1,J)-\psi(I,J)]}}{\psi(I+1,J) - \psi(I,J)} \right] \Delta x(I+1) . \quad (47)$$

Equations (46) and (47), together with the vertical counterpart of (46) derived in the same manner from (43), form the basis for the finite-difference algorithm for the electron density n , which proceeds as follows. Consider any row $J \geq \text{JUNCTN}$ (see Figure 4) which intersects the vertical source and drain "contacts" at the left and right borders where n is known. Starting at the left border, (46) is applied recursively to "march" along that row, toward the right border, until a potential minimum is encountered. When this occurs, then one switches to the right border and applies (47), recursively, to "march" to the left toward the last point at which n was previously calculated. In this manner, the electron member density is filled in row by row, for all rows of the ψ lattice which intersect the source and drain "contacts." Note that the exponentials encountered with this procedure always involve negative exponents.

The next step in the procedure then utilizes the vertical counterpart of (46), derived from (43). In this case, one starts at the row $J = \text{JUNCTN}$, where n is now known, and "marches" vertically downward to the substrate contact, column by column. Again, only negative exponents are encountered in any exponentiation operations required.

To avoid underflow, appropriate approximations are invoked in the subprogram which implements this procedure when the negative exponents encountered become sufficiently large. Similarly, appropriate approximations are applied when the denominators in (46) and (47), and the vertical counterpart of (46) approach zero, to avoid divide checks.

The "marching" algorithm described above is precisely the one suggested by Mock [1], who states that the procedure of switching directions at the point where ψ passes through a minimum suppresses the buildup of roundoff errors. In spite of this assertion, one intuitively feels uneasy about any numerical method which only makes use of information about the solution at one border without "pumping into" the solution some information about the boundary condition at the other border as well. The "marching" method fails to do so, and blithely assumes that, where the two solutions meet, continuity in n will not be violated.

The author felt sufficiently uneasy about this to try a different approach. Combining pairs of equations of the form of (46) by summing them, so as to couple the points $I-1$, I , and $I+1$ in a common row J , a tridiagonal matrix results from the set of equations relating n along that row. Given J_x and ψ as knowns, Gaussian elimination is then implemented to obtain n along such a row. This approach achieves the goal of "pumping into" the equations simultaneous information about the boundary conditions at both ends of the row in question. Interestingly, the two methods are found to give identical results (within the three significant figures printed out) in regions where the electron density is numerically important, i.e., in the inversion layer. Both approaches produce negative electron densities in regions where the numerical magnitude of n is negligible in comparison with the acceptor density N_A . (These nonphysical negative densities are believed due to roundoff errors.) Insofar as these negative densities are concerned, the "marching" method is found superior. With it, they occur with values of n an order of magnitude lower than observed with the more sophisticated tridiagonal matrix approach.

4.0 The Iterative Procedure

The basic equations defined in Section 2, and their finite-difference counterparts developed in Section 3, constitute a set of coupled, nonlinear equations for which a self-consistent solution is obtained by means of an iterative procedure. The one followed is basically the same as that adopted by Mock [1], with one important modification which will be clarified in Section 4.03.

The iterative procedure starts with initial "guesses" for $\psi(x,y)$, $\theta(x,y)$, $n(x,y)$ and $p(x,y)$ which will be discussed in Section 4.04. It then proceeds as follows. Given n and p , the charge Q_p associated with each ψ lattice point P is then known (Subsection 3.01.2). Equation (22) is then solved, using Stone's method, to provide a new estimate for ψ . A new estimate for θ is then generated, followed by new estimates for n and p consistent with the new ψ and θ distributions. The procedure is then repeated until convergence is achieved, as determined by convergence criteria specified as input data by the user. Two differing procedures--PICARD iteration, and GUMMEL's algorithm--are employed in the implementation of this iterative sequence. These will next be discussed.

4.01 Picard Iteration

The Picard iteration procedure utilizes only "past history" to predict the next iterate for ψ , and is employed to achieve "coarse" convergence. Consider the m^{th} iteration step to have just been completed, so that $\psi^{(m)}$, $\theta^{(m)}$, $n^{(m)}$, and $p^{(m)}$ have been determined. (Values for step $(m-1)$ are also available, as needed, except when $m=0$, which corresponds to the initial "guess.") Given these, (22) is solved, yielding a new solution for the potential distribution, which we designate $v^{(m+1)}$. With it, the improved approximation $\psi^{(m+1)}$ for the correct potential $\psi(x,y)$ is obtained from:

$$\psi^{(m+1)} = \psi^{(m)} + \alpha_m [v^{(m+1)} - \psi^{(m)}] + \beta_m [\psi^{(m)} - \psi^{(m-1)}], \quad (48)$$

where α_m and β_m are underrelaxation parameters, adjusted for each iteration step m in the manner to be described next. With $\psi^{(m+1)}$ thus specified, the corresponding new estimates for $\theta^{(m+1)}$, $n^{(m+1)}$ are then determined.

As was done by Mock [1], we adopt the Chebyscheff sequence of relaxation parameters α_m and β_m discussed by Forsythe and Wasow [9] for estimating appropriate values of those parameters at each iteration step m and, as did Mock, we reinitiate the sequence whenever the new residual $|v^{(m+1)} - \psi^{(m)}|_{\max}$ turns out to be greater than the residual found in step m . (Mock interprets this as an indicator that the nonlinearity of the problem is becoming evident.) This sequence of relaxation parameters is given by, [9]:

$$\alpha_m = \frac{4 \cosh(m\omega)}{(b-a) \cosh([m+1]\omega)}, \quad (49)$$

$$\beta_m = \frac{\cosh([m-1]\omega)}{\cosh([m+1]\omega)}, \quad (50)$$

where

$$\omega = \cosh^{-1} \left[\frac{b+a}{b-a} \right]. \quad (51)$$

The parameters b and a in (51) are the upper and lower bounds, respectively, of the eigenvalues of the matrix equation (24). The initial values of this Chebyscheff sequence, as prescribed by Forsythe and Wasow, are determined by,

$$\alpha_0 = 2/(b+a), \quad (52)$$

$$\beta_0 = 0. \quad (53)$$

The implementation of this procedure requires an estimate for the upper and lower bounds b and a of the eigenvalues of the matrix equation (24). The

[9] G.E. Forsythe and W.R. Wasow, Finite-Difference Equations for Partial Differential Equations, pp. 226-235. Wiley, New York (1960).

estimate for a is not critical, but that of b is. Too small an estimate for b leads to failure of the relaxation procedure to converge, while too large an estimate leads to extremely slow convergence. We have adopted the estimate for b suggested by Mock ([1], eq. (21))^{*}:

$$b = \frac{y_{\text{sub}}}{4x_{\text{channel}}} \iint (n+p) dx dy, \quad (54)$$

the double integral being evaluated over the entire rectangular substrate region by application of the trapezoidal rule in two dimensions. The parameter b is evaluated using initial estimates for n and p to be described below.^{**}

Mock [1] points out that since large values of b lead to slow rates of convergence, and since its magnitude is proportional to the total number of free carriers in the substrate region, a savings in computation time can be achieved by applying the Picard iteration process, initially, with a reduced donor density assigned to the source and drain, until coarse convergence criteria are satisfied. Having achieved this, he then assigns the correct donor density to those regions and switches to Gummel's iterative algorithm for the remainder of the computation, with tightened convergence criteria applied.

^{*} Mock's eq. (21) contains a factor ϵ_s which is missing in (54). This is because of differences in Mock's choice of normalized variables and the choice which we have adopted.

^{**} At one time, the program included steps to reevaluate the parameter b each time the Chebyscheff sequence was reinitiated, on the basis that the estimates for n and p at that stage of the computation should be better than the estimates previously employed for that purpose. Computer experiments later showed that not only is this unnecessary but also that it usually caused the number of iterations required for convergence to increase, rather than decrease.

4.02 Gummel's Algorithm

Unlike the Picard iteration method just described, which uses only "past history," Gummel's algorithm [10] incorporates a new prediction for p and n at each iterative step. Because this prediction is based upon a linear approximation of the exponential functions appearing in the Boltzmann relations for those densities, it is efficient in terms of computation speed only when the estimates of ψ , p , and n are close to the "correct" values when it is initiated.

Let $\psi^{(m)}$, $n^{(m)}$ and $p^{(m)}$ be the values obtained at iteration step m . Let $\psi^{(m+1)} = \psi^{(m)} + \delta^{(m+1)}$, and assume that $\delta^{(m+1)} \ll \psi^{(m)}$. Then:

$$e^{\psi^{(m+1)}} \approx e^{\psi^{(m)}} [1 + \delta^{(m+1)}] . \quad (55)$$

Applying this approximation to (2) and (3), one has

$$n^{(m+1)} \approx n^{(m)} [1 + \delta^{(m+1)}] , \quad (56)$$

$$p^{(m+1)} \approx p^{(m)} [1 - \delta^{(m+1)}] , \quad (57)$$

which assumes that the electron quasi-Fermi potential ϕ_n does not change appreciably between iteration steps (m) and $(m+1)$. Assuming these conditions to be met, Poisson's equation, (1), gives for $\psi^{(m+1)}$:

$$\nabla^2 \psi^{(m+1)} - [n^{(m)} + p^{(m)}] \psi^{(m+1)} = [N_A + n^{(m)} - p^{(m)}] - [n^{(m)} + p^{(m)}] \psi^{(m)} , \quad (58)$$

which is Gummel's algorithm.

The finite-difference equivalent of (58) can be cast into the same form as (22). Only the coefficient E_p in (23)

[10] H.K. Gummel, IEEE Trans. Electron Devices ED-11, 455 (1964).

is modified due to additional term $[n^{(m)} + p^{(m)}]\psi^{(m+1)}$ appearing on the left side of (58). Similarly, the charge term Q_p in (23) is modified due to the corresponding additional term on the right side of (58). The resulting matrix equation, corresponding to (24), is solved for $[\psi^{(m+1)}]$, given $[Q^{(m)}]$, using Stone's iterative procedure.

4.03 A Modification of Mock's Iterative Procedure

As described above, Mock uses both the Picard iteration and Gummel's algorithm, the former being used to achieve coarse convergence at reduced donor density, the latter being used to achieve final tightened convergence at full donor density. Initially, the author adopted this same procedure. However, computational experiments with our computer model have revealed that this procedure does not seem to be necessary. The author has found that not only is it possible to apply Gummel's algorithm directly at the outset, with full donor density, but also that the rate of convergence can be substantially enhanced if one applies overrelaxation in so doing. This approach proceeds as follows.

Let $\psi^{(m)}$ be the potential corresponding to the m^{th} iterative step and let $v^{(m+1)}$ be the result of applying Gummel's algorithm at the $(m+1)^{\text{th}}$ iterative step. Then the new potential $\psi^{(m+1)}$ is obtained as:

$$\psi^{(m+1)} = \psi^{(m)} + \Omega(v^{(m+1)} - \psi^{(m)}), \quad (59)$$

where Ω is an empirically determined relaxation parameter having a numerical value greater than unity.

That this procedure can result in a substantial reduction in computation time is illustrated in Figure 8, which plots the number of iterations required to achieve tight convergence ($\max|\psi^{(m+1)} - \psi^{(m)}| \leq .02$) versus gate voltage, with drain voltage fixed, for a particular device. In this

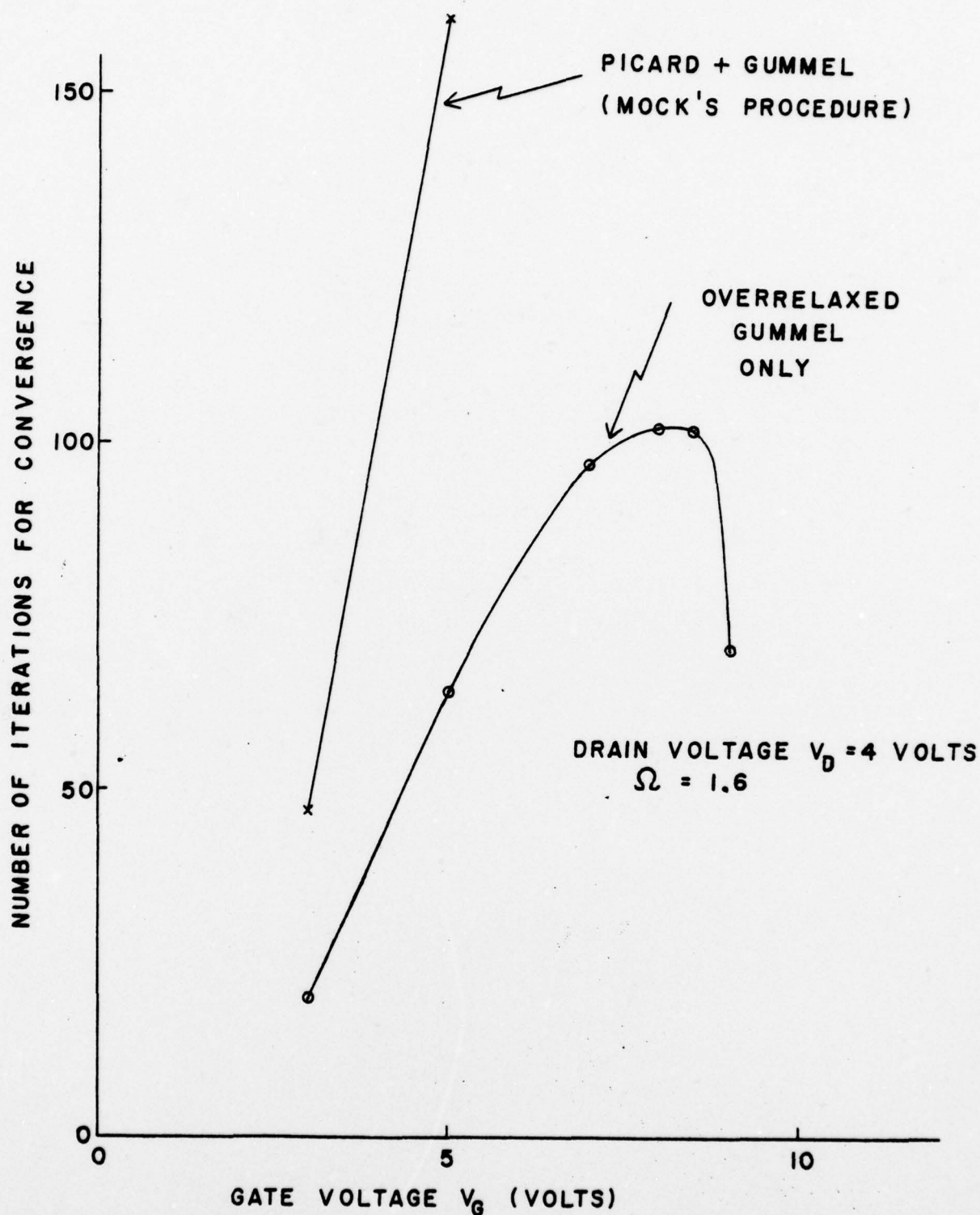


Figure 8 Number of iterations required for convergence of ψ to within $.02 \text{ } kT/q$ versus the gate voltage V_G , comparing Mock's iterative procedure with the overrelaxed Gummel procedure.

case, Ω was set to be 1.6, in the overrelaxation of Gummel's algorithm. In this experiment, four of the six points ($V_G = 3, 5, 7, 9$) shown for the curve labeled "OVER-RELAXED GUMMEL ONLY" were generated in a single computer run requiring 190 seconds of CPU time (the remaining two points were generated in separate runs to fill in further detail). On the other hand, at $V_G = 7$ volts, the combined "PICARD + GUMMEL" procedure failed to converge at all within a 6-minute cut-off time that was specified for that particular run!

Figure 8 reveals that the number of iterations required for convergence is strongly dependent upon the degree of charge inversion in the conducting channel. Computational experiments have also shown that the effectiveness of overrelaxation is much more dramatic in the strong inversion case. This is illustrated in Figure 9, which plots the number of iterations required to achieve convergence with the overrelaxed Gummel procedure versus the overrelaxation parameter Ω . (The threshold voltage for this particular device is ≈ 2.5 volts.) The numerical values shown along the two curves give CPU time, in seconds, required with the Amdahl 470 V/6-II computer used for these experiments, and include compilation time in each instance.

The discovery that the Gummel algorithm alone can be used, and particularly the fact that overrelaxation can be applied with marked success with that algorithm, was made only during the final phases of this project. Consequently, the computer model has been revised so as to allow the user the flexibility of specifying the implementation of either Mock's iterative procedure, or the overrelaxed Gummel procedure alone, by means of a "flag" incorporated as part of the input data specified by him. Similarly, the value of the overrelaxation parameter Ω to be used is at the user's disposal, inasmuch as time did not permit an investigation of possible methods for automatically determining an optimum value (or possibly a sequence of values) for this parameter.

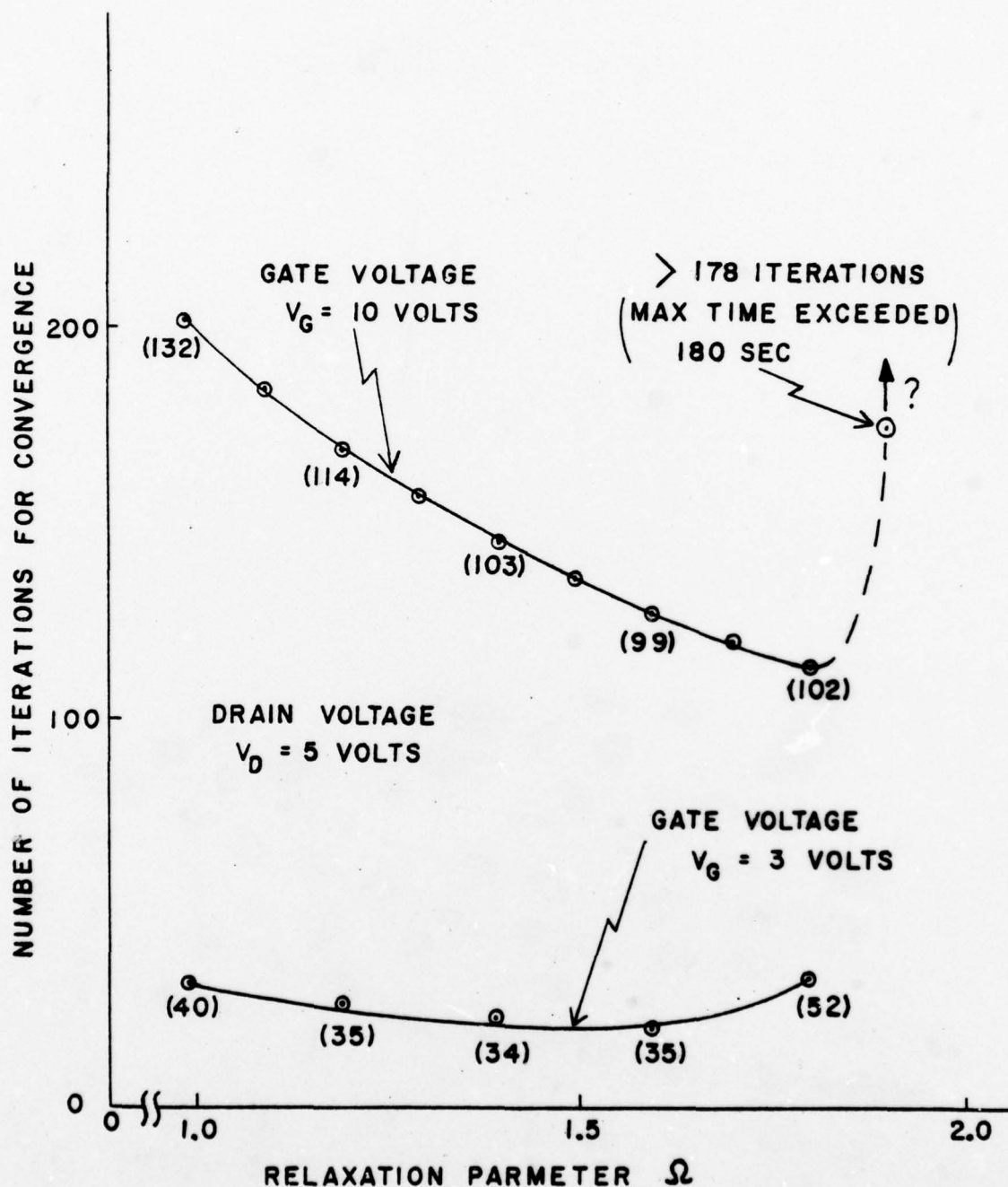


Figure 9 Number of iterations required for convergence of ψ to within $.02 \text{ kT/q}$ versus the overrelaxation parameter Ω used with Gummel's algorithm. The numerical values show CPU time, in seconds, required with an Amdahl 470 V/6-II computer.

4.04 Initial Estimates for $\psi(x,y)$, $\theta(x,y)$, $n(x,y)$, and $p(x,y)$

The initial estimates for ψ , θ , n , and p have been found to be a crucial factor in determining the number of iterations required to achieve convergence to a self-consistent solution. Early versions of our computer model were found to require from two to three times the number of iterations that were required with the IBM program developed by Mock. Much effort has been expended, in developing our model, to improve upon this early experience. These efforts have proven successful. Particularly, when only the Gummel algorithm is utilized, as described above, our model now requires from two to three times less iterations than does the IBM program, in most cases. This is attributed to the adequacy of the algorithms finally adopted for supplying the initial estimates. These will next be described.

4.04.1 Initial Estimate for $\psi(x,y)$

Figure 10(a) shows a sketch of the equipotential contours obtained from a two-dimensional, self-consistent solution of equations (1) through (7) for an MOSFET with a channel length of $5\mu\text{m}$, operating in strong inversion in the saturation mode. The cross-hatched regions shown in the figure identify regions in which $\psi(x,y)$ can be regarded as essentially having one-dimensional dependence, $\psi(x,y) \approx \psi(x)$, where $\psi(x)$ is found, to good approximation, to exhibit the parabolic dependence on x predicted by the widely used depletion approximation of abrupt p-n junction theory. This parabolic dependence in the vicinity of the source and drain "contacts" is sketched in Figure 10(b) as the two dashed curves shown.

The dotted region in Figure 10(a) identifies the charge-neutral region of the substrate, where $\psi = \psi_{eq} + V_{SUB}$, and where $\nabla\psi=0$. The two depletion parabolas of Figure 10(b) merge

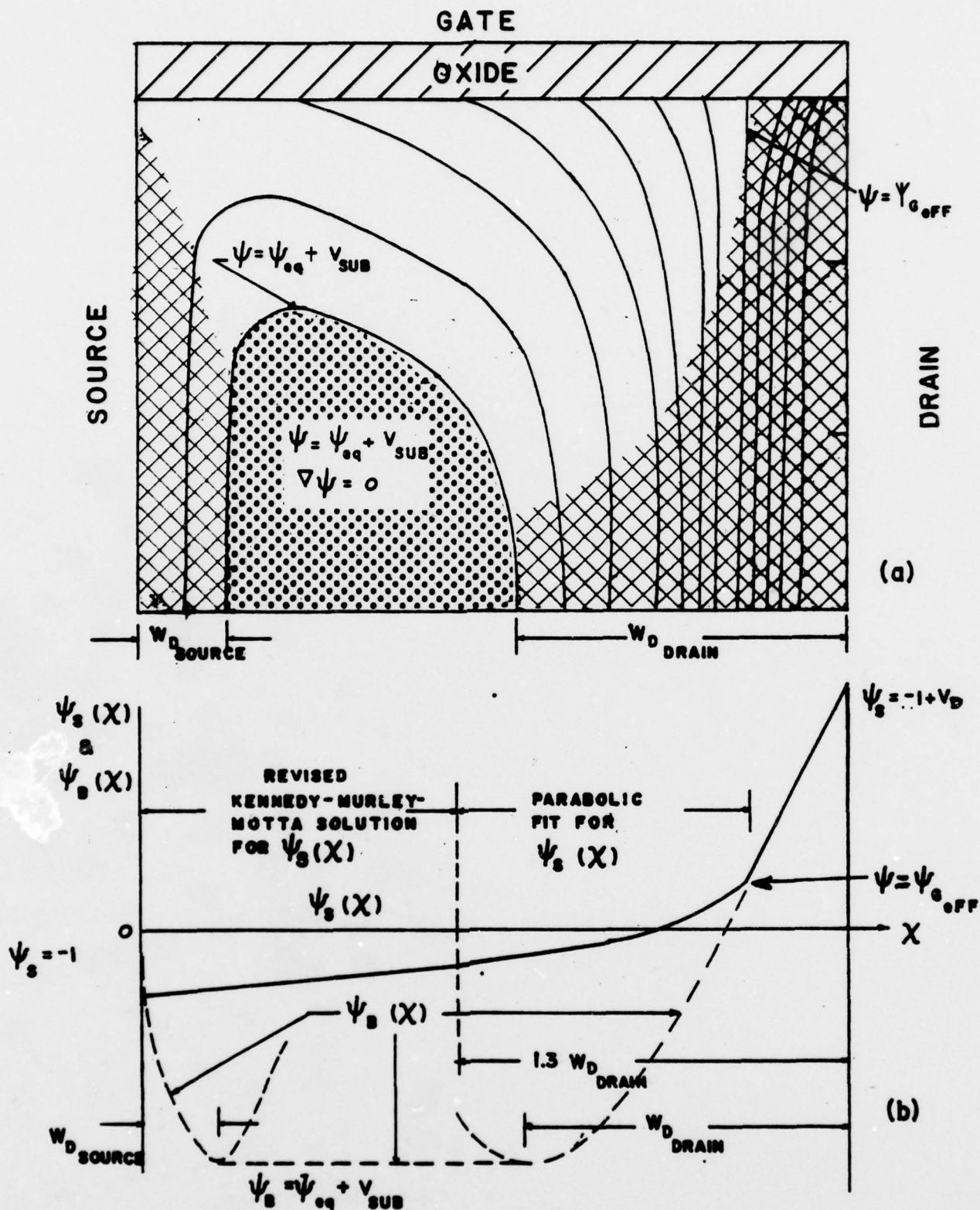


Figure 10 (a) Sketch of the equipotential contours in an MOSFET operating in saturation, providing insight into how to supply an initial estimate for $\psi(x,y)$. (b) Sketch of the potential $\psi_s(x)$ along the oxide-silicon interface, and $\psi_B(x)$ deep within the bulk material.

smoothly into the constant potential existent in that charge-neutral region. The composite dashed curve in Figure 10(b), for these three regions, serves to define the bulk potential $\psi_B(x)$, which is applicable deep within the substrate region, provided that $y < y_{\text{JUNCTION}}$ (see Figure 1(b)).

In contrast with the above regions, the unshaded region in Figure 10(a) depicts the region where $\psi(x,y)$ must be regarded as a two-dimensional function of the position coordinates x and y . At the oxide-silicon interface, $y=0$, it is effectively bounded on the left by the source itself, and on the right by the equipotential contour $\psi = \psi_{G_{\text{eff}}}$, which defines the point along the interface at which the component of electric field, E_y , normal to the interface vanishes. (In terms of the energy band diagrams commonly employed in MOSFET theory, this is the point along the channel at which the flatband condition occurs.) That contour is labelled in Figure 10(a) as $\psi = \psi_{G_{\text{eff}}}$, where:

$$\psi_{G_{\text{eff}}} = \psi_G + (k_{\text{si}}/k_{\text{ox}})y_{\text{ox}}Q_{\text{ss}}, \quad (59)$$

with $\psi_G = \psi_{\text{EQ}} + V_G$, as defined in Figure 3(a). Equation (59) defines the surface potential at the interface ψ_s which leads to vertical electric field reversal. This condition occurs, of course, only in the saturation mode, when the drain potential ψ_D exceeds $\psi_{G_{\text{eff}}}$.

The approach that we have adopted for estimating the two-dimensional potential distribution $\psi(x,y)$ in the unshaded region of Figure 10(a) is the following. An estimate for the surface potential $\psi_s(x)$ is first obtained by using the one-dimensional theory for MOSFET operation developed by Kennedy and Murley [11], as modified by Motta [12]. In principle,

[11] D.P. Kennedy and P.C. Murley, IBM Jour. Res. & Dev., 17, 1 (1973).

[12] R.F. Motta, Steady State Theory for the Metal-Oxide-Semiconductor Field Effect Transistor, Ph.D. Dissertation, University of Florida, 1976.

this solution is applicable up to the value of x at which $\psi_s(x) = \psi_{G^{eff}}$. It has been found empirically, however, that it is better to terminate the Kennedy-Murley-Motta solution for $\psi_s(x)$ at a value of x about 1.3 times the drain depletion width, $W_{D_{drain}}$, from the drain itself, and to extend $\psi_s(x)$ parabolically beyond that point of termination. Said parabolic extension is then matched in magnitude and slope to the Kennedy-Murley-Motta solution at that point, defining two of the three constants required to describe a parabola. The third constant depends upon whether or not the flatband condition is reached at some x between the point at which the parabolic fit is applied and the location of the drain, itself. If $\psi_D < \psi_{G^{eff}}$, the parabolic extension of $\psi_s(x)$ is forced to equal the drain potential ψ_D at $x = x_{channel}$ (see Figure 1). Otherwise, $\psi_s(x)$ is forced to equal $\psi_{G^{eff}}$ at the value of x at which the parabolic drain depletion potential equals $\psi_{G^{eff}}$. The latter case is the one illustrated in Figure 10(b).

Given an estimate for $\psi_s(x)$ and $\psi_B(x)$, as determined in the manner described above, one-dimensional solutions of Poisson's equation (with y the geometric variable) are then obtained along each plane x corresponding to an index I of the ψ lattice. These one-dimensional solutions are forced to: (a) match $\psi = \psi_B(x)$, with zero slope $d\psi/dy$ in the shaded regions of Figure 10(a), and (b) match the "known" solution $\psi = \psi_s(x)$ at the oxide-silicon interface. Furthermore, these one-dimensional solutions are forced to satisfy the boundary condition on $d\psi/dy$ at the oxide-silicon interface by adjusting the electron quasi-Fermi potential ϕ_n so that eq. (25) is satisfied. (The latter function is assumed to be independent of y over the range of y covered by these one-dimensional solutions--an approximation.)

In the above manner, "reasonable" quasi-two-dimensional first estimates for $\psi(x,y)$ are established throughout the silicon substrate. The estimate for $\psi(x,y)$ in the oxide region assumes a linear dependence on y which matches the

"known" surface potential $\psi_s(x)$ at the interface and the gate potential ψ_G at the gate electrode.

4.04.2 Initial Estimate for $\theta(x,y)$

The initial estimate of the stream function $\theta(x,y)$ is based upon the observation that θ takes on the value of unity at about the point at which the electron number density becomes intrinsic (i.e., $n=1$), throughout most of the substrate region. Furthermore, θ is found to be essentially a function only of the coordinate x , except in regions immediately adjacent to the source and drain "contacts." This being the case, the one-dimensional solution for $\psi(y)$, utilized as described above in the unshaded region of Figure 10(a), is then used at the vertical plane corresponding with the edge of the source depletion region to estimate the location y_1 at which $n=1$. A parabolic estimate for $\theta(y)$ is then established which takes on the value of unity, with zero slope, at $y=y_1$, and which takes on the value of zero at the oxide-silicon interface, $y=0$. That parabolic estimate for θ is then assigned along all vertical planes corresponding to the index I of the θ lattice, thereby establishing a one-dimensional initial estimate for θ .

4.04.3 Initial Estimates for $n(x,y)$ and $p(x,y)$

Given initial estimates for $\psi(x,y)$ and $\theta(x,y)$, the corresponding initial estimate for the electron density $n(x,y)$ is obtained using the "marching" method described in Section 3.04. The hole density $p(x,y)$ is obtained by applying the Boltzmann relationship, eq. (3), since the hole quasi-Fermi potential ϕ_p is assumed invariable (eq. (5)), and takes on the value which causes p to equal N_A in the charge-neutral substrate region.

CHAPTER II

Evaluation of the Computer Model's Performance

In this chapter, we show comparisons of the results obtained from our computer model with those obtained for identical cases from the IBM program devised by Mock. We also show comparisons of the predictions obtained from our model with experimental data obtained for a particular MOSFET structure whose processing parameters have been characterized from test sites fabricated as an integral part of its chip.

1.0 Comparisons with Mock's Program

Figures 11 through 34 show comparisons of the results obtained from our model with those obtained from the program developed for IBM by Mock. The figures are ordered in groups of three: (1) $\psi(x)$ versus x along the oxide-silicon interface, (2) $\psi(y)$ versus y along the vertical plane perpendicular to the interface midway between the source and the drain, and (3) $n(y)$ versus y along the same vertical plane. The eight cases represented by these data represent extremes of operation as follows:

- 1) Short channel ($3\mu\text{m}$) ($N_D = 10^{19} \text{ cm}^{-3}$, $N_A = 2 \times 10^{16} \text{ cm}^{-3}$):
 - (a) Weak inversion, triode mode
 - (b) Weak inversion, saturation mode
 - (c) Strong inversion, triode mode
 - (d) Strong inversion, saturation mode
- 2) Long channel ($10\mu\text{m}$) ($N_D = 10^{19} \text{ cm}^{-3}$, $N_A = 2 \times 10^{15} \text{ cm}^{-3}$):
 - (a) Weak inversion, triode mode
 - (b) Weak inversion, saturation mode
 - (c) Strong inversion, triode mode
 - (d) Strong inversion, saturation mode

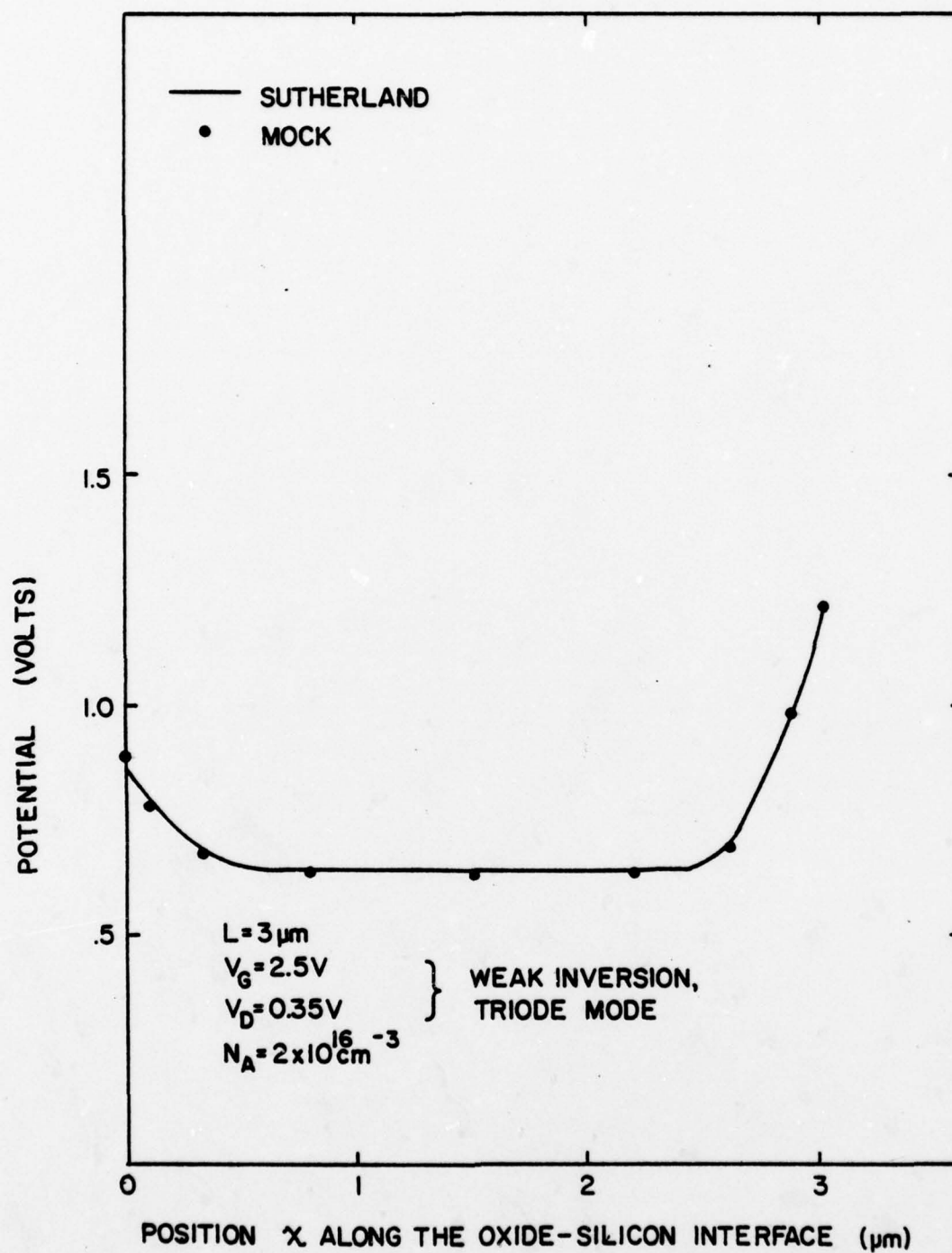


Figure 11 Comparison of the potential $\psi(x)$ along the oxide-silicon interface, generated by this model and by Mock's model.

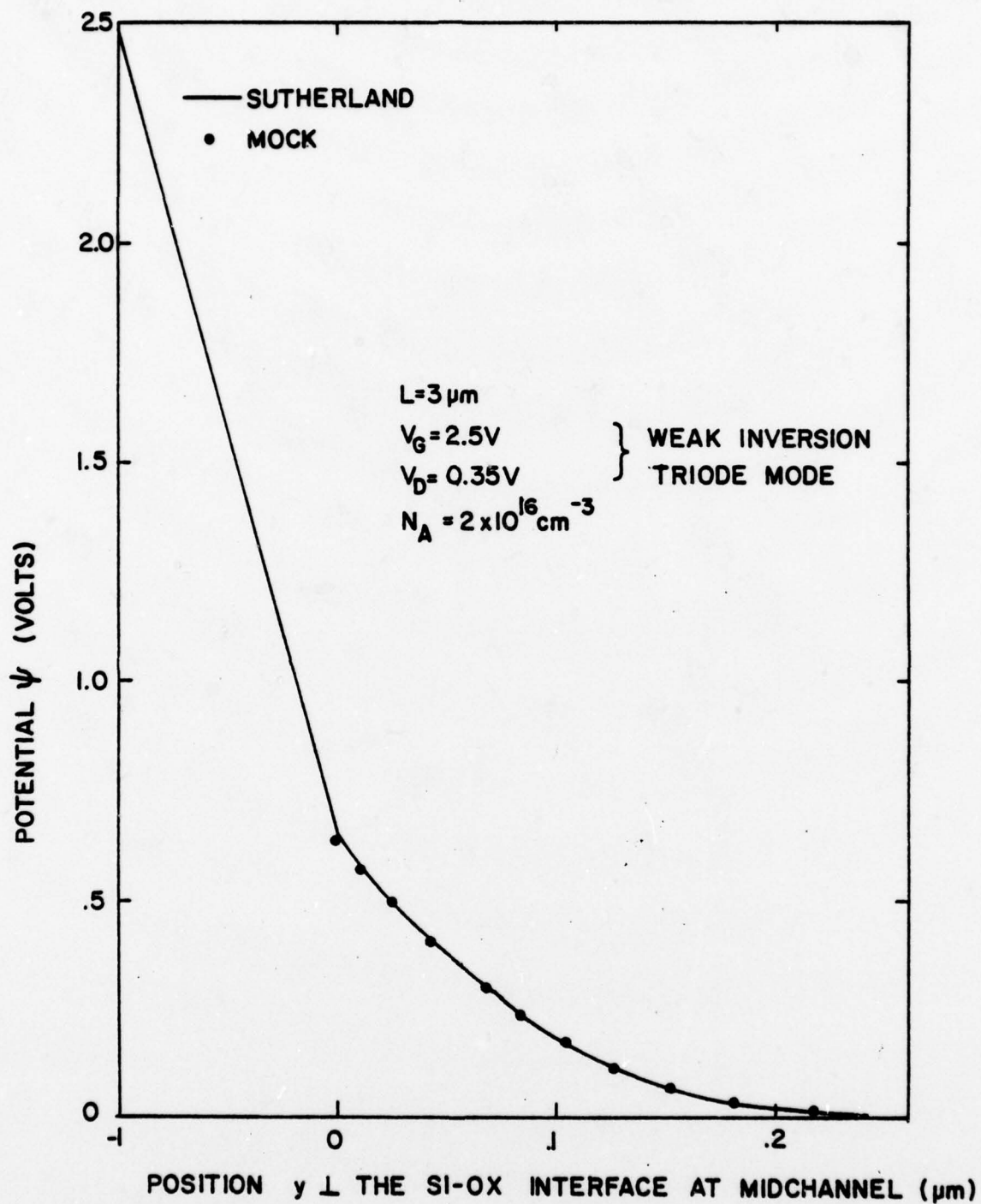


Figure 12 Comparison of the potential $\psi(y)$ along the plane midway between source and drain, generated by this model and by Mock's model.

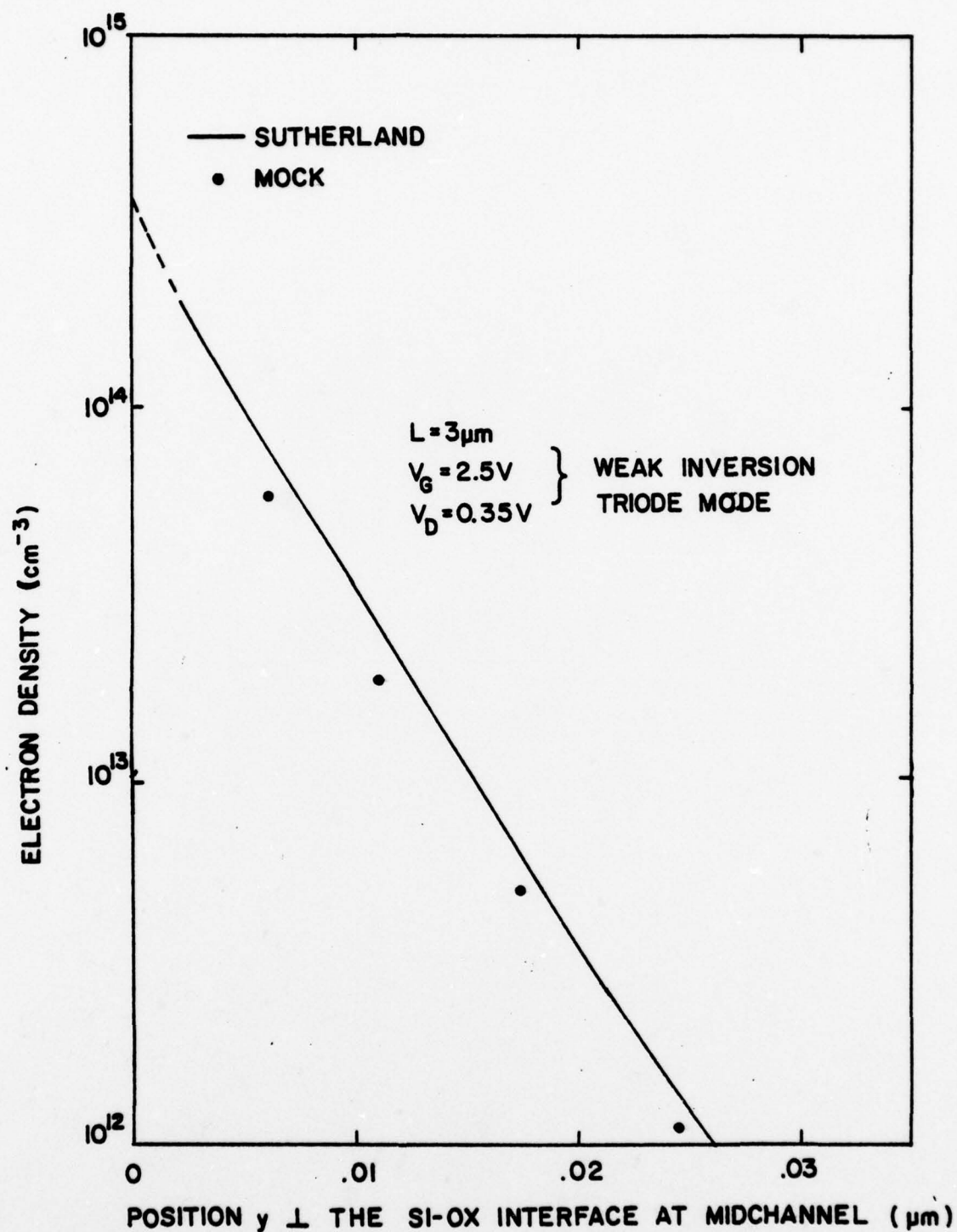


Figure 13 Comparison of the electron number density $n(y)$ along the plane midway between source and drain, generated by this model and by Mock's model.

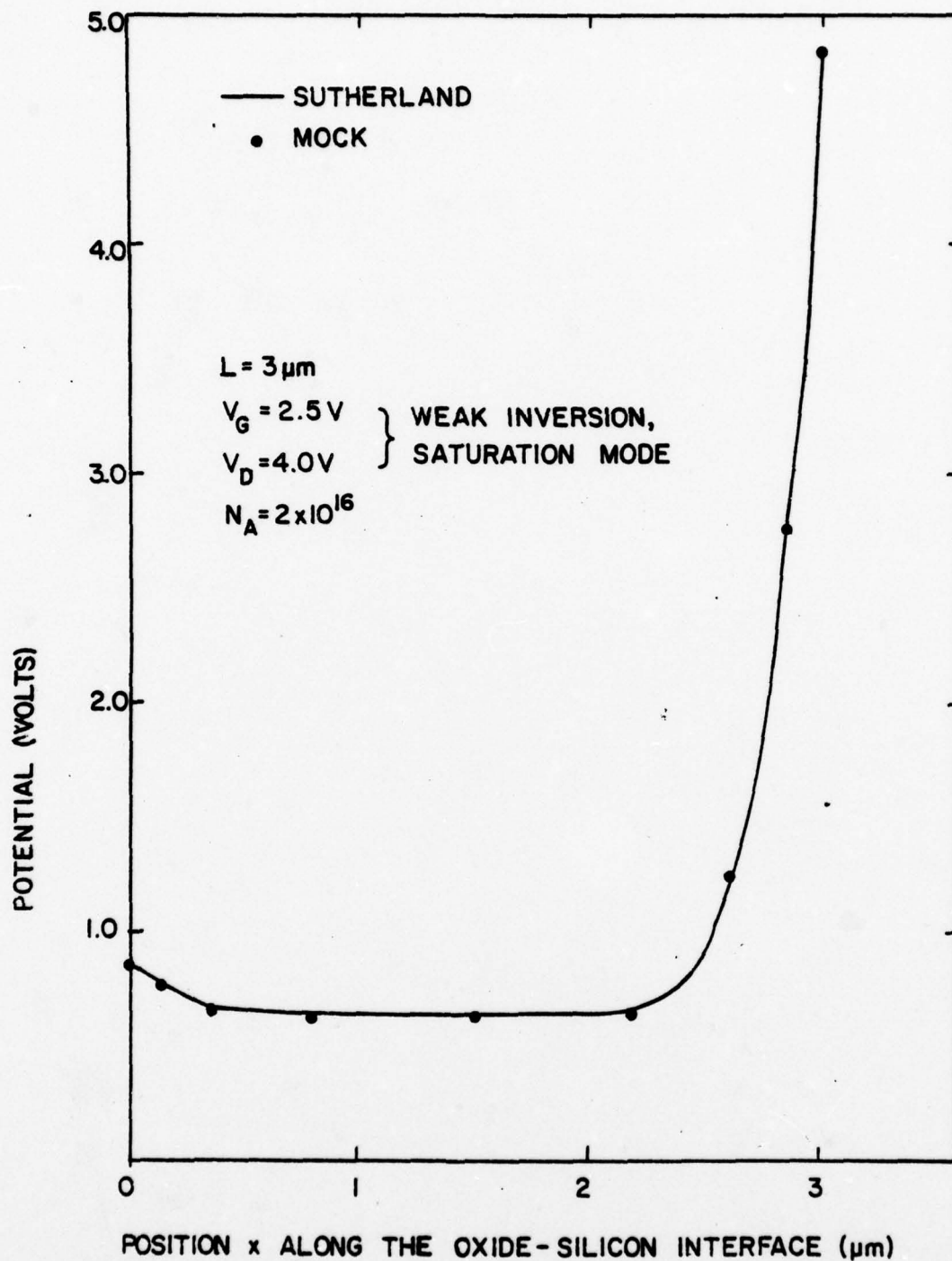


Figure 14 Comparison of the potential $\psi(x)$ along the oxide silicon interface, generated by this model and by Mock's model.

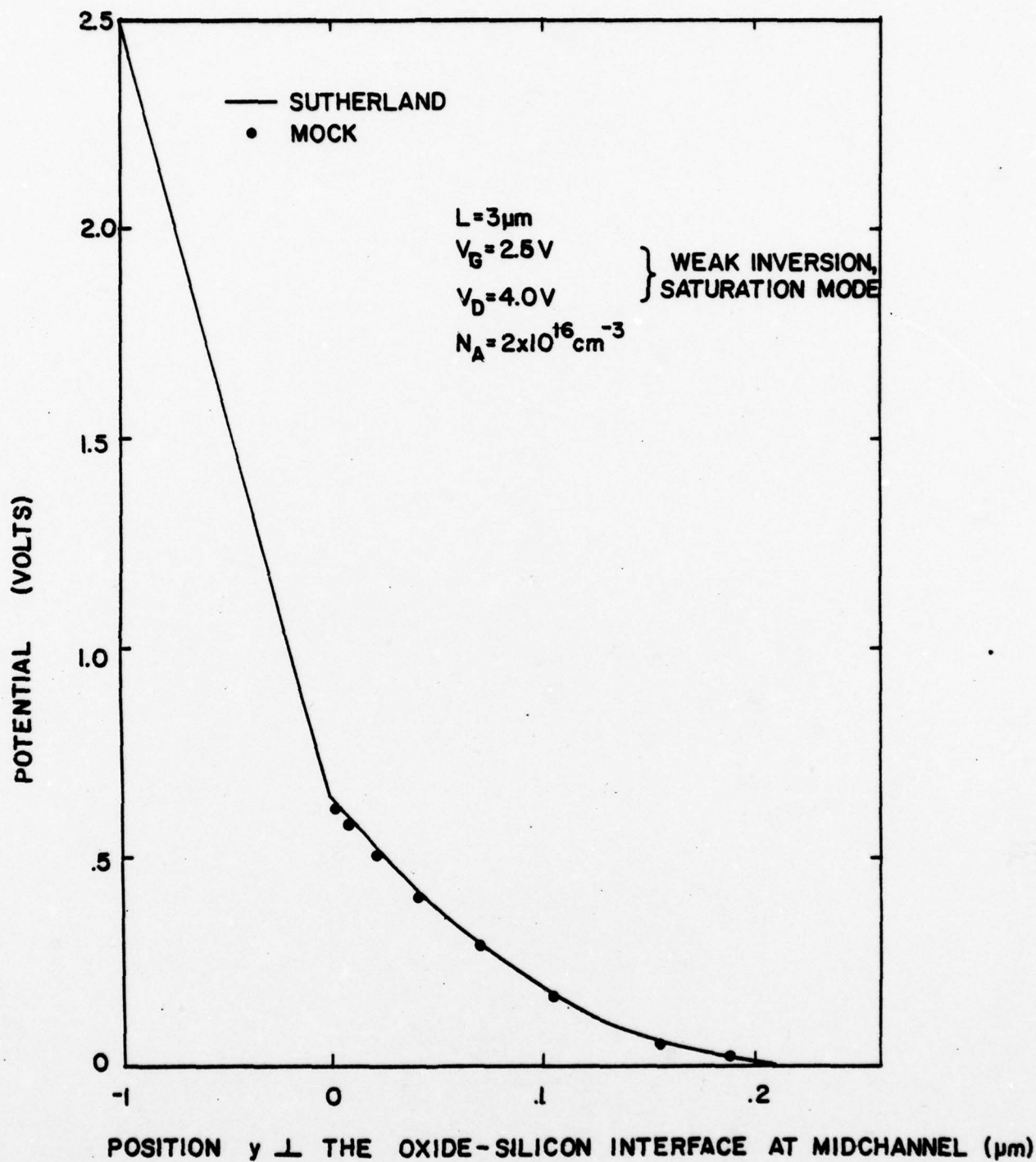


Figure 15 Comparison of the potential $\psi(y)$ along the plane midway between source and drain, generated by this model and by Mock's model.

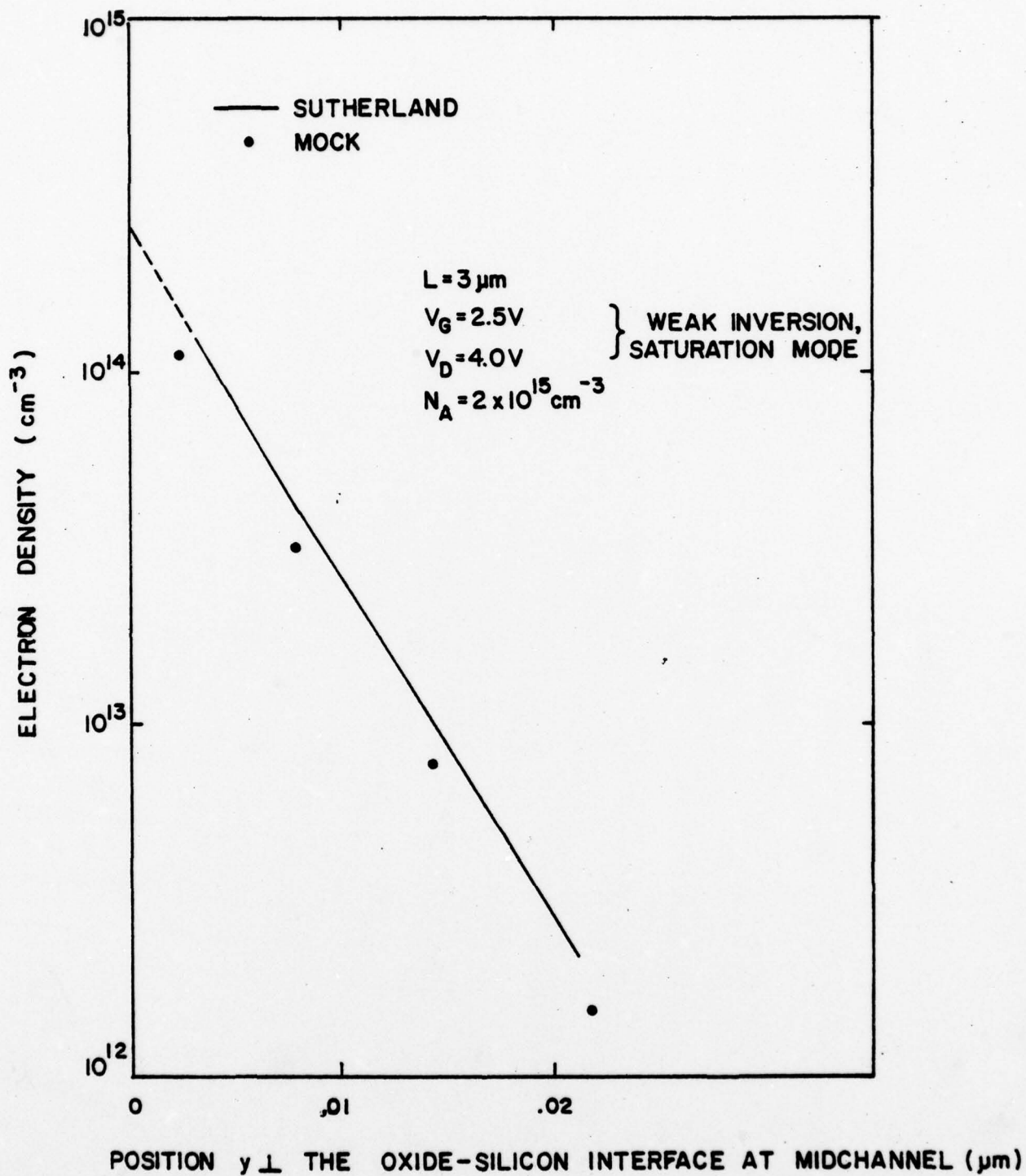


Figure 16 Comparison of the electron number density $n(y)$ along the plane midway between source and drain, generated by this model and by Mock's model.

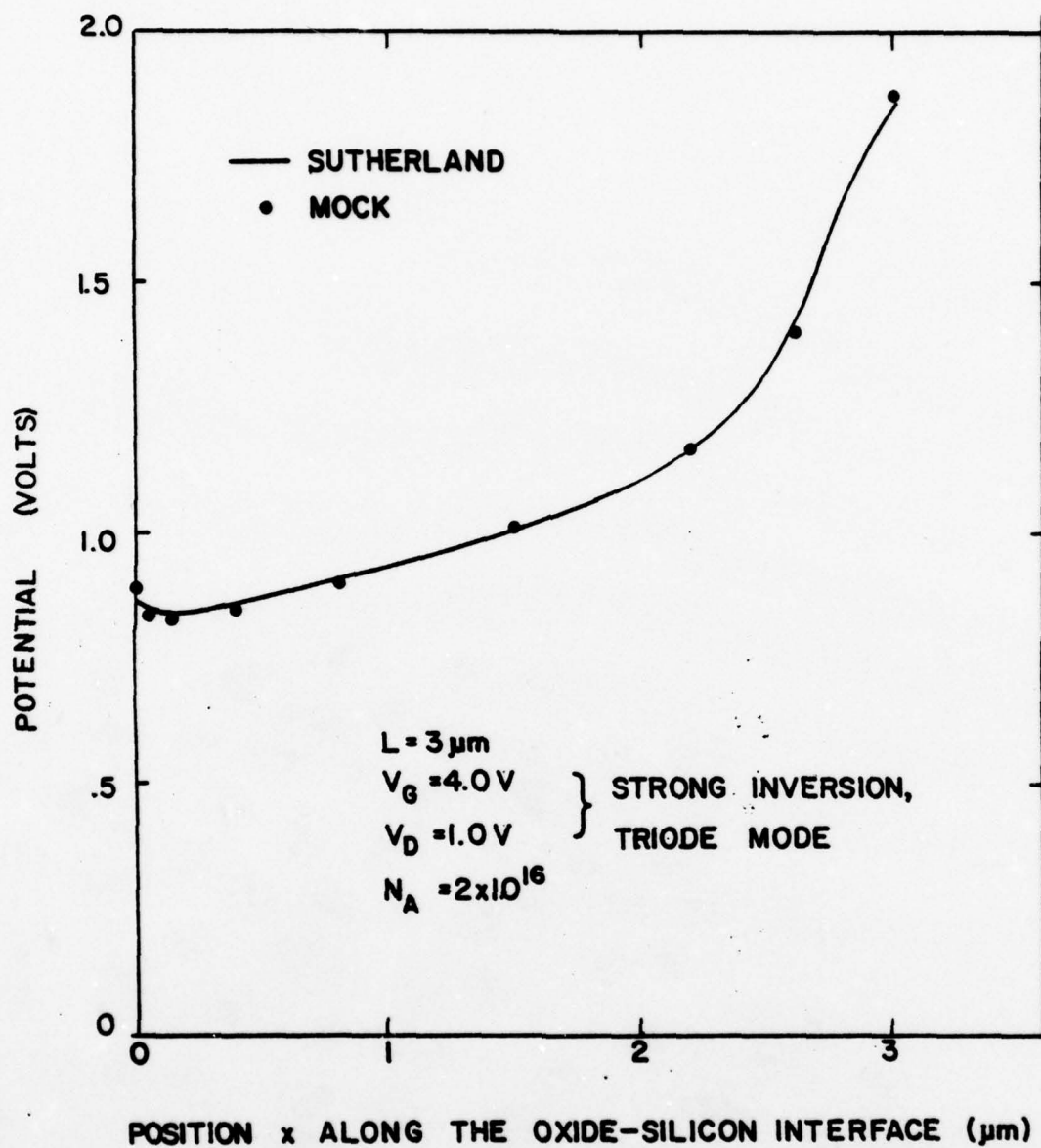


Figure 17 Comparison of the potential $\psi(x)$ along the oxide silicon interface, generated by this model and by Mock's model.

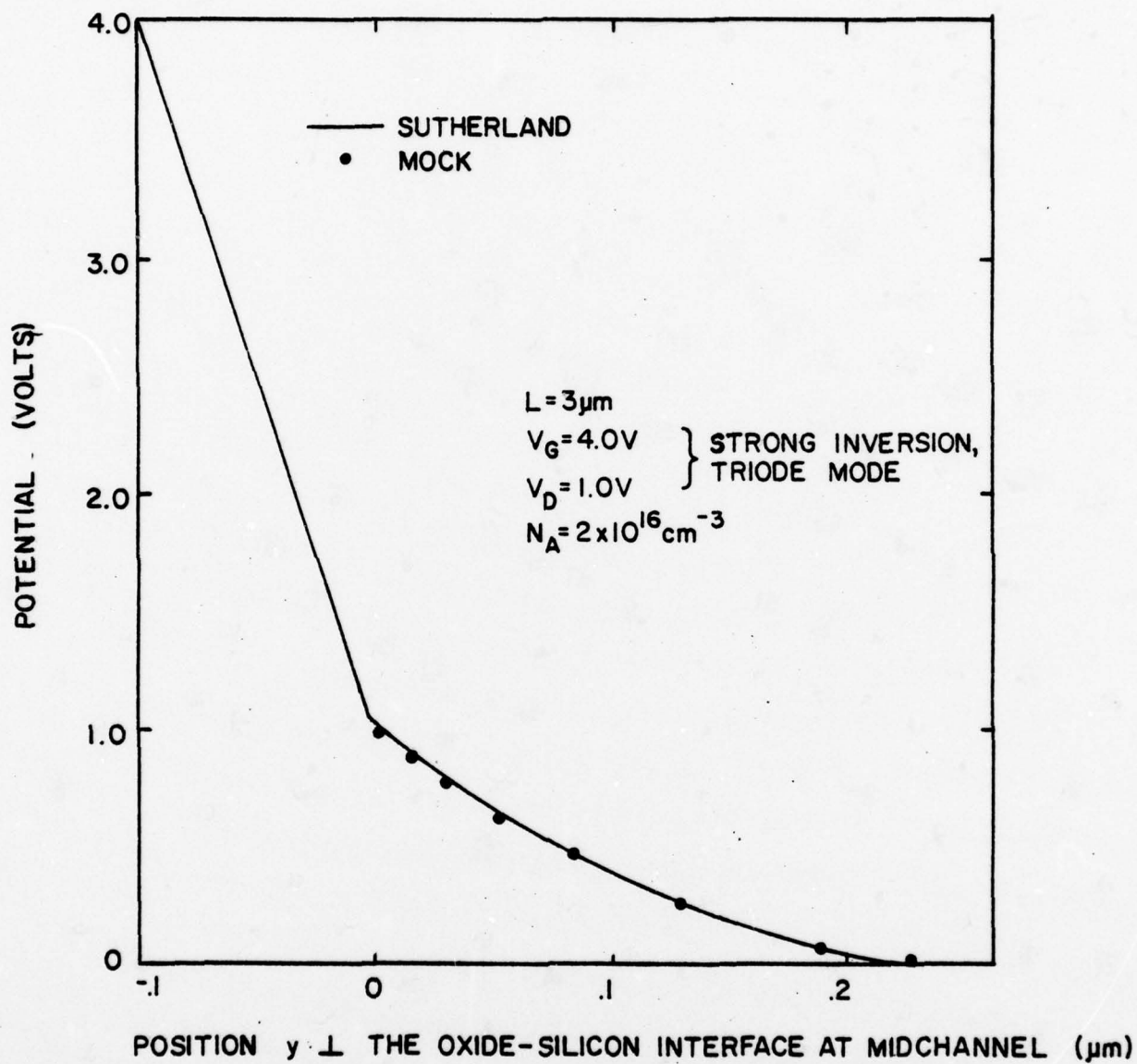


Figure 18 Comparison of the potential $\psi(y)$ along the plane midway between source and drain, generated by this model and by Mock's model.

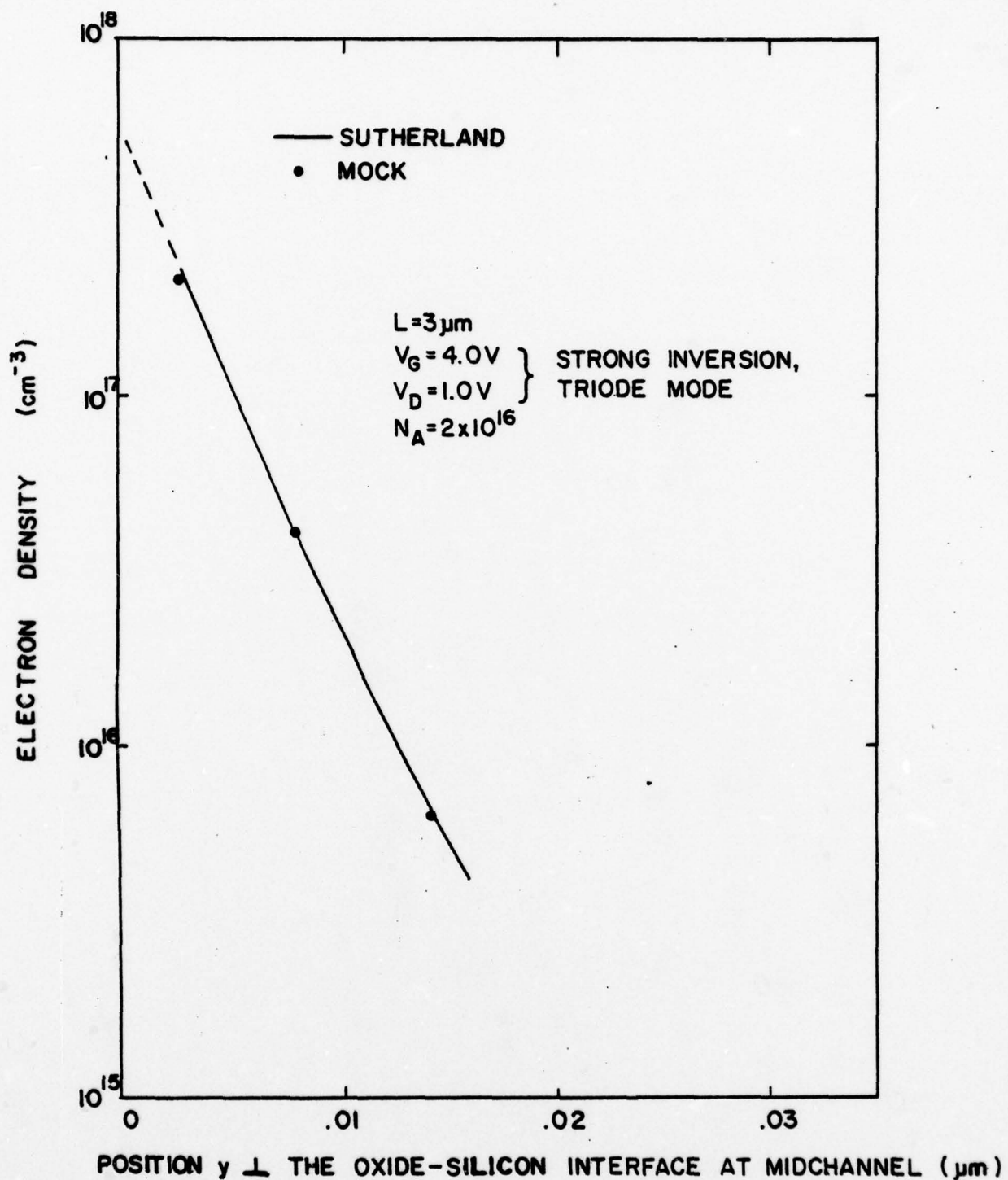


Figure 19 Comparison of the electron number density $n(y)$ along the plane midway between source and drain, generated by this model and by Mock's model.

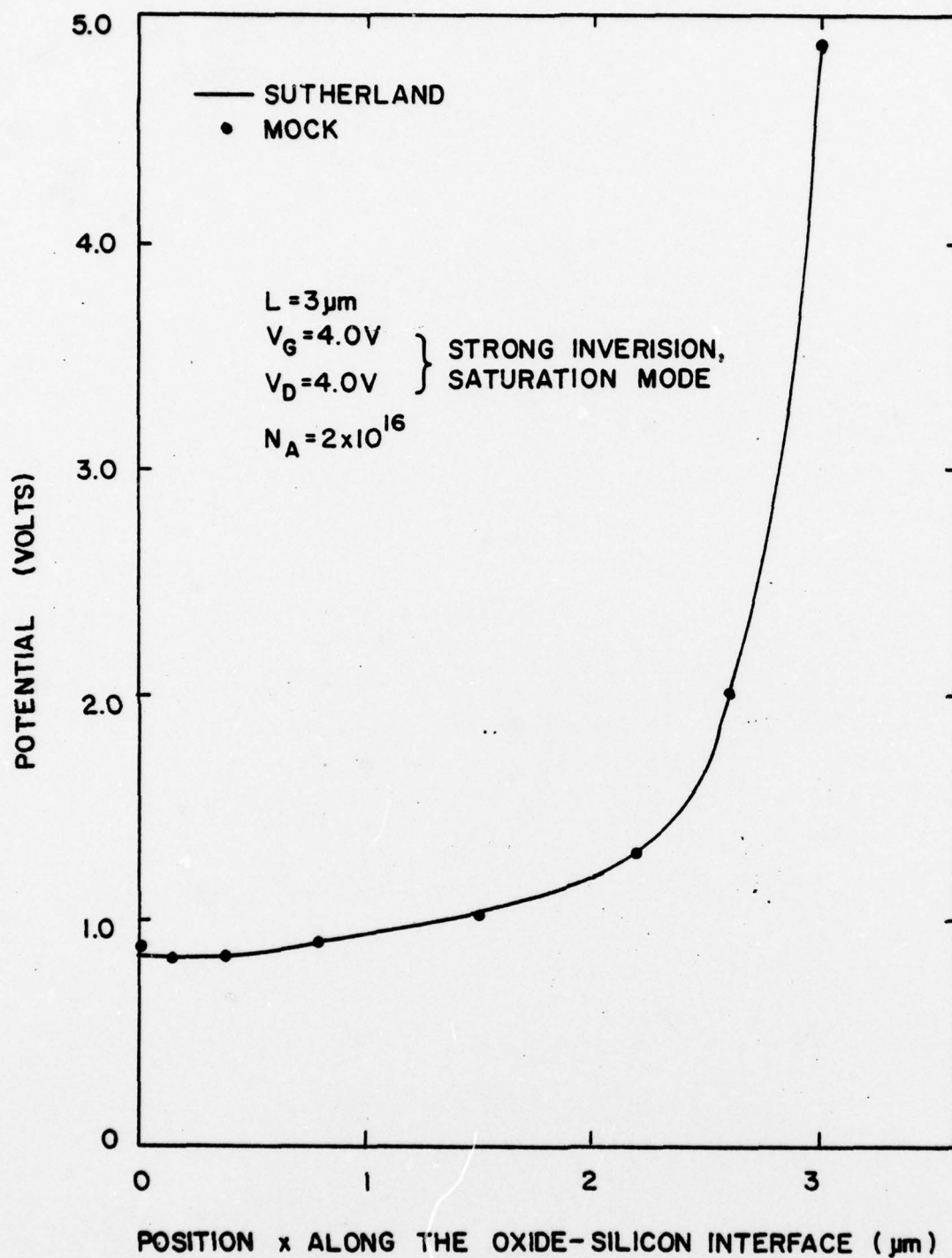


Figure 20 Comparison of the potential $\psi(x)$ along the oxide silicon interface, generated by this model and by Mock's model.

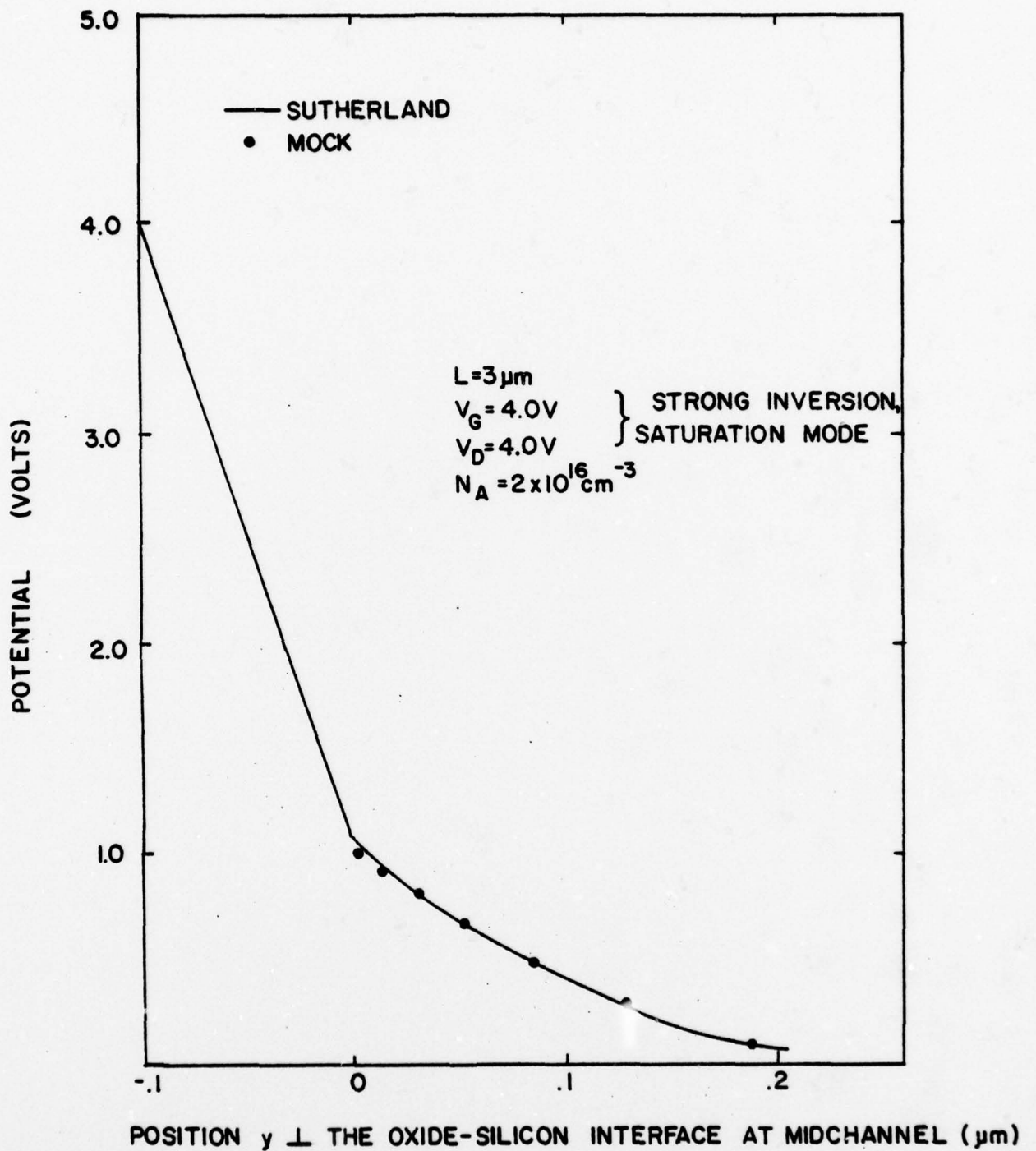


Figure 21 Comparison of the potential $\psi(y)$ along the plane midway between source and drain, generated by this model and by Mock's model.

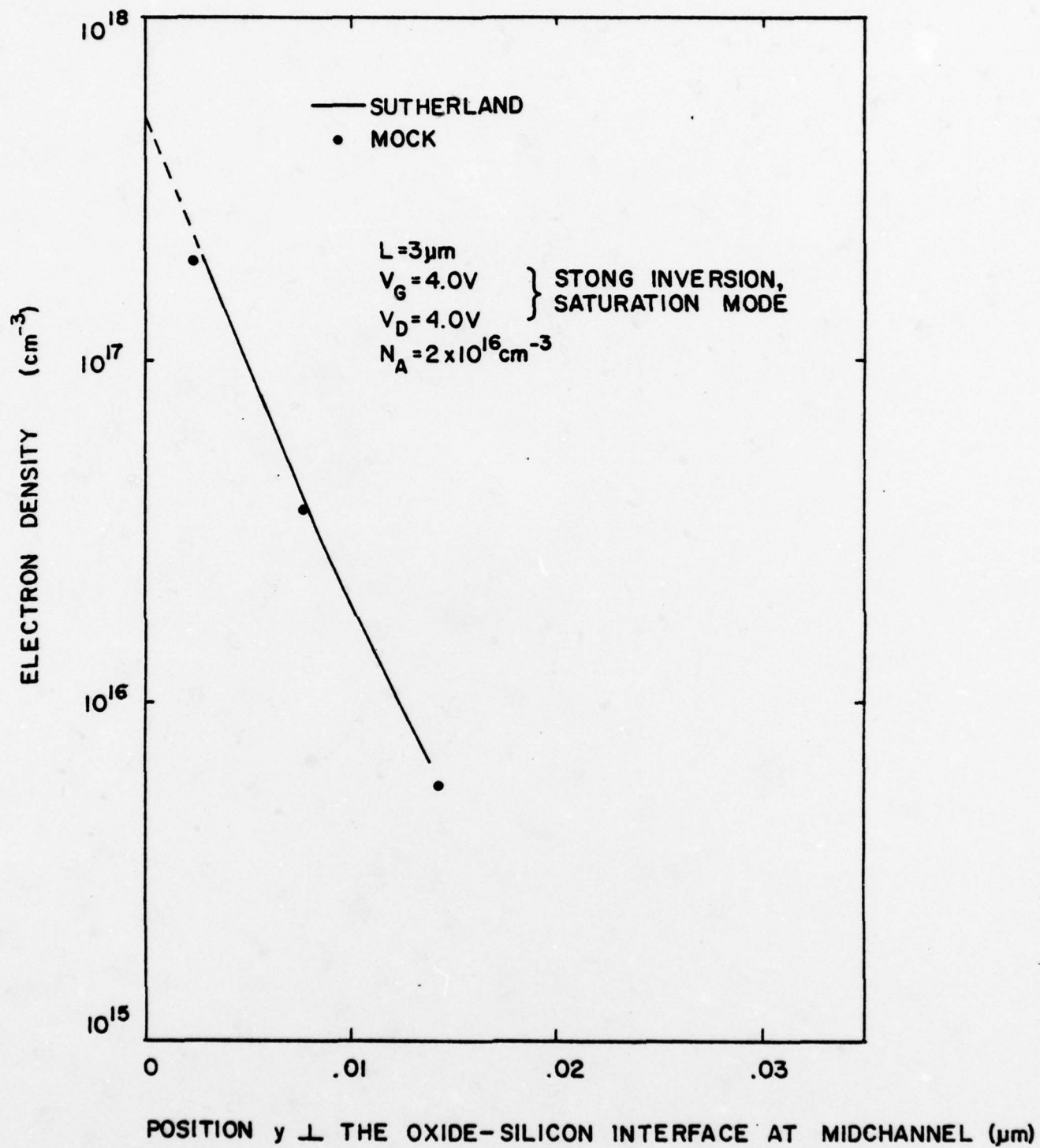


Figure 22 Comparison of the electron number density $n(y)$ along the plane midway between source and drain, generated by this model and by Mock's model.

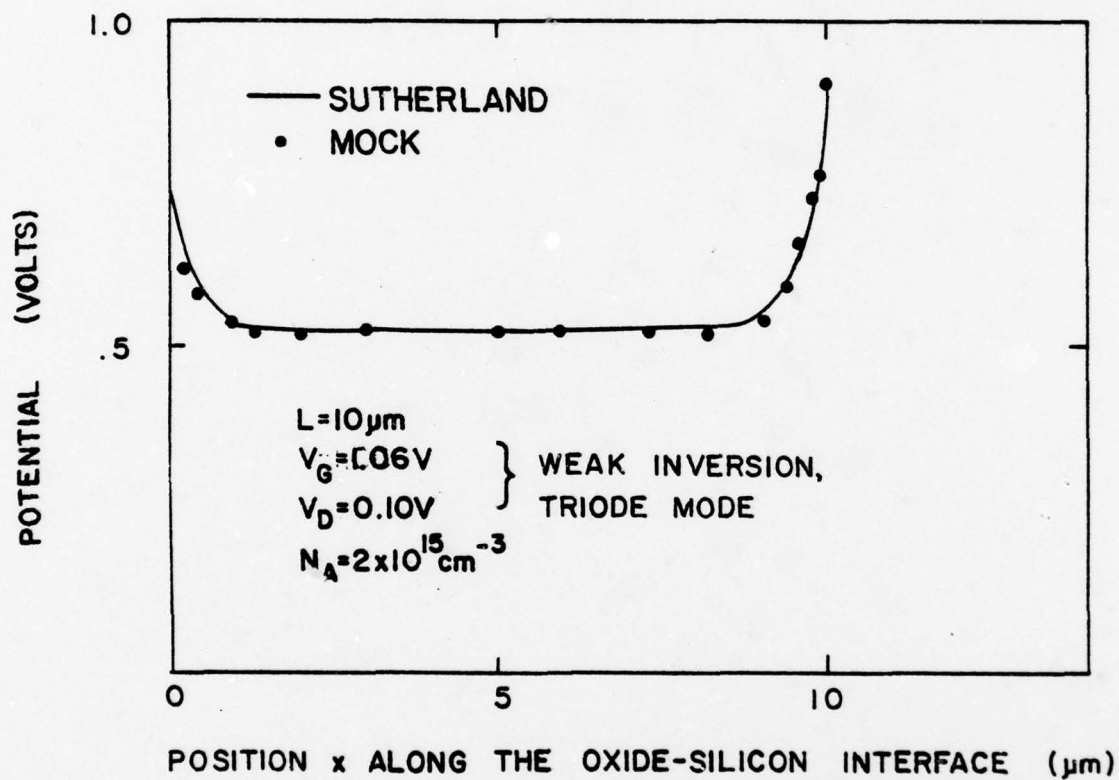


Figure 23 Comparison of the potential $\psi(x)$ along the oxide silicon interface, generated by this model and by Mock's model.

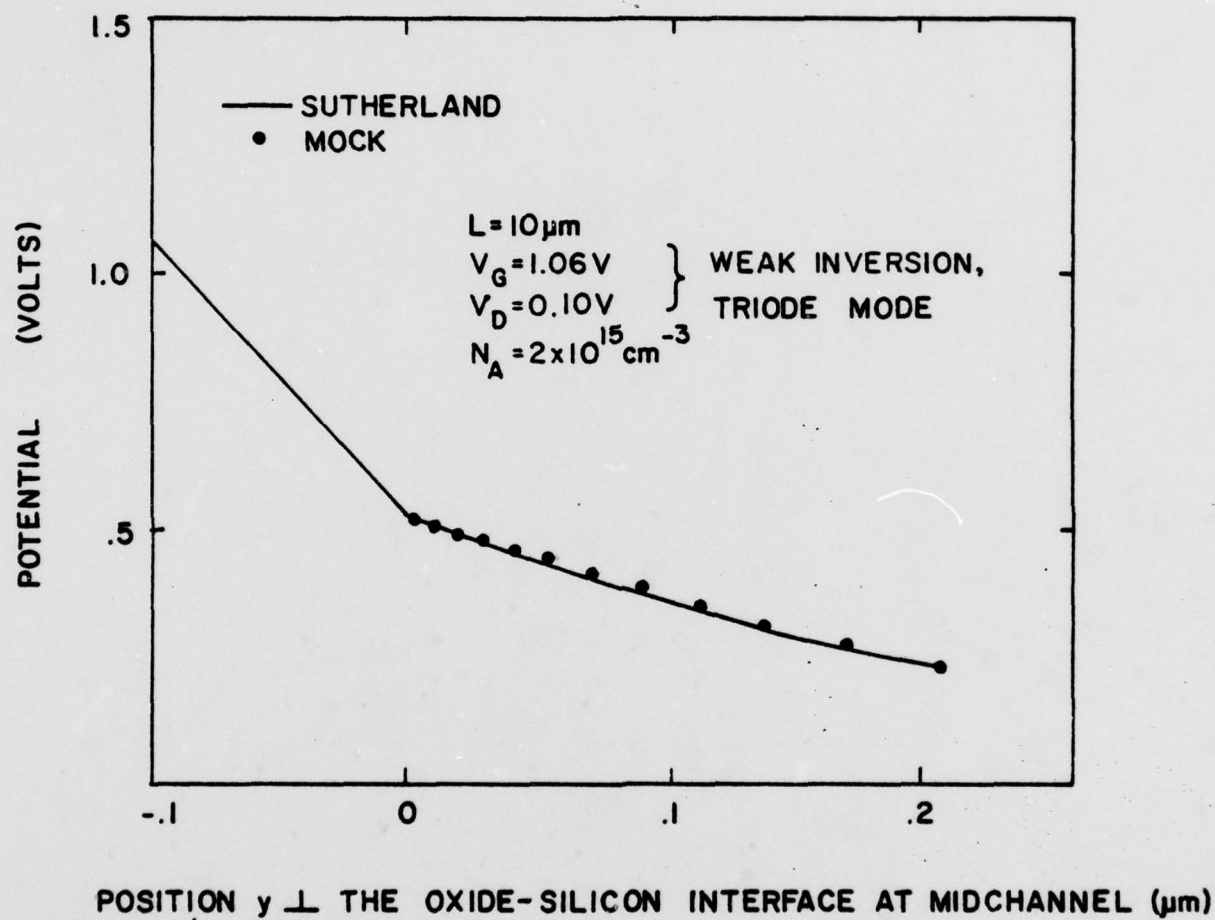


Figure 24 Comparison of the potential $\psi(y)$ along the plane midway between source and drain, generated by this model and by Mock's model.

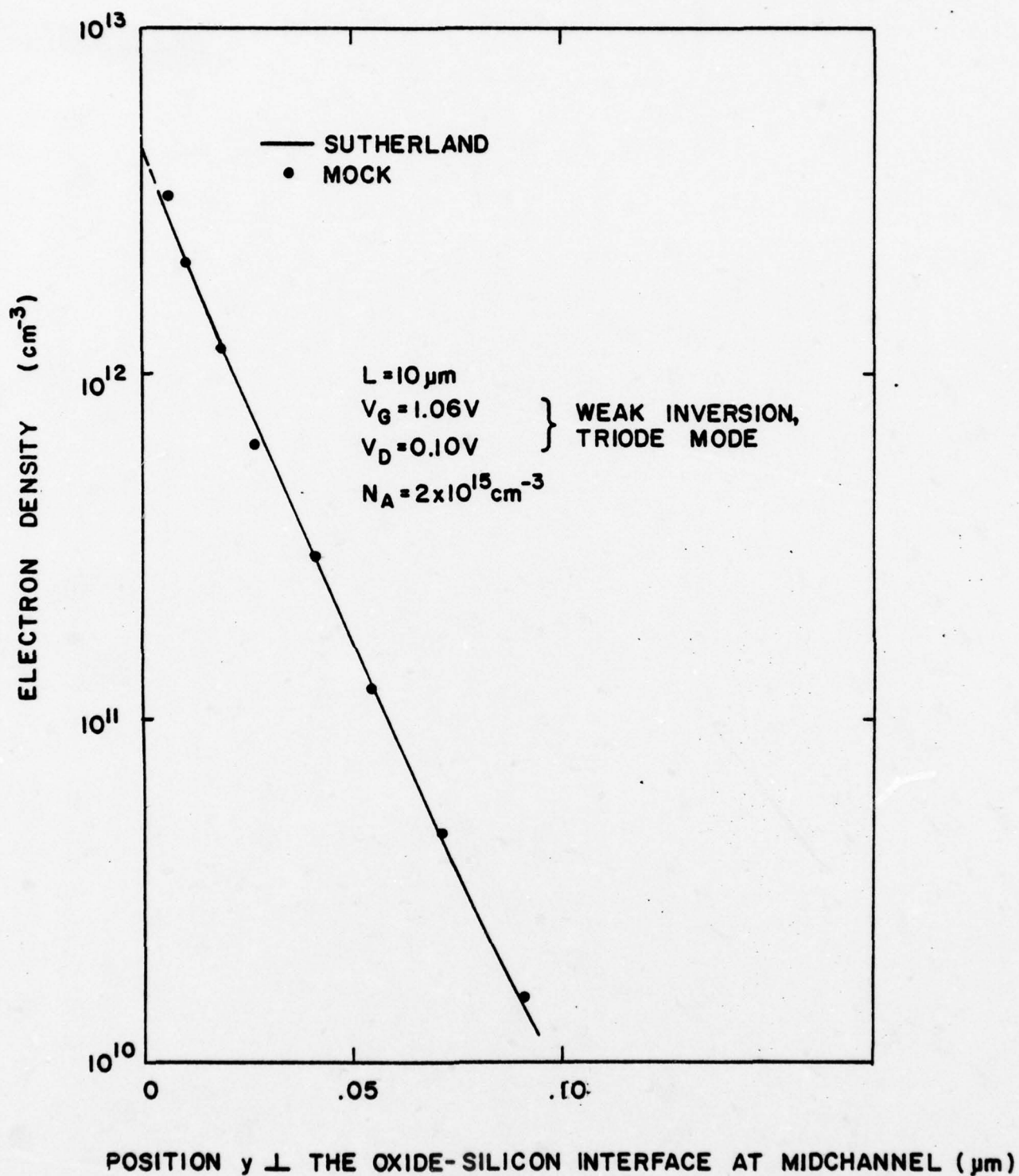


Figure 25 Comparison of the electron number density $n(y)$ along the plane midway between source and drain, generated by this model and by Mock's model.

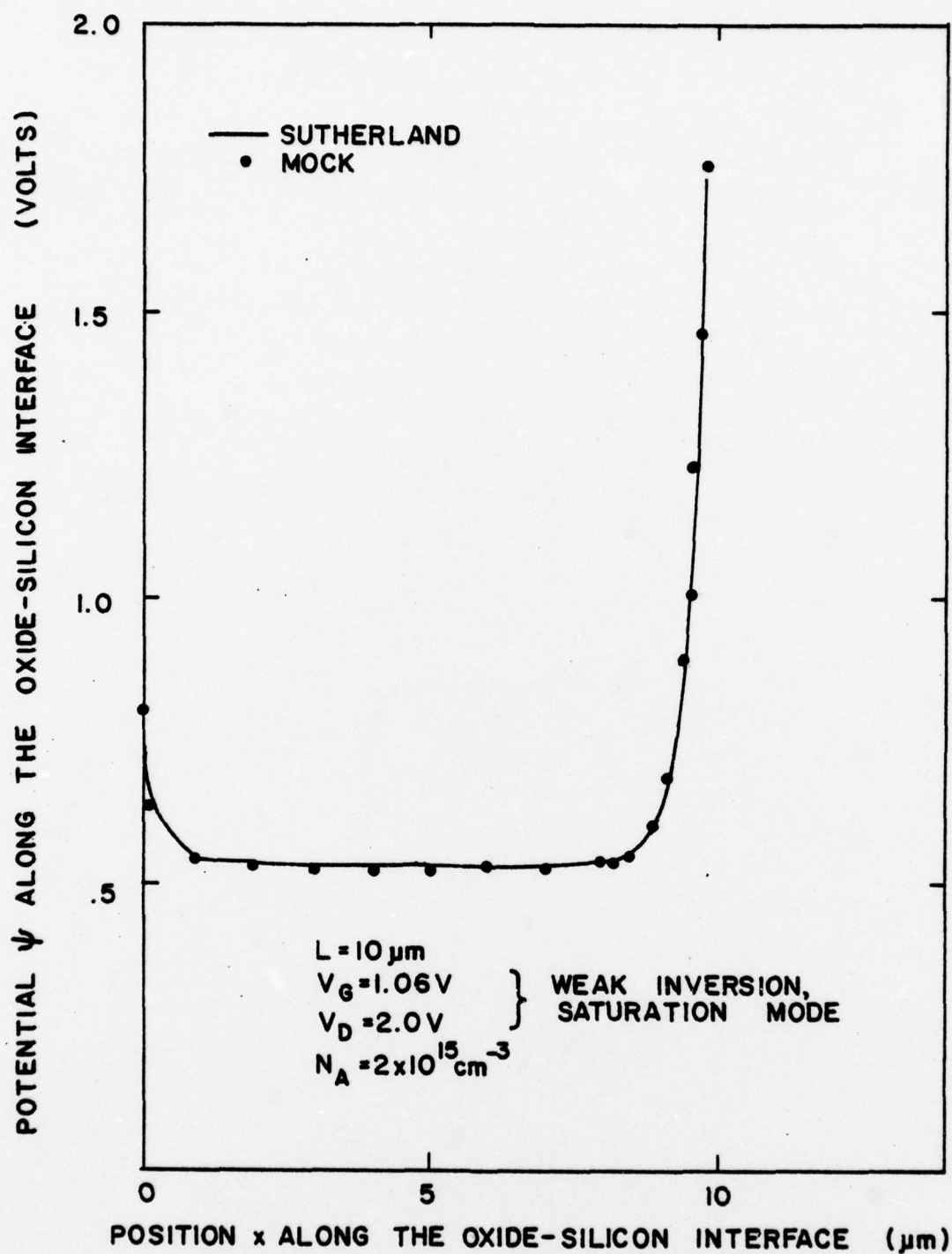


Figure 26 Comparison of the potential $\psi(x)$ along the oxide silicon interface, generated by this model and by Mock's model.

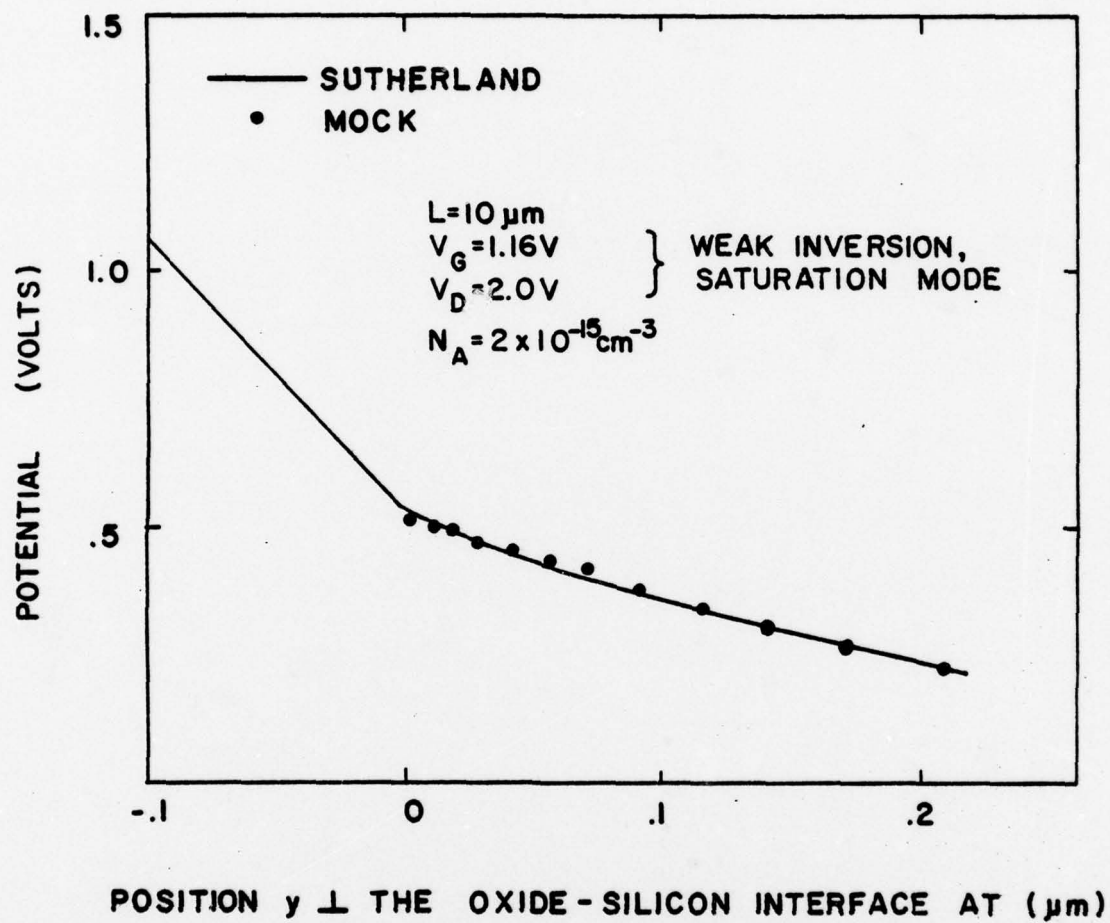
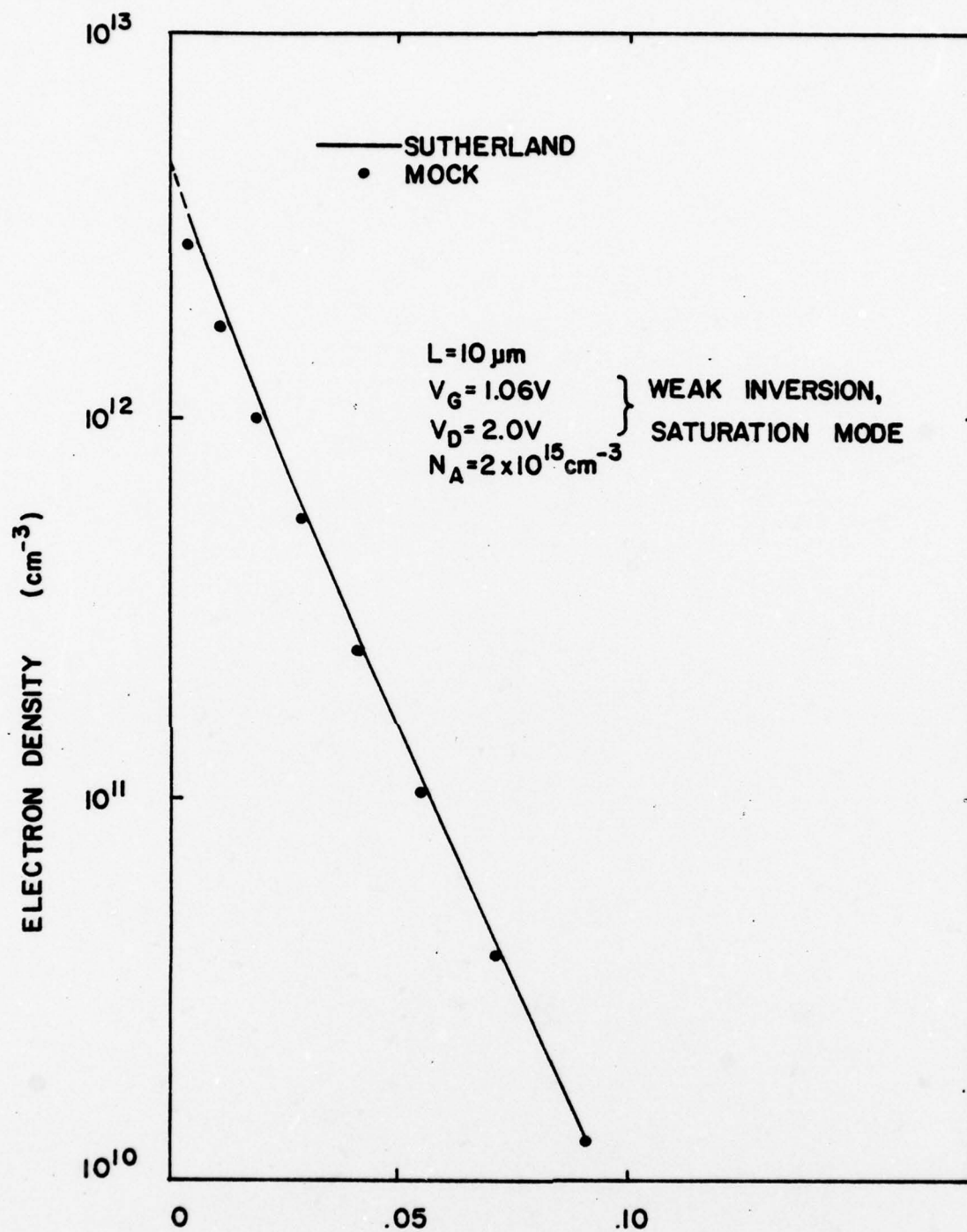


Figure 27 Comparison of the potential $\psi(y)$ along the plane midway between source and drain, generated by this model and by Mock's model.



POSITION $y \perp$ THE OXIDE-SILICON INTERFACE AT MIDCHANNEL (μm)

Figure 28 Comparison of the electron number density $n(y)$ along the plane midway between source and drain, generated by this model and by Mock's model.

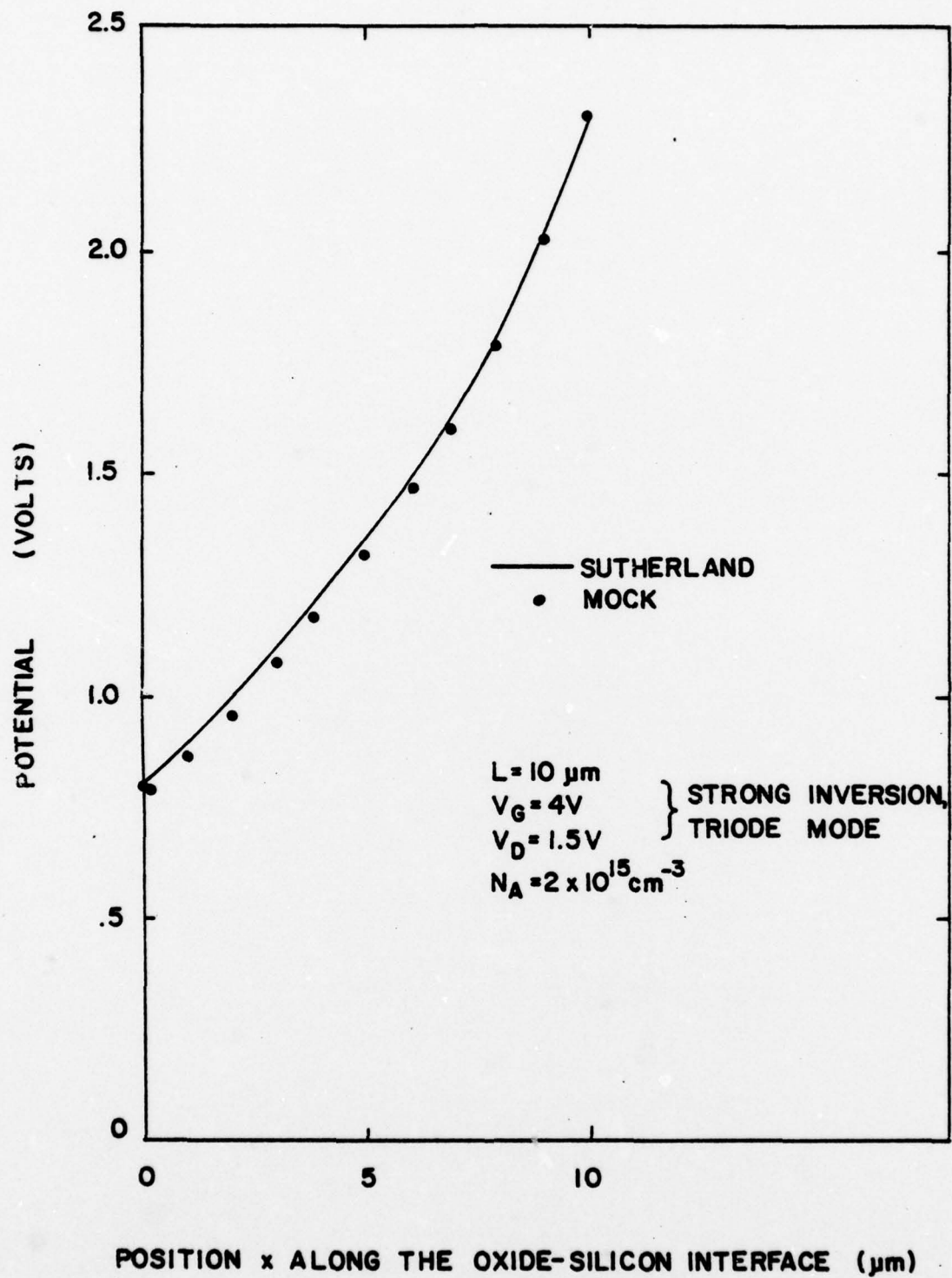


Figure 29 Comparison of the potential $\psi(x)$ along the oxide silicon interface, generated by this model and by Mock's model.

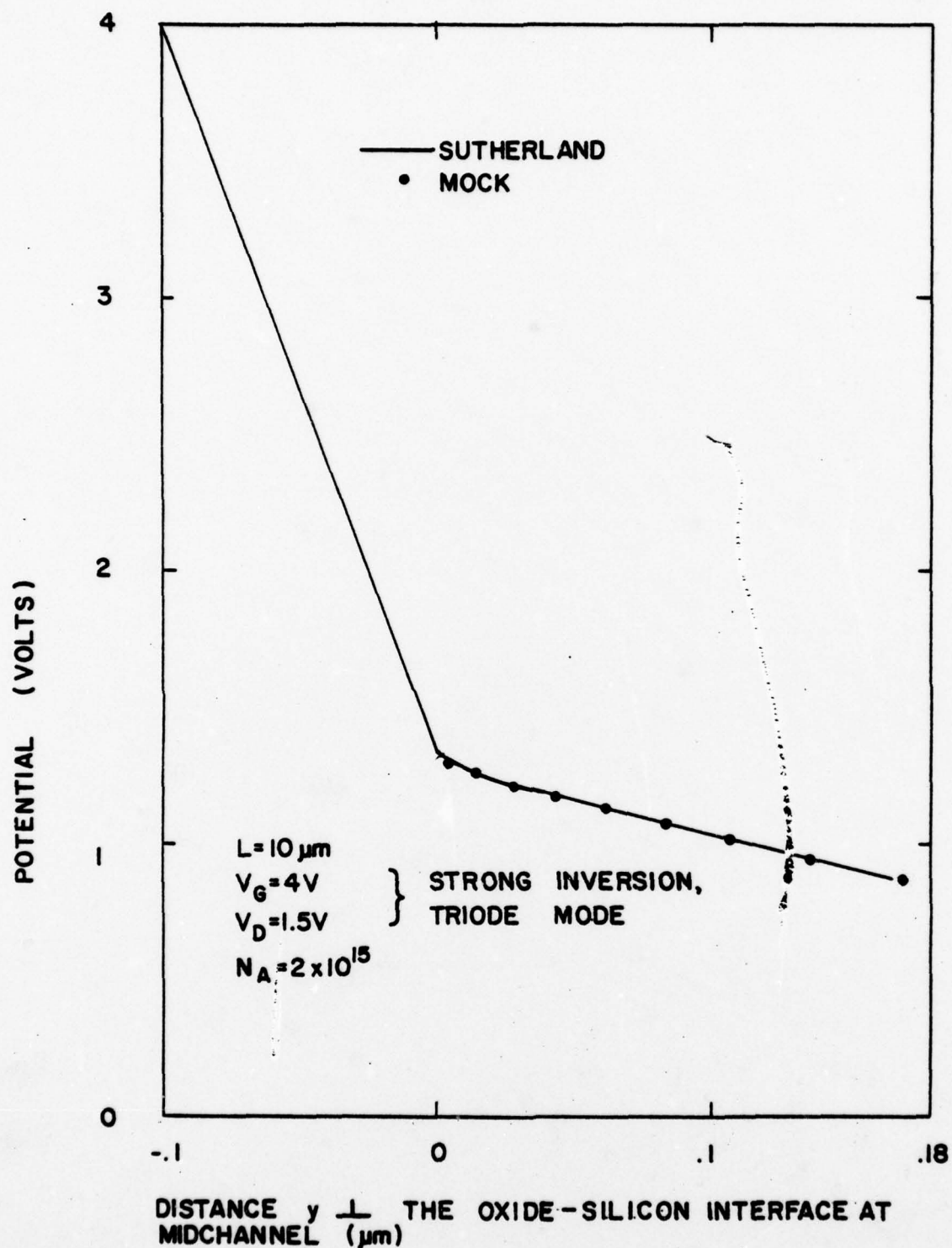
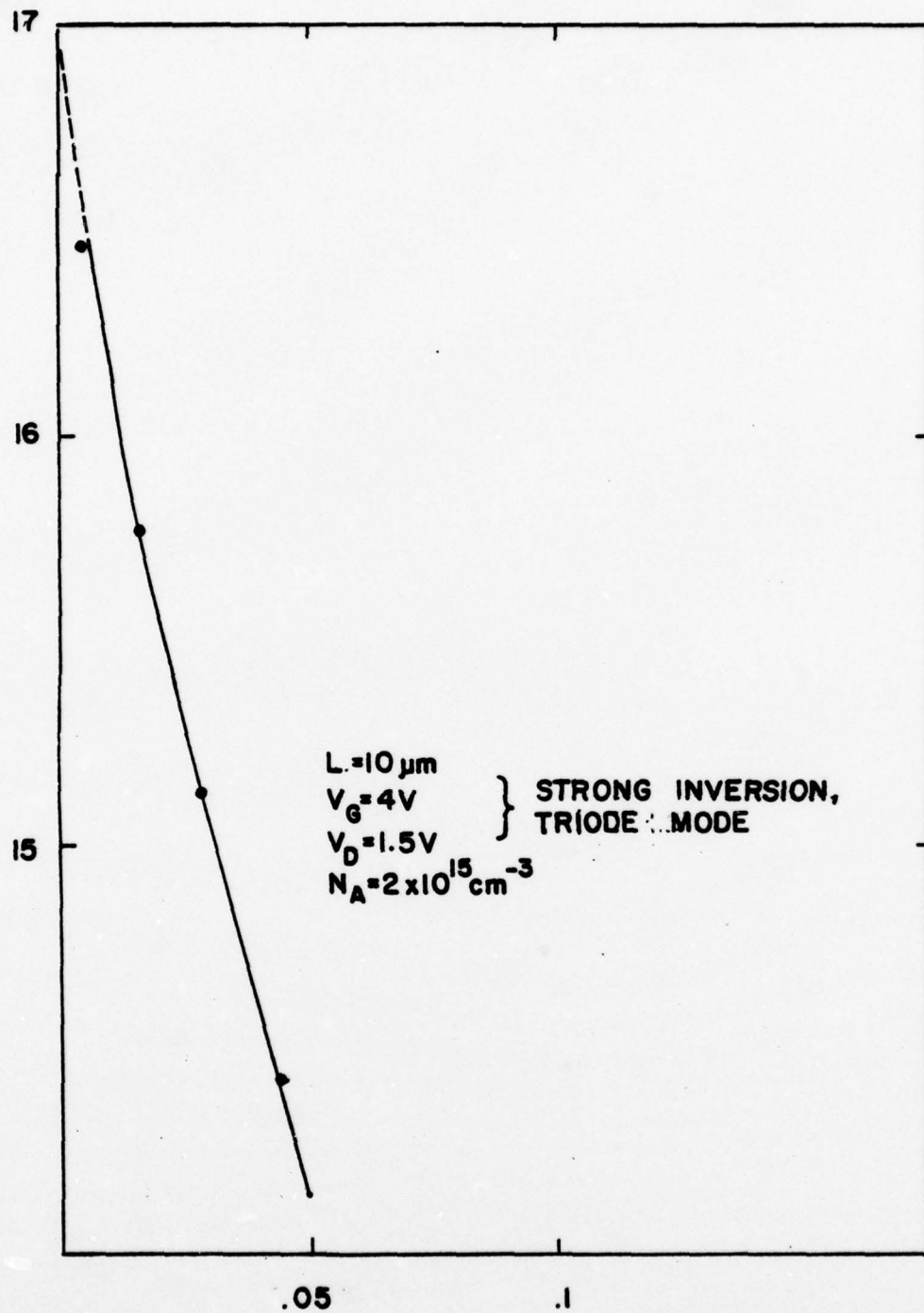


Figure 30 Comparison of the potential $\psi(y)$ along the plane midway between source and drain, generated by this model and by Mock's model.



RUN 8 #3

Figure 31 Comparison of the electron number density $n(y)$ along the plane midway between source and drain, generated by this model and by Mock's model.

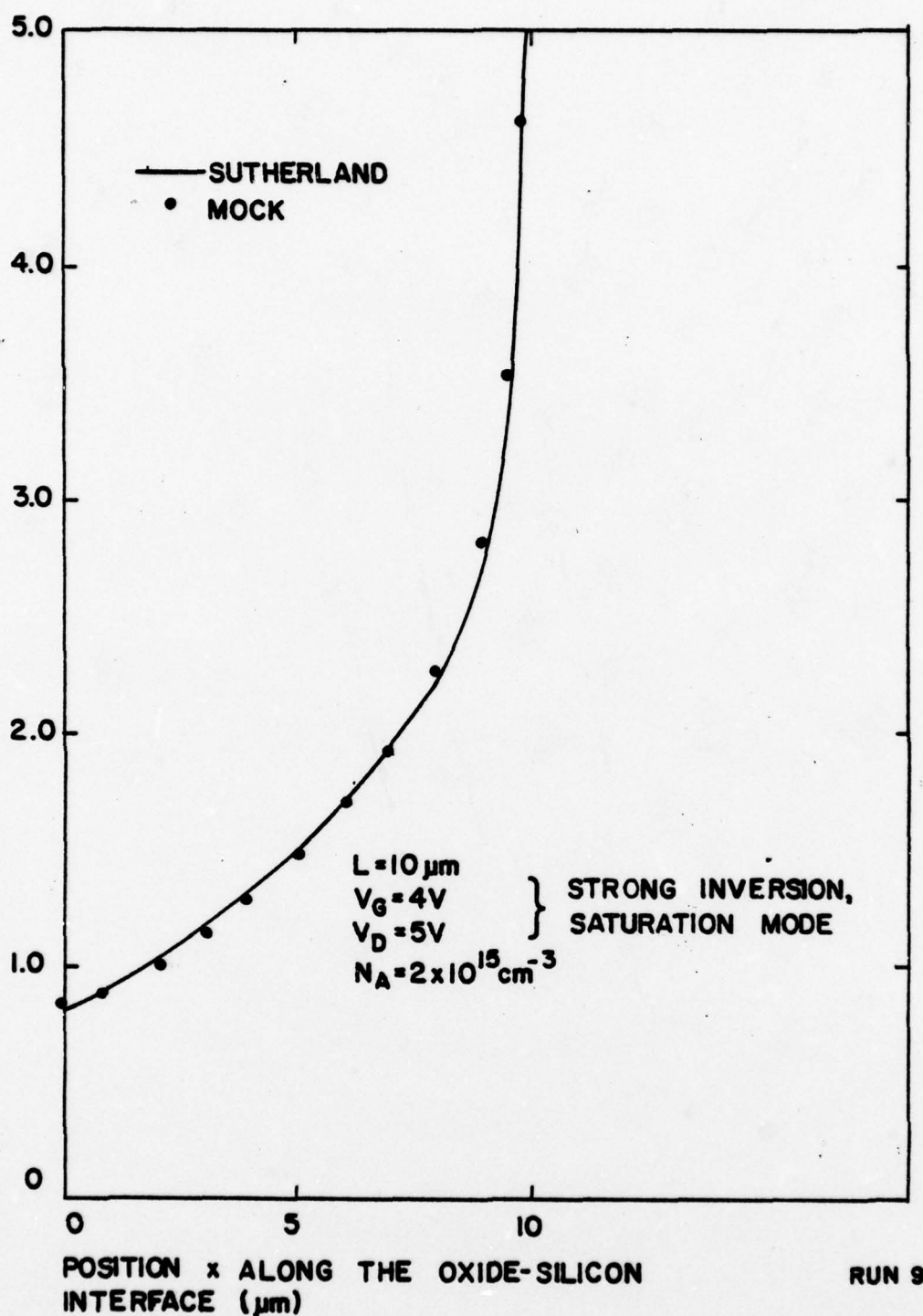


Figure 32 Comparison of the potential $\psi(x)$ along the oxide silicon interface, generated by this model and by Mock's model.

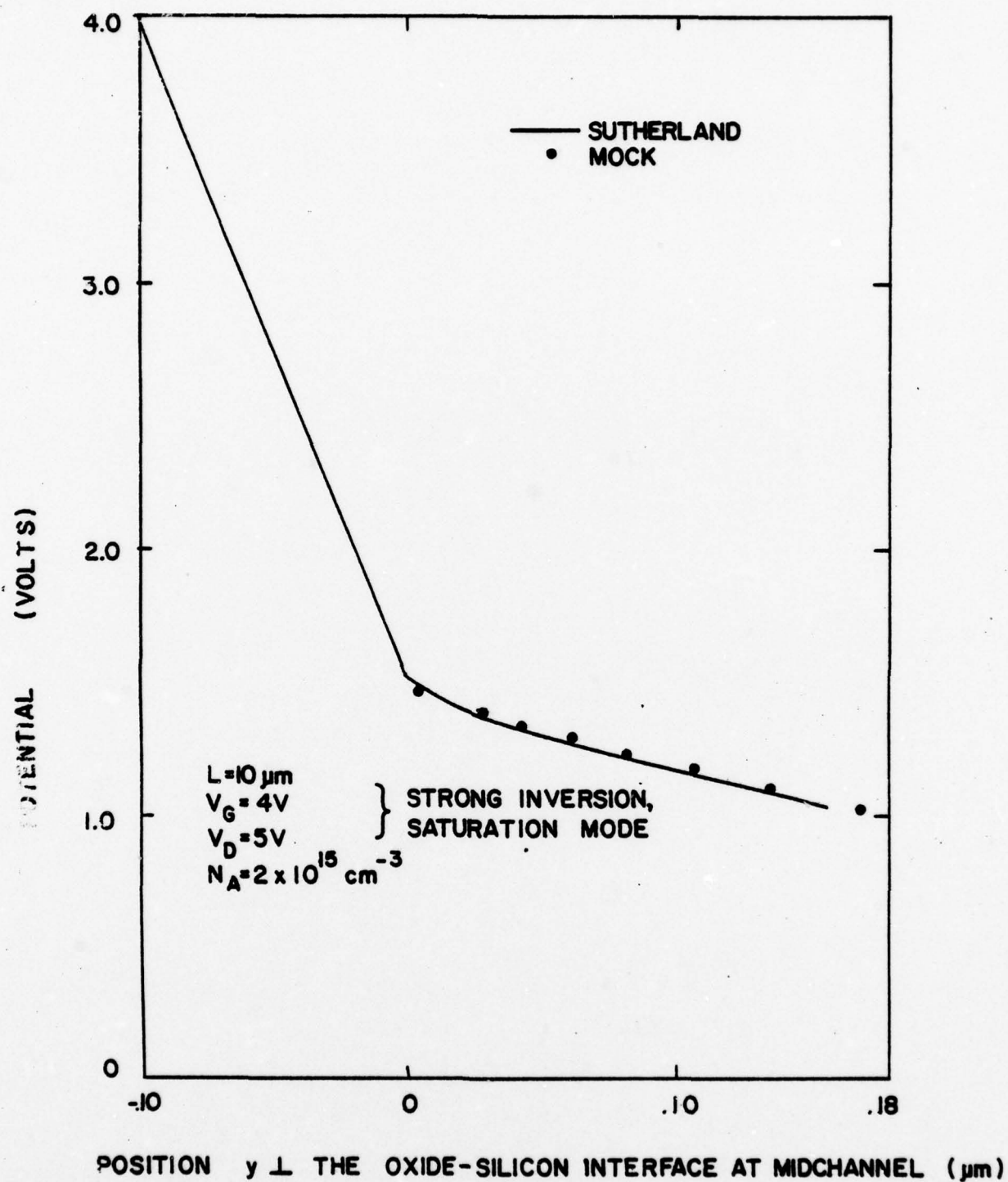


Figure 33 Comparison of the potential $\psi(y)$ along the plane midway between source and drain, generated by this model and by Mock's model.

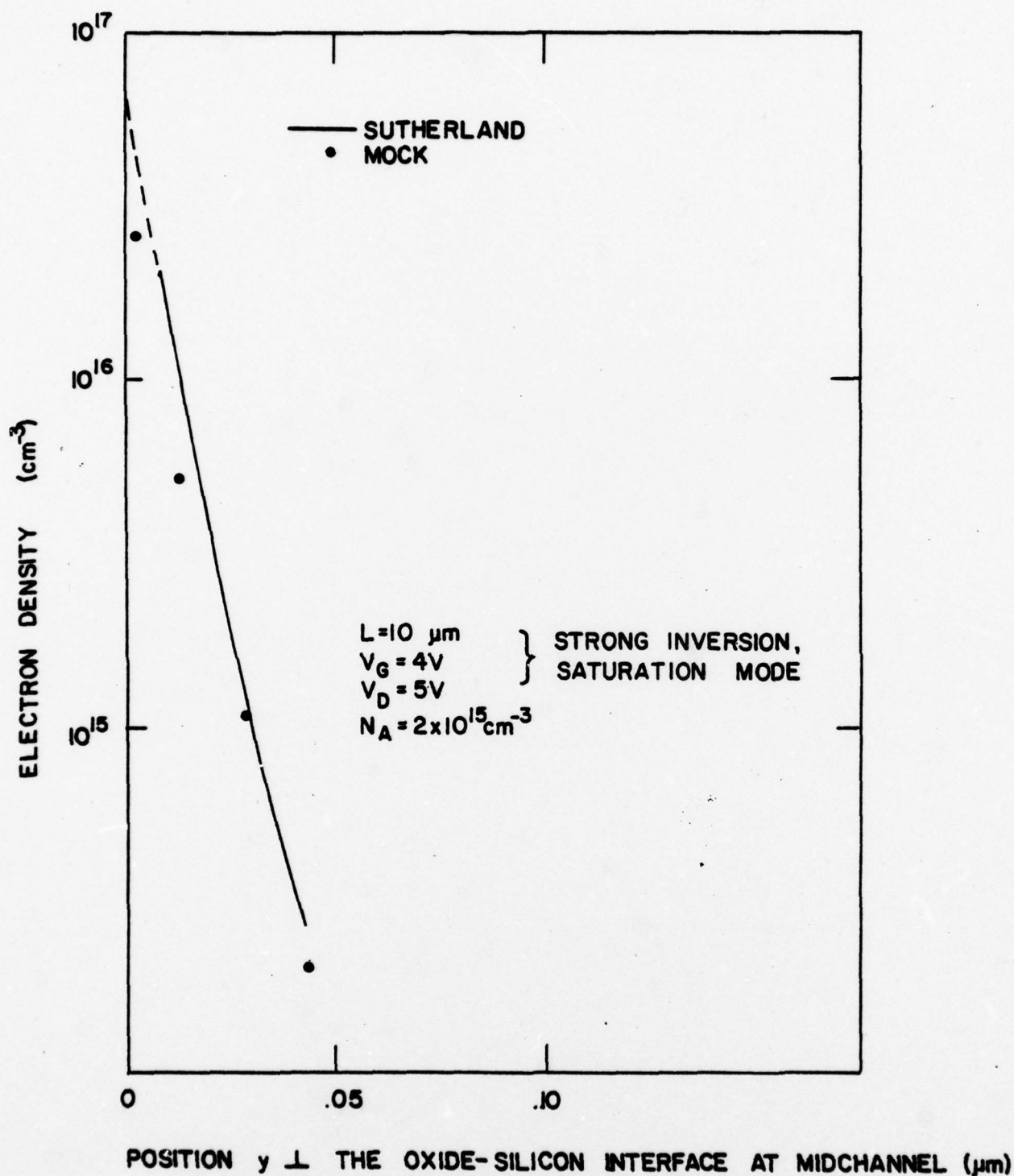


Figure 34 Comparison of the electron number density $n(y)$ along the plane midway between source and drain, generated by this model and by Mock's model.

Table II compares the drain currents calculated by our model with those calculated by Mock's program for these eight cases

TABLE II -- COMPARISON OF DRAIN CURRENT CALCULATIONS
(ma/cm of channel width)

Case		Our Model	Mock
L=3 μ m	Weak inversion, triode	.00164	.00127
	Weak inversion, saturation	.00184	.00148
	Strong inversion, triode	11.4	11.2
	Strong inversion, saturation	12.9	12.95
L=10 μ m	Weak inversion, triode	.000180	.000163
	Weak inversion, saturation	.000193	.000180
	Strong inversion, triode	23.4	22.9
	Strong inversion, saturation	27.8	29.0

It is seen that, in very weak inversion, the drain currents predicted by our model are only in fair agreement with those predicted by Mock's program, but in strong inversion the agreement is quite satisfactory. Insofar as the comparison of solution details is concerned, Figures 11 through 34 show essentially excellent agreement.

2.0 Comparison with Experiment

The experimental data with which we next compare our model were supplied to the author by Dr. D.L. Fraser, Jr. from measurements taken in conjunction with his Ph.D. dissertation [13], using the PMOS reliability test chips supplied

- [13] D.L. Fraser, Jr., "Modeling and Optimization of MOSFET LSI Circuits," Ph.D. Dissertation, University of Florida, 1977. (This work was supported by the National Science Foundation, NSF Grant ENG-75-23078.)

by the National Security Agency, together with data on five additional test chips taken by NSA. The numerous test site configurations available on those chips, in addition to a silicon gate PMOS structure enabled Fraser to characterize the MOS device and its parameters in some detail. Full details are given in [13]. In particular such parameters as the device channel length and width, the oxide thickness, the substrate doping, the source and drain doping, the gate threshold voltage V_T , and the flatband voltage V_{FB} are all deduced from such measurements. From these data, we deduced the effective mobility of holes in the inversion channel, ($182 \text{ cm}^2/\text{volt-sec}$) as well. Thus, this appeared to the author to be an ideal structure for comparing the theoretical predictions of our model with experimental reality.

To utilize our model, which is for n-channel structures, to model the p-channel device, only two steps are necessary: (1) replace the electron mobility with the hole mobility, and (2) reverse the sign of Q_{ss} , since a positive Q_{ss} raises the threshold for a p-channel device, while lowering it for an n-channel device. Hence, to raise the threshold with an n-channel model, negative Q_{ss} should be used. We used an "effective" Q_{ss} ($Q_{ss}^{\text{eff}} = C_{ox} V_{FB}$), with V_{FB} the flatband voltage deduced from Fraser's measurements.

Figures 35 and 36 show comparisons of the drain current predicted with our model with Fraser's measurements. Figure 35 is for a fixed gate voltage putting the device into strong inversion ($V_{GS} = 10\text{V}$, with $V_T = 2.18\text{V}$). Figure 36 gives drain current versus V_{GS} , with the drain connected to the gate, so that $V_{DS} = V_{GS}$, and includes the weak inversion case as well. The results obtained are quite gratifying.

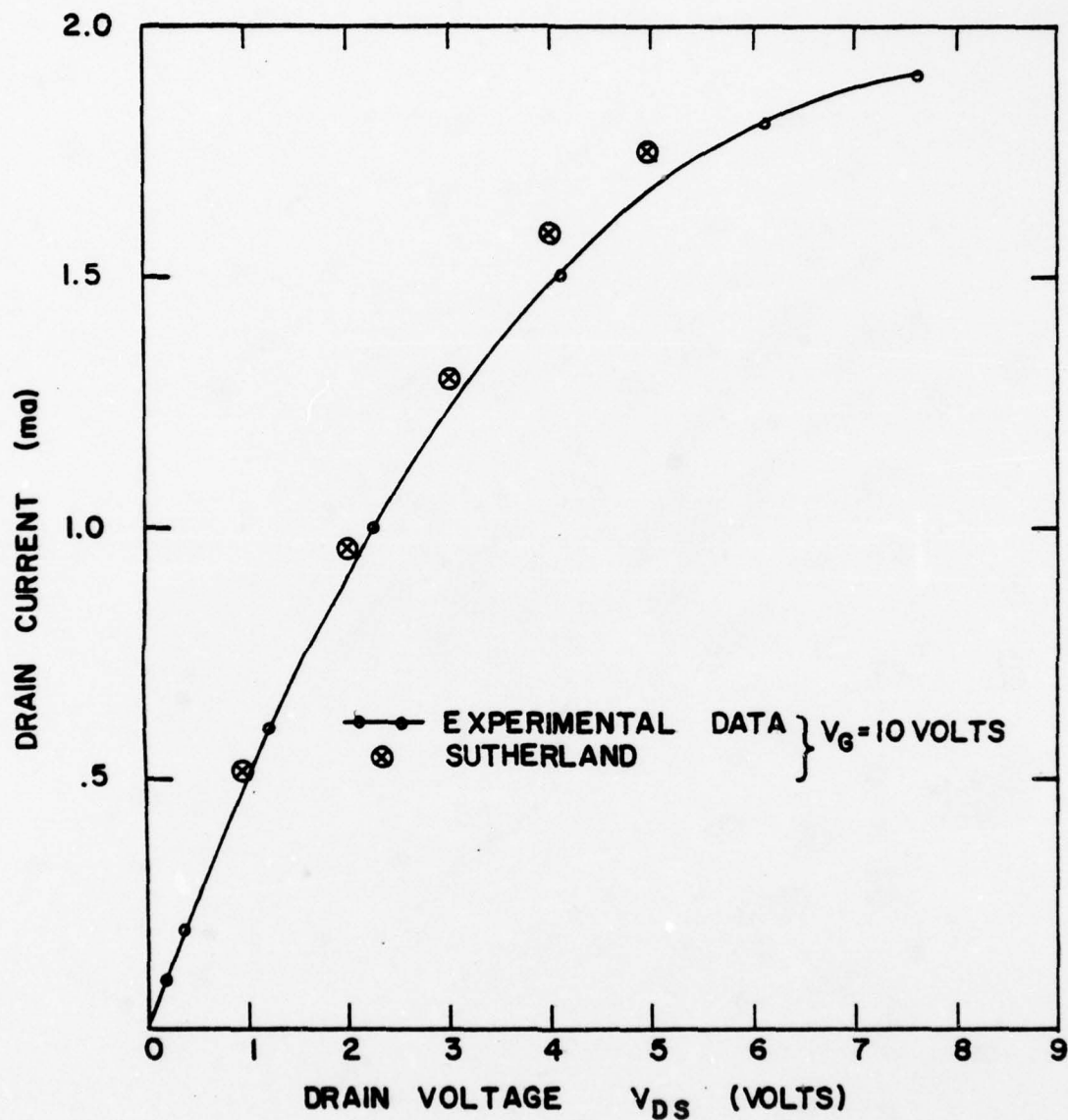


Figure 35 Comparison of the theory with experimental data obtained from a p-channel MOSFET device whose parameters were characterized by means of test sites on its chip. The curve shows I_D versus V_{DS} , with $V_{GS} = 10$ volts.

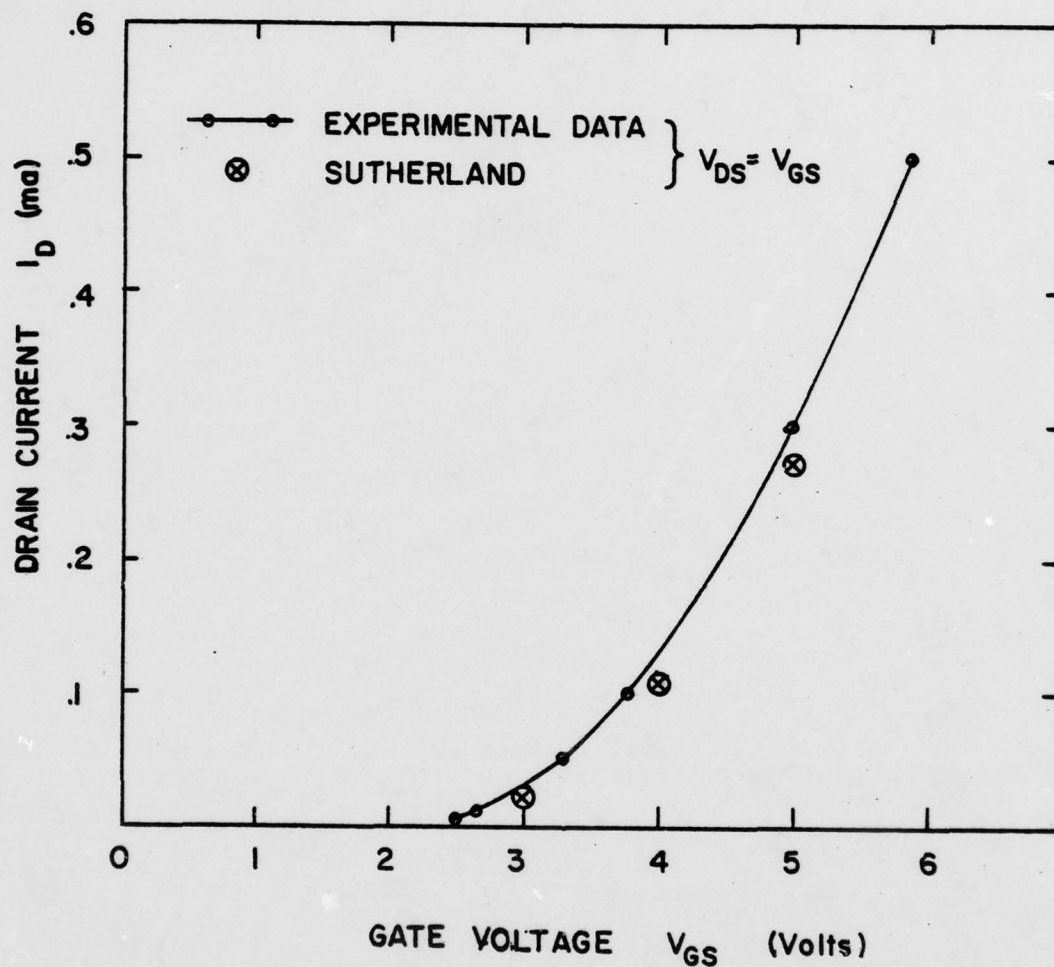


Figure 36 Comparison of the theory with experimental data obtained from a p-channel MOSFET device whose parameters were characterized by means of test sites on its chip. The curve shows I_D versus V_{GS} , with $V_{DS} = V_{GS}$.

CHAPTER III

Instructions for Using the Computer Program

1.0 Input Data

Input data for running the computer model are specified in the form of three NAMELIST data sets: NAMELIST/PRMTRS/, NAMELIST/VOLTGE/, and NAMELIST/CONTRL/. A sample input data set is given in Table III.

TABLE III -- SAMPLE INPUT DATA SET

```
&PRMTRS XCHNL=6.42, YOXIDE=0.100, YJNCTN=0.500, DONOR=9.07D19,  
ACCPTR=8.45D14, QSS=-4.29D-8, EMOB=182.0, XDELTA=0.90, YDELTA=0.85  
IMAX=41, JMAX=25, &END  
&VOLTGE VGDLT=1.00, VGATE0=3.0, VDDLT=1.00, VDRNO=5.00, VSUB=-0.00,  
NGATE=01, NDRAIN=01, &END  
&CONTRL CNVRG1=3.00, CNVRG2=0.02, SIDLT1=.01, SIDLT2=.001,  
THDLT1=.01, THDLT2=.001, ITMAX=200, ITSIMX=200, ITTHMX=200,  
KRSWCH=0, OMEGA=1.6 &END  
EXPERIMENTAL CHECK OF MOSFET MODEL  
A.D. SUTHERLAND  
6/29/77
```

Note that the last 3 cards of the data set provide for a 3-line title by means of which the user may identify the purpose of that particular run. These 3 cards must be present in the data deck, even if left blank. Immediately following the input of these data, a listing of them is printed to provide a record for future reference.

1.01 NAMELIST/PRMTRS/

The data included in this set are:

XCHNL -- Channel length (μm)
YOXIDE -- Oxide thickness (μm)
YJNCTN -- Source and drain junction depth (μm)
DONOR -- Doping density of the source and drain (cm^{-3})
ACCPTR -- Doping density (uniform) of the p-type substrate (cm^{-3})

Q_{SS} -- Surface charge density (coul/cm²)
 $EMOB$ -- Electron mobility (cm²/volt-sec)
 $XDELTA$ -- Graded lattice parameter for the x coordinate
 $YDELTA$ -- Graded lattice parameter for the y coordinate
 $IMAX$ -- # of lattice points in the x direction. This must
 be an odd integer ≤ 41
 $JMAX$ -- # of lattice points in the y direction. This can
 be any integer ≤ 25 .

Regarding Q_{SS} , it is possible to account for work function differences between the gate metallization and the silicon substrate by defining an "effective" Q_{SS} given by $Q_{SS\text{eff}} = C_{ox} V_{FB}$, where C_{ox} is the oxide layer capacitance, $C_{ox} = \kappa_{ox} \epsilon_0 / y_{ox}$ (F/cm²), and where V_{FB} is the flatband voltage of MOS capacitor theory.

The graded lattice parameters $XDELTA$ and $YDELTA$ determine the spacing between lattice points in the following manner. Let $IMID$ be the I-index of the plane midway between the source and the drain. Let $XDLT(IMID)$ be the spacing between that plane and the planes $IMID \pm 1$ immediately to the right and left of the mid-plane. Then the algorithm for determining $XDLT(I)$, given $XDLT(IMID)$, is

$$\begin{aligned}
 XDLT(I-1) &= XDELTA * XDLT(I), & I=3, IMID \\
 XDLT(I+1) &= XDELTA * XDLT(I), & I=IMID+1, IMAX-1
 \end{aligned}$$

where $XDELTA \leq 1$. The graded lattice illustrated in Figure 2, in Chapter I, was generated with $XDELTA = 0.9$, the value suggested by Mock [1]. In a like manner, let $YDLT(2)$ be the vertical lattice spacing at the substrate "contact." Then the algorithm employed for determining $YDLT(J)$, given $YDLT(2)$, is,

$$YDLT(J+1) = YDELTA * YDLT(J), \quad J=3, JMAX-1$$

where $YDELTA \leq 1$. The graded lattice of Figure 2 was generated with $YDELTA = 0.85$, again the value suggested by Mock.

Note that the substrate thickness Y_{SUB} is not specified by the user. It is automatically adjusted to provide a spacing between the substrate contact and the lower edge of the source and drain "contacts" which is 50% greater than the drain space-charge layer width $W_{D, drain}$, calculated from abrupt junction depletion theory, and is readjusted each time the drain voltage changes. This is done to maximize the effectiveness of achieving small spacings between vertically adjacent lattice points in the vicinity of the oxide-silicon interface, while assuring charge neutrality at the substrate "contact."

1.02 NAMELIST/VOLTGE/

The data specified in this set are:

VGDLT -- Gate voltage increment (volts)
 VGATEØ -- Starting gate voltage (volts)
 VDDLTL -- Drain voltage increment (volts)
 VDRNØ -- Starting drain voltage (volts)
 VSUB -- Applied substrate voltage (volts) with $V_{SUB} \leq 0$
 NGATE -- # of gate voltage increments
 NDRAIN -- # of drain voltage increments

The meaning of these parameters is as follows. The program has been written to function in the manner of a curve-tracer which plots families of curves of I_D versus V_{DS} , with V_{GS} varied as a parameter. The initial gate voltage is set equal to $VGATEØ$, and subsequent gate voltages are incremented upward in increments of $VGDLT$, until $NGATE$ such voltages have been treated. The parameter $NDRAIN$ determines the number of drain voltages at which the drain current I_D is to be determined. The lowest drain voltage used is $VDRNØ$. The drain voltage is then incremented upward in increments of $VDDLTL$, until $NDRAIN$ voltage values have been treated. The gate voltage is then incremented, and the process is repeated. During this sequence, the substrate voltage remains fixed. The user should always make an estimate of the threshold gate voltage, and specify $VGATEØ \geq V_T$.

1.03 NAMelist/CONTRL/

The parameters in this data set provide the user a degree of control over the iteration process and, as described in Chapter I, allow him to specify whether the "Picard and Gummel" relaxation procedure devised by Mock, or the "Overrelaxed Gummel" procedure devised by the author is to be used. The parameters appearing in this data set are:

- CNVRG1 -- "Coarse" and "Tight" convergence criteria for
CNVRG2 the Picard and Gummel algorithms.
- SIDLT1 -- "Coarse" and "Tight" convergence criteria for
SIDLT2 Stone's method for finding ψ .
- THDLT1 -- "Coarse" and "Tight" convergence criteria for
THDLT2 the Block-Line iteration for finding θ .
- ITMAX -- Maximum number of iterations to be allowed with
 the Picard and Gummel algorithms.
- ITSIMX -- Maximum number of iterations to be allowed with
 Stone's method.
- ITTHMX -- Maximum number of iterations to be allowed with
 Block-Line iteration.
- KRSWCH -- "Flag" to specify which iteration scheme is to
 be used. KRSWCH=0 causes only Gummel's algorithm
 to be applied, with full donor density and "tight"
 convergence criteria. KRSWCH=1 causes Mock's
 approach to be implemented, viz. Picard iteration
 at reduced donor density until "coarse" convergence
 is achieved, followed by Gummel's algorithm at
 full donor density, with "tight" convergence criteria.
- OMEGA -- Overrelaxation parameter used with the Gummel algo-
 rithm, as described in Section 4.03.

Table IV lists the values of the iteration control parameters which have been found to work well for gate and drain voltages ≤ 10 volts.*

TABLE IV -- RECOMMENDED CONTROL PARAMETERS

CNVRG1 = 3.0
CNVRG2 = .02
SIDLT1 = .01
SIDLT2 = .001
THDLT1 = .01
THDLT2 = .001
ITMAX = 200
ITSIMX = 100
ITTHMX = 100
OMEGA = 1.6

Concerning the three "maximum iterations" parameters, the program will stop, with a "MAXIMUM ITERATIONS EXCEEDED" message being printed, identifying why it stopped, in the event that this condition is encountered. These three parameters were installed by the author as "safety valves" to avoid excessive computation times when things are going awry. The author encountered program stops due to all three "safety valves" during the course of evaluating and improving the computer program and, with the exception of the "ITMAX EXCEEDED" criterion when using Mock's Picard + Gummel iterative procedure, was able to devise corrective measures to eliminate their occurrence. But the user may expect to encounter the "ITMAX EXCEEDED" exit message, especially under

*The range of gate and drain voltages explored with numerous computer runs was $V_T \leq V_G < 10V$ (V_T is the threshold gate voltage for inversion), and $1 \leq V_D \leq 9V$. The recommended value for ITMAX worked well over this range when the overrelaxed Gummel procedure was in use. However, the Picard + Gummel procedures frequently required excessive iterations, especially under conditions of strong inversion.

conditions of strong inversion, if he elects to use that procedure by setting KRSWCH=1. In the author's experience, both Stone's iterative procedure (limited by ITSIMX) and the block-line iterative procedure for the stream function (limited by ITTHMX), require only a small fraction of the "recommended" limits stated in Table IV.

2.0 Output Data

Table V (17 sheets) illustrates the output data printed by the program. A complete set of these data are printed for each pair of voltages V_G, V_D , and the user may not desire all of this data. In that event, he may wish to modify SUBROUTINE OUTPUT to suit his particular needs. Some plotting routines would also be helpful, but the author did not have sufficient time available to develop same.

All output data are listed in physical units, the conversion from normalized to unnormalized variables being implemented in SUBROUTINE OUTPUT. What these data represent will next be described.

Sheet 1 of Table V summarizes the three voltages V_G, V_D , and V_B , then gives the corresponding drain current I_D in milliamperes/cm of channel width. Next, is printed the substrate thickness which is automatically determined in the manner described above. Following this are listed in columns, the following results,

- X -- The x coordinate (μm).
- PSI -- The electrostatic potential at the silicon surface (volts).
- PHIN -- The electron quasi-Fermi potential ϕ'_n along the row $J=J_{\text{MAX}}$, just below the silicon surface.
- QI -- The total inversion charge Q_i (coulombs/cm²) at position x.
- QD -- The total depletion charge Q_D (coulombs/cm²) at position x.
- YI -- The inversion layer thickness (μm) at position x.
- YD -- The depletion layer thickness (μm) at position x.

Note that YI and YD are quantized because they can only be approximated, due to the quantized nature of the lattice of mesh points at which they can be determined.

The remaining data in Table V provide information about selected variables in the bulk silicon substrate. They are,

- PSI(I,J) -- Electrostatic potential ψ' (volts) at the ψ -lattice points corresponding to the lattice indices (I,J). (Sheets 2 and 3)
- EDENS(I,J) -- The electron density n' (cm^{-3}) at the ψ -lattice points corresponding to the lattice indices (I,J). (Sheets 4 and 5)
- HDENS(I,J) -- The hole density p' (cm^{-3}) at the ψ -lattice points corresponding to the lattice indices (I,J). (Sheets 6 and 7)
- THETA(I,J) -- The stream function θ (dimensionless) at the θ -lattice points corresponding to the lattice indices (I,J). (See Figure 4.) (Sheets 8 and 9)
- ESUBX(I,J) -- The x-directed component of the electric field E'_x , (volts/cm) at the θ -lattice coordinates corresponding to the lattice index I, and the ψ -lattice coordinates corresponding to the lattice index J. (Sheets 10 and 11)
- ESUBY(I,J) -- The y-directed component of the electric field, E'_y , (volts/cm) at the ψ lattice coordinates corresponding to the lattice index I, and the θ -lattice coordinates corresponding to the lattice index J. (Sheets 12 and 13)
- JSUBX(I,J) -- The x-directed component of the electron current density, J'_x , (amps/cm^2) at the θ -lattice coordinates corresponding to the lattice index I, and the ψ -lattice coordinates corresponding to the lattice index J. (Sheets 14 and 15)

JSUBY(I,J) -- The y-directed component of the electron current density, J'_y , (amps/cm²) at the ψ -lattice coordinates corresponding to the lattice index I, and the θ -lattice coordinates corresponding to the lattice index J. (Sheets 16 and 17)

In the case of Sheets 2 through 17 of Table IV, the data are formatted in an identical manner. Across the top of the even numbered sheets is listed the x'-coordinate corresponding to the lattice index I. (ψ -lattice, or θ -lattice, as the case may be.) The first two columns list the lattice index J, and the corresponding y'-coordinate. (Again, ψ -lattice or θ -lattice, as the case may be.) Both coordinates are expressed in micrometers. The remaining columns give the values of the variable indicated in the legend printed just below the listing of the x'-coordinate values. One scans each horizontal group of data (corresponding to a given lattice index J) in the manner of reading a printed page. Scanning first the listing of X(I) at the top of the sheet, one finds the corresponding value of the variable of interest in the corresponding location in the listing for the value of Y(J) (Column 2). In this manner, the two-dimensional solution for these variables is obtained.

3.0 Glossary of the Variables Appearing in COMMON Statements

Five COMMON blocks are defined in the computer program: ARRAYS, COEFF, REAL, INTGR, NRMLZE. The FORTRAN variables contained therein are next defined.

3.01 COMMON/ARRAYS/

PSI(41,30) -- The electrostatic potential ψ .

EDENS(41,25) -- The electron density n.

HDENS(41,25) -- The hole density p.

THETA(40,25) -- The stream function θ .

B(41,30)	} -- Stone's coefficients B,D,E,F,H, and Q. (Also used for the Block-line iteration for θ , in the same context.)
D(41,30)	
E(41,30)	
F(41,30)	
H(41,30)	
Q(41,30)	

VG=	3.00U+00	VOLTS
VD=	8.00U+00	VOLTS
VB=	0.0	VOLTS
ID=	-6.17U-01	MILLIAMPERES

SUMMARY OF CONDITIONS ALONG THE SILICON-OXIDE INTERFACE :

YD
 VI
 UD
 QI
 PHIN
 PSI
 X

[illegible]

[illegible]

[illegible]

10	9	8	7	6	5	4	3	2	1
2.260.00	10.010.00	6.450.00	5.200.00	6.350.00	7.160.00	9.180.00	1.000.00	1.280.00	1.510.00

[illegible]

1	2	3	4	5	6	7	8	9	10	11	12	13	14	15	16	17	18	19	20	21	22	23	24	25	26	27	28	29	30	31	32	33	34	35	36	37	38	39	40	41	42	43	44	45	46	47	48	49	50	51	52	53	54	55	56	57	58	59	60	61	62	63	64	65	66	67	68	69	70	71	72	73	74	75	76	77	78	79	80	81	82	83	84	85	86	87	88	89	90	91	92	93	94	95	96	97	98	99	100
1	2	3	4	5	6	7	8	9	10	11	12	13	14	15	16	17	18	19	20	21	22	23	24	25	26	27	28	29	30	31	32	33	34	35	36	37	38	39	40	41	42	43	44	45	46	47	48	49	50	51	52	53	54	55	56	57	58	59	60	61	62	63	64	65	66	67	68	69	70	71	72	73	74	75	76	77	78	79	80	81	82	83	84	85	86	87	88	89	90	91	92	93	94	95	96	97	98	99	100
1	2	3	4	5	6	7	8	9	10	11	12	13	14	15	16	17	18	19	20	21	22	23	24	25	26	27	28	29	30	31	32	33	34	35	36	37	38	39	40	41	42	43	44	45	46	47	48	49	50	51	52	53	54	55	56	57	58	59	60	61	62	63	64	65	66	67	68	69	70	71	72	73	74	75	76	77	78	79	80	81	82	83	84	85	86	87	88	89	90	91	92	93	94	95	96	97	98	99	100
1	2	3	4	5	6	7	8	9	10	11	12	13	14	15	16	17	18	19	20	21	22	23	24	25	26	27	28	29	30	31	32	33	34	35	36	37	38	39	40	41	42	43	44	45	46	47	48	49	50	51	52	53	54	55	56	57	58	59	60	61	62	63	64	65	66	67	68	69	70	71	72	73	74	75	76	77	78	79	80	81	82	83	84	85	86	87	88	89	90	91	92	93	94	95	96	97	98	99	100
1	2	3	4	5	6	7	8	9	10	11	12	13	14	15	16	17	18	19	20	21	22	23	24	25	26	27	28	29	30	31	32	33	34	35	36	37	38	39	40	41	42	43	44	45	46	47	48	49	50	51	52	53	54	55	56	57	58	59	60	61	62	63	64	65	66	67	68	69	70	71	72	73	74	75	76	77	78	79	80	81	82	83	84	85	86	87	88	89	90	91	92	93	94	95	96	97	98	99	100
1	2	3	4	5	6	7	8	9	10	11	12	13	14	15	16	17	18	19	20	21	22	23	24	25	26	27	28	29	30	31	32	33	34	35	36	37	38	39	40	41	42	43	44	45	46	47	48	49	50	51	52	53	54	55	56	57	58	59	60	61	62	63	64	65	66	67	68	69	70	71	72	73	74	75	76	77	78	79	80	81	82	83	84	85	86	87	88	89	90	91	92	93	94	95	96	97	98	99	100
1	2	3	4	5	6	7	8	9	10	11	12	13	14	15	16	17	18	19	20	21	22	23	24	25	26	27	28	29	30	31	32	33	34	35	36	37	38	39	40	41	42	43	44	45	46	47	48	49	50	51	52	53	54	55	56	57	58	59	60	61	62	63	64	65	66	67	68	69	70	71	72	73	74	75	76	77	78	79	80	81	82	83	84	85	86	87	88	89	90	91	92	93	94	95	96	97	98	99	100
1	2	3	4	5	6	7	8	9	10	11	12	13	14	15	16	17	18	19	20	21	22	23	24	25	26	27	28	29	30	31	32	33	34	35	36	37	38	39	40	41	42	43	44	45	46	47	48	49	50	51	52	53	54	55	56	57	58	59	60	61	62	63	64	65	66	67	68	69	70	71	72	73	74	75	76	77	78	79	80	81	82	83	84	85	86	87	88	89	90	91	92	93	94	95	96	97	98	99	100
1	2	3	4	5	6	7	8	9	10	11	12	13	14	15	16	17	18	19	20	21	22	23	24	25	26	27	28	29	30	31	32	33	34	35	36	37	38	39	40	41	42	43	44	45	46	47	48	49	50	51	52	53	54	55	56	57	58	59	60	61	62	63	64	65	66	67	68	69	70	71	72	73	74	75	76	77	78	79	80	81	82	83	84	85	86	87	88	89	90	91	92	93	94	95	96	97	98	99	100
1	2	3	4	5	6	7	8	9	10	11	12	13	14	15	16	17	18	19	20	21	22	23	24	25	26	27	28	29	30	31	32	33	34	35	36	37	38	39	40	41	42	43	44	45	46	47	48	49	50	51	52	53	54	55	56	57	58	59	60	61	62	63	64	65	66	67	68	69	70	71	72	73	74	75	76	77	78	79	80	81	82	83	84	85	86	87	88	89	90	91	92	93	94	95	96	97	98	99	100
1	2	3	4	5	6	7	8	9	10	11	12	13	14	15	16	17	18	19	20	21	22	23	24	25	26	27	28	29	30	31	32	33	34	35	36	37	38	39	40	41	42	43	44	45	46	47	48	49	50	51	52	53	54	55	56	57	58	59	60	61	62	63	64	65	66	67	68	69	70	71	72	73	74	75	76	77	78	79	80	81	82	83	84	85	86	87	88	89	90	91	92	93	94	95	96	97	98	99	100
1	2	3	4	5	6	7	8	9	10	11	12	13	14	15	16	17	18	19	20	21	22	23	24	25	26	27	28	29	30	31	32	33	34	35	36	37	38	39	40	41	42	43	44	45	46	47	48	49	50	51	52	53	54	55	56	57	58	59	60	61	62	63	64	65	66	67	68	69	70	71	72	73	74	75	76	77	78	79	80	81	82	83	84	85	86	87	88	89	90	91	92	93	94	95	96	97	98	99	100
1	2	3	4	5	6	7	8	9	10	11	12	13	14	15	16	17	18	19	20	21	22	23	24	25	26	27	28	29	30	31	32	33	34	35	36	37	38	39	40	41	42	43	44	45	46	47	48	49	50	51	52	53	54	55	56	57	58	59	60	61	62	63	64	65	66	67	68	69	70	71	72	73	74	75	76	77	78	79	80	81	82	83	84	85	86	87	88	89	90	91	92	93	94	95	96	97	98	99	100
1	2	3	4	5	6	7	8	9	10	11	12	13	14	15	16	17	18	19	20	21	22	23	24	25	26	27	28	29	30	31	32	33	34	35	36	37	38	39	40	41	42	43	44	45	46	47	48	49	50	51	52	53	54	55	56	57	58	59	60	61	62	63	64	65	66	67	68	69	70	71	72	73	74	75	76	77	78	79	80	81	82	83	84	85	86	87	88	89	90	91	92	93	94	95	96	97	98	99	100
1	2	3	4	5	6	7	8	9	10	11	12	13	14	15	16	17	18	19	20	21	22	23	24	25	26	27	28	29	30	31	32	33	34	35	36	37	38	39	40	41	42	43	44	45	46	47	48	49	50	51	52	53	54	55	56	57	58	59	60	61	62	63	64	65	66	67	68	69	70	71	72	73	74	75	76	77	78	79	80	81	82	83	84	85	86	87	88	89	90	91	92	93	94	95	96	97	98	99	100
1	2	3	4	5	6	7	8	9	10	11	12	13	14	15	16	17	18	19	20	21	22	23	24	25	26	27	28	29	30	31	32	33	34	35	36	37	38	39	40	41	42	43	44	45	46	47	48	49	50	51	52	53	54	55	56	57	58	59	60	61	62	63	64	65	66	67	68	69	70	71	72	73	74	75	76	77	78	79	80	81	82	83	84	85	86	87	88	89	90	91	92	93	94	95	96	97	98	99	100
1	2	3	4	5	6	7	8	9	10	11	12	13	14	15	16	17	18	19	20	21	22	23	24	25	26	27	28	29	30	31	32	33	34	35	36	37	38	39	40	41	42	43	44	45	46	47	48	49	50	51	52	53	54	55	56	57	58	59	60	61	62	63	64	65	66	67	68	69	70	71	72	73	74	75	76	77	78	79	80	81	82	83	84	85	86	87	88	89	90	91	92	93	94	95	96	97	98	99	100
1	2	3	4	5	6	7	8	9	10	11	12	13	14	15	16	17	18	19	20	21	22	23	24	25	26	27	28	29	30	31	32	33	34	35	36	37	38	39	40	41	42	43	44	45	46	47	48	49	50	51	52	53	54	55	56	57	58	59	60	61	62	63	64	65	66	67	68	69	70	71	72	73	74	75	76	77	78	79	80																				

10	3.20-01	7.50-12	7.40-12	6.00-12	7.50-12	2.20-12	1.00-11	1.20-10	1.00-09	1.00-08	2.70-07
9	3.90-01	0.00-00	0.00-00	0.00-00	0.00-00	0.00-00	0.00-00	0.00-00	0.00-00	0.00-00	0.00-00
8	4.60-01	0.00-00	0.00-00	0.00-00	0.00-00	0.00-00	0.00-00	0.00-00	0.00-00	0.00-00	0.00-00
7	5.30-01	0.00-00	0.00-00	0.00-00	0.00-00	0.00-00	0.00-00	0.00-00	0.00-00	0.00-00	0.00-00
6	6.00-01	0.00-00	0.00-00	0.00-00	0.00-00	0.00-00	0.00-00	0.00-00	0.00-00	0.00-00	0.00-00
5	7.70-01	0.00-00	0.00-00	0.00-00	0.00-00	0.00-00	0.00-00	0.00-00	0.00-00	0.00-00	0.00-00
4	9.10-01	0.00-00	0.00-00	0.00-00	0.00-00	0.00-00	0.00-00	0.00-00	0.00-00	0.00-00	0.00-00
3	1.00-00	0.00-00	0.00-00	0.00-00	0.00-00	0.00-00	0.00-00	0.00-00	0.00-00	0.00-00	0.00-00
2	1.20-00	0.00-00	0.00-00	0.00-00	0.00-00	0.00-00	0.00-00	0.00-00	0.00-00	0.00-00	0.00-00
1	1.50-00	0.00-00	0.00-00	0.00-00	0.00-00	0.00-00	0.00-00	0.00-00	0.00-00	0.00-00	0.00-00

Table V sheet 17

DELTA(41,30) -- The new residual $(v^{(m+1)} - \psi^{(m)})$ calculated by Stone's method (Gummel's δ). See Sections 4.01 and 4.02 of Chapter I.

XPOS(41) -- The x-coordinate corresponding to the ψ -lattice index I.

YPOS(25) -- The y-coordinate corresponding to the ψ -lattice index J.

XTHPOS(41) -- The x-coordinate corresponding to the θ -lattice index I.

YTHPOS(25) -- The y-coordinate corresponding to the θ -lattice index J.

3.02 COMMON/COEFF/

XDLT(42) -- The ψ -lattice spacing $\Delta x(I)$.

YDLT(31) -- The ψ -lattice spacing $\Delta y(J)$.

XTHDLT(41) -- The θ -lattice spacing $\tilde{\Delta x}(I)$.

YTHDLT(25) -- The θ -lattice spacing $\tilde{\Delta y}(J)$.

HNRT(41,30) -- The "north" coefficient $\tilde{\Delta x}(I)/\Delta y(J+1)$, appearing in eq. (23) as H_p .

HEAST(41,30) -- The "east" coefficient $\tilde{\Delta y}(J)/\Delta x(I+1)$, appearing in eq. (23) as F_p .

HSTH(41,30) -- The "south" coefficient $\tilde{\Delta x}(I)/\Delta y(J)$, appearing in eq. (23) as B_p .

HWEST(41,30) -- The "west" coefficient $\tilde{\Delta y}(J)/\Delta x(I)$, appearing in eq. (23) as D_p .

HCNTR(41,30) -- The "center" coefficient appearing in eq. (23) as E_p .

THNRTH(40,25) -- The "north" coefficient $-\Delta x(I+1)/\tilde{\Delta}y(J+1)$ appearing in eq. (40). (The minus sign is used to make the matrix involved in the block-line iteration for θ positive-definite -- a crucial factor for convergence of that iterative scheme.)

THEAST(40,25) -- The "east" coefficient $-\Delta y(J+1)/\tilde{\Delta}x(I+1)$ appearing in eq. (40). (Same reason for the minus sign.)

THSTH(40,25) -- The "south" coefficient $-\Delta x(I+1)/\tilde{\Delta}y(J)$ appearing in eq. (40). (Same reason for the minus sign.)

THWEST(40,25) -- The "west" coefficient $-\Delta y(J+1)/\tilde{\Delta}x(I)$ appearing in eq. (40). (Same reason for the minus sign.)

QAREA(41,25) -- The area $\tilde{\Delta}x(I)\tilde{\Delta}y(J)$ associated with the ψ -lattice point (I,J), for purposes of calculating the charge contained within that "box."

3.03 COMMON/REAL/

XCHNL -- The channel length (spacing between the source and drain "contacts" in the x-direction).

YSUB -- The substrate thickness in the y-direction.

YOXIDE -- The oxide thickness.

YJNCTN -- The source and drain junction depths in the y-direction.

DONOR -- The donor density in the source and drain.

ACCPTR -- The acceptor density in the substrate region (assumed independent of x and y).

VGATE -- The applied gate voltage.

VSUB -- The applied substrate (back gate) voltage
(assumed always to be negative, or zero).

VDRAIN -- The applied drain voltage.

DIELK -- The ratio of dielectric constants (κ_{ox}/κ_{si}).

QSS -- The surface charge density at the oxide-silicon
interface. (This can account for the metal-oxide
work function difference ϕ_{MS} , as discussed in
Section 1.01 of this chapter.)

CURRNT -- The drain current factor J_0 discussed in Section
2.05 of Chapter I.

EDENSØ -- The electron density n in the charge-neutral
region of the silicon substrate.

PSIEQ -- The electrostatic potential of the charge-neutral
region of the substrate ($PSIEQ = -\ln(N_D N_A) + V_{SUB}$).

3.04 COMMON/INTGR/

IMAX -- Maximum of the index I definiting the x-coordinate.

JMAX -- Maximum of the index J defining the y-coordinate
within the silicon substrate.

JMAX5 -- Maximum of the index J defining the y-coordinate
within both the silicon substrate and the oxide
region ($JMAX5 = JMAX + 5$).

JUNCTN -- The J index which defines the lower corner of the
source and drain "contacts."

ITHMAX -- Maximum of the index I for the θ -lattice
($ITHMAX = IMAX - 1$).

3.05 COMMON/NRMLZE/

DNSNRM -- Electron and hole density normalization parameter.

PSINRM -- Electrostatic potential normalization parameter.

DEBYE -- Intrinsic Debye length.

QNORM -- Surface charge normalization parameter.

CRTNRM -- Current density normalization parameter.

3.06 COMMON/CNTRL/

OMEGA -- The overrelaxation parameter Ω used for overrelaxation with Gummel's algorithm.

CHAPTER IV

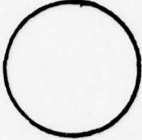
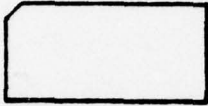

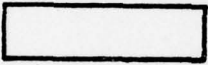
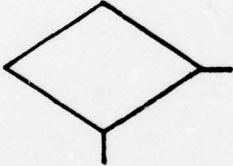

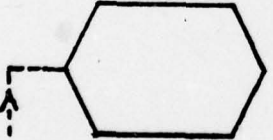
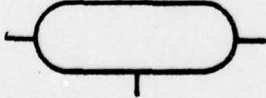

Program Listing, with Flowcharts

With the 41x30 ψ -lattice dimensions specified in the DIMENSION statements incorporated in the program, roughly 336,000 Bytes of core storage are required. The program consists of a main executive program, together with 21 FUNCTION and SUBROUTINE subprograms. (Two of the subprograms, GRELAX, and STONE) are embedded as ENTRY statements in other subprograms, viz. RELAX and STONE.)

Each subprogram is liberally sprinkled with COMMENT statements which, together with the flowcharts provided herein should make the functioning of that subprogram fairly transparent to a reader skilled in FORTRAN IV. We have consistently operated the program using IBM's Level H Extended, Optimization 2, Compiler.

In this chapter, section by section, we provide a brief description of each subprogram, together with a listing, and detailed flowcharts. Regarding the latter, Table VI defines the convention adopted for displaying the various FORTRAN operations in graphic form.

TABLE VI -- SYMBOLS APPEARING IN THE FLOWCHARTS

	ENTRY or EXIT
	READ
	WRITE
	FORMULAS
	IF STATEMENT
	CALL STATEMENT
	DO STATEMENT
	COMPUTED GO TO
	CONNECTOR

1.0 MAIN

This is the executive program which controls the functioning of the overall program. It reads the input data in unnormalized form, records them for future reference by the user, normalizes them, then controls the sequence of operations required to trace out characteristic curves of I_D versus V_{DS} , with V_{GS} varied as a parameter. By means of the parameter KRSWCH, it implements either Mock's iterative procedure -- Picard iteration at reduced donor density for coarse convergence, followed by Gummel's algorithm, with full donor density for tight convergence -- or Gummel's algorithm throughout.

TESTED OPTIONS: NODECK,LOAD,OPT=2, SOURCE,MAP

AS IN EFFECT: NAME(MAIN) OPTIMIZE(2) LINECOUNT(74) SIZE(MAX) AUTODBL(NONE)
SOURCE EBCDIC NULIST NODECK OBJECT MAP NOFORMAT GOSTMT NOXREF ALC NC MAIN EXECUTIVE PROGRAM FOR MOSFET ANALYSIS.
C
C
C
CISN 0002
ISN 0003
ISN 0004
ISN 0005
ISN 0006
ISN 0007
ISN 0008INITIALIZE ALL ARRAYS TO ZERO WITH A BLOCK DATA SUBPROGRAM
BLOCK DATA
IMPLICIT REAL*8(A-H,O-Z)
COMMON/ARRAYS/ADUMMY
COMMON/COEFF/CDUMMY
REAL*8 ADUMMY(13022)/13022*0.00/
REAL*8 CDUMMY(11314)/11314*0.00/
ENDTHIS PAGE IS BEST QUALITY PRACTICABLE
FROM COPY FURNISHED TO DDC

ED CPTIONS: NODCK,LOAD,OPT=2,SOURCE,MAF

IN EFFECT: NAME(MAIN) OPTIMIZL(2) LINECOUNT(74) SIZE(MAX) AUTODBL(NONE)
SOURCE EBCDIC NOLIST NODECK OBJECT MAP NOFORMAT GOSTMT NOXREF ALC NO

```

0002      IMPLICIT REAL*8(A-H,O-Z)
0003      REAL TITLE
C
0004      COMMON/ARRAYS/PSI(41,30),EDENS(41,25),HDENS(41,25),THETA(40,25),
18(41,30),D(41,30),E(41,30),F(41,30),H(41,30),O(41,30),DELTA(41,30),
0005      2,XPOS(41),YPOS(25),XTHPOS(41),YTHPOS(25)
      COMMON/COEFF/XDLT(42),YDLT(31),XTHDLT(41),YTHDLT(25),HNKTH(41,30),
0006      1,HEAST(41,30),HSTH(41,30),HWEEST(41,30),HCNTR(41,30),THNRTH(40,25),
      2,THEAST(40,25),THSTH(40,25),THWEEST(40,25),WAREA(41,25)
      COMMON/REAL/XCHNL,YSUB,YUXIDE,YJNCTN,DONOR,ACCPTR,VGATE,VSUB,
0007      1,VDRNIN,DIELK,QSS,CURRNT,EDENS0,PSIEQ
      COMMON/INTGR/IMAX,JMAX,JMAX5,JUNCTN,ITHMAX
0008      COMMON/NRMLZE/UNSNRM,PSINRM,DEBYE,QNORM,CRNRM
0009      COMMON/CNTRL/UMEGA
C
0010      DIMENSION TITLE(54)
C
0011      NAMELIST/PRMTRS/ XCHNL,YOXIDE,YJNCTN,DONOR,ACCPTR,QSS,EMOB,
1XDELTA,YDELTA,IMAX,JMAX
0012      NAMELIST/VOLTGE/VGDLT,VGATE0,VDDLTVDRNO,VSUB,NGATE,NURAIN
0013      NAMELIST/CNTRL/CNVRG1,CNVRG2,SIDL1,SIDL2,THDLT1,THDLT2,
1ITHMAX,ITSIMX,ITTHMX,KRSWCH,OMEGA
C
C
0014      READ(5,PRMTRS)
0015      READ(5,VOLTGE)
0016      READ(5,CNTRL)
0017      READ(5,1000)(TITLE(I),I=1,54)
0018      1000 FORMAT(18A4/18A4/18A4)
0019      WRITE(6,1010)(TITLE(I),I=1,54)
0020      1010 FORMAT(1H0,30X,18A4,/,30X,18A4,/,30X,18A4,///.5X,'SUMMARY OF INPUT
      1DATA :',//)
0021      WRITE(6,1020) XCHNL,YOXIDE,YJNCTN,DONOR,ACCPTR,QSS,EMOB,
1XDELTA,YDELTA,IMAX,JMAX
0022      1020 FORMAT(1H0,5X,'NAMELIST/PRMTRS/ XCHNL=',1PD11.3,2X,'YOXIDE=',
11PD11.3,2X,'YJNCTN=',1PD11.3,2X,'DONOR=',1PD11.3,2X,'ACCPTR=',
21PD11.3,/,5X,'QSS=',1PD11.3,2X,'EMOB=',1PD11.3,2X,'XDELTA=',
31PD11.3,2X,'YDELTA=',1PD11.3,2X,'IMAX=',13,2X,'JMAX=',13)
0023      WRITE(6,1030) VGDLT,VGATE0,VDDLTVDRNO,VSUB,NGATE,NURAIN
0024      1030 FORMAT(1H0,5X,'NAMELIST/VOLTGE/ VGDLT=',1PD11.3,2X,'VGATE0=',
11PD11.3,2X,'VDDLTVDRNO=',1PD11.3,2X,'VDRNO=',1PD11.3,2X,'VSUB=',
21PD11.3,/,2X,'NGATE=',13,2X,'NURAIN=',13)
0025      WRITE(6,1040) CNVRG1,CNVRG2,SIDL1,SIDL2,THDLT1,THDLT2,ITHMAX,
1ITSIMX,ITTHMX,KRSWCH,OMEGA
0026      1040 FORMAT(1H0,5X,'NAMELIST/CNTRL/ CNVRG1=',1PD11.3,2X,'CNVRG2=',
11PD11.3,2X,'SIDL1=',1PD11.3,2X,'SIDL2=',1PD11.3,/,5X,'THDLT1=',
21PD11.3,2X,'THDLT2=',1PD11.3,2X,'ITHMAX=',13,2X,'ITSIMX=',13,
32X,'ITTHMX=',13,2X,'KRSWCH=',13,2X,'OMEGA=',1PD11.3,///)
0027      JMAX5=JMAX+5
C
C      CALCULATE NORMALIZATION PARAMETERS & NORMALIZE ALL DATA.
C      NORMALIZATIONS ASSUME THE FOLLOWING UNITS FOR INPUT & OUTPUT DATA
C      POTENTIALS----- (VOLTS)
C      LENGTHS----- (MICRONS)
C      DONOR & ACCEPTOR DENSITIES----- (CM**3)
C      MOBILITY----- (CM**2/VOLT-SEC)
C      SURFACE CHARGE DENSITY----- (COULOMBS/CM**2)
C      CURRENT DENSITY----- (AMPERES/CM**2)
C
0028      DEBYE=(11.700*8.854D-14*2.585D-2)/(1.602D-19*1.5D10)
0029      DEBYE=DSQRT(DEBYE)
0030      QNORM=2.585D-2*11.700*8.854D-14/DEBYE
0031      CRNRM=2.585D-2*1.5D10*1.602D-19*EMOB/DEBYE
0032      DEBYE=DEBYE*1.04
0033      UNSNRM=1.5D10
0034      PSINRM=2.585D-2

```

THIS PAGE IS BEST QUALITY PRACTICABLE
FROM COPY FURNISHED TO DDC

```

ISN 0035      XCHNL=XCHNL/DLBYE
ISN 0036      YDABE=YDABE/DLBYE
ISN 0037      YJNCTN=YJNCTN/DLBYE
ISN 0038      DONOR=DONOR/DNSNRM
ISN 0039      ACCPTR=ACCPTR/DNSNRM
ISN 0040      QSS=QSS/QNORM
ISN 0041      VGDLT=VGDLT/PSINRM
ISN 0042      VGATE0=VGATE0/PSINRM
ISN 0043      VDOLT=VDOLT/PSINRM
ISN 0044      VDRNO=VDRNO/PSINRM
ISN 0045      VSUB=VSUB/PSINRM
ISN 0046      DIELK=3.900/11.700
ISN 0047      KEY=0
ISN 0048      IGATE=0
ISN 0049      VGATE=VGATE0-VGDLT

C
C      LOOP STARTS HERE. GATE VOLTAGE IS HELD FIXED WHILE DRAIN VOLTAGE
C      IS INCREMENTED THROUGH THE SPECIFIED RANGE, STARTING AT VD=VDRNO.
C      THEN GATE VOLTAGE IS INCREMENTED AND THE PROCESS IS REPEATED.
C

ISN 0050      100 IGATE=IGATE+1
ISN 0051      IF(IGATE.GT.NGATE) STOP
ISN 0053      VGATE=VGATE+VGDLT
ISN 0054      IDRAIN=1
ISN 0055      VDRAIN=VDRNO
ISN 0056      110 YSUB=USRT(2.00*(DLBG(DONOR*ACCPTR)+VDRAIN-VSUB-1.00)/ACCPTR)
ISN 0057      YSUB=YJNCTN+1.50*YSUB
ISN 0058      CALL GRID(XDELTA,YDELTA,KEY)
ISN 0059      CALL STONE1(IMAX,JMAX,JMAX5)

C
C      IF KRSWCH.EQ.0, APPLY ONLY THE GUMMEL ALGORITHM, WITH FULL DONOR
C      DENSITY AND TIGHT CONVERGENCE CRITERIA. IF KRSWCH.GT.0, APPLY PICAR
C      ITERATION FIRST, WITH LOOSE CONVERGENCE CRITERIA AND REDUCED DONOR
C      DENSITY (IF APPLICABLE), FOLLOWED BY THE GUMMEL ALGORITHM, WITH
C      TIGHT CONVERGENCE CRITERIA AND FULL DONOR DENSITY.
C

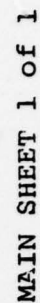
ISN 0060      IF(KRSWCH.GT.0) GO TO 120
ISN 0062      CALL BURDER(0,1,DNR)
ISN 0063      CALL NITIAL(DNR)
ISN 0064      CALL GRELAX(ITMAX,ITSIMX,ITTHMX,CNVRG2,SIDLT2,THDLT2,DNR)
ISN 0065      GO TO 130
ISN 0066      120 CALL BURDER(1,0,DNR)
ISN 0067      CALL NITIAL(DNR)
ISN 0068      CALL RELAX(ITMAX,ITSIMX,ITTHMX,CNVRG1,SIDLT1,THDLT1,DNR)
ISN 0069      IF(DNR.LT.DONOR) CALL BURDER(1,1,DNR)
ISN 0071      CALL GRELAX(ITMAX,ITSIMX,ITTHMX,CNVRG2,SIDLT2,THDLT2,DNR)
ISN 0072      130 CALL OUTPUT

C
C      STEP DRAIN VOLTAGE & REPEAT UNLESS MAX DRAIN VOLTAGE WAS USED.
C      IF SO, STEP GATE VOLTAGE & REINITIATE DRAIN VOLTAGE SEQUENCE.
C

ISN 0073      IDRAIN=IDRAIN+1
ISN 0074      IF(IDRAIN.GT.NDRAIN) GO TO 100
ISN 0076      VDRAIN=VDRAIN+VDOLT
ISN 0077      GO TO 110
ISN 0078      END

```

THIS PAGE IS BEST QUALITY PRACTICABLE
FROM COPY FURNISHED TO DDC



2.0 GRID

This subprogram establishes the ψ and θ -lattice spacings $\Delta x(I)$, $\Delta y(J)$, $\tilde{\Delta} x(I)$, $\tilde{\Delta} y(J)$, following the procedure devised by Mock [1] for generating the graded lattice illustrated in Figure 2 of Chapter I. It then calculates the finite-difference coefficients required in the implementation of Stone's method and of Block-Line iteration. The special procedures for treating the boundary conditions at the oxide-silicon interface, described in Chapter I, Section 3.01.1, are implemented in this subprogram.

REC OPTIONS: NODACK,LOAD,OPT=2,SOURCE,MAP

5 IN EFFECT: NAME(MAIN) OPTIMIZE(2) LINECOUNT(74) SIZE(MAX) AUTODBL(NONE)
SOURCE EDDIC NULIST NODACK OBJECT MAP NOFORMAT GOSTMT NOAREF ALL N

```

0002      SUBROUTINE GRID(XDELTA,YDELTA,KEY)
      C
      C      SETS UP LATTICE PARAMETERS FOR PSI & THETA. CALCULATES COEFF FOR
      C      THE FINITE-DIFFERENCE EQUATIONS.
0003      IMPLICIT REAL*8(A-H,U-Z)
      C
0004      COMMON/ARRAYS/PSI(41,30),EDENS(41,25),HDENS(41,25),THETA(40,25),
      1B(41,30),D(41,30),E(41,30),F(41,30),H(41,30),Q(41,30),DELTA(41,3
      2,XPOS(41),YPOS(25),XTHPOS(41),YTHPOS(25)
0005      COMMON/CUEFF/XDLT(42),YDLT(31),XTHDLT(41),YTHDLT(25),HNRKTH(41,30
      1HEAST(41,30),HSTH(41,30),HWEEST(41,30),HCNIR(41,30),THNRKTH(40,25)
      2THEAST(40,25),THSTH(40,25),THWEST(40,25),UAREA(41,25)
0006      COMMON/REAL/XCHNL,YSUB,YOXIDE,YJUNCTN,DUNUR,ACCPTR,VGATE,VSUB,
      1VDRAIN,DIELK,GSS,CURRNT,EDENS0,PSIEQ
0007      COMMON/INTGR/IMAX,JMAX,JMAX5,JUNCTN,ITHMAX
      C
      C
      C      BY-PASS XDLT & XTHDLT COMPUTATION IF KEY GT 0.
0008      IF(KEY.GT.0) GO TO 150
0010      IMID=(IMAX-1)/2
0011      I=2*IMID+1
0012      IF(I.EQ.IMAX) GO TO 100
0014      WRITE(6,1000)
0015      1000 FORMAT(1H1,5X,'ERROR IN INPUT DATA. PARAMETER IMAX MUST BE ODD',
0016      STOP
0017      100 IMID=IMID+1
0018      IMAX=IMID-2
0019      SUM=0.
      C
      C
      C      HORIZONTAL LATTICE PARAMETERS
0020      DO 110 I=1,IMAXX
0021      110 SUM=SUM+XDELTA**I
0022      XDLT(IMID)=XCHNL/(2.00*(1.00+SUM))
0023      IMAXX=IMID-1
0024      DO 120 I=2,IMAXX
0025      J=IMID+1-I
0026      120 XDLT(J)=XDLT(J+1)*XDELTA
0027      DO 130 I=2,IMID
0028      J=IMAX+2-I
0029      130 XDLT(J)=XDLT(I)
0030      XDLT(1)=XDLT(2)
0031      XDLT(IMAX+1)=XDLT(IMAX)
      C
      C
      C      THETA LATTICE
0032      ITHMAX=IMAX-1
0033      DO 140 I=1,IMAX
0034      140 XTHDLT(I)=(XDLT(I)+XDLT(I+1))/2.00
      C
      C
      C      VERTICAL LATTICE PARAMETERS
0035      150 JMAXX=JMAX-2
0036      SUM=0.
0037      DO 160 J=1,JMAXX
0038      160 SUM=SUM+YDELTA**J
0039      YDLT(2)=YSUB/(1.00+SUM)
0040      DO 170 J=3,JMAX
0041      170 YDLT(J)=YDLT(J-1)*YDELTA
      C
      C
      C      OXIDE REGION
0042      YDLT(JMAX+1)=YDLT(JMAX)*YDELTA
0043      UXDLTA=(YOXIDE-YDLT(JMAX+1)*DIELK/(1.00+DIELK))/4.00
0044      JMINN=JMAX+2

```

THIS PAGE IS BEST QUALITY PRACTICABLE
FROM COPY FURNISHED TO DDG

```

SN 0045      DO 180 J=JMINN,JMAX5
SN 0046      YDLT(J)=DXDLTA
SN 0047      YDLT(1)=YDLT(2)
SN 0048      YDLT(JMAX5+1)=YDLT(JMAX5)
SN 0049      JMAXX=JMAX-1
C
C      THETA LATTICE
C
SN 0050      DO 190 J=1,JMAXX
SN 0051      YTHDLT(J)=(YDLT(J)+YDLT(J+1))/2.00
SN 0052      YTHDLT(JMAX)=YDLT(JMAX)/2.00+YDLT(JMAX+1)/(1.00+DIELK)
C
C      FINITE-DIFFERENCE COEFFICIENTS
C
SN 0053      DO 210 I=1,IMAX
C
C      SILICON REGION
C
SN 0054      DO 200 J=1,JMAXX
SN 0055      QAREA(I,J)=XTHDLT(I)*YTHDLT(J)
SN 0056      HSTH(I,J)=XTHDLT(I)/YDLT(J)
SN 0057      HWEST(I,J)=YTHDLT(J)/XDLT(I)
SN 0058      HEAST(I,J)=YTHDLT(J)/XDLT(I+1)
SN 0059      HNRTH(I,J)=XTHDLT(I)/YDLT(J+1)
SN 0060      MCNTR(I,J)=-(HSTH(I,J)+HWEST(I,J)+HEAST(I,J)+HNRTH(I,J))
C
C      THE TWO ROWS BRACKETING THE SI-GX INTERFACE
C
SN 0061      J=JMAX
SN 0062      QAREA(I,J)=XTHDLT(I)*(YDLT(J)/2.00+YDLT(J+1)/(1.00+DIELK))
SN 0063      HSTH(I,J)=XTHDLT(I)/YDLT(J)
SN 0064      HWEST(I,J)=YTHDLT(J)/XDLT(I)
SN 0065      HEAST(I,J)=YTHDLT(J)/XDLT(I+1)
SN 0066      HNRTH(I,J)=XTHDLT(I)/(2.00*YDLT(J+1)/(1.00+DIELK))
SN 0067      MCNTR(I,J)=-(HSTH(I,J)+HWEST(I,J)+HEAST(I,J)+HNRTH(I,J))
SN 0068      J=JMAX+1
SN 0069      AVG=YDLT(J+1)/2.00+YDLT(J)*DIELK/(1.00+DIELK)
SN 0070      HSTH(I,J)=XTHDLT(I)/(2.00*YDLT(J)*DIELK/(1.00+DIELK))
SN 0071      HWEST(I,J)=AVG/XDLT(I)
SN 0072      HEAST(I,J)=AVG/XDLT(I+1)
SN 0073      HNRTH(I,J)=XTHDLT(I)/YDLT(J+1)
SN 0074      MCNTR(I,J)=-(HSTH(I,J)+HWEST(I,J)+HEAST(I,J)+HNRTH(I,J))
C
C      OXIDE REGION
C
SN 0075      DO 210 J=JMINN,JMAX5
SN 0076      AVG=(YDLT(J)+YDLT(J+1))/2.00
SN 0077      HSTH(I,J)=XTHDLT(I)/YDLT(J)
SN 0078      HWEST(I,J)=AVG/XDLT(I)
SN 0079      HEAST(I,J)=AVG/XDLT(I+1)
SN 0080      HNRTH(I,J)=XTHDLT(I)/YDLT(J+1)
SN 0081      MCNTR(I,J)=-(HSTH(I,J)+HWEST(I,J)+HEAST(I,J)+HNRTH(I,J))
C
C      MODIFY THE SOUTH COEFFICIENTS FOR THE TWO POINTS JUST NORTH OF
C      THE INTERFACE AT THE SOURCE & DRAIN CONTACTS.
C
SN 0082      HSTH(1,JMAX+1)=XTHDLT(1)/(YDLT(JMAX+1)*DIELK/(1.00+DIELK))
SN 0083      HSTH(IMAX,JMAX+1)=HSTH(1,JMAX+1)
SN 0084      MCNTR(1,JMAX+1)=-(HSTH(1,JMAX+1)+HWEST(1,JMAX+1)+HNRTH(1,JMAX+1)
SN 0085      +HEAST(1,JMAX+1))
SN 0086      MCNTR(IMAX,JMAX+1)=MCNTR(1,JMAX+1)
C
C      THETA COEFFICIENTS
C
SN 0086      DO 220 I=1,ITHMAX
SN 0087      DO 220 J=1,JMAXX
SN 0088      THSTH(I,J)=-XDLT(I+1)/YTHDLT(J)
SN 0089      THWEST(I,J)=-YDLT(J+1)/XTHDLT(I)
SN 0090      THEAST(I,J)=-YDLT(J+1)/XTHDLT(I+1)
SN 0091      THNRTH(I,J)=-XDLT(I+1)/YTHDLT(J+1)
C
C      TABULATE PSI & THETA LATTICE COORDINATES.

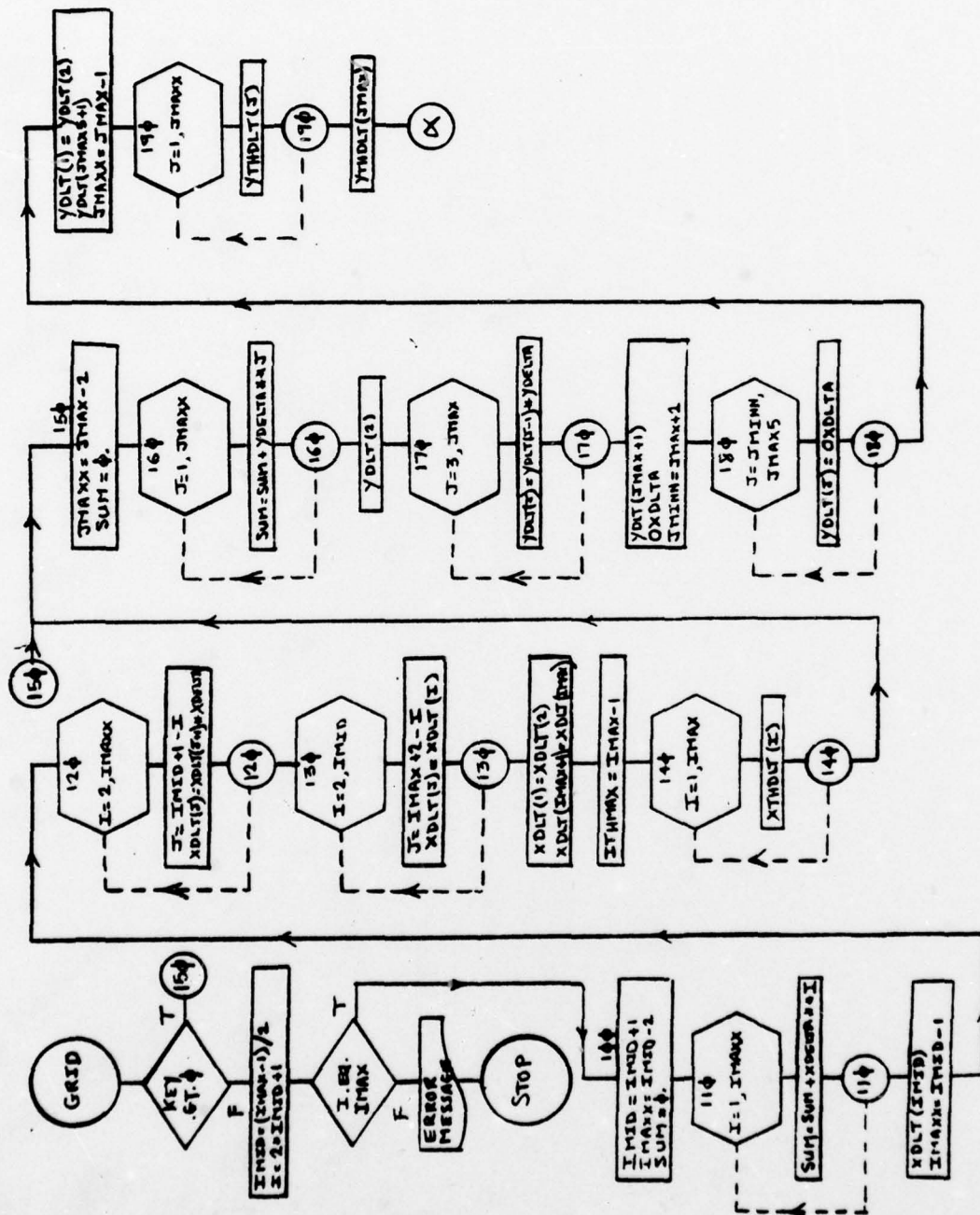
```

THIS PAGE IS BEST QUALITY PRACTICABLE
FROM COPY FURNISHED TO DDG

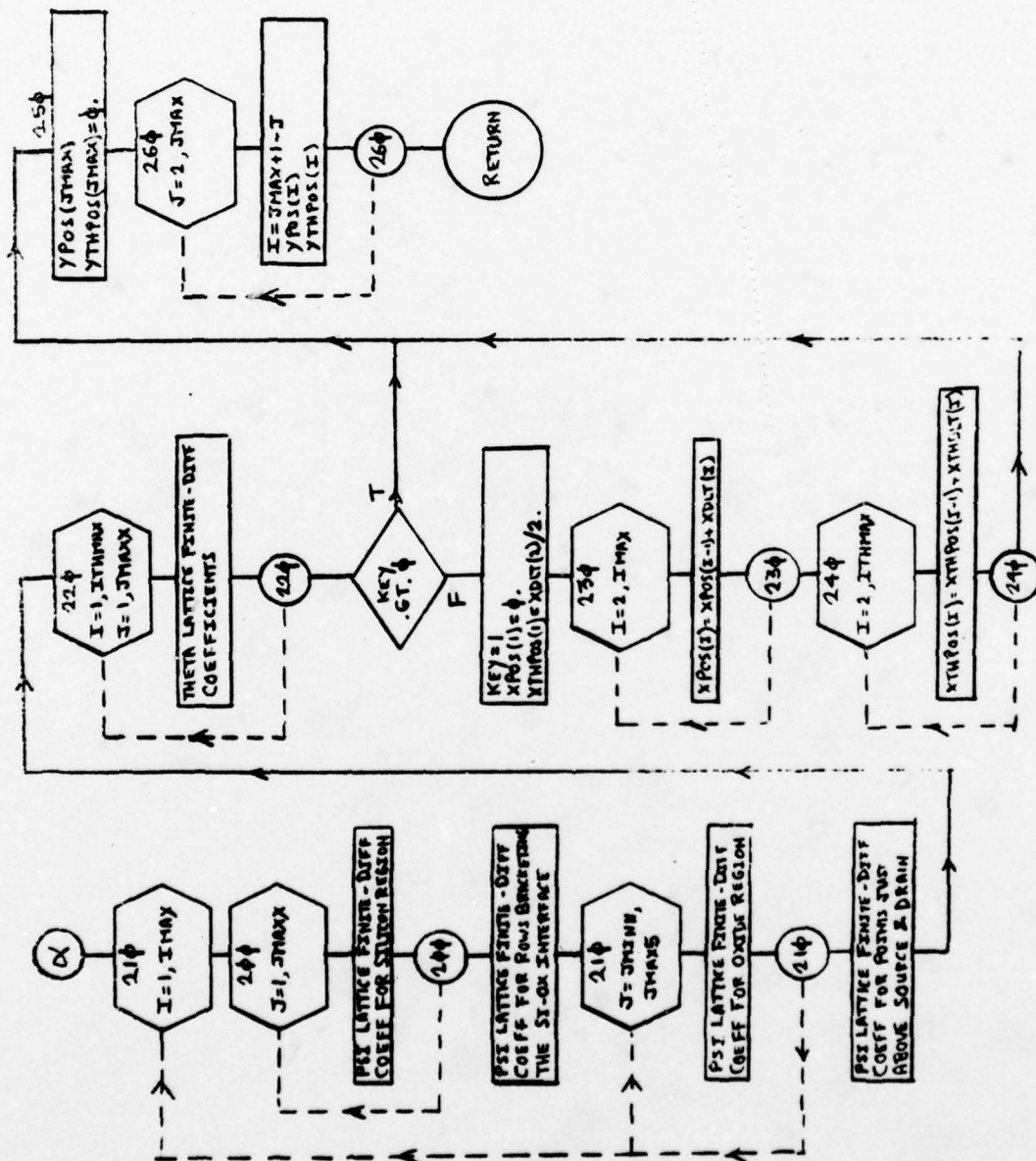

```
C
0092      IF (KEY.GT.0) GO TO 250
0094      KEY=1
0095      XPUS(1)=0.
0096      XTHPUS(1)=XDLT(2)/2.00
0097      DO 230 I=2,IMAX
0098 230    XPUS(I)=XPUS(I-1)+XDLT(I)
0099      DO 240 I=2,ITHMAX
0100 240    XTHPUS(I)=XTHPUS(I-1)+XTHDLT(I)
0101 250    YPCS(JMAX)=YDLT(JMAX+1)/(1.00+DIELK)
0102      YTHPUS(JMAX)=0.
0103      DO 260 J=2,JMAX
0104      I=JMAX+1-J
0105      YPCS(I)=YPCS(I+1)+YDLT(I+1)
0106 260    YTHPUS(I)=YTHPUS(I+1)+YTHDLT(I+1)
0107      RETURN
0108      END
```

THIS PAGE IS BEST QUALITY PRACTICABLE
FROM COPY FURNISHED TO DDC

THIS PAGE IS BEST QUALITY PRACTICABLE
FROM COPY FURNISHED TO DDG



GRID SHEET 1 of 2



3.0 BORDER

This subprogram assigns the boundary conditions on ψ , n , and p at the borders of the lattice. Since the substrate potential ($\psi_{\text{SUB}} = -\ln(N_D N_A) + V_{\text{SUB}}$) depends upon the donor density N_D , and since the latter is generally a reduced value if the Picard iteration method has been used (i.e., if Mock's iterative procedure is being employed) it is necessary to shift the level of the array $\text{PSI}(I,J)$, as determined from convergence of the Picard iteration, to account for the increased donor density which will next be used for Gummel's algorithm. This is done by BORDER, the flags KRSWCH and KDOPE determining whether this is necessary.

EL OPTICNS: NUDECK,LOCAL,OPT=2,SOURCE,MAP

IN EFFECT: NAME(MAIN) OPTIMIZL(2) LINECOUNT(74) SIZE(MAX) AUTODBL(NONE)
SOURCE CUDIC NOLIST NUDECK OBJECT MAP NOFORMAT GUSTMT NOXREF ALC NL

```

0002      SUBROUTINE BORDER(KRSWCH,KDCPE,DNR)
C
C      SETS BOUNDARY CONDITIONS ALONG THE FOUR BORDERS. IF REDUCED
C      DONOR DENSITY WAS PREVIOUSLY USED (KRSWCH.EQ.1 AND KDCPE.GT.0),
C      MODIFIES THE POTENTIAL PREVIOUSLY OBTAINED BY CONVERGENCE
C      OF RELAX TO ACCOUNT FOR THE CHANGE IN SUBSTRATE POTENTIAL DUE
C      TO THE INCREASE IN DONOR DENSITY TO ITS CORRECT VALUE.
C
0003      IMPLICIT REAL*8(A-H,O-Z)
C
0004      COMMON/ARRAYS/PSI(41,30),EDENS(41,25),HDENS(41,25),THETA(40,25),
1B(41,30),D(41,30),E(41,30),F(41,30),H(41,30),Q(41,30),DELTA(41,30)
2,XPLS(41),YPOS(25),XTHPOS(41),YTHPOS(25)
0005      COMMON/CUEFF/XDLT(42),YDLT(31),XTHDLT(41),YTHDLT(25),HNRTH(41,30),
1HEAST(41,30),HSTH(41,30),HWEST(41,30),HCNTR(41,30),THNRTH(40,25),
2THEAST(40,25),TMSTH(40,25),TWEST(40,25),QAREA(41,25)
0006      COMMON/REAL/XCHNL,YSUB,YOXIDE,YJUNCT,DONOR,ACCPTR,VGATE,VSUB,
1VDRAIN,DIELK,GSS,CURRNT,EDENS0,PSIEQ
0007      COMMON/INTGR/IMAX,JMAX,JMAX5,JUNCTN,ITHMAX
C
C      KDCPE .EQ.0 SIGNIFIES USE REDUCED DONOR DOPING. KDCPE .EQ.1
C      SIGNIFIES USE FULL DOPING.
C
0008      DNR=DONOR
0009      IMAX5=IMAX-1
0010      DLTPSI=0.
0011      IF(KRSWCH.GT.0.AND.KDCPE.GT.0) DLTPSI=PSIEQ-VSUB
0013      IF(KDCPE.GT.0) GO TO 110
0015      RATIO=DONOR/ACCPTR
0016      IF(RATIO.LT.1.02) GO TO 110
0018      DNR=ACCPTR*1.02
0019      110 PSIEQ=-DLUG(DNR*ACCPTR)
0020      IF(KRSWCH.GT.0.AND.KDCPE.GT.0) DLTPSI=PSIEQ-DLTPSI
0022      EDENS0=1.00/ACCPTR
C
C      THE HORIZONTAL BORDERS
C
0023      DO 120 I=1,IMAX
0024      PSI(1,JMAX5)=PSIEQ+VGATE
0025      PSI(1,1)=PSIEQ+VSUB
0026      EDENS(1,1)=EDENS0
0027      120 HDENS(1,1)=ACCPTR
C
C      REGION BORDERED BY THE SOURCE & DRAIN.
C
0028      J=JMAX
0029      SUM=YPLS(JMAX)
0030      130 IF(SUM.GT.YJUNCTN) GO TO 150
0032      DO 140 I=2,IMAX
0033      140 PSI(1,J)=PSI(1,J)+DLTPSI
0034      PSI(1,J)=-1.00
0035      PSI(IMAX,J)=-1.00+VDRAIN
0036      EDENS(1,J)=DNR/DEXP(1.00)
0037      EDENS(IMAX,J)=EDENS(1,J)
0038      HDENS(1,J)=1.00/EDENS(1,J)
0039      HDENS(IMAX,J)=HDENS(1,J)
0040      SUM=SUM+YDLT(J)
0041      J=J-1
0042      GO TO 130
C
C      THE REGION NOT BORDERED BY THE SOURCE & DRAIN
C
0043      150 DO 160 JJ=2,J
0044      DO 160 I=1,IMAX
0045      160 PSI(I,JJ)=PSI(1,JJ)+DLTPSI
0046      JUNCTN=J+1
C

```

THIS PAGE IS BEST QUALITY PRACTICABLE
FROM COPY FURNISHED TO DDG

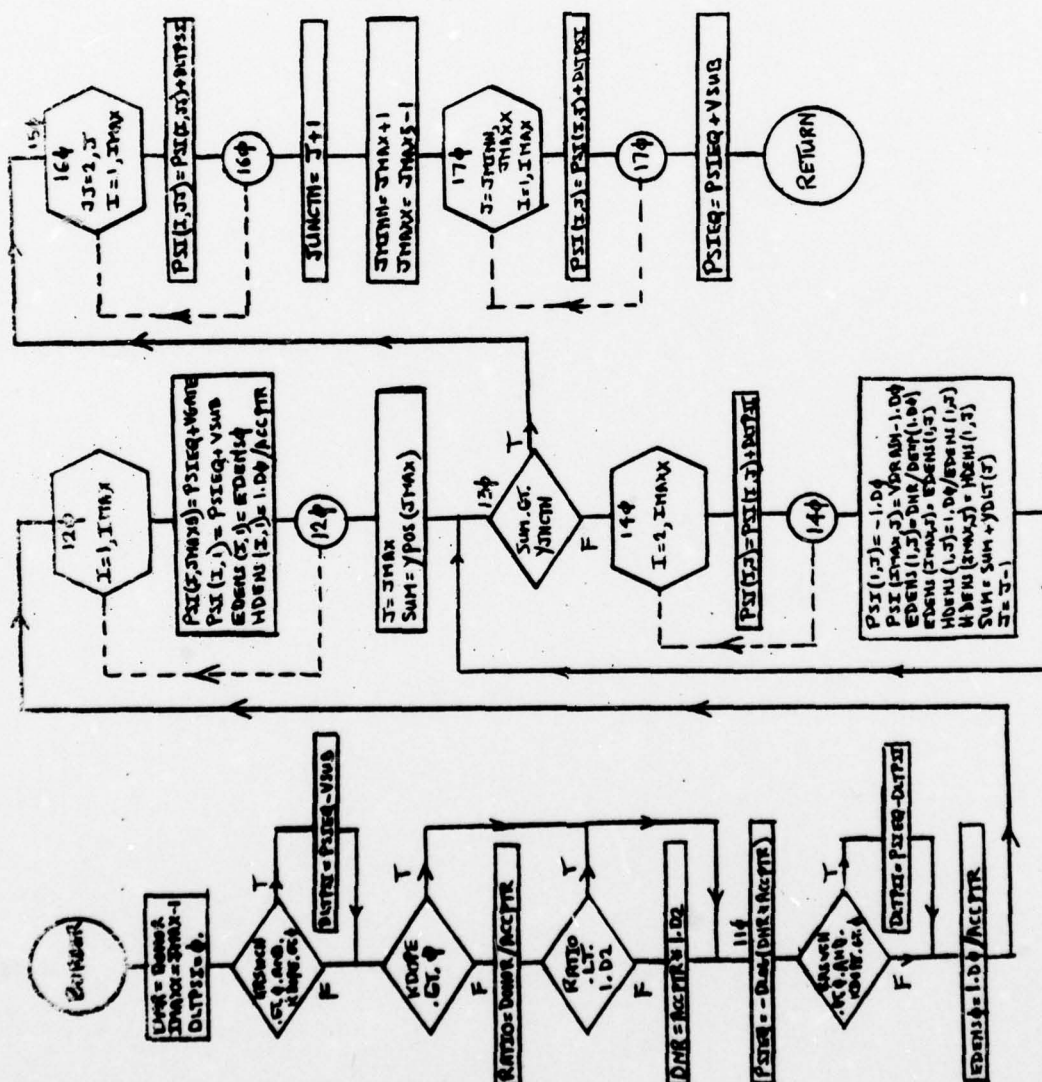
C
C

THE OXIDE REGION

```
0047 JMINN=JMAX+1
0048 JMAXX=JMAX-1
ISN 0049 DO 170 J=JMINN,JMAXX
ISN 0050 DO 170 I=1,IMAX
ISN 0051 170 PSI(I,J)=PSI(I,J)+DLTPSI
ISN 0052 PSIEG=PSIEG+VSUB
ISN 0053 RETURN
ISN 0054 END
```

THIS PAGE IS BEST QUALITY PRACTICABLE
FROM COPY FURNISHED TO DDG

THIS PAGE IS BEST QUALITY PRACTICABLE
FROM COPY FURNISHED TO DDC



BORDER SHEET 1 of 1

4.0 NITIAL

This subprogram calculates the initial estimates for $\psi(x,y)$ and $\theta(x,y)$. It first assigns $\psi = -\ln(N_D N_A) + V_{SUB}$ throughout the silicon substrate, then overwrites this with the potential determined from depletion theory to create space-charge "sheaths" in contact with the source and drain. (An interpolation scheme is applied to provide smooth transitions in the corner regions at the lower edges of the source and drain "contacts.") This procedure establishes $\psi_B(x)$ -- the curve shown dotted in Figure 10(b). The Kennedy-Murley-Motta equations are then used to determine the potential $\psi_S(x)$ along the oxide-silicon interface for $0 < x < (x_{channel} - 1.3W_{D_{drain}})$, with a parabolic equation extending $\psi_S(x)$ beyond that point in the manner described in Chapter I, Section 4.04.1. Then, given $\psi_S(x)$ and $\psi_B(x)$, one-dimensional solutions of Poisson's equation for $\psi(y)$ are generated vertically downward from the interface, matching $\psi_B(x)$, with zero $d\psi/dy$, deep within the substrate, and matching $\psi_S(x)$ at the interface. For each such vertical solution, the electron quasi-Fermi level ϕ_n (assumed not to vary with y in these one-dimensional solutions) is adjusted to satisfy the boundary condition on $d\psi/dy$ which must be satisfied at the oxide-silicon interface. The potential within the oxide region is approximated to vary linearly with y , matching $\psi = \psi_S(x)$ at the interface, and $\psi = \psi_{gate}$ at the gate contact.

The initial estimate for $\theta(x,y)$ uses the one-dimensional parabolic estimate discussed in Chapter I, Section 4.04.2, established along the vertical plane corresponding to the edge of the space-charge sheath adjacent to the source.

TEL OPTIONS: NODACK,LOAD,OPT=2,SOURCE,MAP

S IN EFFECT: NAME(MAIN) OPTIMIZE(2) LINECOUNT(74) SIZE(MAX) AUTODEL(NONE)
SOURCE EBCDIC NULIST NODACK OBJECT MAP NOFORMAT GUSTMT NOXREF ALC N

```

0002      SUBROUTINE INITAL(DNR)
          C
          C PROVIDES INITIAL ESTIMATES FOR PSI & THETA.
          C
0003      IMPLICIT REAL*8(A-H,O-Z)
          C
0004      COMMON/ARRAYS/PSI(41,30),EDENS(41,25),MDENS(41,25),THETA(40,25),
          1B(41,30),D(41,30),E(41,30),F(41,30),H(41,30),G(41,30),DELTA(41,3
          2,XFUS(41),YFUS(25),XTHPUS(41),YTHPUS(25)
0005      COMMON/COEFF/ADLT(42),YDLT(31),XTHDLT(41),YTHDLT(25),HNRTH(41,30
          1HEAST(41,30),HSTH(41,30),HWEST(41,30),HCNTR(41,30),THNRTH(40,25)
          2THEAST(40,25),THSTH(40,25),THWEST(40,25),GAREA(41,25)
0006      COMMON/REAL/XCHNL,YSUB,YOXIDE,YJUNCTN,DUNDR,ACCPTR,VGATE,VSUB,
          1VDRAIN,DIELK,QSS,CURRNT,EDENS0,PSIEQ
0007      COMMON/INTGR/IMAX,JMAX,JMAX5,JUNCTN,ITHMAX
          C
0008      JMAX5=JMAX5-1
0009      JMINN=JMAX+1
0010      YY=YDLT(JMINN)*DIELK/(1.D0+DIELK)
0011      YY=YY-YDLT(JMINN)
0012      DO 90 J=JMINN,JMAXX
0013      YY=YY+YDLT(J)
0014      PSI(1,J)=(PSI(1,JMAX5)-PSI(1,JMAX))*YY/YOXIDE+PSI(1,JMAX)
0015      90 PSI(IMAX,J)=(PSI(IMAX,JMAX5)-PSI(IMAX,JMAX))*YY/YOXIDE+
          1PSI(IMAX,JMAX)
          C
0016      JMINN=JUNCTN-1
0017      IMID=(IMAX-1)/2+1
0018      DLTA=1.D-2
0019      DO 100 J=2,JMINN
0020      DO 100 I=1,IMAX
0021      100 PSI(I,J)=PSIEQ
0022      DO 110 J=JUNCTN,JMAX
0023      DO 110 I=2,ITHMAX
0024      110 PSI(I,J)=PSIEQ
          C
          C PROVIDE SPACE-CHARGE SHEATHS ADJACENT ON THE SOURCE & DRAIN CONT
          C
          C KEY=1 SIGNIFIES THE SOURCE REGION,KEY=2 THE DRAIN REGION
          C
0025      KEY=1
0026      I=1
0027      II=1
0028      IDLT=1
0029      XX=0.
0030      IBDUER=1
0031      GO TO 130
0032      120 KEY=2
0033      I=1
0034      II=IMAX
0035      IDLT=-1
0036      XX=0.
0037      IBDUER=IMAX
          C
          C SOURCE & DRAIN SHEATHS USE THE DEPLETION APPROXIMATION.
          C
0038      130 SI=PSI(II,JMAX)-PSIEQ
0039      WD=DSQRT(2.D0*SI/ACCPTR)
0040      J=JUNCTN
0041      YY=0.
          C
          C SHEATH EDGE BELOW SOURCE (OR DRAIN) CONTACTS.
          C
0042      140 YY=YY+YDLT(J)
0043      JSTOP=J
0044      J=J+1
0045      IF(J.EQ.1) GO TO 150
0046      IF(YY.GT.WD) GO TO 150
0047      PSI(II,J)=(YY-WD)*(YY-WD)*ACCPTR/2.D0+PSIEQ
0048
0049

```

THIS PAGE IS BEST QUALITY PRACTICABLE
FROM COPY FURNISHED TO DDG

```

SN 0050      GO TO 140
C
C      SHEATH HORIZONTALLY ALONG ROW J=JUNCTN.
C
SN 0051      150 J=JUNCTN
SN 0052      I=I+1
SN 0053      II=II+IDLT
SN 0054      XX=XA+XDLT(I)
SN 0055      IF(I.EQ.IMAX) GO TO (120,200).KEY
SN 0056      IF(XX.GT.WD) GO TO (120,200).KEY
SN 0057      PSI(II,J)=(XX-WD)*(XX-WD)*ACCPTR/2.00+PSIEQ
C
C      FILL IN PSI VERTICALLY UPWARD ALONG SOURCE (OR DRAIN) REGION.
C
SN 0060      160 J=J+1
SN 0061      IF(J.GT.JMAX) GO TO 170
SN 0062      PSI(II,J)=PSI(II,JUNCTN)
SN 0063      GO TO 160
C
C      OXIDE REGION ABOVE THE SHEATH.
C
SN 0065      170 YY=YDLT(J)*DIELK/(1.00+DIELK)
SN 0066      YY=YY-YDLT(J)
SN 0067      JMINN=J
SN 0068      DO 180 J=JMINN,JMAXX
SN 0069      YY=YY+YDLT(J)
SN 0070      180 PSI(II,J)=(PSI(II,JMAXX)-PSI(II,JMAX))*YY/YOXIDE+PSI(II,JMAX)
C
C      CORNER REGIONS BELOW SOURCE (OR DRAIN), USING AN INTERPOLATION
C      SCHEME TO PROVIDE A SMOOTH TRANSITION
C
SN 0071      J=JUNCTN
SN 0072      190 J=J-1
SN 0073      IF(J.LT.JSTOP) GO TO 150
SN 0074      PSI(II,J)=(PSI(16ORDER,J)-PSIEQ)*(PSI(II,JUNCTN)-PSIEQ)/
SN 0075      1(PSI(16ORDER,JUNCTN)-PSIEQ)+PSIEQ
SN 0076      GO TO 190
C
C      THE KENNEDY-MURLEY 1-D THEORY, AS MODIFIED BY MOTTA, IS NEXT USED
C      TO ESTIMATE THE POTENTIAL ALONG THE SI-OX INTERFACE FOR VALUES OF
C      X.LT.(XCHNL-1.3*WD). THIS CUTOFF HAS BEEN EMPIRICALLY SELECTED.
C
C      FIRST FIND THE EQUILIBRIUM (MOS CAPACITOR) VALUE U0, USING AN
C      EQUIVALENT GATE POTENTIAL UG WHICH ACCOUNTS FOR QSS. (ALL "U"
C      FUNCTIONS USE ZERO REFERENCE POTENTIAL AS THE CHARGE-NEUTRAL
C      SUBSTRATE REGION.)
C
SN 0077      200 UG=PSI(IMID,JMAXX)-PSIEQ+QSS*YOXIDE/DIELK
SN 0078      UD=PSI(IMAX,JMAX)-PSIEQ
SN 0079      ALPHA=USRT(2.00*ACCPTR)*YOXIDE/DIELK
SN 0080      BB=1.00/(ACCPTR*ACCPTR)
SN 0081      U0=VZERO(UG,ALPHA,BB)
C
C      IF THE DRAIN VOLTAGE IS ZERO (MOS CAPACITOR CASE), ONLY A SINGLE
C      1-D INTEGRATION VERTICALLY DOWNWARD ALONG THE COLUMN I=IMID WILL
C      SUFFICE FOR FILLING IN PSI IN THE REMAINDER OF THE REGION (KEY=1).
C      OTHERWISE, 1-D INTEGRATIONS ALONG EACH COLUMN EXTERNAL TO THE
C      SHEATHS ARE NECESSARY (KEY=2 FOR THE KENNEDY-MURLEY-MOTTA REGION
C      FOR THE SURFACE POTENTIAL US, KEY=3 FOR THE SUTHERLAND "PARABOLIC
C      FIT" REGION FOR US).
C
SN 0082      IF(VDRAIN.GT.0.) GO TO 230
SN 0083      KEY=1
SN 0084      US=U0
SN 0085      I=IMID
SN 0086      GO TO 320
SN 0087      210 IMID=IMID-1
SN 0088      DO 220 I=2,IMID
SN 0089      DO 220 J=2,JMAXX
SN 0090      IF(PSI(I,J).GT.PSI(IMID+1,J)) GO TO 220
SN 0091      PSI(I,J)=PSI(IMID+1,J)
SN 0092      PSI(IMAX+1-I,J)=PSI(I,J)
SN 0093
SN 0094

```

THIS PAGE IS BEST QUALITY PRACTICABLE
FROM COPY FURNISHED TO DDG

```

0095      220 CONTINUE
0096      GO TO 360

C
C      SET UP COEFFICIENTS FOR THE KENNEDY-MURLEY-MOTTA SOLUTION FOR US
C
0097      230 AA=ALPHA/DSQRT(UG-1.00)
0098      FACTOR=ULAP(U0)/ACCPTR
0099      FACTOR=FACTOR/(FACTOR+2.00*ACCPTR)
C100      XLMBDA=(1.00+AA/2.00)/(UG-U0+1.00-(U0-1.500)*AA)
U101      AA=(1.00-XLMBDA)/(UG-U0)
U102      UC=U0+VDRAIN
U103      IF(UG.LE.UC) UC=UG
U105      XC=XCHNL-U0*(1.00-DSQRT(UC/UD))
U106      EXPNT=(XLMBDA+AA)/AA
U107      E0=FACTOR*(1.00-(1.00-AA*(UC-U0))*EXPNT)/XC
U108      EXPNT=1.00/EXPNT

C
C      THE KENNEDY-MURLEY -MOTTA SOLUTION FOR US IS APPLIED FOR XX.LT.
C      (XCHNL-1.3*U0). BEYOND THAT A PARABOLIC SOLUTION FOR US IS
C      APPLIED, DETERMINED EMPIRICALLY BY SUTHERLAND.
C
0109      XC=XCHNL-1.300*U0
0110      IF(XC.GE.1.0-1*XCHNL) GO TO 235
0112      WRITE(6,1000)
0113      1000 FORMAT(1H0,5X,'RUN TERMINATED IN SUBROUTINE INITIAL. ',/,
1' THE DRAIN VOLTAGE EXCEEDS THAT FOR WHICH THE PROGRAM ',/,
2' WAS DESIGNED. (THE LOGIC FAILS FOR PARABOLIC EXTENSION',/,
3' OF THE KENNEDY-MURLEY-MOTTA SOLUTION FOR PSI ALONG THE',/,
4' SI-UX INTERFACE',//)
C
C      STOP NOT SHOWN IN THE FLOWCHART
C
0114      235 KEY=2
0115      I=1
0116      XX=0.
0117
0118      240 J=JMAX
0119      I=I+1
0120      XX=XX+XDLT(I)
0121      IF(XX.GT.XC) GO TO 250
0123      US=U0+(1.00-(1.00-E0*XX))*EXPNT/AA
0124      GO TO 310

C
C      SET UP COEFFICIENTS FOR PARABOLIC SOLUTION FOR US.
C
0125      250 KEY=3
0126      UST=US
0127      XX=XX-XDLT(I)
0128      I=I+1
0129      IMINN=I
0130      FACTOR=XLMBDA+AA
0131      EXPNT=XLMBDA/FACTOR
0132      BB=(E0/FACTOR)/((1.00-E0*XX))*EXPNT)

C
C      TERMINATION POINT FOR THE PARABOLIC SOLUTION DEPENDS ON WHETHER
C      UG.GT.UD. IF SO, TERMINATION IS AT XCHNL. IF NOT, TERMINATION
C      OCCURS WHEN US.GT.UG.
C
0133      IF(UG.GE.UD) GO TO 280
0135      DD=0.
0136      I=I+1
0137      IF(I.GT.IMAX) GO TO 270
0139      DD=DD+XDLT(I)
0140      US=PSI(1,J)-PSIEU
0141      IF(US.LT.UG) GO TO 260
0143      270 AA=(US-UST-BB*DD)/(DU*UD)
0144      IMAXX=I-1
0145      GO TO 290
0146      280 DD=XCHNL-XX
0147      AA=(UD-UST-BB*DD)/(DU*DD)
0148      IMAXX=IMAX-1
0149      290 I=IMINN
0150      XX=0.

C
C      PARABOLIC EQUATION FOR US IN THE INTERVAL WHERE IT APPLIES.

```

THIS PAGE IS BEST QUALITY PRACTICABLE
FROM COPY FURNISHED TO DDG


```

C
ISN 0151      300 J=JMAX
ISN 0152      I=I+1
ISN 0153      IF(I.GT.IMAXX) GO TO 360
ISN 0154      XX=XX+XDLT(I)
ISN 0155      US=AA*XX*XX+BB*XX+UST
C
C      ASSIGN US TO THE SURFACE POINT ONLY IF IT EXCEEDS THE POTENTIAL
C      ALREADY THERE DUE TO THE SHEATHS.
ISN 0157      310 IF(US.GT.(PSI(1,J)-PSIEQ)) GO TO 320
ISN 0159      IF(KEY.EQ.2) GO TO 240
ISN 0161      GO TO 300
C
C      FIRST FILL IN THE OXIDE POTENTIALS ABOVE THE INTERFACE.
C
ISN 0162      320 J=JMAX+1
ISN 0163      YY=YDLT(J)*DIELK/(1.00+DIELK)
ISN 0164      YY=YY+YDLT(J)
ISN 0165      JMINN=J
ISN 0166      DO 330 J=JMINN,JMAXX
ISN 0167      YY=YY+YDLT(J)
ISN 0168      330 PSI(1,J)=(PSI(1,JMAX5)-PSIEQ)-US)*YY/YOXIDE+US+PSIEQ
C
C      SET UP TO INTEGRATE A 1-D POISSON EQ FROM THE SURFACE DOWNWARD,
C      WHICH MATCHES THE POTENTIAL UB WITH ZERO DERIVATIVE THERE.
C
ISN 0169      UB=PSI(1,JUNCTN)-PSIEQ
ISN 0170      UDLT=US-UB
ISN 0171      IF(UDLT.GT.0) GO TO 335
ISN 0172      WRITE(6,1010)
ISN 0173
ISN 0174
1010 FORMAT(1H0,5X,'RUN TERMINATED IN SUBROUTINE INITIAL.',/,
1' THE GATE VOLTAGE IS NOT HIGH ENOUGH TO CAUSE THE',/,
2' ELECTRIC FIELD AT THE SI-OX INTERFACE TO BE DIRECTED',/,
3' VERTICALLY DOWNWARD-- A CONDITION WHICH MUST BE SAT',/,
4' ISFIED FOR THE 1-D SOLUTIONS USED IN INITIAL TO APPLY.',/)
STOP
C      NOT SHOWN IN THE FLOWCHART
ISN 0175      335 FACTOR=0.
ISN 0176      IF(UB.LT.1.01) FACTOR=DEXP(-UB)
ISN 0177      QF=-(1.00-FACTOR)
ISN 0179      UGTERM=((UG-US)/ALPHA)*((UG-US)/ALPHA)
ISN 0180      IF(UDLT.GT.1.0-4) QF=(UGTERM-UDLT-FACTOR*(DEXP(-UDLT)-1.00))/
ISN 0181      1(DEXP(UDLT)-1.00)
ISN 0183      J=JMAX
ISN 0184      Y=0.
ISN 0185      YY=XDLT(J+1)/(1.00+DIELK)
ISN 0186      DY=YY/3.00
ISN 0187      SI=US
ISN 0188      YZERU=0.
ISN 0189      SIZERU=SI
ISN 0190      KNT=0
ISN 0191      KFLAG=0
C
C      USE PREDICTOR-CORRECTOR INTEGRATION UNTIL Y & YZERU BRACKET YY.
C
ISN 0192      340 KNT=KNT+1
ISN 0193      YNEG=YZERU
ISN 0194      SINEG=SIZERU
ISN 0195      YZERU=Y
ISN 0196      SIZERU=SI
ISN 0197      CALL UNEDIM(SI,UB,FACTOR,QF,DY,DLTA,KNT,KFLAG)
C
C      TERMINATE IF KFLAG.GT.0. ( THE 1-D SOLUTION REACHED A MINIMUM VAL
C
ISN 0198      IF(KFLAG.GT.0) GO TO(210,240,300).KEY
C
C      TEST FOR BRACKETING. CONTINUE INTEGRATION IF NOT.
C
ISN 0200      Y=Y+DY
ISN 0201      350 IF(Y.LT.YY) GO TO 340
C
C      SINCE BRACKETING OCCURRED. INTERPOLATE FOR PSI AT YY.

```

THIS PAGE IS BEST QUALITY PRACTICABLE
FROM COPY FURNISHED TO DDC


```

C
V 0203      SITEMP=JTEMP(Y,YZERO,YNEG,SI,SIZERO,SINEG,YY)
V 0204      DLT=OABS(SITEMP-UB)
V 0205      IF(DLT.LT.1.D-2) GO TO (210,240,300),KEY
V 0207      SITEMP=SITEMP+PSIEU
V 0208      IF(SITEMP.LT.PSI(1,J)) GO TO (210,240,300),KEY
V 0210      PSI(1,J)=SITEMP
V 0211      YY=YY+YDLT(J)
V 0212      J=J-1
V 0213      IF(J.EQ.1) GO TO (210,240,300),KEY
V 0215      GO TO 350

C
C      SUPPLY AN INITIAL ESTIMATE FOR THE STREAM FUNCTION.
C
V 0216      360 I=1
V 0217          J=JUNCTN
V 0218          SI=PSI(1,J)
V 0219      370 I=I+1
V 0220          IF(PSI(1,J).GE.SI) GO TO 380
V 0222          SI=PSI(1,J)
V 0223          GO TO 370
V 0224      380 J=JMAX
V 0225          US=(PSI(1,J)+PSI(1,J+1))/2.D0+USS*YPOS(J)/2.D0-PSIEU
V 0226          UGTERM=((UG-US)/ALPHA)*((UG-US)/ALPHA)
V 0227          QF=(UGTERM-US-DEXP(-US)+1.D0)/(DEXP(US)-1.D0)
V 0228          SI=-DLUG(ACCPTR*QF)+PSIEU
V 0229          YY=0.
V 0230      390 IF(SI.GT.PSI(1,J)) GO TO 400
V 0232          YY=YTHPUS(J)
V 0233          J=J-1
V 0234          IF(J.EQ.1) GO TO 400
V 0236          GO TO 390
V 0237      400 Y=YY
V 0238          JMAXX=J
V 0239          DO 410 J=1,JMAXX
V 0240              DO 410 I=1,ITHMAX
V 0241      410          THETA(1,J)=1.D0
V 0242              JMINN=JMAXX+1
V 0243              DO 420 J=JMINN,JMAX
V 0244                  DO 420 I=1,ITHMAX
V 0245                      YY=YTHPUS(J)/Y
V 0246      420          THETA(1,J)=YY*(2.D0-YY)
V 0247          RETURN
V 0248          ENL

```

THIS PAGE IS BEST QUALITY PRACTICABLE
FROM COPY FURNISHED TO DDC

TESTED OPTIONS: NOCHECK,LOAD,OPT=2,SOURCE,MAP

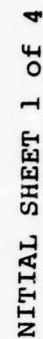
IONS IN EFFECT: NAME(MAIN) OPTIMIZE(2) LINECOUNT(74) SIZE(MAX) AUTODBL(NONE)
SOURCE LBCDIC NULIST NOCHECK OBJECT MAP NOFORMAT GOSTMT NOAREF ALC

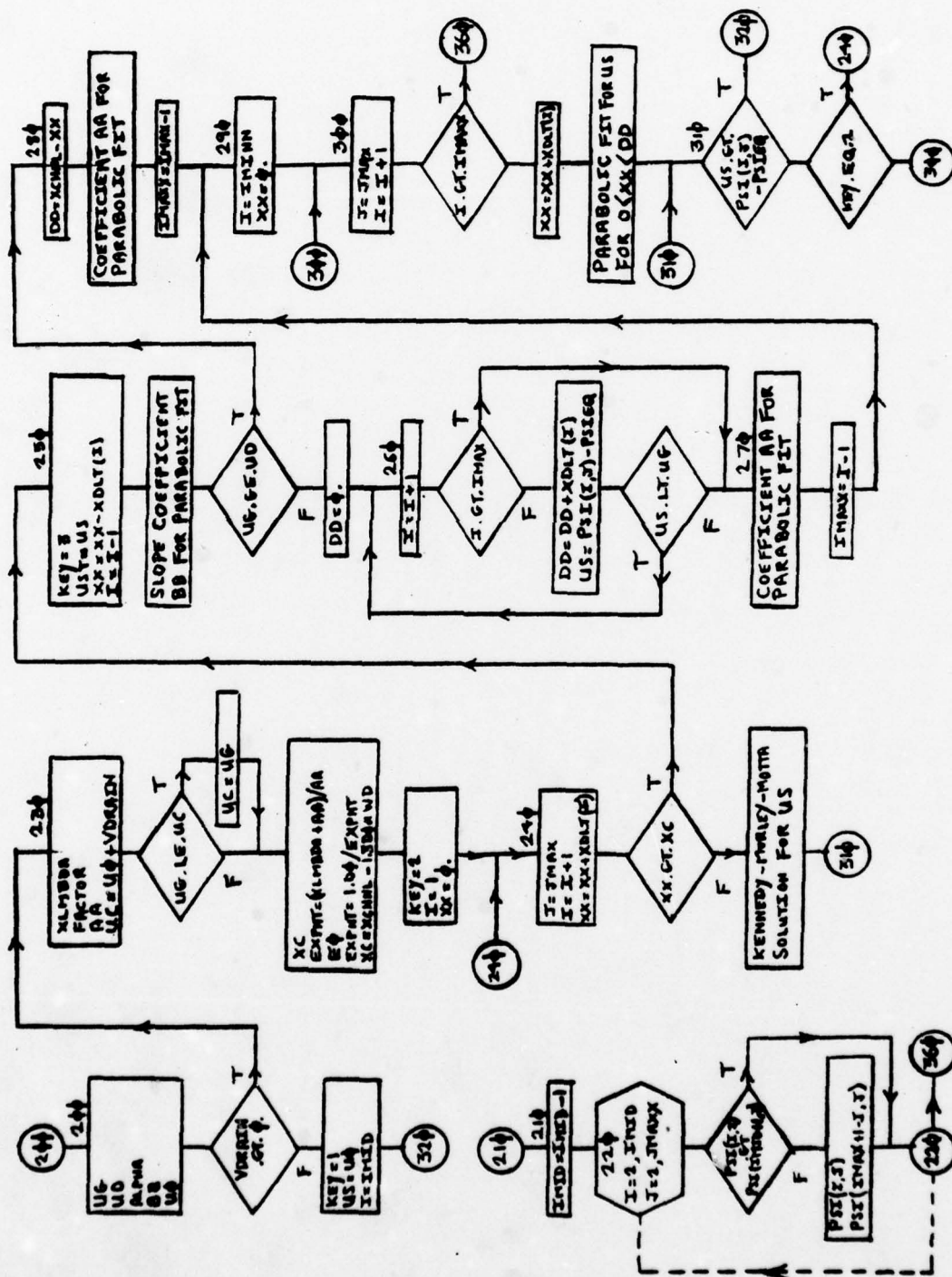
```

ISN 0002      FUNCTION QTERP(YP,YO,YN,FP,FO,FN,YY)
               C
               C      PARABOLIC INTERPOLATION WITH UNEQUAL INTERVALS FOR SUBROUTINE
               C      INITIAL
ISN 0003      C      IMPLICIT REAL*8(A-H,J-Z)
ISN 0004      DP=YP-YO
ISN 0005      DN=YO-YN
ISN 0006      DY=YY-YO
ISN 0007      DENOM=DP*DN*(DP+DN)
ISN 0008      A=(DN*FP+DP*FN-(DP+DN)*FO)/DENOM
ISN 0009      DP=DP*DP
ISN 0010      DN=DN*DN
ISN 0011      B=(DN*FP-DP*FN+(DP-DN)*FO)/DENOM
ISN 0012      QTERP=DY*(A*DY+B)+FO
ISN 0013      RETURN
ISN 0014      END

```

THIS PAGE IS BEST QUALITY PRACTICABLE
FROM COPY FURNISHED TO DDC





NITIAL SHEET 2 OF 4

5.0 VZERO & DERIV

FUNCTION VZERO solves a transcendental equation for the surface potential V_0 of the Kennedy-Motta-Murley theory. (This is the result of a one-dimensional solution of Poisson's equation in y which assumes that equilibrium conditions, viz. $\phi_n = \phi_p$, apply close to the source, as in MOS capacitor theory.) The subprogram uses the method of secants [14] to achieve this, and implicitly assumes that the energy band bending will always be in the direction which causes inversion at the silicon surface. Thus, when attempting to model p-channel structures by using this n-channel model (as was described in Chapter III) the user must assure that the above condition is not violated. Otherwise, an error message will be printed and the run will terminate.

FUNCTION DERIV provides the derivatives $d\psi/dy$ required by ONEDIM, which generates the one-dimensional solutions for $\psi(y)$ needed in implementing NITIAL, as discussed in the preceding section.

[14] F.S. Acton, NUMERICAL METHODS THAT WORK, Harper & Row, New York, 1970, p. 52.

DATE 77.183

```
ECT: NAME(MAIN) OPTIMIZE(2) LINECOUNT(74) SIZE(MAX) AUTODBL(NONE)
SOURCE E9CDIC NOLIST NODECK OBJECT MAP NOFORMAT GOSTMT NOXREF ALC NOANSF NOT
```

```
COC
FUNCTION DERIV(PRM,U,UB,FACTOR,QF,KFLAG)
PROVIDES DPSIDY/DY FOR SUBROUTINE ONEDIM.

IMPLICIT REAL*8(A-H,O-Z)
UDLT=U-UB
R=UDLT+FACTOR*(DEXP(-UDLT)-1.00)+QF*(DEXP(UDLT)-1.00)
IF(R.LT.0) GO TO 100
DERIV=PRM*DNSQRT(R)
RETURN
100 KFLAG=1
    RETURN
END
```

THIS PAGE IS BEST QUALITY PRACTICABLE
FROM COPY FURNISHED TO DDG

TED OPTIONS: NODUCK,LOAD,DPT=2,SOURCE,MAP

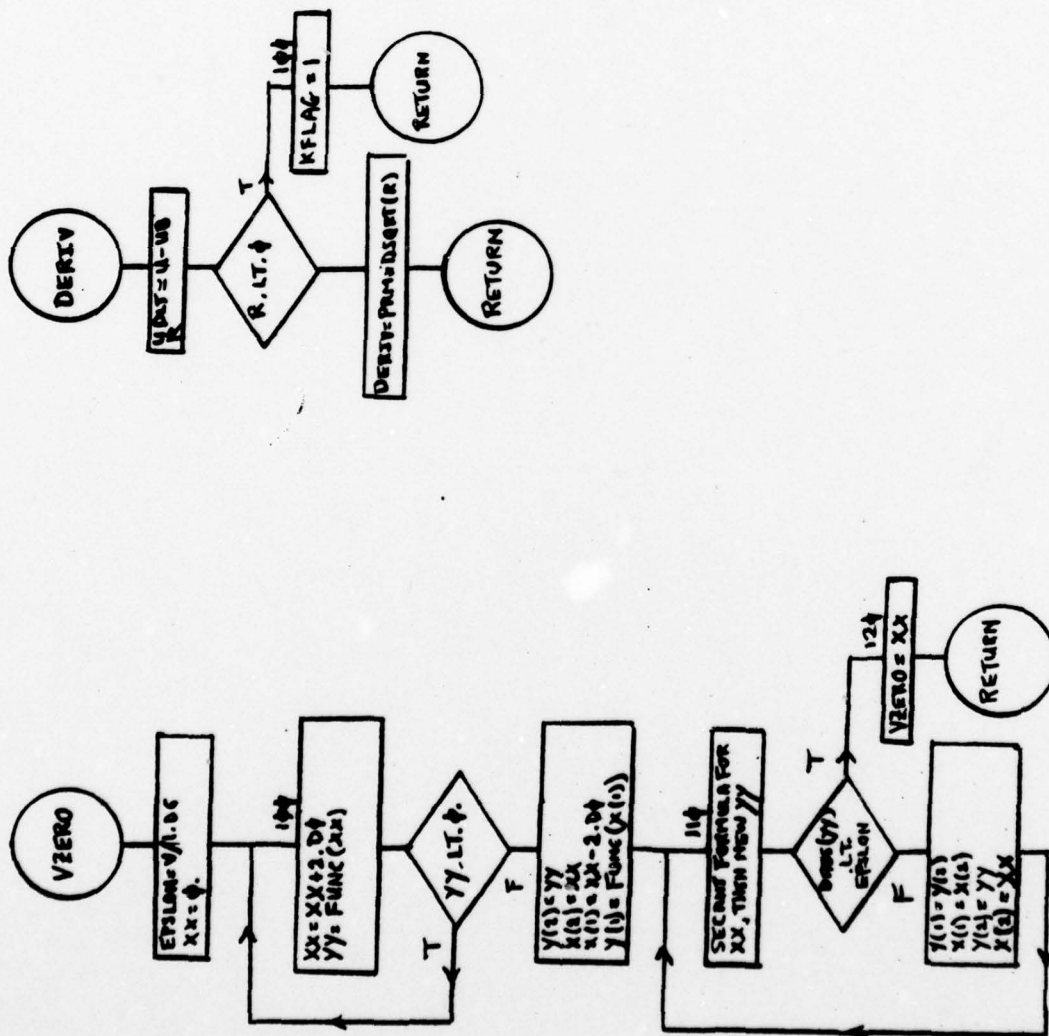
S IN EFFECT: NAME(MAIN) OPTIMIZE(2) LINECOUNT(74) SIZE(MAX) AUTODBL(NONE)
SOURCE EBCDIC NOLIST NODUCK OBJECT MAP NOFORMAT GOSTMT NOXRLF ALC N

```

0002      FUNCTION VZERO(V,A,B)
      C
      C      CALCULATES V0 OF THE ONE DIMENSIONAL KENNEDY MODEL
      C
0003      IMPLICIT REAL*8(A-H,O-Z)
0004      DIMENSION X(2),Y(2)
0005      FUNC(X)=X+A*DSQRT(DEXP(-X)+X-1.00+B*(DEXP(X)-1.00))-V
0006      EPSLON=V/1.06
0007      XX=0.
      C
      C      INCREMENT XX UNTIL YY CHANGES SIGN FROM MINUS TO PLUS.
      C
0008      100 XX=XX+2.00
0009      YY=FUNC(XX)
0010      IF(YY.LT.0.) GO TO 100
      C
      C      USE METHOD OF SECANTS TO REDUCE YY BELOW EPSLON.
      C
0012      Y(2)=YY
0013      X(2)=XX
0014      X(1)=XX-2.00
0015      Y(1)=FUNC(X(1))
0016      110 XX=(X(2)*Y(1)-X(1)*Y(2))/(Y(1)-Y(2))
0017      YY=FUNC(XX)
0018      IF(DABS(YY).LT.EPSLON) GO TO 120
0020      Y(1)=Y(2)
0021      X(1)=X(2)
0022      Y(2)=YY
0023      X(2)=XX
0024      GO TO 110
0025      120 VZERO=XX
0026      RETURN
0027      END

```

THIS PAGE IS BEST QUALITY PRACTICABLE
FROM COPY FURNISHED TO DDC



FUNCTIONS VZERO & DERIV SHEET 1 OF 1

6.0 ONEDIM

This subroutine implements the Adams-Bashforth-Moulton predictor-corrector algorithm [15], with a simple modification to improve its accuracy [16], to obtain the one-dimensional solutions of Poisson's equation required for NITIAL. It utilizes a 4th order Runge-Kutta starting procedure [17] to initialize the solution. Interval halving and doubling are invoked when tests show that these measures are acceptable.

[15] F.S. Acton, loc. cit., p. 146.

[16] ENCYCLOPAEDIC DICTIONARY OF MATHEMATICS FOR ENGINEERS AND APPLIED SCIENTISTS, Pergamon Press, 1976, (I.N. Sneddon, Editor), p. 182.

[17] J.B. Scarborough, NUMERICAL MATHEMATICAL ANALYSIS, Fifth Edition, Johns Hopkins Press, 1962, p. 357.

TESTED OPTIONS: NOCHECK, LOAD, OPT=2, SOURCE, MAP

IONS IN EFFECT: NAME(MAIN) OPTIMIZE(2) LINECOUNT(74) SIZE(MAX) AUTODBL(NONE)
SOURCE EBCDIC NOLIST NOCHECK OBJECT MAP NOFORMAT GOSTMT NOXREF ALC NO

```

ISN 0002      SUBROUTINE UNEDIM(SI,UB,FACTOR,QF,DY,DLTA,KNT,KFLAG)
C
C      USED ADAMS-DASHFORD-MOULTON PREDICTOR-CORRECTOR (WITH RUNGE-KUTTA
C      STARTING PROCEDURE) TO INTEGRATE 1-D SOLUTION OF POISSON'S EQ FOR
C      SUBROUTINE INITIAL.
ISN 0003      IMPLICIT REAL*8(A-H,D-Z)
C
ISN 0004      COMMON/ARRAYS/PSI(41,30),EDENS(41,25),HDENS(41,25),THETA(40,25),
18(41,30),D(41,30),E(41,30),F(41,30),H(41,30),U(41,30),DELTA(41,30),
2,XPLS(41),YPOS(25),XTHPOS(41),YTHPOS(25)
ISN 0005      COMMON/CUEFF/XDLT(42),YDLT(31),XTHDLT(41),YTHDLT(25),HNRTH(41,30),
1HEAST(41,30),HSTH(41,30),HWEST(41,30),HCNTR(41,30),THNRTH(40,25),
2THEAST(40,25),THSTH(40,25),THWEST(40,25),JAREA(41,25)
ISN 0006      COMMON/REAL/XCHNL,YSUB,YUXIDE,YJUNCT,DUNOR,ACCPTR,VGATE,VSUB,
1VURAIN,DIELK,QSS,CURRNT,EDENS0,PSIEU
ISN 0007      COMMON/INTGR/IMAX,JMAX,JMAX5,JUNCTN,ITHMAX
C
ISN 0008      DIMENSION USI(7)
C
C      USE RUNGE-KUTTA FOR THE FIRST FOUR INTEGRATION STEPS.
C
ISN 0009      IF(KNT.EQ.1) PRM=-DSQRT(2.00*ACCPTR)
ISN 0011      IF(KNT.GT.4) GO TO 100
ISN 0013      UK1=DERIV(PRM,SI,UB,FACTOR,QF,KFLAG)
ISN 0014      ETA=SI+UK1*DY/2.00
ISN 0015      DK2=DERIV(PRM,ETA,UB,FACTOR,QF,KFLAG)
ISN 0016      ETA=SI+UK2*DY/2.00
ISN 0017      UK3=DERIV(PRM,ETA,UB,FACTOR,QF,KFLAG)
ISN 0018      ETA=SI+UK3*DY
ISN 0019      UK4=DERIV(PRM,ETA,UB,FACTOR,QF,KFLAG)
ISN 0020      USI(KNT+3)=(UK1+2.00*(UK2+UK3)+DK4)/6.00
ISN 0021      SI=SI+USI(KNT+3)*DY
ISN 0022      KDLT=3
ISN 0023      USI(KNT+3)=DERIV(PRM,SI,UB,FACTOR,QF,KFLAG)
ISN 0024      GO TO 150
C
C      PREDICTOR-CORRECTOR USING PRESENT INTERVAL.
C
ISN 0025      100 PRDICT=(55.00*USI(7)-59.00*USI(6)+37.00*USI(5)-9.00*USI(4))*
1DY/24.00
ISN 0026      ETA=SI+PRDICT
ISN 0027      USINEW=DERIV(PRM,ETA,UB,FACTOR,QF,KFLAG)
ISN 0028      CORRECT=(9.00*USINEW+19.00*USI(7)-5.00*USI(6)+USI(5))*DY/24.00
ISN 0029      DLT=DABS(PRDICT-CORRECT)
C
C      HALVE THE INTERVAL IF DLT EXCEEDS DLTA.
C
ISN 0030      IF(DLT.LT.DLTA) GO TO 110
C
C      PARABOLIC INTERPOLATION COEFFICIENTS FOR THE HALF INTERVAL VALUE.
C
ISN 0032      AA=(USI(7)-2.00*USI(6)+USI(5))/(2.00*DY*DY)
ISN 0033      BB=(USI(7)-USI(5))/(2.00*DY)
ISN 0034      AAA=(USI(6)-2.00*USI(5)+USI(4))/(2.00*DY*DY)
ISN 0035      BBB=(USI(6)-USI(4))/(2.00*DY)
ISN 0036      DY=DY/2.00
ISN 0037      USI(1)=USI(4)
ISN 0038      USI(3)=USI(5)
ISN 0039      USI(5)=USI(6)
ISN 0040      USI(2)=DY*(AAA*DY-BBB)+USI(3)
ISN 0041      USI(4)=DY*(AA*DY-BB)+USI(5)
ISN 0042      USI(6)=DY*(AA*DY+BB)+USI(5)
ISN 0043      GO TO 100
C
C      TENTATIVELY DOUBLE THE INTERVAL, BUT ONLY IF 3 STEPS HAVE BEEN
C      TAKEN SINCE THE LAST DOUBLING, AND ONLY IF DLT IS LESS THAN

```



```

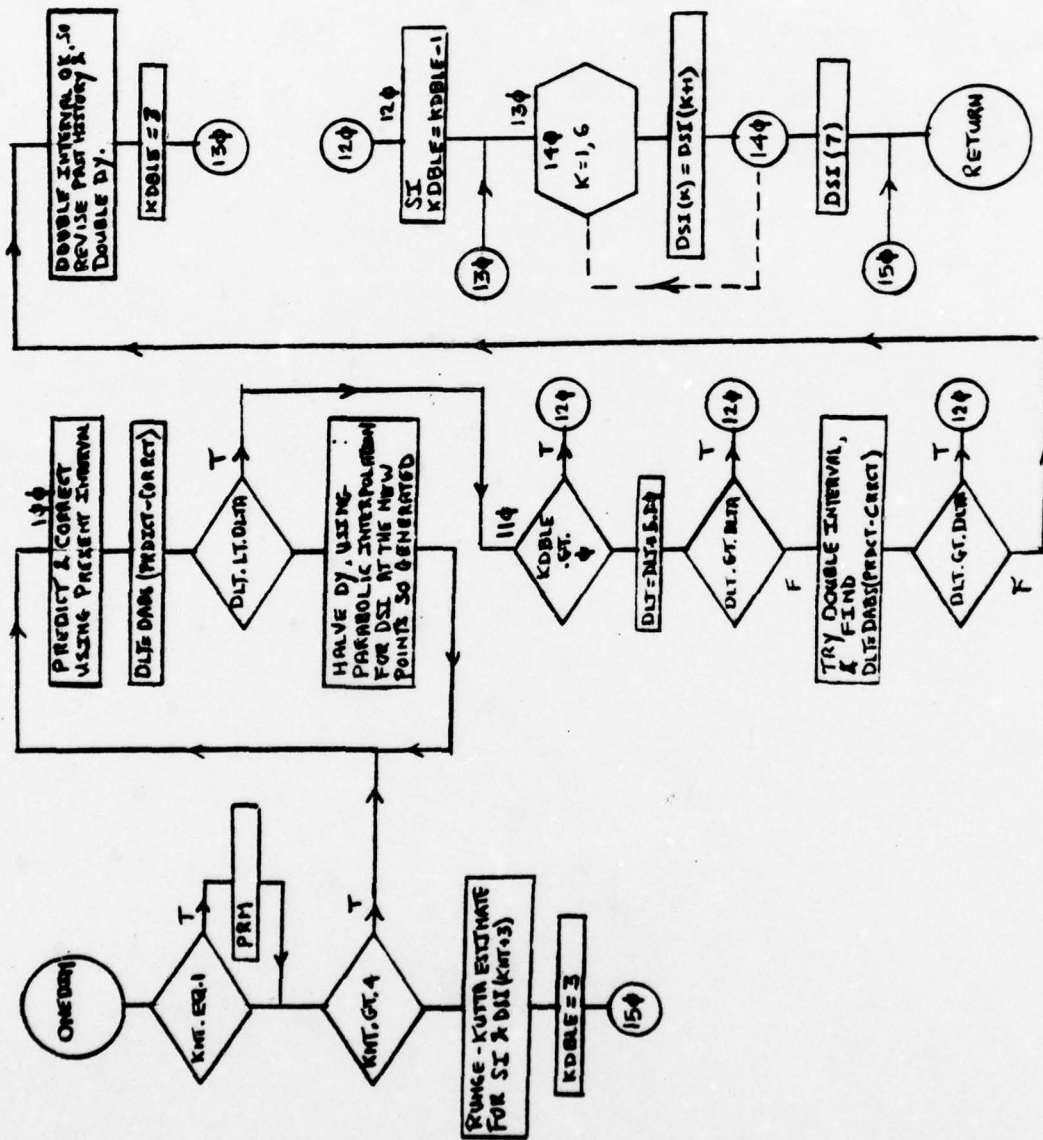
C      ONE FIFTH OF DELTA.
C
0044      110 IF(KDOUBLE.GT.0) GO TO 120
0046          DLT=DLT*5.00
0047          IF(DLT.GT.DELTA) GO TO 120
0049          PRDCT=(55.00*DSI(7)-59.00*DSI(5)+37.00*DSI(3)-9.00*DSI(1))*
          DY/12.00
0050          ETA=SI+PRDCT
0051          USINE*=DERIV(PRM,ETA,UB,FACTOR,GF,KFLAG)
0052          CRRCT=(9.00*USINE*+19.00*DSI(7)-5.00*DSI(5)+DSI(3))*DY/12.00
0053          DLT=DABS(PRDCT-CRRCT)
0054          IF(DLT.GT.DELTA) GO TO 120

C      DOUBLE INTERVAL IS OK. SO DO IT.
C
0056          DSI(6)=DSI(5)
0057          DSI(5)=DSI(3)
0058          DSI(4)=DSI(1)
0059          DY=2.00*DY
0060          SI=SI+(19.00*PRDCT+251.00*CRRCT)/270.00
0061          KDOUBLE=3
0062          GO TO 130

C      NO DOUBLING OCCURRED. COMPUTE NEW SI & SHIFT DERIVATIVES LEFT
C      FOR THE NEXT INTEGRATION STEP, UPDATING THE PRESENT DERIVATIVE.
C
0063      120 SI=SI+(19.00*PRDCT+251.00*CRRCT)/270.00
0064          KDOUBLE=KDOUBLE-1
0065      130 DO 140 K=1,6
0066      140 DSI(K)=DSI(K+1)
0067          DSI(7)=DERIV(PRM,SI,UB,FACTOR,GF,KFLAG)
0068      150 RETURN
0069      END

```

**THIS PAGE IS BEST QUALITY PRACTICABLE
FROM COPY FURNISHED TO DDC**



ONEDIM SHEET 1 of 1

7.0 RELAX & GRELAX

This subprogram implements the Picard iteration method described in Chapter I, Section 4.01. It calculates and applies the Chebyscheff sequence of relaxation parameters, reinitiating said sequence whenever the maximum residual at step $(m+1)$ is detected to exceed that encountered at step (m) , as suggested by Mock.

7.01 GRELAX

GRELAX, which appears as an ENTRY statement in RELAX (in order to reduce storage requirements because it utilizes some arrays also used by RELAX), implements the overrelaxed Gummel's algorithm, described in Chapter I, Section 4.02.

DELETED OPTIONS: NUDECK,LOAD,OPT=2,SOURCE,MAP

OPTIONS IN EFFECT: NAME(MAIN) OPTIMIZE(2) LINECOUNT(74) SIZE(MAX) AUTODBL(NONE)
SOURCE EBCDIC NULIST NUDECK OBJECT MAP NOFORMAT GOSTMT NOXREF ALLOCN

```

ISN 0002      SUBROUTINE RELAX(ITMAX,ITSIMX,ITTHMX,CONVRG,SIDLT,THDLT,DNR)
C
C      IMPLEMENTS CHEBYSCHIEFF RELAXATION SEQUENCE FOR THE PICARD
C      ITERATION (KEY=0) OR GUMMEL'S ALGORITHM (KEY=1) FOR A SELF-
C      CONSISTENT SOLUTION FOR PSI,EDENS, & THETA. SEE FORSYTHE & WASOW
C      "FINITE-DIFFERENCE METHODS FOR PARTIAL DIFFERENTIAL EQUATIONS",
C      WILEY,1960, P235.
ISN 0003      IMPLICIT REAL*8(A-H,O-Z)
C
ISN 0004      COMMON/ARRAYS/PSI(41,30),EDENS(41,25),HDENS(41,25),THETA(40,25),
1J(41,30),D(41,30),E(41,30),F(41,30),H(41,30),Q(41,30),DELTA(41,30),
2,XPOS(41),YPOS(25),XTHPOS(41),YTHPOS(25)
ISN 0005      COMMON/CLEFF/XDLT(42),YDLT(31),XTHDLT(41),YTHDLT(25),HNRTH(41,30)
1HEAST(41,30),HSTH(41,30),HWEST(41,30),HCNTR(41,30),THNRTH(40,25)
2THEAST(40,25),THSTH(40,25),THWEST(40,25),CAREA(41,25)
ISN 0006      COMMON/REAL/XCHNL,YSUB,YOXIDE,YJUNCT,DUNOR,ACCPTR,VGATE,VSUB,
1VDRAIN,DIELK,QSS,CURRNT,EDENS0,PSIEG
ISN 0007      COMMON/INTG/IMAX,JMAX,JMAX5,JUNCTN,ITHMAX
ISN 0008      COMMON/CNTRL/ OMEGA
C
ISN 0009      DIMENSION DLT(41,30), RESID(41,30)
C
ISN 0010      KEY=0
ISN 0011      JMAX5=JMAX5-1
ISN 0012      KNT=1
ISN 0013      IT=1
ISN 0014      DLTMAX1=1.D50
C
C      GIVEN THE INITIAL ESTIMATE FOR PSI FROM SUBROUTINE INITAL, FIND
C      THE CORRESPONDING INITIAL ESTIMATES FOR THETA,EDENS, & HDENS.
C
ISN 0015      CALL STREAM(ITTHMX,THDLT)
ISN 0016      CALL CURDNS(DNR)
ISN 0017      CALL DENSITY(DNR)
C
C      ESTIMATE THE RANGE(AA,BB) OF THE MATRIX EIGENVALUES.
C
ISN 0018      CALL EIGEN(AA,BB)
C
C      ITERATION LOOP STARTS AT 100, ENDS JUST BEFORE 190.
C
ISN 0019      100 CALL PUSSN(ITSIMX,SIDLT,KEY)
ISN 0020      DLTMAX2=0.
C
C      FIND MAXIMUM RESIDUAL & TERMINATE IF IT IS LESS THAN THE
C      SPECIFIED MAXIMUM VALUE.
C
ISN 0021      DO 110 I=2,ITHMAX
ISN 0022      DO 110 J=2,JMAX5
ISN 0023      DLTMAX2=DMAX1(DABS(DELTA(I,J)),DLTMX2)
ISN 0024      110 CONTINUE
ISN 0025      IF(DLTMAX2.LE.CONVRG) GO TO 190
ISN 0027      IF(IT.GT.ITMAX) GO TO 200
C
C      INITIALIZE CHEBYSCHIEFF SEQUENCE IF KNT=1
C
ISN 0029      IF(KNT.GT.1) GO TO 140
ISN 0031      120 CUSH=(BB+AA)/(BB-AA)
ISN 0032      CSHF=CUSH
ISN 0033      CSH0=1.D0
ISN 0034      ALPHA=2.D0/(BB+AA)
ISN 0035      DO 130 I=1,IMAX
ISN 0036      DO 130 J=2,JMAX5
ISN 0037      TMP=PSI(I,J)
ISN 0038      DELTA(I,J)=DELTA(I,J)
ISN 0039      PSI(I,J)=SI(I,J)+ALPHA*DELTA(I,J)

```



```

0040      130 RESIDL(I,J)=PSI(I,J)-TMP
0041      DLTMA1=DLTMA2
0042      IT=IT+1
0043      KNT=KNT+1
0044      GO TO 180

C
C      IF THE MAXIMUM DELTA HAS INCREASED, RATHER THAN DECREASED,
C      REINITIALIZE THE CHEBYSCHIEFF SEQUENCE. USE THE PREVIOUS VALUES OF
C      DELTA & PSI, UNLESS THE SEQUENCE WAS JUST PREVIOUSLY RESET.
C      OTHERWISE USE PRESENT VALUES TO AVOID AN ENDLESS LOOP.
C
0045      140 IF(DLTMA2.LT.DLTMA1) GO TO 160
0047      IF(KNT.EQ.2) GO TO 120
0049      DO 150 I=1,IMAX
0050      DO 150 J=2,JMAXX
0051      DELTA(I,J)=DLTA(I,J)
0052      150 PSI(I,J)=PSI(I,J)-RESIDL(I,J)
0053      KNT=1
0054      GO TO 120

C
C      CHEBYSCHIEFF SEQUENCE OF ALPHAS & BETAS, USING A RECURSIVE
C      FORMULA FOR THE REQUIRED HYPERBOLIC FUNCTIONS.
C
0055      160 COSHN=COSH0
0056      COSH0=CUSHP
0057      CUSHP=2.00*CUSH*CUSH0-COSH0
0058      ALPHA=4.00*CUSH0/(CUSHP*(DD-AA))
0059      BETA=COSH0/CUSHP
0060      DO 170 I=1,IMAX
0061      DO 170 J=2,JMAXX
0062      TMP=PSI(I,J)
0063      DLTMA(I,J)=DELTA(I,J)
0064      PSI(I,J)=PSI(I,J)+ALPHA*DELTA(I,J)+BETA*RESIDL(I,J)
0065      170 RESIDL(I,J)=PSI(I,J)-TMP
0066      DLTMA1=DLTMA2
0067      IT=IT+1
0068      KNT=KNT+1

C
C      UPDATE THETA, EDENS, & HDENS THEN CONTINUE ITERATION.
C
0069      180 CALL STREAM(IT,THMX,THDLT)
0070      CALL CURONS(DNK)
0071      CALL DENSITY(DNK)
0072      GO TO 100

C
C      TERMINATION MESSAGES.
C
0073      190 WRITE(6,1000) IT
0074      1000 FORMAT(1H0,5X,15,' ITERATIONS WERE REQUIRED IN RELAX')
0075      RETURN
0076      200 IT=IT-1
0077      WRITE(6,1010) IT,DLTMA2,DLTMA1,CONVRG
0078      1010 FORMAT(1H0,5X,' MAXIMUM ITERATIONS (ITMAX=',15,' ) WERE EXCEEDED
0079      1IN RELAX.',3X,' DLTMA2=',1PD10.2,' DLTMA1=',1PD10.2,' CONVRG=',
0080      21PD10.2,/)
0081      STOP

C
C      ENTRY GRELAX IMPLEMENTS GUMMEL'S ALGORITHM
C
0080      ENTRY GRELAX(ITMAX,ITSIMX,ITTHMX,CONVRG,SIDLT,THDLT,DNK)
0081      JMAXX=JMAX5-1
0082      IT=1
0083      KEY=1
0084      210 DLTMA2=0.
0085      CALL STREAM(IT,THMX,THDLT)
0086      CALL CURONS(DNK)
0087      CALL DENSITY(DNK)
0088      CALL PUISSN(ITSIMX,SIDLT,KEY)
0089      DO 220 I=1,IMAX
0090      DO 220 J=2,JMAXX
0091      DLTMA2=DMA1(DABS(DELTA(I,J)),DLTMA2)
0092      DLT=DABS(DELTA(I,J))

```

ISN 0093
ISN 0095
ISN 0096
ISN 0097
ISN 0098
ISN 0099
ISN 0100
ISN 0101
ISN 0103
ISN 0104
ISN 0106
ISN 0107
ISN 0109

IF (DLT.LI.DLTMX2) GO TO 220
IMAX=1
JMAX=J
220 CONTINUE
DO 230 I=1,IMAX
DO 230 J=2,JMAX
PSI(I,J)=PSI(I,J)+OMEGA*DELTA(I,J)
IF (PSI(I,J).LT.PSIEG) PSI(I,J)=PSIEG
230 CONTINUE
IF (DLTMX2.LE.CONVRG) GO TO 240
IT=IT+1
IF (IT.GT.ITMAX) GO TO 250
GO TO 210

↑
↑
↑
THESE INSTRUCTIONS ARE NEEDED. THEY WERE INSERTED FOR DEBUGGING & WERE INADVERTENTLY INCLUDED WHEN RUNNING THIS LISTING.

C
C
C

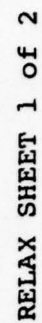
TERMINATION MESSAGES

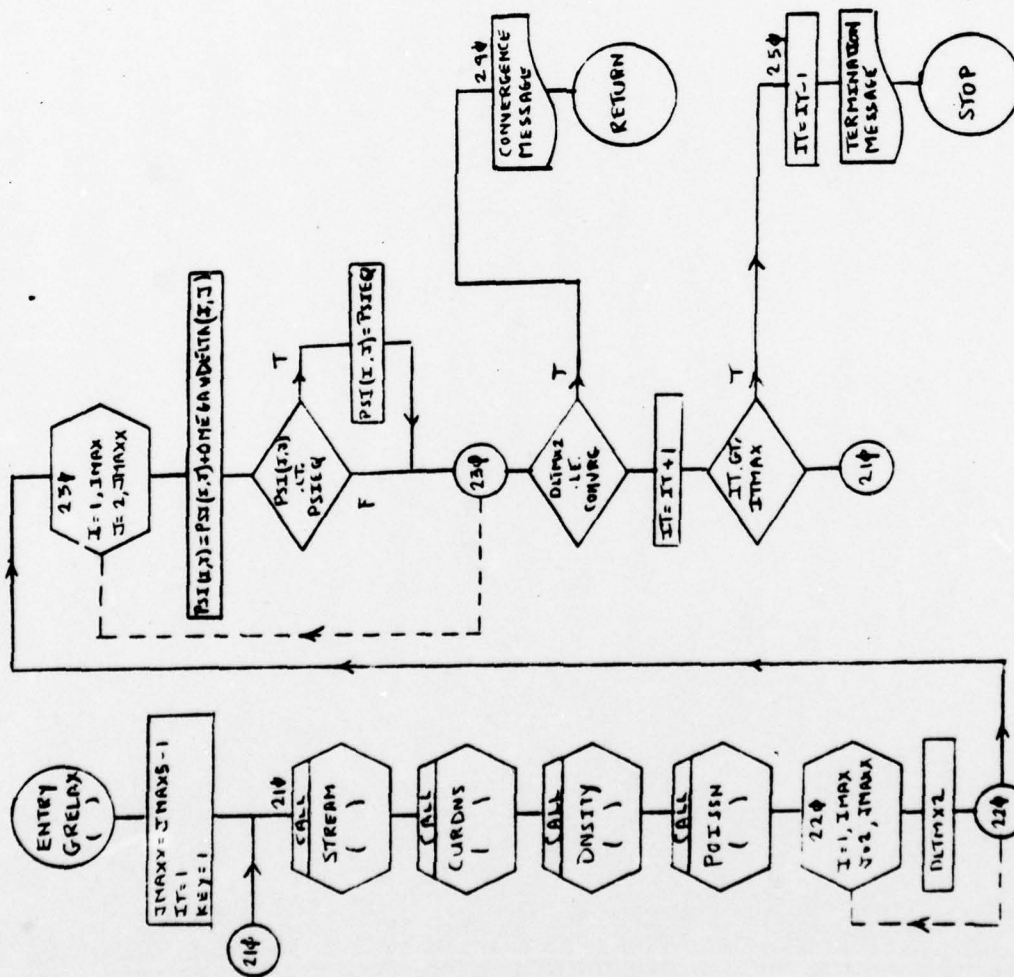
ISN 0110
ISN 0111
ISN 0112
ISN 0113
ISN 0114
ISN 0115

240 WRITE(6,1030) IT
1030 FORMAT(1H0,5X,15,' ITERATIONS WERE REQUIRED IN GRELAX',//)
RETURN
250 IT=IT-1
WRITE(6,1040) IT,DLTMX2,CONVRG
1040 FORMAT(1H0,5X,'MAXIMUM ITERATIONS(ITMAX=',15,') WERE EXCEEDED IN GRELAX.',3X,'DLTMX2=',1P010.2,' CONVRG=',21P010.2,//)
STOP
END

ISN 0116
ISN 0117

THIS PAGE IS BEST QUALITY PRACTICABLE
FROM COPY FURNISHED TO DDC





RELAX SHEET 2 of 2

8.0 STREAM

This subprogram solves for the stream function $\theta(x,y)$, and controls the Block-Line iteration algorithm until convergence is achieved. Given the potentials at the four ψ -lattice points NE, SE, SW, and NW of the θ -lattice point under consideration, it selects the one of 16 possible cases which assures that only negative exponents will be encountered in the operation $\text{DEXP}(x)$, and that only differences in potential between adjacent ψ -lattice points will appear as such exponents. It calls subroutine BLOCK, each iteration, to implement the algorithm. It calls upon function programs SIFUNC and EXPFNC to evaluate exponential functions which supply, in turn, appropriate approximations when exponential underflow, or division by zero operations are imminent.

TESTED OPTIONS: NDECK,LOAD,OPT=2,SOURCE,MAP

INS IN EFFECT: NAME(MAIN) OPTIMIZE(2) LINECOUNT(74) SIZE(MAX) AUTODBL(NONE)
SOURCE EBCDIC NULIST NDECK OBJECT MAP NOFORMAT GOSTMT NOXREF ALC

```

ISN 0002      SUBROUTINE STREAM(ITHMAX,RDELT)
C
C      SOLVES FOR THE STREAM FUNCTION THETA.
ISN 0003      IMPLICIT REAL*8(A-H,O-Z)
C
ISN 0004      COMMON/ARRAYS/PSI(41,30),EDENS(41,25),HDENS(41,25),THETA(40,25),
1B(41,30),U(41,30),E(41,30),F(41,30),H(41,30),Q(41,30),DELTA(41,
2,XPOS(41),YPOS(25),XTHPOS(41),YTHPOS(25)
ISN 0005      COMMON/CUEFF/XDLT(42),YDLT(31),XTHDLT(41),YTHDLT(25),HNRTH(41,30),
1HEAST(41,30),HSTH(41,30),HWEST(41,30),HCNTR(41,30),THNRTH(40,25),
2THEAST(40,25),THSTH(40,25),THWEST(40,25),QAREA(41,25)
ISN 0006      COMMON/REAL/XCHNL,YSUB,YOXIDE,YJUNCTN,DONOR,ACCPTR,VGATE,VSUB,
1VDRAIN,DIELK,QSS,CURRNT,EDENS0,PSIEQ
ISN 0007      COMMON/INTGR/IMAX,JMAX,JMAX5,JUNCTN,ITHMAX
C
C
C      SET UP THE ITERATION. LOOP STARTS AT 100, ENDS JUST ABOVE 300
ISN 0008      ITH=1
ISN 0009      J=JMAX
ISN 0010      100 J=J-1
ISN 0011      IF(J.LT.1) GO TO 300
ISN 0012      I=0
ISN 0013      110 I=I+1
ISN 0014      IF(I.GT.ITHMAX) GO TO 100
ISN 0015
C
C      TO AVOID EXPONENT OVERFLOW OR UNDERFLOW, THE FINITE-DIFFERENCE
C      EQUATION IS FACTORED BY DEXP(PSIMIN), WHERE PSIMIN IS THE MINIM.
C      VALUE OF PSI AT THE FOUR POINTS OF THE PSI LATTICE SURROUNDING
C      THE POINT (I,J). THE COEFFICIENTS ARE FURTHER MANIPULATED SO TH.
C      ONLY DIFFERENCES IN PSI APPEAR AS EXPONENTS WHICH ARE NEGATIVE
C      SO THAT SUITABLE APPROXIMATIONS CAN BE MADE WHEN LARGE NEGATIVE
C      EXPONENTS ARE ENCOUNTERED. FUNCTION SUBPROGRAMS SIFUNC(DSI) AND
C      EXPFNC(DSI) HANDLE THESE APPROXIMATIONS.
C
C      FIRST FIND PSIMIN AND ITS LOCATION. THE POINTS SW,SE,NE,WNW OF
C      THE POINT (I,J) ARE DESIGNATED 1,2,3,4, RESPECTIVELEY.
ISN 0017      S11=PSI(I,J)
ISN 0018      S12=PSI(I+1,J)
ISN 0019      S13=PSI(I+1,J+1)
ISN 0020      S14=PSI(I,J+1)
ISN 0021      SIMIN=UMIN1(S11,S12,S13,S14)
ISN 0022      IF(S11.EQ.SIMIN) GO TO 120
ISN 0023      IF(S12.EQ.SIMIN) GO TO 160
ISN 0024      IF(S13.EQ.SIMIN) GO TO 190
ISN 0025      GO TO 220
ISN 0026
ISN 0027
C
C      POINT #1 (SW) IS THE LOCATION OF PSIMIN.
ISN 0029      120 DSI=S12-S11
ISN 0030      FS=SIFUNC(DSI)
ISN 0031      DSI=S14-S11
ISN 0032      FW=SIFUNC(DSI)
ISN 0033      IF(S13.GT.S12) GO TO 130
ISN 0034      DSI=S12-S13
ISN 0035      FE=SIFUNC(DSI)
ISN 0036      DSI=S13-S11
ISN 0037      FE=FE*EXPFNC(DSI)
ISN 0038      GO TO 140
ISN 0039      130 DSI=S13-S12
ISN 0040      FE=SIFUNC(DSI)
ISN 0041      DSI=S12-S11
ISN 0042      FE=FE*EXPFNC(DSI)
ISN 0043      140 IF(S13.GT.S14) GO TO 150
ISN 0044      DSI=S14-S13
ISN 0045

```

THIS PAGE IS BEST QUALITY PRACTICABLE
FROM COPY FURNISHED TO DDO

2.1 (JAN 75)

STREAM

US/360 FORTRAN H EXTENDED

0A1

```

0047      FN=SIFUNC(DSI)
0048      DSI=SI3-SI1
0049      FN=FN*EXPFC(DSI)
0050      GO TO 250
0051 150    DSI=SI3-SI4
0052      FN=SIFUNC(DSI)
0053      DSI=SI4-SI1
0054      FN=FN*EXPFC(DSI)
0055      GO TO 250

```

```

C
C      POINT #2 (SE) IS THE LOCATION OF PSIMIN.
C

```

```

0056 160    DSI=SI1-SI2
0057      FS=SIFUNC(DSI)
0058      DSI=SI3-SI2
0059      FE=SIFUNC(DSI)
0060      IF(SI4.GT.SI3) GO TO 170
0062      DSI=SI3-SI4
0063      FN=SIFUNC(DSI)
0064      DSI=SI4-SI2
0065      FN=FN*EXPFC(DSI)
0066      GO TO 175
0067 170    DSI=SI4-SI3
0068      FN=SIFUNC(DSI)
0069      DSI=SI3-SI2
0070      FN=FN*EXPFC(DSI)
0071 175    IF(SI4.GT.SI1) GO TO 180
0073      DSI=SI1-SI4
0074      FW=SIFUNC(DSI)
0075      DSI=SI4-SI2
0076      FW=FW*EXPFC(DSI)
0077      GO TO 250
0078 180    DSI=SI4-SI1
0079      FW=SIFUNC(DSI)
0080      DSI=SI1-SI2
0081      FW=FW*EXPFC(DSI)
0082      GO TO 250

```

```

C
C      POINT #3 (NE) IS THE LOCATION OF PSIMIN.
C

```

```

0083 190    DSI=SI2-SI3
0084      FE=SIFUNC(DSI)
0085      DSI=SI4-SI3
0086      FN=SIFUNC(DSI)
0087      IF(SI1.GT.SI2) GO TO 200
0089      DSI=SI2-SI1
0090      FS=SIFUNC(DSI)
0091      DSI=SI1-SI3
0092      FS=FS*EXPFC(DSI)
0093      GO TO 205
0094 200    DSI=SI1-SI2
0095      FS=SIFUNC(DSI)
0096      DSI=SI2-SI3
0097      FS=FS*EXPFC(DSI)
0098 205    IF(SI1.GT.SI4) GO TO 210
0100      DSI=SI4-SI1
0101      FW=SIFUNC(DSI)
0102      DSI=SI1-SI3
0103      FW=FW*EXPFC(DSI)
0104      GO TO 250
0105 210    DSI=SI1-SI4
0106      FW=SIFUNC(DSI)
0107      DSI=SI4-SI3
0108      FW=FW*EXPFC(DSI)
0109      GO TO 250

```

```

C
C      POINT #4 (NW) IS THE LOCATION OF PSIMIN.
C

```

```

0110 220    DSI=SI1-SI4
0111      FW=SIFUNC(DSI)
0112      DSI=SI3-SI4
0113      FN=SIFUNC(DSI)

```

THIS PAGE IS BEST QUALITY PRACTICABLE
FROM COPY FURNISHED TO DDG

```

ISN 0114      IF(S12.GT.S11) GO TO 230
ISN 0116      DS1=S11-S12
ISN 0117      FS=SIFUNC(DS1)
ISN 0118      DS1=S12-S14
ISN 0119      FS=FS*EXPFNC(DS1)
ISN 0120      GO TO 235
ISN 0121      230 DS1=S12-S11
ISN 0122      FS=SIFUNC(DS1)
ISN 0123      DS1=S11-S14
ISN 0124      FS=FS*EXPFNC(DS1)
ISN 0125      235 IF(S12.GT.S13) GO TO 240
ISN 0127      DS1=S13-S12
ISN 0128      FE=SIFUNC(DS1)
ISN 0129      DS1=S12-S14
ISN 0130      FE=FE*EXPFNC(DS1)
ISN 0131      GO TO 250
ISN 0132      240 DS1=S12-S13
ISN 0133      FE=SIFUNC(DS1)
ISN 0134      DS1=S13-S14
ISN 0135      FE=FE*EXPFNC(DS1)

C
C      HAVING CALCULATED THE AVERAGE EXP(-PSI) FUNCTIONS FOR THE
C      MIDPOINTS E,W,N,S OF THE POINT (I,J) (MUCK'S "A" FUNCTIONS)
C      NOW CALCULATE THE MATRIX COEFFICIENTS B,D,E,F,H,AND Q FOR THE
C      POINT (I,J).

ISN 0136      250 B(I,J)=THSTH(I,J)*FS
ISN 0137      D(I,J)=THWEST(I,J)*FW
ISN 0138      F(I,J)=THEAST(I,J)*FE
ISN 0139      H(I,J)=THNRTH(I,J)*FN
ISN 0140      E(I,J)=-B(I,J)+D(I,J)+F(I,J)+H(I,J)
ISN 0141      Q(I,J)=0.

C
C      MODIFY THE COEFFICIENTS ALONG THE BOTTOM ROW.

ISN 0142      IF(J.GT.1) GO TO 260
ISN 0144      Q(1,1)=-B(1,1)

C
C      SIMILARLY ALONG THE LEFT BORDER

ISN 0145      260 IF(I.GT.1) GO TO 280
ISN 0147      IF(J.LT.JUNCTN) GO TO 270
ISN 0149      E(1,J)=E(1,J)+D(1,J)
ISN 0150      GO TO 110
ISN 0151      270 Q(1,J)=Q(1,J)-D(1,J)
ISN 0152      GO TO 110

C
C      SIMILARLY ALONG THE RIGHT BORDER

ISN 0153      280 IF(I.LT.ITHMAX) GO TO 110
ISN 0155      IF(J.LT.JUNCTN) GO TO 290
ISN 0157      E(1,J)=E(1,J)+F(1,J)
ISN 0158      GO TO 110
ISN 0159      290 Q(1,J)=Q(1,J)-F(1,J)
ISN 0160      GO TO 110

C
C      FIND THETA USING BLOCK-LINE ITERATION (SLUR).

ISN 0161      300 CALL BLOCK(RESID)
ISN 0162      IF(RESID.LE.RDELT) RETURN
ISN 0164      ITH=ITH+1
ISN 0165      IF(ITH.GT.ITHMAX) GO TO 310
ISN 0167      GO TO 300
ISN 0168      310 WRITE(6,1000)
ISN 0169      1000 FORMAT(1H0,5X,'MAXIMUM ITERATIONS EXCEEDED IN STREAM',//)
ISN 0170      STOP
ISN 0171      END

```


TED OPTIONS: NUDECK,LOAD,DPT=2,SOURCE,MAP

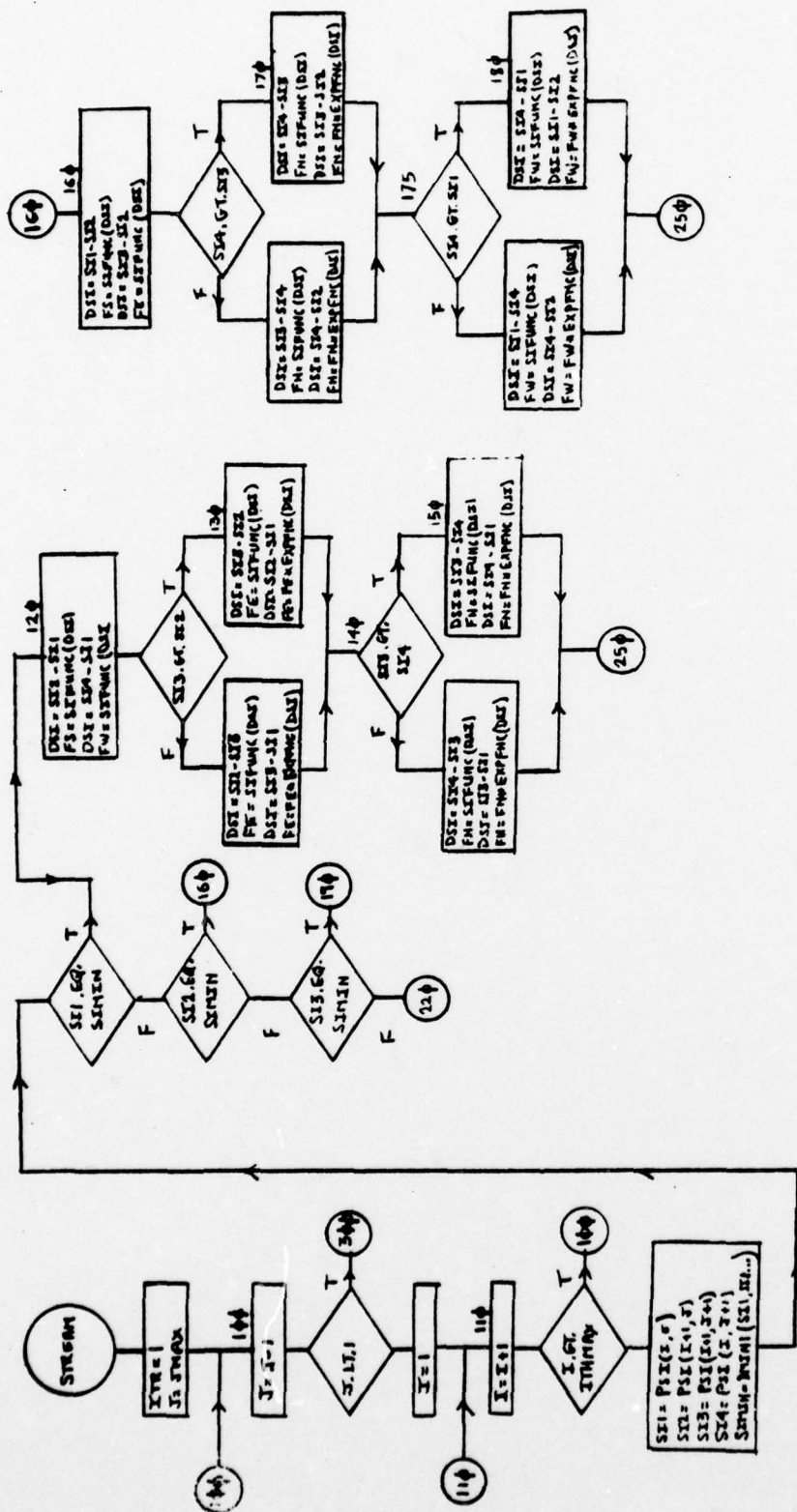
5 IN EFFECT: NAME(MAIN) OPTIMIZE(2) LINECOUNT(74) SIZE(MAX) AUTODBL(NONE)
SOURCE EBCDIC NOLIST NUDECK OBJECT MAP NOFORMAT GOSTMT NOXREF ALC N

```
0002      FUNCTION SIFUNC(DSI)
          C
          C      CALCULATES MUCK'S "A" FUNCTIONS OF PSI FOR SUBROUTINE STREAM.
          C
0003      IMPLICIT REAL*8(A-H,D-Z)
0004      IF(DSI.GT.1.7D2) GO TO 100
0006      IF(DSI.LT.1.D-9) GO TO 110
0008      SIFUNC=(1.D0-DEXP(-DSI))/DSI
0009      RETURN
0010      100 SIFUNC=1.D0/DSI
0011      RETURN
0012      110 SIFUNC=1.D0
0013      RETURN
0014      END
```

TESTED OPTIONS: NODECK, LOAD, OPT=2, SOURCE, MAP

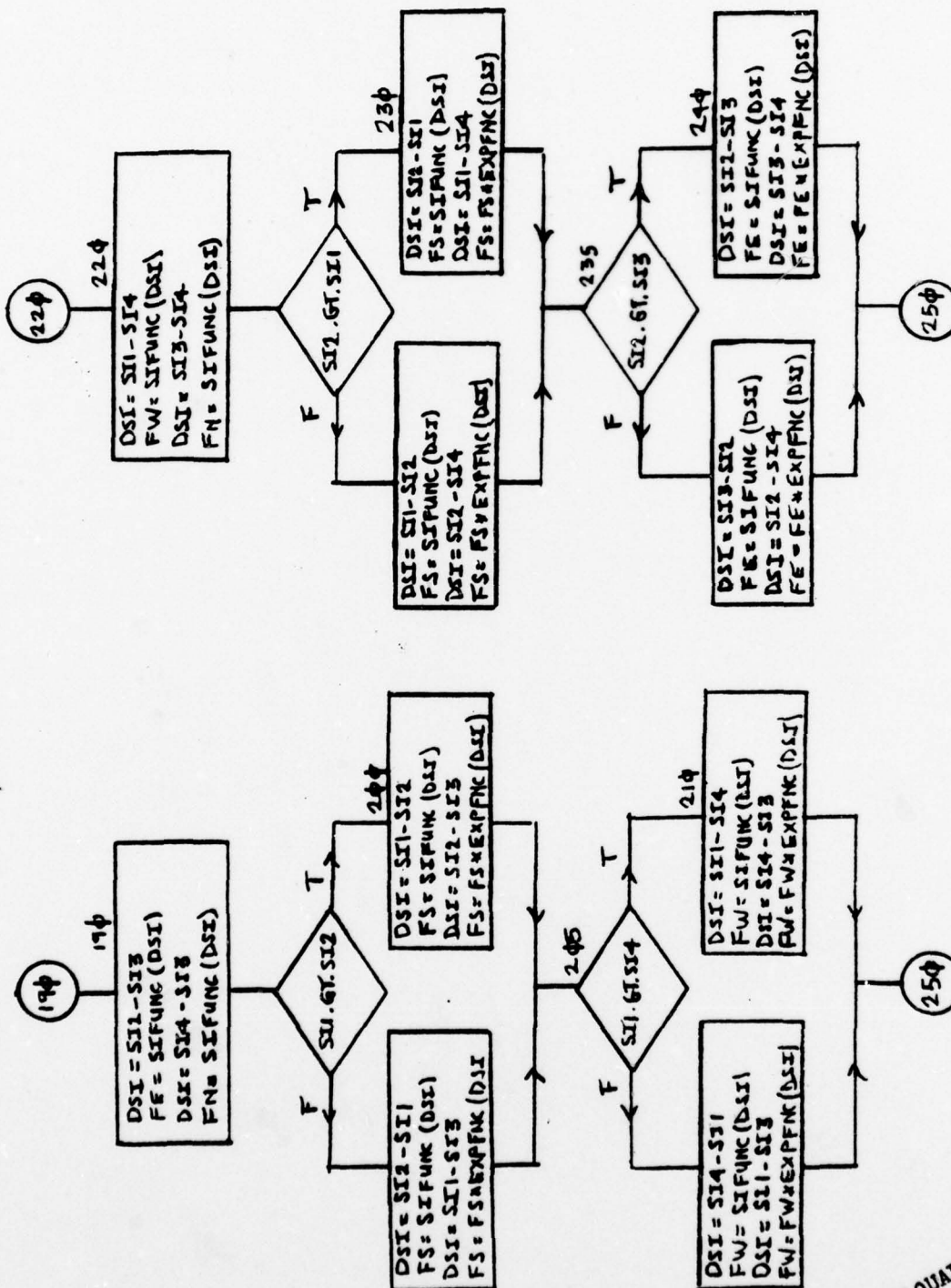
IONS IN EFFECT: NAME(MAIN) OPTIMIZE(2) LINECOUNT(74) SIZE(MAX) AUTODBL(NONE)
SOURCE LBCDIC NOLIST NODECK OBJECT MAP NOFORMAT GOSTMT NOXREF ALC NO

```
C 0002      FUNCTION EXPFNC(DSI)
C
C      CALCULATES DEXP(-DSI) FOR SUBROUTINE STREAM.
C
ISN 0003      IMPLICIT REAL*8(A-H,O-Z)
ISN 0004      IF (DSI.GT.1.7D2) GO TO 100
ISN 0005      EXPFNC=DEXP(-DSI)
ISN 0006      RETURN
ISN 0007      100 EXPFNC=0.
ISN 0008      RETURN
ISN 0009      END
ISN 0010
```

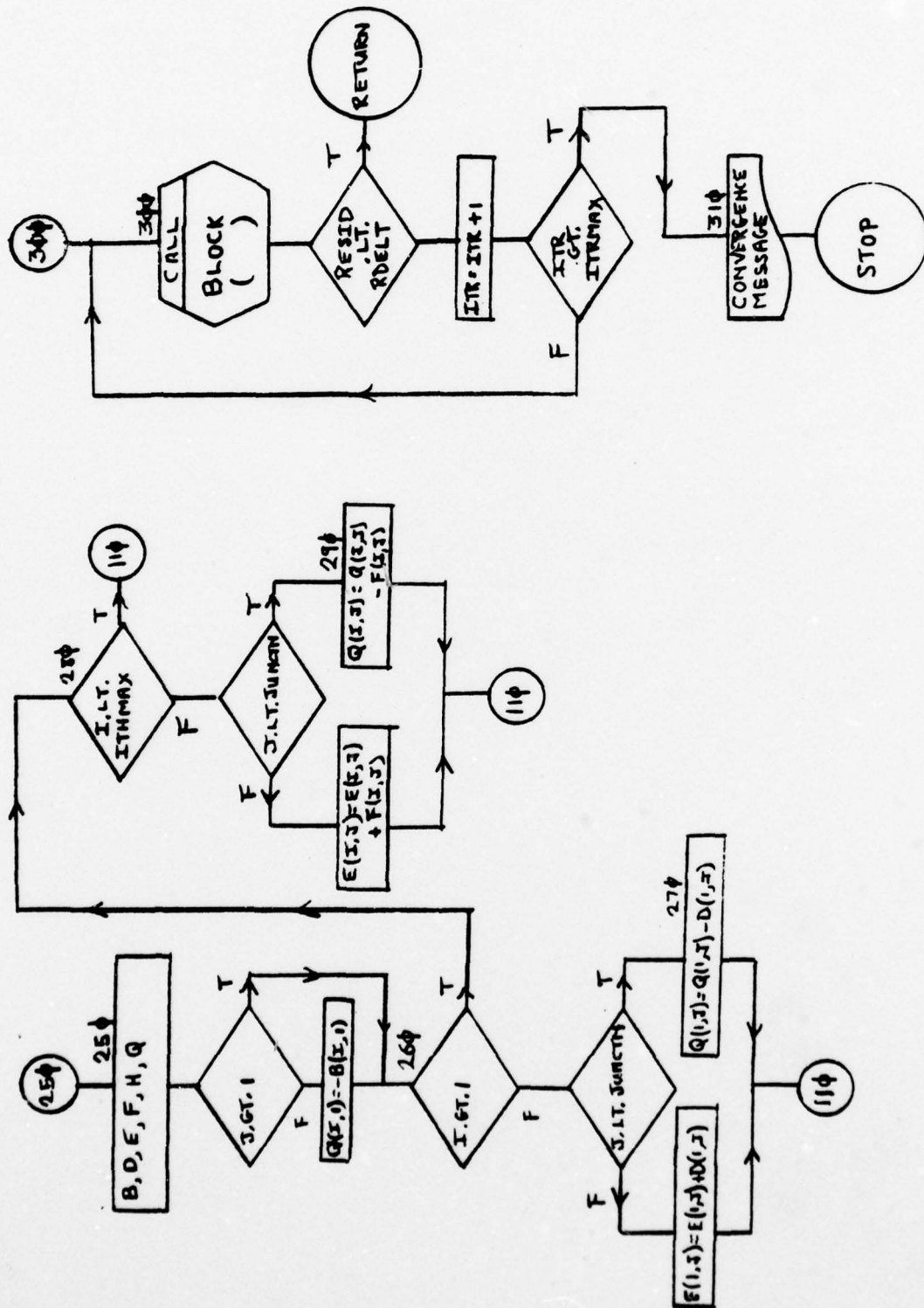


STREAM SHEET 1 of 3

THIS PAGE IS BEST QUALITY PRACTICABLE
FROM COPY FURNISHED TO DDG



STREAM SHEET 2 of 3



9.0 BLOCK

This subprogram implements the Block-Line iteration method for matrix inversion described by Varga [18], the iteration procedure itself being controlled by subroutine STREAM.

-
- [18] R.S. Varga, MATRIX ITERATIVE ANALYSIS, Prentice-Hall, 1962, pp. 195-199.

ED OPTIONS: NODUCK,LOAD,OPT=2,SOURCE,MAP

IN EFFECT: NAME(MAIN) OPTIMIZE(2) LINECOUNT(74) SIZE(MAX) AUTODBL(NONE)
SOURCE EBCDIC NOLIST NODUCK OBJECT MAP NOFORMAT GUSTMT NOXREF ALC NL

```

0002      SUBROUTINE BLOCK(RESID)
      C
      C      IMPLEMENTS BLOCK-LINE ITERATION FOR SOLVING FOR THE STREAM
      C      FUNCTION THETA. SEE VARGA "ITERATIVE MATRIX ANALYSIS", PRENTICE-
      C      HALL, 1962. PP. 194-199.
0003      C      IMPLICIT REAL*8(A-H,O-Z)
0004      C      COMMON/ARRAYS/PSI(41,30),EDENS(41,25),HDENS(41,25),THETA(40,25),
      C      1B(41,30),D(41,30),E(41,30),F(41,30),H(41,30),G(41,30),DELTA(41,30),
      C      2,XPOS(41),YPOS(25),XTHPOS(41),YTHPOS(25)
0005      C      COMMON/CUEFF/XDLT(42),YDLT(31),XTHDLT(41),YTHDLT(25),HNRTH(41,30),
      C      1HEAST(41,30),HSTH(41,30),HWEST(41,30),HCNTR(41,30),THNETH(40,25),
      C      2THEAST(40,25),THSTH(40,25),THWEST(40,25),JAREA(41,25)
0006      C      COMMON/REAL/XCHNL,YSUB,YOXIDE,YJUNCT,DUNOR,ACCPTR,VGATE,VSUB,
      C      1VDRAIN,DIELK,USC,CURKNT,EDENSO,PSIEQ
0007      C      COMMON/INTGR/IMAX,JMAX,JMAX5,JUNCTN,ITHMAX
0008      C      DIMENSION W(40),G(40),TH(40),VECTOR(40)
0009      C      IMAXX=ITHMAX-1
0010      C      JMAXX=JMAX-1
0011      C      J=JMAXX
      C
      C      OMIT THE ROW J=JMAX, WHERE THETA IS FIXED AT ZERO.
      C      INDEX DOWNWARD BY ROWS. KEY IS USED AS A SWITCH FOR THE
      C      COMPUTED GO TO STATEMENT FOLLOWING STATEMENT # 180 BELOW.
0012      C      KEY=1
0013      110 J=J-1
0014      C      IF(J.EQ.1) GO TO 130
      C
      C      ALL INTERIOR ROWS.
0016      C      DO 120 I=1,ITHMAX
0017      120 VECTOR(I)=-B(I,J)*THETA(I,J-1)-H(I,J)*THETA(I,J+1)+Q(I,J)
0018      C      GO TO 150
      C
      C      THE ROW J=1. (SET KEY = 2 TO FLAG THIS AS THE LAST ROW TREATED.)
0019      C      130 KEY=2
0020      C      DO 140 I=1,ITHMAX
0021      140 VECTOR(I)=-H(I,J)*THETA(I,J+1)+Q(I,J)
      C
      C      RECURSIVE DETERMINATION OF THETA(I,J). FIRST SET UP THE VECTORS
      C      W AND G DEFINED BY VARGA.
0022      C      150 W(1)=F(1,J)/E(1,J)
0023      C      G(1)=VECTOR(1)/E(1,J)
0024      C      DO 160 I=2,IMAXX
0025      C      DENOM=E(1,J)-D(1,J)*W(I-1)
0026      C      W(I)=F(1,J)/DENOM
0027      C      160 G(I)=(VECTOR(I)-D(1,J)*G(I-1))/DENOM
      C
      C      CALCULATE THETA(I,J) USING VARGA'S EQ (6.46*)
0028      C      TH(ITHMAX)=(VECTOR(ITHMAX)-D(ITHMAX,J)*G(IMAXX))/
      C      1(E(ITHMAX,J)-D(ITHMAX,J)*W(IMAXX))
0029      C      IF(J.EQ.JMAXX) RESID=0.
0030      C      DO 170 I=1,IMAXX
0031      C      I=IMAXX+1-I
0032      C      TH(I)=G(I)-W(I)*TH(I+1)
0033      C      RR=DABS(THETA(I,J)-TH(I))
0034      C      170 RESID=DMAX1(DABS(RR),RESID)
0035      C
      C      FILL IN NEW THETA (USING OMEGA=1.0) FOR ROW J. REPEAT PROCEDURE
      C      FOR ROW J-1 UNLESS J=1 (FLAGGED BY KEY=2). OTHERWISE TERMINATE.

```

C

ISN 0036
ISN 0037
ISN 0038
ISN 0039
ISN 0040
ISN 0041

OMEGA=1.000
DO 180 I=1,ITHMAX
180 THETA(I,J)=OMEGA*(TH(I)-THETA(I,J))+THETA(I,J)
GO TO (110,190).KEY
190 RETURN
END

10.0 DENSITY

This subprogram implements Mock's "marching method," described in Chapter I, Section 3.04, for determining the electron density $n(x,y)$. It applies appropriate approximations for $\text{DEXP}(-x)$ when x is sufficiently large.

TEC OPTIONS: NODUCK,LOAD=OPT=2,SOURCE,MAP

S IN EFFECT: NAME(MAIN) OPTIMIZE(2) LINECOUNT(74) SIZE(MAX) AUTODBL(NONE)
SOURCE EDDIC NOLIST NODUCK OBJECT MAP NOFORMAT GUSTMT NOXREF ALC NO

```

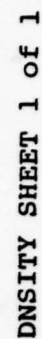
0002      SUBROUTINE DENSITY(DNR)
          C
          C      USES MUCKS INTEGRAL METHOD FOR FINDING ELECTRON DENSITY. USES
          C      THE GULTZMANN RELATIONSHIP FOR HOLE DENSITY.
0003      IMPLICIT REAL*8(A-H,U-Z)
0004      COMMON/ARRAYS/PSI(41,30),EDENS(41,25),HDENS(41,25),THETA(40,25),
          1B(41,30),U(41,30),E(41,30),F(41,30),H(41,30),Q(41,30),DELTA(41,30),
          2,XFUS(41),YPOS(25),XTHPOS(41),YTHPOS(25)
0005      COMMON/COEFF/XDLT(42),YDLT(31),XTHDLT(41),YTHDLT(25),HNRTH(41,30),
          1HEAST(41,30),HSTH(41,30),HWEST(41,30),HCNTR(41,30),THNRTH(40,25),
          2THEAST(40,25),THSTH(40,25),THWEST(40,25),GAREA(41,25)
0006      COMMON/REAL/XCHNL,YSUB,YOXIDE,YJUNCTN,DUNOR,ACCPTR,VGATE,VSUB,
          1VDRAIN,DIELK,QSS,CURRNT,EDENS0,PSIEQ
0007      COMMON/INTGR/IMAX,JMAX,JMAX5,JUNCTN,ITHMAX
          C
          C      ELECTRON DENSITY IN THE REGION "IN CONTACT WITH" THE SOURCE &
          C      DRAIN.
          C
          C      INTEGRATE AWAY FROM SOURCE UNTIL THE POTENTIAL MINIMUM IS
          C      ENCOUNTERED.
          C
0008      DO 180 J=JUNCTN,JMAX
0009      I=1
0010      100 XCRNT=CURRNT*(THETA(I,J-1)-THETA(I,J))/YTHDLT(J)
0011      PSIDL=PSI(I+1,J)-PSI(I,J)
0012      IF(PSIDL.GT.0.) GO TO 140
0014      IF(PSIDL.GT.-1.D-9) GO TO 110
0016      IF(PSIDL.LT.-2.D1) GO TO 120
0018      EDENS(I+1,J)=EDENS(I,J)*DEXP(PSIDL)+XCRNT*XDLT(I+1)*
          1(DEXP(PSIDL)-1.D0)/PSIDL
0019      GO TO 130
0020      110 EDENS(I+1,J)=EDENS(I,J)+XCRNT*XDLT(I+1)
0021      GO TO 130
0022      120 EDENS(I+1,J)=-XCRNT*XDLT(I+1)/PSIDL
0023      130 CONTINUE
0024      I=I+1
0025      IF(I.LT.IMAX) GO TO 100
0027      GO TO 180
          C
          C      INTEGRATE AWAY FROM DRAIN FOR X BEYOND POTENTIAL MINIMUM.
          C
0028      140 IMINN=1
0029      IF(IMINN.EQ.1) IMINN=2
0031      I=IMAX
0032      150 XCRNT=CURRNT*(THETA(I-1,J-1)-THETA(I-1,J))/YTHDLT(J)
0033      PSIDL=PSI(I-1,J)-PSI(I,J)
0034      IF(PSIDL.GT.-1.D-9) GO TO 155
0036      IF(PSIDL.LT.-2.D1) GO TO 160
0038      EDENS(I-1,J)=EDENS(I,J)*DEXP(PSIDL)-XCRNT*XDLT(I)*
          1(DEXP(PSIDL)-1.D0)/PSIDL
0039      GO TO 170
0040      155 EDENS(I-1,J)=EDENS(I,J)-XCRNT*XDLT(I)
0041      GO TO 170
0042      160 EDENS(I-1,J)=XCRNT*XDLT(I)/PSIDL
0043      170 CONTINUE
0044      I=I-1
0045      IF(I.GT.IMINN) GO TO 150
0047      180 CONTINUE
          C
          C      INTEGRATE DOWNWARD FROM THE ROW CONTACTING THE LOWER BOUNDARY OF
          C      THE SOURCE & DRAIN TO FILL IN THE SUBSTRATE REGION BELOW THAT ROW
          C
0048      DO 200 I=1,IMAX
0049      J=JUNCTN
0050      190 IF(I.EQ.1) GO TO 200

```

```

ISN 0052      IF(I.EQ.IMAX) GO TO 210
ISN 0054      YCRNT=-CURRENT*(THETA(I,J-1)-THETA(I-1,J-1))/XTHDLT(I)
ISN 0055      GO TO 220
ISN 0056      200 YCRNT=-CURRENT*(THETA(I,J-1)-1.00)/XTHDLT(I)
ISN 0057      GO TO 220
ISN 0058      210 YCRNT=-CURRENT*(1.00-THETA(IMAX,J-1))/XTHDLT(IMAX)
ISN 0059      220 PSIDL1=PSI(I,J-1)-PSI(I,J)
ISN 0060      IF(PSIDL1.GT.-1.0-9) GO TO 230
ISN 0062      IF(PSIDL1.LT.-2.01) GO TO 240
ISN 0064      EDENS(I,J-1)=EDENS(I,J)*DEXP(PSIDL1)+YCRNT*YDLT(J)*
      1(DEXP(PSIDL1)-1.00)/PSIDL1
ISN 0065      GO TO 250
ISN 0066      230 EDENS(I,J-1)=EDENS(I,J)+YCRNT*YDLT(J)
ISN 0067      GO TO 250
ISN 0068      240 EDENS(I,J-1)=-YCRNT*YDLT(J)/PSIDL1
ISN 0069      250 CONTINUE
ISN 0070      J=J-1
ISN 0071      IF(J.GT.2) GO TO 190
ISN 0073      260 CONTINUE
C
C      CALCULATE THE HOLE DENSITY
C
ISN 0074      DO 280 I=1,IMAX
ISN 0075      DO 280 J=1,JMAX
ISN 0076      EXPNT=VSUB-PSI(I,J)
ISN 0077      IF(EXPNT.LT.-2.01) GO TO 270
ISN 0079      HDENS(I,J)=DEXP(EXPNT)/DNR
ISN 0080      GO TO 280
ISN 0081      270 HDENS(I,J)=2.000-9
ISN 0082      280 CONTINUE
ISN 0083      RETURN
ISN 0084      END

```

11.0 CURDNS

This subprogram calculates the drain current factor J_0 , as described in Chapter I, Section 3.03. The trapezoidal rule is invoked in evaluating the integral discussed there along the row of the ψ -lattice just below the oxide-silicon interface.

TED OPTIONS: NODECK,LOAD,OPT=2,SOURCE,MAP

S IN EFFECT: NAME(MAIN) OPTIMIZE(2) LINECOUNT(74) SIZE(MAX) AUTODBL(NONE)
SOURCE EBCDIC NULIST NODECK OBJECT MAP NOFORMAT GOSTMT NOAREF ALC NL

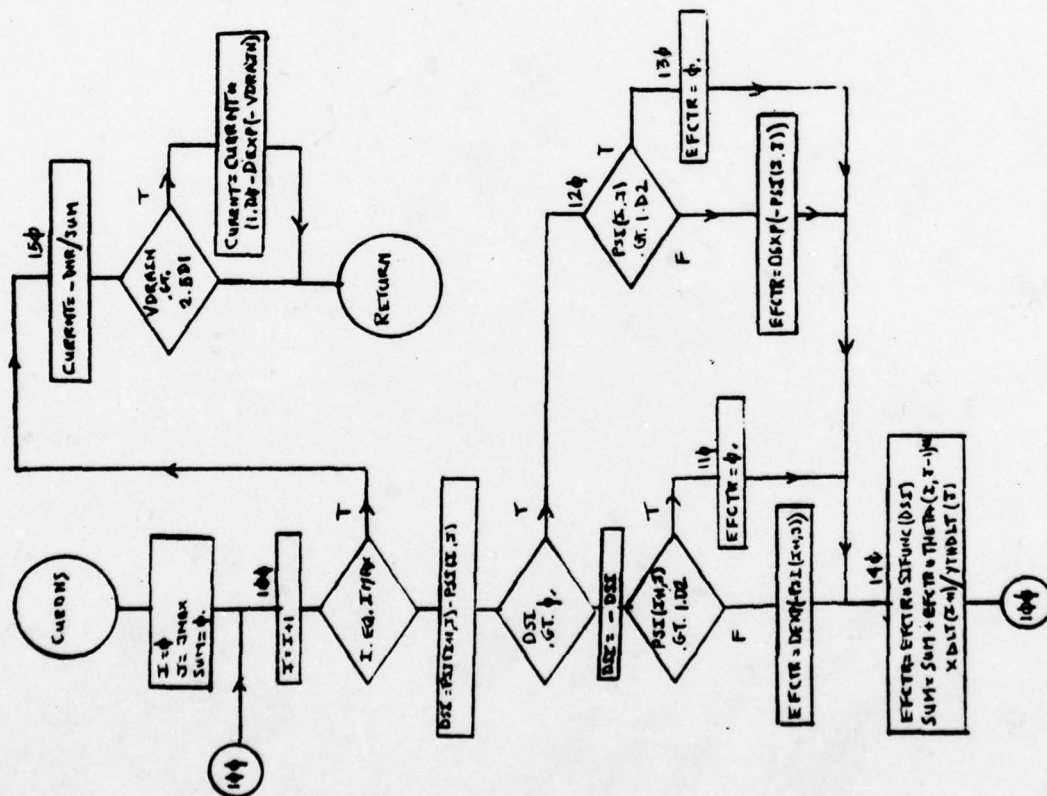
```

0002      SUBROUTINE CURRNS(DNR)
          C
          C      CALCULATES THE CURRENT DENSITY SCALE FACTOR JO (CURRNT) BY
          C      INTEGRATING FROM SOURCE TO DRAIN ALONG THE ROW JUST BELOW THE
          C      SI-OA INTERFACE.
0003      IMPLICIT REAL*8(A-H,O-Z)
          C
0004      COMMON/ARRAYS/PSI(41,30),EDENS(41,25),HDENS(41,25),THETA(40,25),
          1B(41,30),D(41,30),E(41,30),F(41,30),H(41,30),Q(41,30),DELTA(41,30),
          2,XPOS(41),YPOS(25),XTHPOS(41),YTHPOS(25)
0005      COMMON/CUEFF/XDLT(42),YDLT(31),XTHDLT(41),YTHDLT(25),HNRTH(41,30),
          1HEAST(41,30),HSTH(41,30),HWEST(41,30),HCNTR(41,30),THNRTH(40,25),
          2THEAST(40,25),THSTH(40,25),THWEST(40,25),CAKEA(41,25)
0006      COMMON/REAL/XCHNL,YSUB,YOXIDE,YJUNCTN,DONOR,ACCPTR,VGATE,VSUB,
          1VDRAIN,DIELK,CSS,CURRNT,EDENS0,PSIEQ
0007      COMMON/INTGR/IMAX,JMAX,JMAX5,JUNCTN,ITHMAX
          C
0008      IF(VDRAIN.GT.0.) GO TO 90
0010      CURRNT=0.
0011      RETURN
          C
          C      EVALUATE THE LINE INTEGRAL OF EXP(-PSI)*(OTHETA/DY) ALONG THE ROW
          C      JUST BELOW THE INTERFACE. THE IF STATEMENTS BELOW ARE TO AVOID
          C      OVERFLOW OR UNDERFLOW DUE TO LARGE POSITIVE OR NEGATIVE EXPONENTS
          C      AS WELL AS OVERFLOW DUE TO DIVISION BY A NUMBER CLOSE TO ZERO.
0012      90 I=0
0013          J=JMAX
0014          SUM=0.
0015      100 I=I+1
0016          IF(I.EQ.IMAX) GO TO 150
0018          DSI=PSI(I+1,J)-PSI(I,J)
0019          IF(DSI.GT.0) GO TO 120
0021          DSI=-DSI
0022          IF(PSI(I+1,J).GT.1.7D2) GO TO 110
0024          EFCTR=DEXP(-PSI(I+1,J))
0025          GO TO 140
0026      110 EFCTR=0.
0027          GO TO 140
0028      120 IF(PSI(I,J).GT.1.7D2) GO TO 130
0030          EFCTR=DEXP(-PSI(I,J))
0031          GO TO 140
0032      130 EFCTR=0.
0033      140 EFCTR=EFCTR*SI-UNC(DSI)
0034          SUM=SUM+EFCTR*THETA(I,J-1)*XDLT(I+1)/YTHDLT(J)
0035          GO TO 100
0036      150 CURRNT=-DNR/SUM
0037          IF(VDRAIN.LT.1.7D2) CURRNT=CURRNT*(1.00-DEXP(-VDRAIN))
0039          RETURN
0040      END

```

THIS PAGE IS BEST QUALITY PRACTICABLE
FROM COPY FURNISHED TO DDG

THIS PAGE IS BEST QUALITY PRACTICABLE
FROM COPY FURNISHED TO DDC



CURDENS SHEET 1 of 1

12.0 EIGEN

This subprogram evaluates the upper and lower bounds, b and a , of the eigenvalues of equation (24), the finite-difference equation for ψ described in Chapter I, Section 4.01. The lower bound, a , is set to unity, since its value is not critical for the Picard iteration. The upper bound, b , is evaluated from eq. (54), using a two-dimensional trapezoidal rule to approximate the integral contained therein.

REQUESTED OPTIONS: NODACK,LLAD,CPT=2,SOURCE,MAP

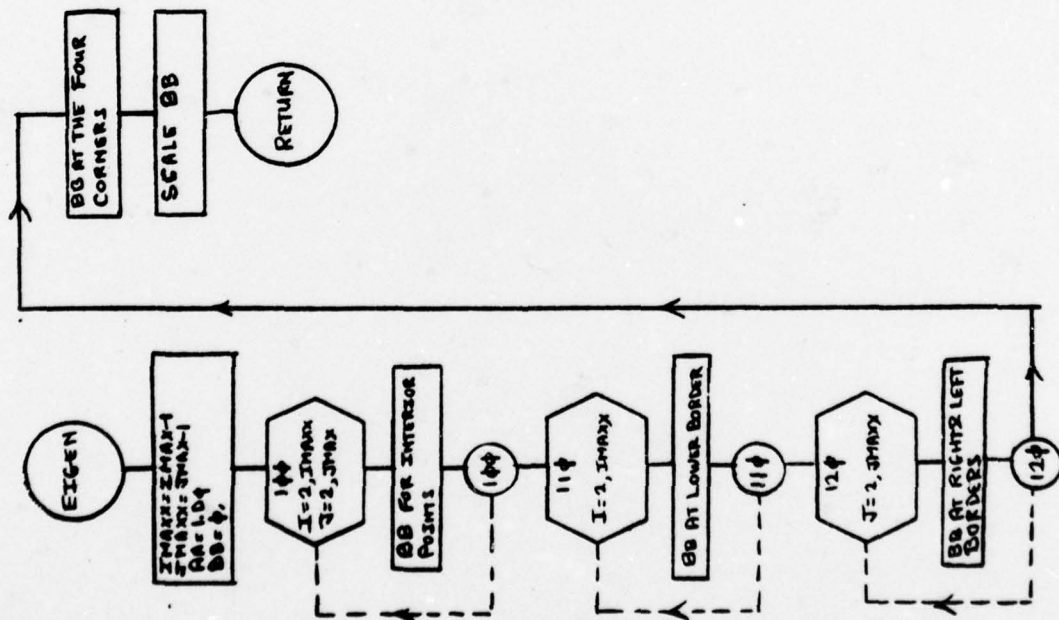
CTIONS IN EFFECT: NAME(MAIN) OPTIMIZE(2) LINECOUNT(74) SIZE(MAX) AUTODBL(NONE)
SOURCE EDDIC NULIST NODACK OBJECT MAP NOFORMAT GOSTMT NOXREF ALC N

```

ISN 0002      SUBROUTINE EIGEN(AA,BB)
C
C      ESTIMATES THE UPPER & LOWER BOUNDS BB AND AA OF THE EIGENVALUES
C      THE MATRIX USED WITH THE PICARD ALGORITHM. INTEGRATES (EDENS+HDEN
C      OVER THE SUBSTRATE REGION. USING THE TRAPEZOIDAL RULE.
ISN 0003      IMPLICIT REAL*8(A-H,O-Z)
C
ISN 0004      COMMON/ARRAYS/PSI(41,30),EDENS(41,25),HDENS(41,25),THETA(40,25),
1B(41,30),D(41,30),E(41,30),F(41,30),H(41,30),Q(41,30),DELTA(41,3
2,XFUS(41),YPUS(25),XTHPOS(41),YTHPOS(25)
ISN 0005      COMMON/COEFF/XDLT(42),YDLT(31),XTHDLT(41),YTHDLT(25),HNRTH(41,30
1HEAST(41,30),HSTH(41,30),HWEEST(41,30),HCNTR(41,30),THNRTH(40,25)
2THEAST(40,25),THSTH(40,25),THWEST(40,25),QAREA(41,25)
ISN 0006      COMMON/REAL/XCHNL,YSUB,YOXIDE,YJUNCTN,DUNDR,ACCPTR,VGATE,VSUB,
1VDRAIN,CIELK,QSS,CURRNT,EDENSO,PSIEQ
ISN 0007      COMMON/INTGR/IMAX,JMAX,JMAX5,JUNCTN,ITHMAX
C
C      THE REGION EXCLUDING THE BORDERS
ISN 0008      IMAXX=IMAX-1
ISN 0009      JMAXX=JMAX-1
ISN 0010      AA=1.00
ISN 0011      BB=0.
ISN 0012      DO 100 I=2,IMAXX
ISN 0013      DO 100 J=2,JMAXX
ISN 0014      100 BB=BB+(EDENS(I,J)+HDENS(I,J))*XTHDLT(I)*YTHDLT(J)
C
C      THE LOWER BORDER, EXCLUDING THE CORNERS.
ISN 0015      DO 110 I=2,IMAXX
ISN 0016      110 BB=BB+(EDENS(I,1)+HDENS(I,1))*XTHDLT(I)*YDLT(2)/2.00
C
C      THE RIGHT AND LEFT BORDERS EXCLUDING THE CORNERS.
ISN 0017      DO 120 J=2,JMAXX
ISN 0018      BB=BB+(EDENS(1,J)+HDENS(1,J))*XDLT(2)*YTHDLT(J)/2.00
ISN 0019      120 BB=BB+(EDENS(IMAX,J)+HDENS(IMAX,J))*XDLT(IMAX)*YTHDLT(J)/2.00
C
C      THE FOUR CORNERS
ISN 0020      BB=BB+(EDENS(1,1)+HDENS(1,1))*XDLT(2)*YDLT(2)/4.00
ISN 0021      BB=BB+(EDENS(IMAX,1)+HDENS(IMAX,1))*XDLT(IMAX)*YDLT(2)/4.00
ISN 0022      BB=BB+(EDENS(1,JMAX)+HDENS(1,JMAX))*XDLT(2)*YTHDLT(JMAX)/2.00
ISN 0023      BB=BB+(EDENS(IMAX,JMAX)+HDENS(IMAX,JMAX))*XDLT(IMAX)*YTHDLT(JMAX)
1/2.00
ISN 0024      BB=BB*YSUB/(4.00*XCHNL)
ISN 0025      BB=BB+1.00
ISN 0026      RETURN
ISN 0027      END

```

THIS PAGE IS BEST QUALITY PRACTICABLE
FROM COPY FURNISHED TO DDC



EIGEN SHEET 1 of 1

13.0 POISSN

This subprogram controls Stone's iterative method for finding $\psi(x,y)$, given the charge densities n , p , and N_A . It calls upon subroutines CHARGE (to calculate the charge term Q_p) and STONE (to apply Stone's method), during each iteration.

ED OPTIONS: NODACK,LOAD,OPT=2,SOURCE,MAP

, IN EFFECT: NAME(MAIN) OPTIMIZE(2) LINECOUNT(74) SIZE(MAX) AUTODBL(NONE)
SOURCE EBCDIC NOLIST NODACK OBJECT MAP NOFORMAT GUSTMT NOAREF ALLOC NO

```

0002      SUBROUTINE POISSN(ITRMAX,RDELT,KEY)
          C
          C      SOLVES POISSONS EQUATION FOR POTENTIAL USING STONES METHOD.
          C
0003      IMPLICIT REAL*8(A-H,O-Z)
0004      COMMON/ARRAYS/PSI(41,30),EDENS(41,25),HDENS(41,25),THETA(40,25),
          1B(41,30),D(41,30),E(41,30),F(41,30),H(41,30),G(41,30),DELTA(41,30)
          2,XPOS(41),YPOS(25),XTHPOS(41),YTHPOS(25)
0005      COMMON/COEFF/XDLT(42),YDLT(31),XTHDLT(41),YTHDLT(25),HNRTH(41,30),
          1HEAST(41,30),HSTH(41,30),HWEST(41,30),HCNTR(41,30),THNRTH(40,25),
          2THEAST(40,25),THSTH(40,25),THWEST(40,25),UAREA(41,25)
0006      COMMON/REAL/XCHNL,YSUB,YOXIDE,YJUNCTN,DONOR,ACCPTR,VGATE,VSUB,
          1VDRAIN,DIELK,GSS,CURRNT,EDENS0,PSIEG
0007      COMMON/INTGR/IMAX,JMAX,JMAX5,JUNCTN,ITHMAX
0008      DIMENSION PSINEW(41,30)
          C
          C      SET UP COEFFICIENTS FOR SUBROUTINE STONE
          C
0009      ISTONE=0
0010      ITR=1
0011      JMAXX=JMAX5-1
0012      DO 100 I=1,IMAX
0013      DO 100 J=1,JMAX5
0014      100 PSINEW(I,J)=PSI(I,J)
          C
          C      GENERAL EXPRESSIONS FOR STONE'S COEFFICIENTS. SPECIAL VALUES FOR
          C      THE BOUNDARIES ARE SUBSTITUTED BELOW.
          C
0015      DO 110 I=1,IMAX
0016      DO 110 J=2,JMAXX
0017      B(I,J)=HSTH(I,J)
0018      D(I,J)=HWEST(I,J)
0019      E(I,J)=HCNTR(I,J)
0020      F(I,J)=HEAST(I,J)
0021      110 H(I,J)=HNRTH(I,J)
          C
          C      CHARGE DENSITY THROUGH SUBSTRATE.
          C
0022      CALL CHARGE(KEY)
          C
          C      SUPPLY COEFFICIENTS ALONG THE GATE & SUBSTRATE CONTACTS.
          C
0023      DO 130 I=1,IMAX
0024      B(I,1)=0.
0025      D(I,1)=0.
0026      E(I,1)=1.00
0027      F(I,1)=0.
0028      H(I,1)=0.
0029      G(I,1)=PSIEG
0030      B(1,JMAX5)=0.
0031      D(1,JMAX5)=0.
0032      E(1,JMAX5)=1.00
0033      F(1,JMAX5)=0.
0034      H(1,JMAX5)=0.
0035      130 G(1,JMAX5)=PSI(2,JMAX5)
          C
          C      MODIFY COEFFICIENTS ALONG LEFT & RIGHT BORDERS
          C
0036      DO 140 J=2,JMAXX
0037      D(1,J)=0.
0038      F(1,J)=2.00*F(1,J)
0039      D(IMAX,J)=2.00*D(IMAX,J)
0040      140 F(IMAX,J)=0.
          C
          C      MODIFY WHAT WAS JUST DONE ALONG SOURCE & DRAIN CONTACTS.

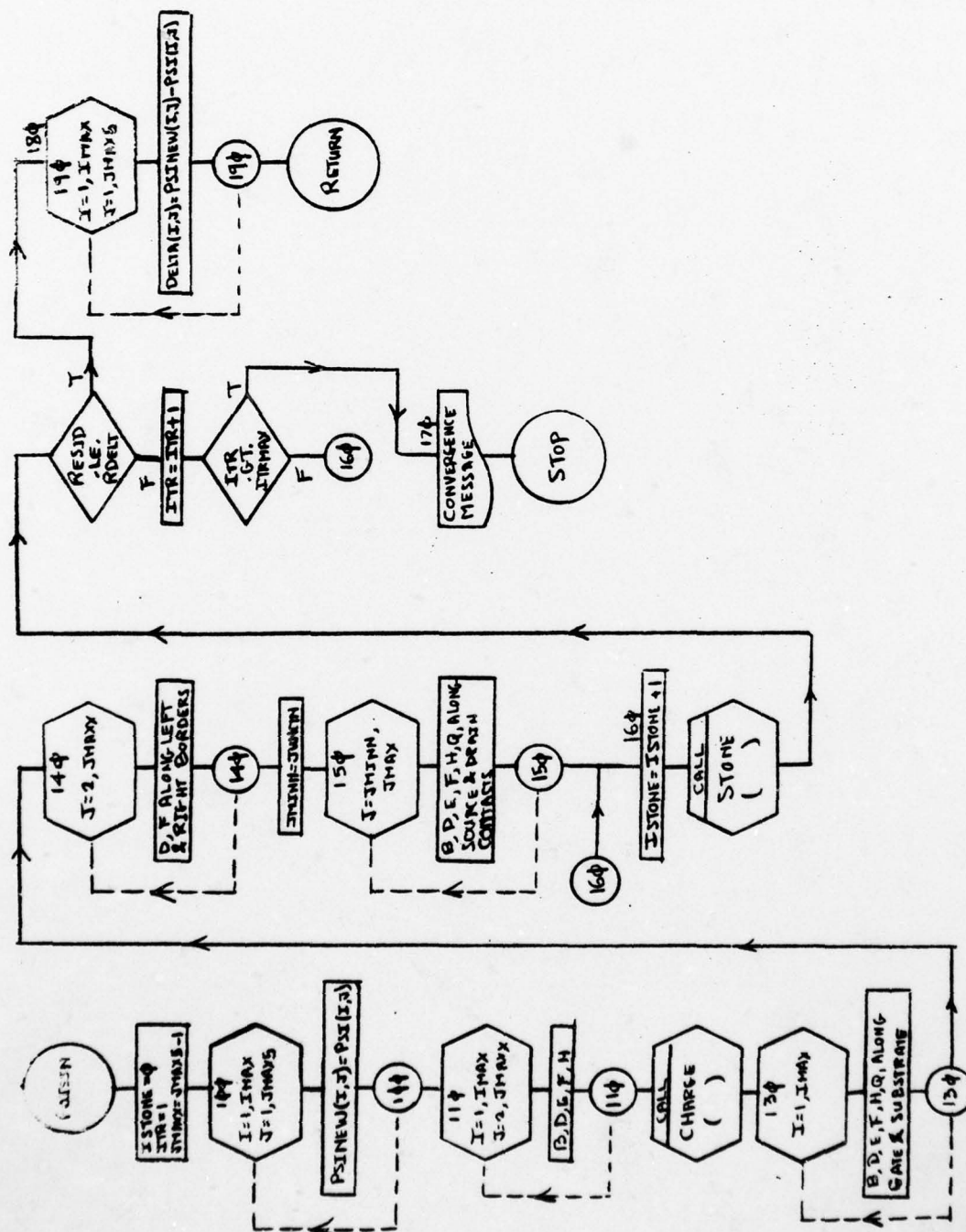
```

```

C
ISN 0041      JM INN=JUNCTN
ISN 0042      DO 150 J=JMINN,JMAX
ISN 0043      B(1,J)=0.
ISN 0044      E(1,J)=1.00
ISN 0045      F(1,J)=0.
ISN 0046      H(1,J)=0.
ISN 0047      G(1,J)=PSI(1,J)
ISN 0048      B(IMAX,J)=0.
ISN 0049      D(IMAX,J)=0.
ISN 0050      E(IMAX,J)=1.00
ISN 0051      F(IMAX,J)=0.
ISN 0052      H(IMAX,J)=0.
ISN 0053      150 G(IMAX,J)=PSI(IMAX,J)
C
C      ITERATIVE STONES METHOD
C
ISN 0054      160 ISTONE=ISTONE+1
ISN 0055      CALL STONE(ISTONE,IMAX,JMAX5,RESID,PSINew)
ISN 0056      IF(RESID.LE.KDELTA) GO TO 180
ISN 0057      ITR=ITR+1
ISN 0058      IF(ITR.GT.ITRMAX) GO TO 170
ISN 0059      GO TO 160
ISN 0060      170 WRITE(6,1000)
ISN 0061      1000 FORMAT(1H0,5X,'MAXIMUM ITERATIONS EXCEEDED IN POISSN',//)
ISN 0062      STOP
ISN 0063      180 DO 190 I=1,IMAX
ISN 0064      DO 190 J=1,JMAX5
ISN 0065      190 DELTA(I,J)=PSINew(I,J)-PSI(I,J)
ISN 0066      RETURN
ISN 0067      END
ISN 0068
ISN 0069

```

THIS PAGE IS BEST QUALITY PRACTICABLE
FROM COPY FURNISHED TO DDG



14.0 STONE & STONE1

This subprogram implements Stone's method for determining $\psi(x,y)$, given the charge term $\rho(x,y)$ in Poisson's equation. The iterative scheme necessary is controlled by subroutine POISSN. This particular subprogram uses a notation which deviates from the notation utilized in other subprograms to make it more transparent to those who study Stone's paper [7]. For example, the indices (I,J) used elsewhere become (J,K), as defined by Stone. Similarly, the potential $\psi(x,y)$ used elsewhere becomes T(x,y), since Stone discusses solving Poisson's equation in the context of a heat flow problem. The variables AA, BB, etc., represent Stone's a, b, etc. The intention in doing this was to make STONE a "utility" program which can be extracted and used in other situations by those who wish to implement Stone's method for their purposes.

14.01 STONE1

This subprogram, which appears as an ENTRY statement in STONE, implements Stone's suggested sequence of his relaxation parameters, α , and initializes the arrays which are internal to STONE. Some of the notation utilized here (e.g., XCHHL, (YSUB+YOXIDE), JMAX5) would require revision were the reader desirous of extracting STONE for use as a "utility" program.

FEC OPTIONS: NODUCK,LOAD,OPT=2,SCURCL,MAP

5 IN EFFECT: NAME(MAIN) OPTIMIZE(2) LINECOUNT(74) SIZE(MAX) AUTODBL(NONE)
SOURCE EDDIC NOLIST NODUCK OBJECT MAP NOFORMAT GUSTMT NOXREF ALC NO.

```

0002      SUBROUTINE STONE(ISTONE,JMAX,KMAX,RESID,T)
          C
          C      IMPLEMENTS STONE'S METHOD FOR MATRIX FACTORIZATION.
          C
0003      IMPLICIT REAL*8(A-H,O-Z)
          C
0004      COMMON/ARRAYS/PS1(41,30),EDENS(41,25),FDENS(41,25),THETA(40,25),
          1B(41,30),U(41,30),E(41,30),F(41,30),H(41,30),Q(41,30),DELTA(41,30),
          2,XPOS(41),YPOS(25),XTHPOS(41),YTHPOS(25)
0005      COMMON/COEFF/XDLT(42),YDLT(31),XTHDLT(41),YTHDLT(25),HNRTH(41,30),
          1HEAST(41,30),HSTH(41,30),HWEST(41,30),HCNTR(41,30),THNRTH(40,25),
          2THEAST(40,25),THSTH(40,25),THWEST(40,25),GAREA(41,25)
0006      COMMON/REAL/XCHNL,YSUB,YOXIDE,YJNCTN,DUNOR,ACCPTR,VGATE,VSUB,
          1VDRAIN,DIELK,QSS,CURRNT,EDENS0,PSIEQ
          C
0007      DIMENSION T(JMAX,KMAX)
0008      DIMENSION EL(41,30),FF(41,30),V(41,30),ALPHA(18)
          C
          C      DEFINE FREQUENTLY USED FUNCTIONS. (N FOR FORWARD K,R FOR REVERSE).
          C
0009      BN(B,E)=B/(1.00+ALPH*E)
0010      CN(D,F)=D/(1.00+ALPH*F)
0011      DN1(E,F)=BB*(ALPH*E-F)
0012      DN2(F,E)=CC*(ALPH*F-E)
0013      EN(F,E)=(F-ALPH*BB*E)/DD
0014      FN(H,F)=(H-ALPH*CC*F)/DD
0015      BR(H,E)=H/(1.00+ALPH*E)
0016      CR(D,F)=D/(1.00+ALPH*F)
0017      DR1(E,F)=BB*(ALPH*E-F)
0018      DR2(F,E)=CC*(ALPH*F-E)
0019      ER(F,E)=(F-ALPH*BB*E)/DD
0020      FR(D,F)=(D-ALPH*CC*F)/DD
          C
          C
          C      ISTONE FLAGS WHICH ALPHA TO USE AND WHETHER FORWARD (ISTONE ODD)
          C      OR REVERSE (ISTONE EVEN) INDEXING OF K IS TO BE IMPLEMENTED.
          C
0021      IF(ISTONE.GT.18) ISTONE=1
0022      ALPH=ALPHA(ISTONE)
0023      JMAXX=JMAX-1
0024      KMAXX=KMAX-1
0025      J=2*(ISTONE/2)
0026      IF(J.EQ.1) GO TO 170
0027
          C
          C      ISTONE IS ODD. INDEX K FORWARD
          C
          C
          C
          C      THE CORNER POINT (1,1)
          C
0029      DD=E(1,1)
0030      EE(1,1)=F(1,1)/DD
0031      FF(1,1)=H(1,1)/DD
0032      R=Q(1,1)-(E(1,1)*T(1,1)+F(1,1)*T(2,1)+H(1,1)*T(1,2))
0033      RR=DABS(R)
0034      RESID=RR
0035      V(1,1)=R/DD
          C
          C
          C      THE ROW K=1, EXCLUDING THE RIGHT CORNER POINT.
          C
0036      DO 100 J=2,JMAXX
0037      JP=J+1
0038      JN=J-1
0039      CC=CN(U(J,1),FF(JN,1))
0040      DD=E(J,1)+DN2(FF(JN,1),EE(JN,1))
0041      EE(J,1)=F(J,1)/DD
0042      FF(J,1)=FN(H(J,1),FF(JN,1))

```

THIS PAGE IS BEST QUALITY PRACTICABLE
FROM COPY FURNISHED TO DDG

```

ISN 0043      R=U(J,1)-(U(J,1)*T(JN,1)+E(J,1)*T(J,1)+F(J,1)*T(JP,1)+H(J,1)*
ISN 0044      1T(J,2))
ISN 0045      RR=DABS(R)
ISN 0046      IF(KR.GT.RESID) RESID=RR
ISN 0047      100 V(J,1)=(R-CC*V(JN,1))/DD
C
C      THE CORNER POINT (JMAX,1)
C
ISN 0048      J=JMAX
ISN 0049      JN=JMAXX
ISN 0050      CC=LN(U(J,1),FF(JN,1))
ISN 0051      DD=E(J,1)+DN2(FF(JN,1),EE(JN,1))
ISN 0052      EE(J,1)=0.
ISN 0053      FF(J,1)=FN(H(J,1),FF(JN,1))
ISN 0054      R=U(J,1)-(U(J,1)*T(JN,1)+E(J,1)*T(J,1)+H(J,1)*T(J,2))
ISN 0055      RR=DABS(R)
ISN 0056      IF(KR.GT.RESID) RESID=RR
ISN 0058      V(J,1)=(R-CC*V(JN,1))/DD
C
C      ALL ROWS EXCEPT ROW KMAX
C
ISN 0059      DO 120 K=2,KMAXX
ISN 0060      KP=K+1
ISN 0061      KN=K-1
C
C      THE LEFT BORDER POINT
C
ISN 0062      BB=BN(B(1,K),EE(1,KN))
ISN 0063      DD=E(1,K)+DN1(EE(1,KN),FF(1,KN))
ISN 0064      EE(1,K)=EN(F(1,K),EE(1,KN))
ISN 0065      FF(1,K)=H(1,K)/DD
ISN 0066      R=U(1,K)-(B(1,K)*T(1,KN)+E(1,K)*T(1,K)+F(1,K)*T(2,K)+H(1,K)*
ISN 0067      1T(1,KP))
ISN 0068      RR=DABS(R)
ISN 0068      IF(KR.GT.RESID) RESID=RR
ISN 0070      V(1,K)=(R-BB*V(1,KN))/DD
C
C      THE ROW K EXCLUDING THE RIGHT BORDER POINT.
C
ISN 0071      DO 110 J=2,JMAXX
ISN 0072      JP=J+1
ISN 0073      JN=J-1
ISN 0074      BB=BN(B(J,K),EE(J,KN))
ISN 0075      CC=LN(U(J,K),FF(JN,K))
ISN 0076      DD=E(J,K)+DN1(EE(J,KN),FF(J,KN))+DN2(FF(JN,K),EE(JN,K))
ISN 0077      EE(J,K)=EN(F(J,K),EE(J,KN))
ISN 0078      FF(J,K)=FN(H(J,K),FF(JN,K))
ISN 0079      R=U(J,K)-(B(J,K)*T(J,KN)+D(J,K)*T(JN,K)+E(J,K)*T(J,K)+
ISN 0080      1F(J,K)*T(JP,K)+H(J,K)*T(J,KP))
ISN 0081      RR=DABS(R)
ISN 0081      IF(KR.GT.RESID) RESID=RR
ISN 0083      110 V(J,K)=(R-BB*V(J,KN)-CC*V(JN,K))/DD
C
C      THE RIGHT BORDER POINT
C
ISN 0084      J=JMAX
ISN 0085      JN=JMAXX
ISN 0086      BB=BN(B(J,K),EE(J,KN))
ISN 0087      CC=LN(U(J,K),FF(JN,K))
ISN 0088      DD=E(J,K)+DN1(EE(J,KN),FF(J,KN))+DN2(FF(JN,K),EE(JN,K))
ISN 0089      EE(J,K)=0.
ISN 0090      FF(J,K)=FN(H(J,K),FF(JN,K))
ISN 0091      R=U(J,K)-(B(J,K)*T(J,KN)+D(J,K)*T(JN,K)+E(J,K)*T(J,K)+H(J,K)*
ISN 0092      1T(J,KP))
ISN 0093      RR=DABS(R)
ISN 0093      IF(KR.GT.RESID) RESID=RR
ISN 0095      120 V(J,K)=(R-BB*V(J,KN)-CC*V(JN,K))/DD
C
C      THE CORNER POINT (1,KMAX)
C
ISN 0096      K=KMAXX
ISN 0097      KN=KMAXX

```

THIS PAGE IS BEST QUALITY PRACTICABLE
FROM COPY FURNISHED TO DDG

```

0098      BB=BN(B(1,K),EE(1,KN))
0099      DD=L(1,K)+DN1(EE(1,KN),FF(1,KN))
0100      EE(1,K)=EN(F(1,K),EE(1,KN))
0101      FF(1,K)=0.
0102      R=L(1,K)-(B(1,K)*T(1,KN)+E(1,K)*T(1,K)+F(1,K)*T(2,K))
0103      RR=DABS(R)
0104      IF(RR.GT.RESID) RESID=RR
0106      V(1,K)=(R-BB*V(1,KN))/DD

C
C
C      THE ROW KMAX, EXCLUDING THE CORNER POINT (JMAX,KMAX)

0107      DO 130 J=2,JMAXX
0108      JP=J+1
0109      JN=J-1
0110      BB=BN(B(J,K),EE(J,KN))
0111      CC=CN(D(J,K),FF(JN,K))
0112      DD=E(J,K)+DN1(EE(J,KN),FF(J,KN))+DN2(FF(JN,K),EE(JN,K))
0113      EE(J,K)=EN(F(J,K),EE(J,KN))
0114      FF(J,K)=0.
0115      R=U(J,K)-(B(J,K)*T(J,KN)+D(J,K)*T(JN,K)+E(J,K)*T(J,K)+F(J,K)*
1      T(JP,K))
0116      RR=DABS(R)
0117      IF(RR.GT.RESID) RESID=RR
0119      130 V(J,K)=(R-BB*V(J,KN)-CC*V(JN,K))/DD

C
C
C      THE CORNER POINT (JMAX,KMAX)

0120      J=JMAX
0121      JN=JMAXX
0122      BB=BN(B(J,K),EE(J,KN))
0123      CC=CN(D(J,K),FF(JN,K))
0124      DD=E(J,K)+DN1(EE(J,KN),FF(J,KN))+DN2(FF(JN,K),EE(JN,K))
0125      EE(J,K)=0.
0126      FF(J,K)=0.
0127      R=U(J,K)-(B(J,K)*T(J,KN)+D(J,K)*T(JN,K)+E(J,K)*T(J,K))
0128      RR=DABS(R)
0129      IF(RR.GT.RESID) RESID=RR
0131      V(J,K)=(R-BB*V(J,KN)-CC*V(JN,K))/DD

C
C
C      INDEX K AND J IN REVERSE TO FIND DELTA

C
C      THE CORNER POINT (JMAX,KMAX)

0132      K=KMAX
0133      DELTA(JMAX,K)=V(JMAX,K)

C
C
C      THE ROW KMAX

0134      DO 140 JJ=1,JMAXX
0135      J=JMAXX+1-JJ
0136      JP=J+1
0137      140 DELTA(J,K)=V(J,K)-EE(J,K)*DELTA(JP,K)

C
C
C      THE ROW K, TREATING THE RIGHT BORDER FIRST.

0138      DO 150 KK=1,KMAXX
0139      K=KMAXX+1-KK
0140      KP=K+1
0141      DELTA(JMAX,K)=V(JMAX,K)-FF(JMAX,K)*DELTA(JMAX,KP)
0142      DO 150 JJ=1,JMAXX
0143      J=JMAXX+1-JJ
0144      JP=J+1
0145      150 DELTA(J,K)=V(J,K)-EE(J,K)*DELTA(JP,K)-FF(J,K)*DELTA(J,KP)
0146      GO TO 240

C
C
C      ISTONE IS EVEN, INDEX K IN REVERSE ORDER.

C
C      THE CORNER POINT (1,KMAX)

0147      170 K=KMAX
0148      KN=KMAXX
0149      UD=E(1,K)

```

THIS PAGE IS BEST QUALITY PRACTICABLE
FROM COPY FURNISHED TO DDG


```

ISN 0150      EE(1,K)=F(1,K)/DD
ISN 0151      FF(1,K)=D(1,K)/DD
ISN 0152      R=G(1,K)-(B(1,K)*T(1,KN)+E(1,K)*T(1,K)+F(1,K)*T(2,K))
ISN 0153      RR=DABS(R)
ISN 0154      RESID=RR
ISN 0155      V(1,K)=R/DD

C
C      THE ROW KMAX
C
ISN 0156      DO 180 J=2,JMAXX
ISN 0157      JP=J+1
ISN 0158      JN=J-1
ISN 0159      CC=CR(D(J,K),FF(JN,K))
ISN 0160      DD=E(J,K)+DR2(FF(JN,K),EE(JN,K))
ISN 0161      EE(J,K)=F(J,K)/DD
ISN 0162      FF(J,K)=FR(B(J,K),FF(JN,K))
ISN 0163      R=G(J,K)-(B(J,K)*T(J,KN)+D(J,K)*T(JN,K)+E(J,K)*T(J,K)+F(J,K)*
180      T(JP,K))
ISN 0164      RR=DABS(R)
ISN 0165      IF(RR.GT.RESID) RESID=RR
ISN 0167      V(J,K)=(R-CC*V(JN,K))/DD

C
C      THE CORNER POINT (JMAX,KMAX)
C
ISN 0168      J=JMAX
ISN 0169      JN=JMAXX
ISN 0170      CC=CR(D(J,K),FF(JN,K))
ISN 0171      DD=E(J,K)+DR2(FF(JN,K),EE(JN,K))
ISN 0172      EE(J,K)=0.
ISN 0173      FF(J,K)=FR(B(J,K),FF(JN,K))
ISN 0174      R=G(J,K)-(B(J,K)*T(J,KN)+D(J,K)*T(JN,K)+E(J,K)*T(J,K))
ISN 0175      RR=DABS(R)
ISN 0176      IF(RR.GT.RESID) RESID=RR
ISN 0178      V(J,K)=(R-CC*V(JN,K))/DD

C
C      ALL ROWS EXCEPT THE ROW K=1
C
ISN 0179      DO 200 KK=2,KMAXX
ISN 0180      K=KMAXX+2-KK
ISN 0181      KP=K+1
ISN 0182      KN=K-1

C
C      THE LEFT BORDER POINT (1,K)
C
ISN 0183      BB=BR(H(1,K),EE(1,KP))
ISN 0184      DD=E(1,K)+DR1(EE(1,KP),FF(1,KP))
ISN 0185      EE(1,K)=ER(F(1,K),EE(1,KP))
ISN 0186      FF(1,K)=D(1,K)/DD
ISN 0187      R=G(1,K)-(B(1,K)*T(1,KN)+E(1,K)*T(1,K)+F(1,K)*T(2,K)+H(1,K)*
180      T(1,KP))
ISN 0188      RR=DABS(R)
ISN 0189      IF(RR.GT.RESID) RESID=RR
ISN 0191      V(1,K)=(R-BB*V(1,KP))/DD

C
C      THE ROW K EXCLUDING THE RIGHT BORDER POINT
C
ISN 0192      DO 190 J=2,JMAXX
ISN 0193      JP=J+1
ISN 0194      JN=J-1
ISN 0195      BB=BR(H(J,K),EE(J,KP))
ISN 0196      CC=CR(D(J,K),FF(JN,K))
ISN 0197      DD=E(J,K)+DR1(EE(J,KP),FF(J,KP))+DR2(FF(JN,K),EE(JN,K))
ISN 0198      EE(J,K)=ER(F(J,K),EE(J,KP))
ISN 0199      FF(J,K)=FR(B(J,K),FF(JN,K))
ISN 0200      R=G(J,K)-(B(J,K)*T(J,KN)+D(J,K)*T(JN,K)+E(J,K)*T(J,K)+F(J,K)*
190      T(JP,K)+H(J,K)*T(J,KP))
ISN 0201      RR=DABS(R)
ISN 0202      IF(RR.GT.RESID) RESID=RR
ISN 0204      V(J,K)=(R-BB*V(J,KP)-CC*V(JN,K))/DD

C
C      THE RIGHT BORDER POINT

```

THIS IS AN ERROR & /
SHOULD BE DELETED.

THIS PAGE IS BEST QUALITY PRACTICABLE
FROM COPY FURNISHED TO DDG


```

0205      J=JMAX
0206      JN=JMAXX
0207      BB=ER(H(J,K),EE(J,KP))
0208      CC=CR(D(J,K),FF(JN,K))
0209      DD=E(J,K)+DR1(EE(J,KP),FF(J,KP))+DR2(FF(JN,K),EE(JN,K))
0210      EE(J,K)=0.
0211      FF(J,K)=FR(B(J,K),FF(JN,K))
0212      R=U(J,K)-(B(J,K)*T(J,KN)+D(J,K)*T(JN,K)+E(J,K)*T(J,K)+H(J,K)*
      1T(J,KP))
0213      RR=DABS(R)
0214      IF(RR.GT.RESID) RESID=RR
0215      200 V(J,K)=(R-BB*V(J,KP)-CC*V(JN,K))/DD
      C
      C      THE CORNER POINT (1,1)
      C
0217      BB=ER(H(1,1),EE(1,2))
0218      DD=E(1,1)+DR1(EE(1,2),FF(1,2))
0219      EE(1,1)=ER(F(1,1),EE(1,2))
0220      FF(1,1)=0.
0221      R=U(1,1)-(E(1,1)*T(1,1)+F(1,1)*T(2,1)+H(1,1)*T(1,2))
0222      RR=DABS(R)
0223      IF(RR.GT.RESID) RESID=RR
0224      V(1,1)=(R-BB*V(1,2))/DD
      C
      C      THE ROW K=1, EXCLUDING THE RIGHT CORNER POINT.
      C
0226      DO 210 J=2,JMAXX
0227      JP=J+1
0228      JN=J-1
0229      BB=ER(H(J,1),EE(J,2))
0230      CC=CR(D(J,1),FF(JN,1))
0231      DD=E(J,1)+DR1(EE(J,2),FF(J,2))+DR2(FF(JN,1),EE(JN,1))
0232      EE(J,1)=ER(F(J,1),EE(J,2))
0233      FF(J,1)=0.
0234      R=U(J,1)-(D(J,1)*T(JN,1)+E(J,1)*T(J,1)+F(J,1)*T(JP,1)+H(J,1)*
      1T(J,2))
0235      RR=DABS(R)
0236      IF(RR.GT.RESID) RESID=RR
0237      210 V(J,1)=(R-BB*V(J,2)-CC*V(JN,1))/DD
      C
      C      THE CORNER POINT (JMAX,1)
      C
0239      J=JMAX
0240      JN=JMAXX
0241      BB=ER(H(J,1),EE(J,2))
0242      CC=CR(D(J,1),FF(JN,1))
0243      DD=E(J,1)+DR1(EE(J,2),FF(J,2))+DR2(FF(JN,1),EE(JN,1))
0244      EE(J,1)=0.
0245      FF(J,1)=0.
0246      R=U(J,1)-(D(J,1)*T(JN,1)+E(J,1)*T(J,1)+H(J,1)*T(J,2))
0247      RR=DABS(R)
0248      IF(RR.GT.RESID) RESID=RR
0249      V(J,1)=(R-BB*V(J,2)-CC*V(JN,1))/DD
      C
      C      INDEX K FORWARD & J REVERSE TO FIND DELTA
      C
      C      THE POINT (JMAX,1)
      C
0251      DELTA(JMAX,1)=V(JMAX,1)
      C
      C      THE ROW K=1
      C
0252      DO 220 JJ=1,JMAXX
0253      J=JMAXX+1-JJ
0254      JP=J+1
0255      220 DELTA(J,1)=V(J,1)-EE(J,1)*DELTA(JP,1)
      C
      C      ALL REMAINING ROWS
      C
0256      DO 230 K=2,KMAX
0257      KN=K-1

```

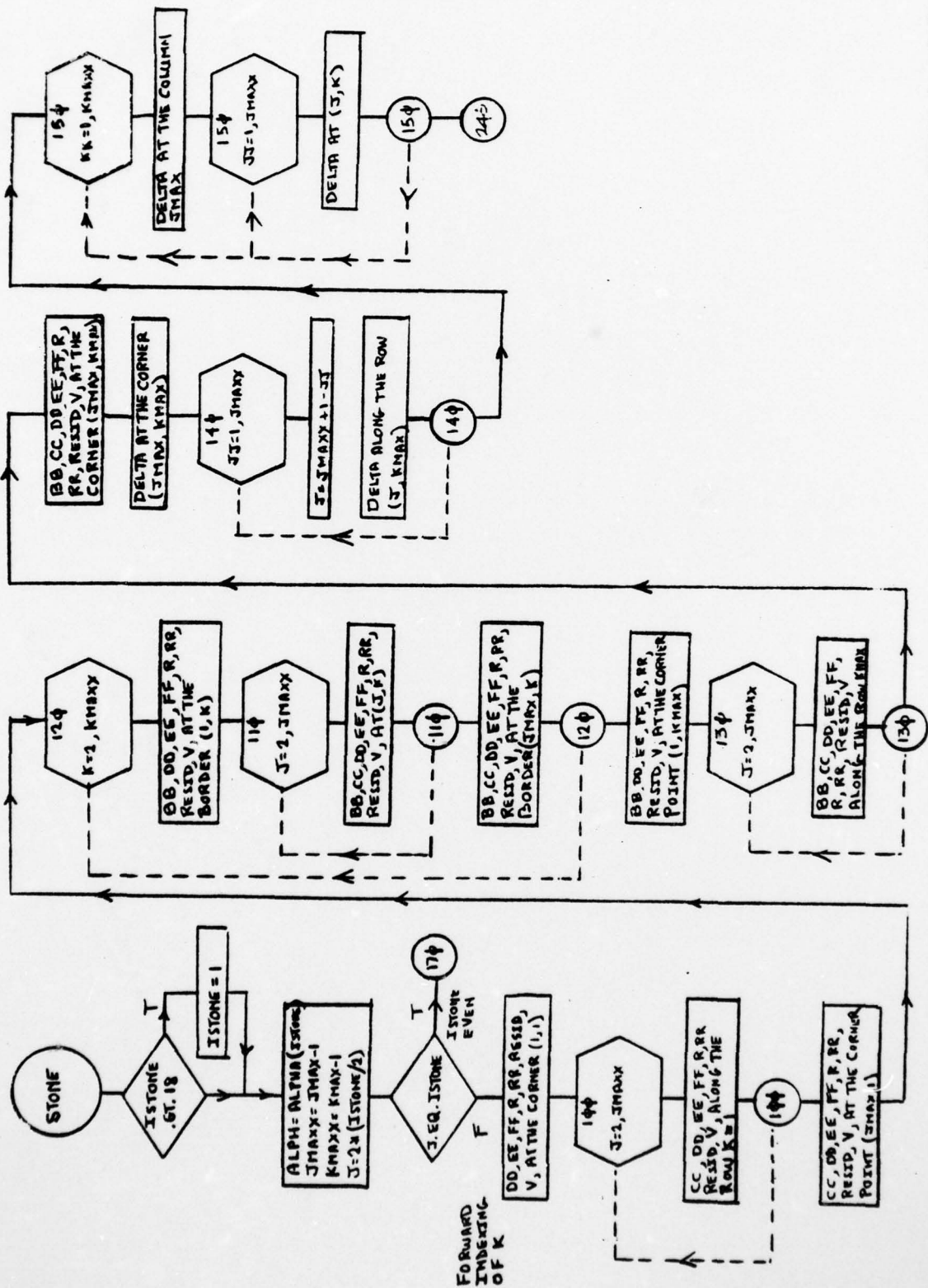
THIS PAGE IS BEST QUALITY PRACTICABLE
FROM COPY FURNISHED TO DDG

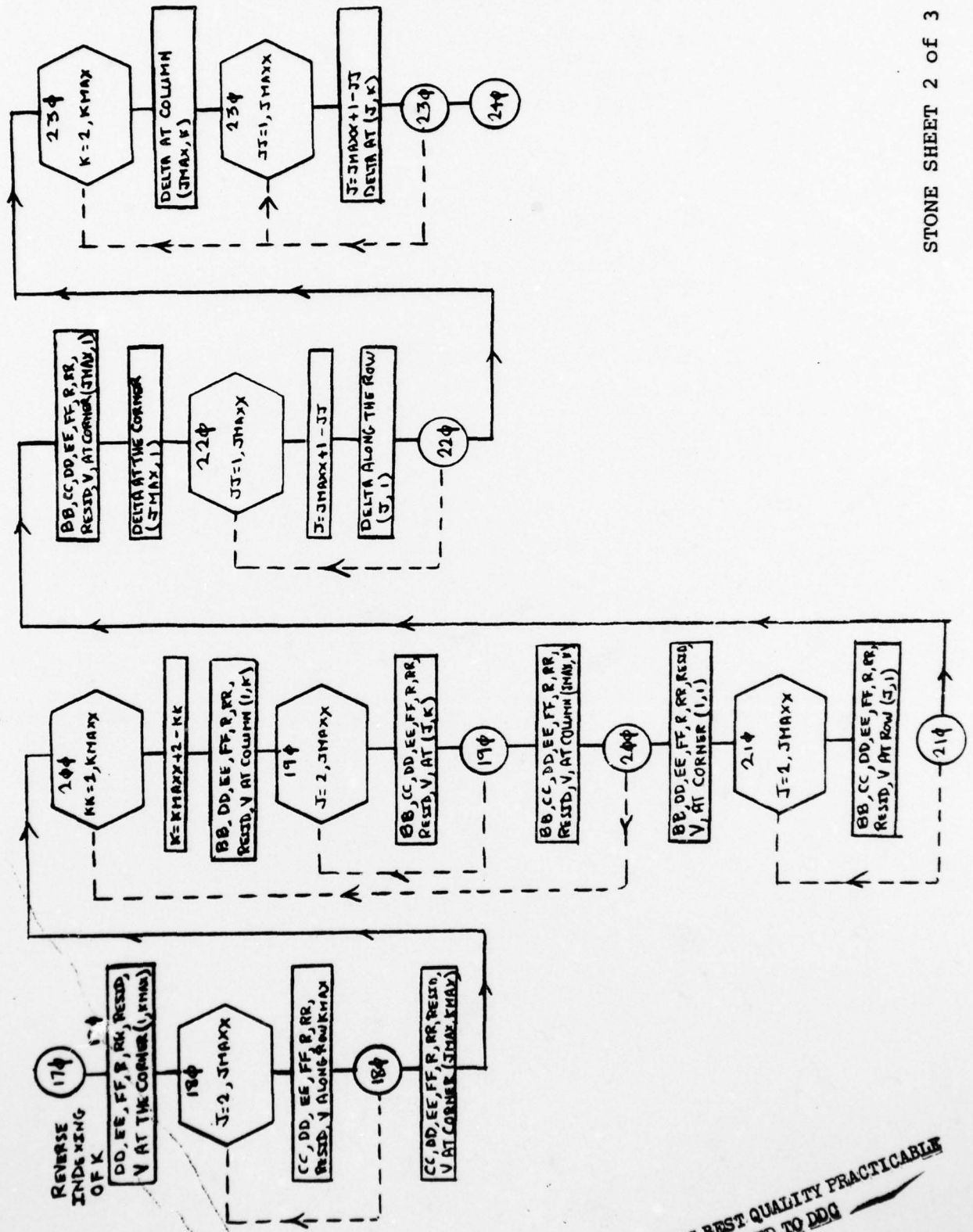
```

C      THE RIGHT BORDER POINT
C
SN 0258      DELTA(JMAX,K)=V(JMAX,K)-FF(JMAX,K)*DELTA(JMAX,KN)
C
C      ALL REMAINING POINTS OF THE ROW
C
SN 0259      DO 230 JJ=1,JMAXX
SN 0260      J=JMAXX+1-JJ
SN 0261      JP=J+1
SN 0262      230 DELTA(J,K)=V(J,K)-EE(J,K)*DELTA(JP,K)-FF(J,K)*DELTA(J,KN)
C
C      CALCULATE NEW T(J,K)
C
SN 0263      240 DO 250 J=1,JMAX
SN 0264      DO 250 K=1,KMAX
SN 0265      250 T(J,K)=T(J,K)+DELTA(J,K)
SN 0266      RETURN
C
C      ENTRY STONE1 SETS UP ALPHA VALUES & INITIALIZES ALL ARRAYS
C
SN 0267      ENTRY STONE1(IMAX,JMAX,JMAX5)
C
SN 0268      DO 320 J=2,IMAX
SN 0269      DO 320 K=2,JMAX5
SN 0270      DX=ADLT(J)/XCHNL
SN 0271      DY=ADLT(K)/(YSUB+YUXIDE)
SN 0272      320 EE(J,K)=2.00/(1.00/(DX*DX)+1.00/(DY*DY))
C
C      FIND AVERAGE
C
SN 0273      ALPHA=0.
SN 0274      DO 330 J=2,IMAX
SN 0275      DO 330 K=2,JMAX5
SN 0276      330 ALPHA=ALPHA+EE(J,K)
SN 0277      ALPHA=ALPHA/(IMAX*JMAX5)
C
C      IMPLEMENT STONE'S EQ(27)
C
SN 0278      DO 340 J=1,9
SN 0279      ALPHY=J-1
SN 0280      ALPHY=ALPHY/8.00
SN 0281      340 EE(J,1)=ALPHX**ALPHY
C
C      IMPLEMENT THE SEQUENCE OF 18 ALPHAS SUGGESTED BY STONE
C
SN 0282      ALPHA(1)=EE(9,1)
SN 0283      ALPHA(3)=EE(6,1)
SN 0284      ALPHA(5)=EE(3,1)
SN 0285      ALPHA(7)=EE(8,1)
SN 0286      ALPHA(9)=EE(5,1)
SN 0287      ALPHA(11)=EE(2,1)
SN 0288      ALPHA(13)=EE(7,1)
SN 0289      ALPHA(15)=EE(4,1)
SN 0290      ALPHA(17)=EE(1,1)
SN 0291      DO 350 J=2,18,2
SN 0292      350 ALPHA(J)=ALPHA(J-1)
SN 0293      DO 360 J=1,18
SN 0294      360 ALPHA(J)=1.00-ALPHA(J)
C
C      INITIALIZE ALL ARRAYS INTERNAL TO STONE TO ZERO.
C
SN 0295      DO 370 J=1,IMAX
SN 0296      DO 370 K=1,JMAX5
SN 0297      EE(J,K)=0.
SN 0298      FF(J,K)=0.
SN 0299      V(J,K)=0.
SN 0300      370 DELTA(J,K)=0.
SN 0301      RETURN
SN 0302      END

```

THIS PAGE IS BEST QUALITY PRACTICABLE
FROM COPY FURNISHED TO DDG





15.0 CHARGE

This subprogram calculates the charge term Q_p defined in eq. (23) of Chapter I, Section 3.01.2, using eq. (36) if the Picard iterative procedure is in use. As explained in Section 4.02 of Chapter I, it invokes appropriate modifications of both Q_p and E_p , in eq. (23), if Gummel's algorithm is in use. These procedures are almost trivial, and hardly call for a separate subroutine for their implementation. The fact that Subroutine CHARGE exists as such is a vestige of the fact that, at one time during the development, more elaborate procedures for calculating Q_p were tried; procedures which were ultimately found unnecessary.

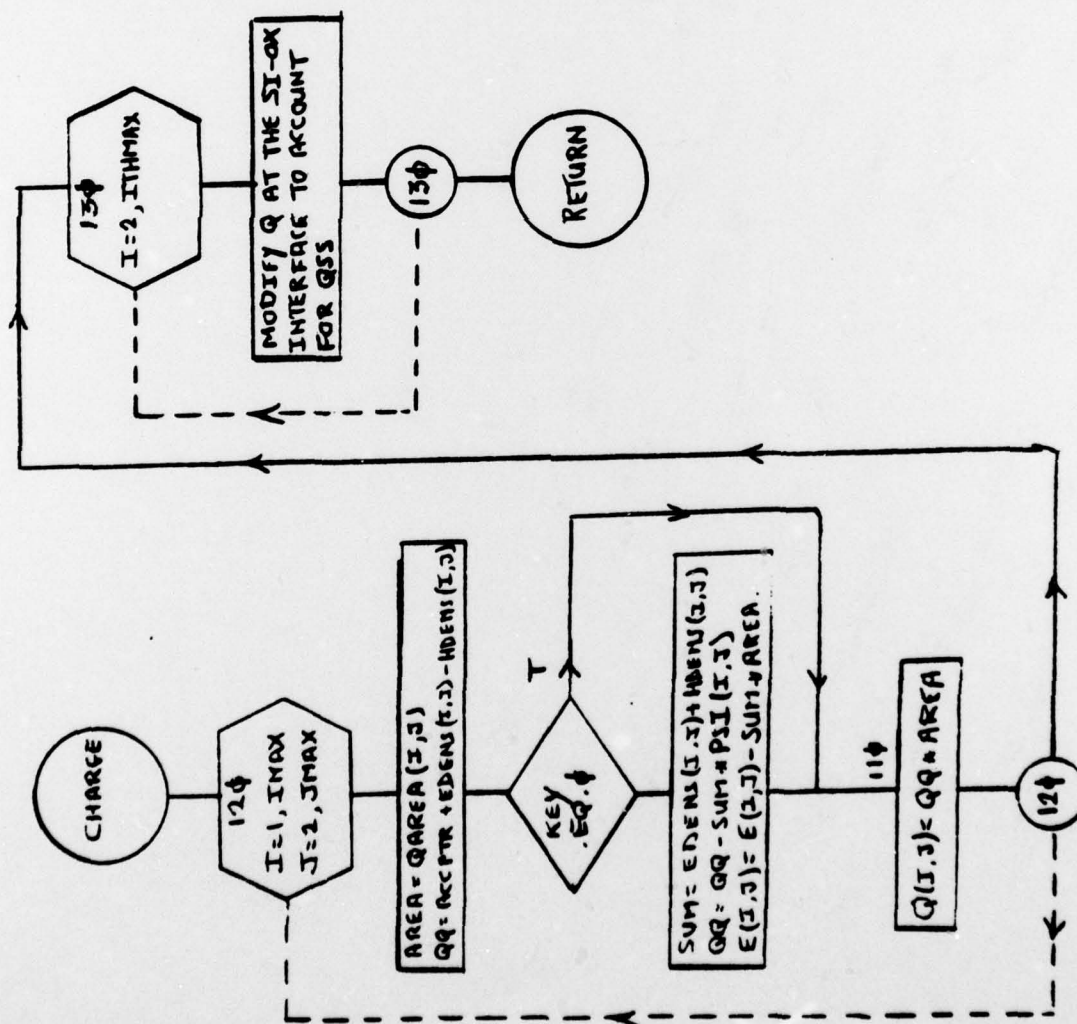
TED OPTIONS: NUDECK,LOAD,OPT=2,SOURCE,MAP

S IN EFFECT: NAME(MAIN) OPTIMIZE(2) LINECOUNT(74) SIZE(MAX) AUTGDBL(NONE)
SOURCE EBCDIC NOLIST NUDECK OBJECT MAP NOFORMAT GOSTMT NOXREF ALC NO

```

0002      SUBROUTINE CHARGE(KEY)
      C
      C      CALCULATES THE CHARGE TERM APPEARING IN THE PICARD & GUMMEL
      C      FINITE-DIFFERENCE EQUATIONS FOR PSI.
0003      IMPLICIT REAL*8(A-H,O-Z)
0004      COMMON/ARRAYS/PSI(41,30),EDENS(41,25),HDENS(41,25),THETA(40,25),
      1B(41,30),D(41,30),E(41,30),F(41,30),H(41,30),Q(41,30),DELTA(41,30),
      2,XPOS(41),YPOS(25),XTHPOS(41),YTHPOS(25)
0005      COMMON/COEFF/XDLT(42),YDLT(31),XTHDLT(41),YTHDLT(25),HNRTH(41,30),
      1HEAST(41,30),HSTH(41,30),HWEST(41,30),HCNTR(41,30),THNRTH(40,25),
      2THEAST(40,25),THSTH(40,25),THWEST(40,25),QAREA(41,25)
0006      COMMON/REAL/XCHNL,YSUB,YOXIDE,YJNCTN,DUNOK,ACCPTR,VGATE,VSUB,
      1VDRAIN,DIELK,QSS,CURHNT,EDENS0,RSIEQ
0007      COMMON/INTGR/IMAX,JMAX,JUNCTN,ITHMAX
0008      COMMON/CNTRL/ UMEGA
      C
0009      DO 120 I=1,IMAX
0010      DO 120 J=2,JMAX
0011      100 AREA=QAREA(I,J)
0012      QQ=ACCPTR+EDENS(I,J)-HDENS(I,J)
0013      IF(KEY.EQ.0) GO TO 110
      C
      C      MODIFY E & Q FOR THE GUMMEL ALGORITHM
      C
0015      SUM=EDENS(I,J)+HDENS(I,J)
0016      QQ=QQ-SUM*PSI(I,J)
0017      E(I,J)=E(I,J)-SUM*AREA
0018      110 Q(I,J)=QQ*AREA
0019      120 CONTINUE
      C
      C      MODIFY Q AT THE SI-OX INTERFACE TO ACCOUNT FOR QSS.
      C
0020      DO 130 I=2,ITHMAX
0021      Q(I,JMAX)=Q(I,JMAX)-QSS*XTHDLT(I)/2.00
0022      130 Q(I,JMAX+1)=-QSS*XTHDLT(I)/(2.00*DIELK)
0023      RETURN
0024      END

```



CHARGE SHEET 1 of 1

16.0 OUTPUT

This subprogram performs the obvious function of providing for the printing of output data concerning the solution. It should be transparent to the user, and is the one subprogram which he is most likely to wish to modify to suit his own needs. About the only aspect of OUTPUT that needs clarification is the method used to calculate the inversion charge Q_I , and the depletion charge Q_D . In both instances, piece-wise exponential "fits" are utilized to approximate the electron and hole densities as a function of the vertical coordinate y between adjacent lattice points, and an analytic evaluation of the integrals required for those parameters is applied. No flowchart for OUTPUT is included herein, because it is deemed unnecessary.

REQUESTED OPTIONS: NODUCK,LOAD,OPT=2,SOURCE,MAP

TRANS IN EFFECT: NAME(MAIN) OPTIMIZE(2) LINECOUNT(74) SIZE(MAX) AUTODBL(NONE)
SOURCE EDCDIC NOLIST NODUCK OBJECT MAP NOFORMAT GOSTMT NOXREF ALC N

```

ISN 0002      SUBROUTINE COUTPUT
ISN 0003      C      IMPLICIT REAL*8(A-H,O-Z)
ISN 0004      C      COMMON/ARRAYS/PSI(41,30),EDENS(41,25),HDENS(41,25),THETA(40,25),
ISN 0005      1B(41,30),J(41,30),E(41,30),F(41,30),H(41,30),G(41,30),DELTA(41,3
ISN 0006      2,XPOS(41),YPOS(25),XTHPOS(41),YTHPOS(25)
ISN 0007      COMMON/CCEFF/XDLT(42),YDLT(31),XTHDLT(41),YTHDLT(25),HNRTH(41,30
ISN 0008      1HEAST(41,30),HSTH(41,30),HWEEST(41,30),HCNTR(41,30),THNRTH(40,25)
ISN 0009      2THEAST(40,25),THSTH(40,25),THWEST(40,25),QAREA(41,25)
ISN 0010      COMMON/REAL/XCHNL,YSUB,YOXIDE,YJUNCTN,DONOR,ACCPTR,VGATE,VSUB,
ISN 0011      1VDRAIN,DIELK,GSS,CURRNT,EDENS0,PSIEQ
ISN 0012      COMMON/INTEGR/IMAX,JMAX,JMAX5,JUNCTN,ITHMAX
ISN 0013      COMMON/NRMLZE/DNSNRM,PSINRM,DEBYE,QNORM,CRTNRM
ISN 0014      C
ISN 0015      DIMENSION X(41),SISURF(41),PHIN(41),QI(41),QD(41),SCRATCH(41),
ISN 0016      1YD(41),YI(41)
ISN 0017      C
ISN 0018      C      INTEGRATE JSUBX ALONG THE DRAIN TO OBTAIN THE DRAIN CURRENT.
ISN 0019      C
ISN 0020      J=JMAX
ISN 0021      YY=YSUB*DEBYE
ISN 0022      VD=VDRAIN*PSINRM
ISN 0023      VG=VGATE*PSINRM
ISN 0024      VB=VSUB*PSINRM
ISN 0025      CRNT=CURRNT*CRTNRM*DEBYE/1.01
ISN 0026      WRITE(6,1000) VG,VD,VB,CRNT
ISN 0027      WRITE(6,1010) YY
ISN 0028      1000 FORMAT(1H1,///,9X,'CURRENT VOLTAGE RESULT :',//,13X,'VG=',1PD10.
ISN 0029      11X,'VOLTS',/,13X,'VD=',1PD10.2,1X,'VOLTS',/,13X,'VB=',1PD10.2,1X
ISN 0030      2,'VOLTS',/,13X,'ID=',1PD10.2,1X,'MILLIAMPS/CM OF CHANNEL *IDTH',/
ISN 0031      1010 FORMAT(9X,'SUBSTRATE THICKNESS (AUTOMATICALLY DETERMINED) IS YS
ISN 0032      1',1PD11.3,' MICROMETERS',//)
ISN 0033      C
ISN 0034      C      CALCULATE THE INTERFACE SURFACE PARAMETERS.
ISN 0035      C
ISN 0036      DYSURF=YPOS(JMAX)
ISN 0037      I=1
ISN 0038      100 I=I+1
ISN 0039      IF(I.GT.ITHMAX) GO TO 190
ISN 0040      X(I)=XPOS(I)*DEBYE
ISN 0041      SISURF(I)=(PSI(I,JMAX)+PSI(I,JMAX+1))/2.00+GSS*DYSURF/2.00
ISN 0042      PHIN(I)=PSI(I,JMAX)-DLOG(EDENS(I,JMAX))
ISN 0043      DSI=SISURF(I)-PSI(I,JMAX)
ISN 0044      QGI=EDENS(I,JMAX)*DYSURF*(DEXP(DSI)-1.00)/DSI
ISN 0045      QGL=ACCPTR*DYSURF
ISN 0046      YD(I)=DYSURF*DEBYE
ISN 0047      YI(I)=DYSURF*DEBYE
ISN 0048      KFLAGI=0
ISN 0049      KFLAGD=0
ISN 0050      J=JMAX+1
ISN 0051      C
ISN 0052      C      INVERSION CHARGE
ISN 0053      C
ISN 0054      110 J=J+1
ISN 0055      IF(J.GT.1) GO TO 120
ISN 0056      GO TO 100
ISN 0057      120 IF(KFLAGI.GT.0) GO TO 150
ISN 0058      IF(EDENS(I,J).LE.1.00.OR.EDENS(I,J-1).LT.0) GO TO 140
ISN 0059      YI(I)=YI(I)+YDLT(J)*DEBYE
ISN 0060      RATIO=EDENS(I,J-1)/EDENS(I,J)
ISN 0061      IF(RATIO.GT.0.9500.AND.RATIO.LT.1.0500) GO TO 130
ISN 0062      QGI=QGI+(EDENS(I,J-1)-EDENS(I,J))*YDLT(J)/DLOG(RATIO)
ISN 0063      GO TO 150
ISN 0064      130 QGI=QGI+EDENS(I,J)*YDLT(J)/(1.00-(EDENS(I,J-1)-EDENS(I,J))/(2.0
ISN 0065      1EDENS(I,J)))
ISN 0066      GO TO 150

```

THIS PAGE IS BEST QUALITY PRACTICABLE
FROM COPY FURNISHED TO DDC

```

0052      140 KFLAGI=1
      C
      C      DEPLETION CHARGE
      C
0053      150 IF(KFLAGD.GT.0) GO TO 180
0055      IF(HDENS(I,J).GT.0.9500*ACCPTR.OR.J.EQ.2) GO TO 170
0057      YD(I)=YD(I)+YDLT(J)*DEBYE
0058      RATIO=HDENS(I,J-1)/HDENS(I,J)
0059      IF(RATIO.GT.0.9500.AND.RATIO.LT.1.0500) GO TO 160
0061      QQU=QUQ+(ACCPTR-(HDENS(I,J-1)-HDENS(I,J))/DLOG(RATIO))*YDLT(J)
0062      GO TO 110
0063      160 QQU=QUQ+(ACCPTR-HDENS(I,J)/(1.00-(HDENS(I,J-1)-HDENS(I,J))/
      12.00*HDENS(I,J)))*YDLT(J)
      C      GO TO 110
0064      170 KFLAGD=1
0065      180 IF(KFLAGI.EQ.0) GO TO 110
0066      QI(I)=QI*QNORM
0068      QU(I)=QU*QNORM
0069      SISURF(I)=SISURF(I)*PSINRM
0070      PHIN(I)=PHIN(I)*PSINRM
0071      GO TO 100
0072
      C
      C      WRITE THE INTERFACE PARAMETERS
      C
0073      190 J=JMAX
0074      QI(I)=0.
0075      QD(I)=0.
0076      QI(I)=0.
0077      QD(I)=0.
0078      SISURF(I)=PSI(I,J)*PSINRM
0079      SISURF(I)=PSI(I,J)*PSINRM
0080      PHIN(I)=(PSI(I,J)-DLOG(EDENS(I,J)))*PSINRM
0081      PHIN(I)=(PSI(I,J)-DLOG(EDENS(I,J)))*PSINRM
0082      X(I)=0.
0083      X(I)=XPOS(I)*DEBYE
0084      YD(I)=0.
0085      YI(I)=0.
0086      YD(I)=0.
0087      YI(I)=0.
0088      WRITE(6,1020)
0089      1020 FORMAT(1H0,9X,'SUMMARY OF CONDITIONS ALONG THE SILICON-OXIDE INTE
      1FACE :',15X,'X',9X,'PSI',8X,'PHIN',7X,'QI',10X,'QD',
      210X,'YI',10X,'YD',//)
      DO 200 I=1,IMAX
0090      200 WRITE(6,1030)X(I),SISURF(I),PHIN(I),QI(I),QD(I),YI(I),YD(I)
0091      1030 FORMAT(11X,1P7D11.3)
      C
      C      BULK PARAMETERS
      C
0093      WRITE(6,1040)
0094      1040 FORMAT(1H1,5X,'X(I),I=1,IMAX',//)
0095      WRITE(6,1050)(X(I),I=1,IMAX)
0096      1050 FORMAT(20X,1P10D10.2)
0097      WRITE(6,1060)
0098      1060 FORMAT(1H0,5X,'J',9X,'Y(J)',15X,'PSI(I,J),I=1,IMAX',//)
0099      YY=-YCALDE*DEBYE
0100      DO 220 JJ=1,JMAX5
0101      J=JMAX5+1-JJ
0102      DO 210 I=1,IMAX
0103      210 SCRTCH(I)=PSI(I,J)*PSINRM
0104      WRITE(6,1070)J,YY,(SCRTCH(I),I=1,10)
0105      1070 FORMAT(15,5X,1P010.2,1P10D10.2)
0106      WRITE(6,1080)(SCRTCH(I),I=11,IMAX)
0107      1080 FORMAT(20X,1P10D10.2)
0108      220 YY=YY+YDLT(J)*DEBYE
0109      WRITE(6,1040)
0110      WRITE(6,1050)(X(I),I=1,IMAX)
0111      WRITE(6,1090)
0112      1090 FORMAT(1H0,5X,'J',9X,'Y(J)',15X,'EDENS(I,J),I=1,IMAX',//)
0113      YY=DYSURF*DEBYE
0114      DO 240 JJ=1,JMAX
0115      J=JMAX+1-JJ

```

THIS PAGE IS BEST QUALITY PRACTICABLE
FROM COPY FURNISHED TO DDG


```

ISN 0116      DO 230 I=1,IMAX
ISN 0117      230 SCRTCH(I)=EDENS(I,J)*DNSNRM
ISN 0118          WRITE(6,1070)J,YY,(SCRTCH(I),I=1,10)
ISN 0119          *WRITE(6,1080)(SCRTCH(I),I=11,IMAX)
ISN 0120      240 YY=YY+YDLT(J)*DEBYE
ISN 0121          WRITE(6,1040)
ISN 0122          WRITE(6,1050)(X(I),I=1,IMAX)
ISN 0123          *WRITE(6,1100)
ISN 0124      1100 FORMAT(1H0,5X,'J',9X,'Y(J)',15X,'HDENS(I,J),I=1,IMAX',//)
ISN 0125          YY=DYSURF*DEBYE
ISN 0126          DO 260 JJ=1,JMAX
ISN 0127          J=JMAX+1-JJ
ISN 0128          DO 250 I=1,IMAX
ISN 0129      250 SCRTCH(I)=HDENS(I,J)*DNSNRM
ISN 0130          WRITE(6,1070)J,YY,(SCRTCH(I),I=1,10)
ISN 0131          *WRITE(6,1080)(SCRTCH(I),I=11,IMAX)
ISN 0132      260 YY=YY+YDLT(J)*DEBYE
ISN 0133          DO 270 I=1,ITHMAX
ISN 0134      270 X(I)=ATHPUS(I)*DEBYE
ISN 0135          *WRITE(6,1110)
ISN 0136      1110 FORMAT(1H1,5X,'ATH(I),I=1,ITHMAX',//)
ISN 0137          *WRITE(6,1050)(X(I),I=1,ITHMAX)
ISN 0138          *WRITE(6,1120)
ISN 0139      1120 FORMAT(1H0,5X,'J',9X,'YTH(J)',13X,'THETA(I,J),I=1,ITHMAX')
ISN 0140          YY=0.
ISN 0141          DO 290 JJ=1,JMAX
ISN 0142          J=JMAX+1-JJ
ISN 0143          DO 280 I=1,ITHMAX
ISN 0144      280 SCRTCH(I)=THETA(I,J)
ISN 0145          *WRITE(6,1130)J,YY,(SCRTCH(I),I=1,10)
ISN 0146      1130 FORMAT(1H0,14,5X,1P10,2,1P10D10,2)
ISN 0147          *WRITE(6,1080)(SCRTCH(I),I=11,ITHMAX)
ISN 0148      290 YY=YY+YTHDLT(J)*DEBYE
ISN 0149          WRITE(6,1110)
ISN 0150          *WRITE(6,1050)(X(I),I=1,ITHMAX)
ISN 0151          *WRITE(6,1140)
ISN 0152      1140 FORMAT(1H0,5X,'J',9X,'Y(J)',15X,'ESUBX(I,J),I=1,ITHMAX')
ISN 0153          YY=DYSURF*DEBYE
ISN 0154          DO 310 JJ=2,JMAX
ISN 0155          J=JMAX+2-JJ
ISN 0156          DO 300 I=1,ITHMAX
ISN 0157      300 SCRTCH(I)=(PSI(I,J)-PSI(I+1,J))*PSINRM*1.D4/(XDLT(I+1)*DEBYE)
ISN 0158          *WRITE(6,1130)J,YY,(SCRTCH(I),I=1,10)
ISN 0159          *WRITE(6,1080)(SCRTCH(I),I=11,ITHMAX)
ISN 0160      310 YY=YY+YDLT(J)*DEBYE
ISN 0161          DO 315 I=1,IMAX
ISN 0162      315 X(I)=APUS(I)*DEBYE
ISN 0163          WRITE(6,1040)
ISN 0164          *WRITE(6,1050)(X(I),I=1,IMAX)
ISN 0165          *WRITE(6,1150)
ISN 0166      1150 FORMAT(1H0,5X,'J',9X,'YTH(J)',13X,'ESUBY(I,J),I=1,IMAX',//)
ISN 0167          YY=0.
ISN 0168          DO 320 I=2,ITHMAX
ISN 0169      320 SCRTCH(I)=(SISURF(I)-PSI(I,JMAX)*PSINRM)*1.D4/(DYSURF*DEBYE)
ISN 0170          SCRTCH(1)=0.
ISN 0171          SCRTCH(IMAX)=0.
ISN 0172          WRITE(6,1070)JMAX,YY,(SCRTCH(I),I=1,10)
ISN 0173          *WRITE(6,1080)(SCRTCH(I),I=11,IMAX)
ISN 0174          YY=YY+YTHDLT(JMAX)*DEBYE
ISN 0175          JMAXX=JMAX-1
ISN 0176          DO 340 JJ=1,JMAXX
ISN 0177          J=JMAXX+1-JJ
ISN 0178          DO 330 I=1,IMAX
ISN 0179      330 SCRTCH(I)=(PSI(I,J+1)-PSI(I,J))*PSINRM*1.D4/(YDLT(J+1)*DEBYE)
ISN 0180          *WRITE(6,1070)J,YY,(SCRTCH(I),I=1,10)
ISN 0181          *WRITE(6,1080)(SCRTCH(I),I=11,IMAX)
ISN 0182      340 YY=YY+YTHDLT(J)*DEBYE
ISN 0183          DO 350 I=1,ITHMAX
ISN 0184      350 X(I)=ATHPOS(I)*DEBYE
ISN 0185          WRITE(6,1110)
ISN 0186          *WRITE(6,1050)(X(I),I=1,ITHMAX)
ISN 0187          *WRITE(6,1160)

```

THIS PAGE IS BEST QUALITY PRACTICABLE
FROM COPY FURNISHED TO DDG


```

0188      1160 FORMAT(1H0,5X,'J',9X,'Y(J)',10X,'JSUBX(1,J),I=1,ITHMAX')
0189      YY=DISC*DEBYE
0190      DO 370 JJ=2,JMAX
0191      J=JMAX+2-JJ
0192      DO 360 I=1,ITHMAX
0193      SCRTCH(I)=CURKNT*(THETA(I,J-1)-THETA(I,J))*CRTNRM/YTHDLT(J)
0194      *WRITE(6,1130)J,YY,(SCRTCH(I),I=1,10)
0195      *WRITE(6,1080)(SCRTCH(I),I=11,ITHMAX)
0196      370 YY=YY+YDLT(J)*DEBYE
0197      DO 375 I=1,IMAX
0198      375 X(I)=XPOS(I)*DEBYE
0199      *WRITE(6,1040)
0200      *WRITE(6,1050)(X(I),I=1,IMAX)
0201      *WRITE(6,1170)
0202      1170 FORMAT(1H0,5X,'J',9X,'YTH(J)',13X,'JSUBY(1,J),I=2,ITHMAX')
0203      YY=0.
0204      DO 390 JJ=1,JMAX
0205      J=JMAX+1-JJ
0206      SCRTCH(1)=0.
0207      DO 380 I=2,ITHMAX
0208      380 SCRTCH(I)=CURKNT*(THETA(I-1,J)-THETA(I,J))*CRTNRM/XTHDLT(I)
0209      *WRITE(6,1130)J,YY,(SCRTCH(I),I=1,10)
0210      *WRITE(6,1080)(SCRTCH(I),I=11,ITHMAX)
0211      390 YY=YY+YTHDLT(J)*DEBYE
0212      RETURN
0213      ENL

```

THIS PAGE IS BEST QUALITY PRACTICABLE
FROM COPY FURNISHED TO DDC

CHAPTER V

Conclusions

The two-dimensional model for an MOSFET described herein has proven to produce results in good agreement with those of the predecessor program developed by Mock. A single check with an experimental p-channel structure, whose parameters have been well characterized by means of "test sites" has also shown good agreement with experiment.

It has been found that Gummel's iterative algorithm, when overrelaxed, proves to be impressively efficient in terms of rate of convergence, when compared with Mock's, Picard and Gummel procedure. The author is unaware of instances in which such overrelaxation procedures have been previously used for solving the nonlinear equations involved with semiconductor devices, although they have been widely used for the equations encountered with vacuum tube devices. In view of the success of this approach, further investigations of the procedure, in the interest of optimization of convergence rates would appear desirable.

DISTRIBUTION LIST

	<u># of Copies</u>		<u># of Copies</u>
Defense Documentation Center ATTN: ODC-TCA Cameron Station (Bldg 5) Alexandria, VA 22314	2	Commander US Army Materiel Development and Readiness Command ATTN: DRCDE-R 5001 Eisenhower Ave Alexandria, VA 22333	1
Office of Naval Research Code 427 Arlington, VA 22217	1	NASA Scientific & Tech Info Facility ATTN: Acquisition Br (S-AK/DL) PO Box 33 College Park, MD 20740	2
Naval Ship Engineering Center ATTN: CODE 6157D Prince Georges Center Hyattsville, MD 20782	1	Advisory Group on Electron Devices 201 Varick Street, 9th Floor New York, NY 10014	2
Commander Naval Electronics Lab Center ATTN: Library San Diego, CA 92152	1	Director Naval Research Laboratory ATTN: Code 2627 Washington, DC 20375	1
Commander US Naval Ordnance Lab ATTN: Technical Library White Oak Silver Springs, MD 20910	1	USA Security Agency ATTN: IARDA Arlington Hall Station Arlington, VA 22212	1
Rome Air Development Center ATTN: Documents Library (TILD) Griffiss AFB, NY 13441	1	Director Defense Communications Agency Technical Library Center Code 25 Washington, DC 20305	1
HQ ESD (ORI) L.G. Hanscom Field Bedford, MA 01731	1	Director Naval Research Laboratory ATTN: Mr. Eliot Cohen Code 5211 Washington, DC 20375	1
Deputy for Science & Technology Office, Assist Sec Army (R&D) Washington, DC 20310	1	Commander Harry Diamond Laboratories ATTN: Library 2800 Powder Mill Road Adelphi, MD 20783	1
Commander US Army Missile Command Redstone Scientific Info Ctr ATTN: Chief, Documents Section Redstone Arsenal, AL 35809	2	**GIDEP Engineering & Support Dept - TE Section P. O. Box 398 Norco, CA 91760	1

**Do not submit if report is not
releasable to public

	<u># of Copies</u>		<u># of Copies</u>
Institute of Defense Analysis Arlington, VA 22209	1	Dr. Barry Dunbridge TRW Systems Group One Space Park Redondo Beach, CA 90278	1
Mr. Jack Kilby 5924 Royal Lane Suite 150 Dallas, TX 75230	1	Dr. Paul E. Greene Hewlett-Packard Co. 1501 Page Mill Road Palo Alto, CA 94304	1
Commander Harry Diamond Laboratories ATTN: Mr. A. J. Baba 2800 Powder Mill Road Adelphi, MD 20783	1	Naval Research Laboratory ATTN: L. J. Palkutti Code 5216 Washington, DC 20375	1
Naval Research Laboratory ATTN: Dr. David F. Barbe (Code 5260) 4555 Overlook Ave., S.W. Washington, DC 20375	1	Bell-Northern Research IC Design Aids ATTN: D. M. Cauchy P. O. Box 3511, Station C Ottawa, Ontario K1Y Canada	1
Commander Naval Electronics Laboratory Ctr ATTN: Mr. C. E. Holland Jr. 271 Catalina Blvd San Diego, CA 92152	1	Dr. Gordon E. Moore Intel Corporation 3065 Bowers Road Santa Clara, CA 95951	1
Air Force Avionics Lab ATTN: AFAL/DHE (Mr. Stanley Wagner) Wright-Patterson AFB, OH 45433	1	Naval Electronics Systems Cmd. ATTN: Mr. L. W. Sumney (Code 3042) Washington, DC 20360	1
Commander Rome Air Development Center ATTN: Mr. Joseph E. Brauer (RBRM) Griffiss AFB, NY 13441	1	Mr. Fred Sharf Actron, Dept 515 700 Royal Oaks Drive Monrovia, California 91016	1
Dr. Gerald B. Herzog Solid-State Technology Center RCA David Sarnoff Research Center Princeton, NJ 08540	1	Mr. Jim Mader Harris Electronic Systems Div P. O. Box 37 MS: 15/966 Melbourne, Florida 32901	1
Mr. Harold D. Toombs Texas Instruments, Inc. P.O. Box 5474; M/S 72 Dallas, TX 75222	1	Mr. Wesley Jones Bendix LSI Design Center East Joppa Road Baltimore, Maryland 21204	1
Dr. George E. Smith Bell Telephone Labs, Inc. Room 2A-323 Murray Hill, NJ 07974	1	Mr. Charles Gwyn Sandia Laboratories Division 2142 Albuquerque, New Mexico 87115	1

	<u># of Copies</u>		<u># of Copies</u>
Mr. David Ford	1	Commander	
Dept 631, Magnavox		ATTN: DRSEL-MS-TI	2
Government & Industrial Elec. Co.		ATTN: DRSEL-TL-DT	1
4624 Executive Blvd		ATTN: DRSEL-TL-E	1
Fort Wayne, Indiana 46808		ATTN: DRSEL-TL-M	1
		ATTN: DRSEL-TL-P	1
Mr. Dick Rath	1	ATTN: DRSEL-PL-ST	1
Hughes Aircraft Co.		ATTN: DRSEL-TL-B	1
P. O. Box 92919		ATTN: DRSEL-TL-I	1
Airport Station		ATTN: DRSEL-TL-I (CPC File)	2
Los Angeles, CA 90009		ATTN: DRSEL-TL-IT	1
		ATTN: DRSEL-TL-IC	1
Mr. Don Gibson	1	ATTN: DRSEL-TL-ID	1
Rockwell International		ATTN: DRSEL-TL-IR	1
Collins Radio Group		ATTN: DRSEL-TL-IG	5
MOS/CSI Marketing Development		ATTN: DRSEL-TL-IS	1
Newport Beach, CA 92663		ATTN: DRSEL-TL-IJ	1
		ATTN: DRSEL-TL-DD	1
Mr. Jeff Steinwedel	1	Fort Monmouth, NJ 07703	
Solid State Scientific			
Montgomeryville Industrial Ctr			
Montgomeryville, PA 18936			
Mr. John Travalent	1		
Sperry Univac			
M.S. UZU25			
Univac Park, P. O. Box 3525			
St. Paul, Minn. 55165			
Mr. Ralph Alspaugh	1		
ITT Semiconductors			
3301 Electronics Way			
West Palm Beach, FLA. 33407			
Commanding Officer	1		
Naval Avionics Facility			
ATTN: Mr. Bob Murphy			
Code 908, 6000 East 21st St.			
Indianapolis, Indiana 46218			
Commander	1		
Naval Electronics Lab			
Dr. I. Lagnado, Code 4800			
271 Catalina Blvd.			
San Diego, California 92152			
RAC	1		
RADC			
ATTN: Mr. I. L. Krulac			
Griffiss AFB, NY 13441			